UNITED STATES DEPARTMENT OF THE INTERIOR

GEOLOGICAL SURVEY

The Purcell Lava
Glacier National Park, Montana

by

Robert G. McGimsey[1]

Open-File Report 85-0543

1985

This report is preliminary and has not been reviewed
for conformity with U.S. Geological Survey
editoral standards and stratigraphic nomenclature

[1]Denver, Colorado

CONTENTS

FIGURES

TABLES

NOTE

Standard 2" by 2" color slides are available at cost through the U.S. Geological Survey Photo Library, MS-914, Box 25046, Federal Center, Denver, CO 80225. Telephone (303) 236-1010.

ABSTRACT

The Purcell Lava, a sequence of Proterozic mafic lava facies, is an important marker in the lower Missoula Group of the Belt Supergroup in both Canada and the United States. Based on the flow structure and morphology, the Purcell in Glacier National Park is informally divisible into a lower pillow lava facies, and an upper pahoehoe facies. Locally, two minor facies--vent rocks and a hypabyssal diabase sill--can be distinguished. The pillow facies, ranging in thickness from 9-15 m, consists entirely of subaqueously emplaced pillow lava and hyaloclastite breccia; it is the only volcanic unit that can be correlated throughout the Park. Thickness of the facies corresponds to the water depth in this part of the Belt basin at the time of lava extrusion.

The pahoehoe facies, emplaced subaerially above the pillow facies, is a variably thick (0-54 m), compound flow sequence that consists of multiple flow units (10 cm-6 m thick). Individual flow units extend laterally for only a few hundred meters. Most have ropy tops and internal structures similar to modern pahoehoe flows.

The vent facies is as much as 10 m thick and is a chaotic breccia composed of variably-sized cognate fragments and accidental blocks of sedimentary country rock in a tuffaceous matrix. The facies, which occurs within the upper part of the pillowed facies in the northernmost part of the Park, is linearly distributed along a northwest-southeast trend. Transverse cross sections are lens-shaped. The facies appears to represent explosive vent products associated with a fissure eruption.

The hypabyssal diabase sill is as much as 21 m thick, is spatially correlative with the vent facies, and generally occurs about 5 m below the base of the pillow lava facies. The sill was emplaced subsequent to eruption of the pillowed facies.

The Purcell Lava has been extensively altered mineralogically and geochemically by diagenesis related to burial. The original rock type was that of continental alkaline basalt.

The Purcell is apparently neither cogenetic nor coeval with a large gabbroic sill (middle Belt carbonate sill) that is conspicuous throughout the Park.

ACKNOWLEDGMENTS

This manuscript is a reformated version of my M.S. thesis, which was directed by Edwin E. Larson, University of Colorado. The study was made possible by the U.S. Geological Survey's Glacier National Park Project, in cooperation with the National Park Service, and a grant from the Geology Department at the University of Colorado, Boulder, CO.

I want to thank Bob Earhart for introducing me to the problem and supporting my first year's work. Special thanks go to Jim Whipple for allowing me a second field season and for his continuous support and encouragement. Thanks also to Paul Carrara for his inspiration, and for showing me the lighter side of geology.

I will always be indebted to Ed Larson for his guidance, instruction, and friendship during the course of this study. His patience with me and critical reviews of the manuscript were invaluable.

I wish also to thank Chuck Stern and Jim Munoz for serving on my committee and reviewing the manuscript, and Jack Harrison and Omer Raup for their interest and technical advice. I am grateful to Jim Whipple and Ren Thompson for reviewing this version of the report. Thanks also to the folks in USGS Field Records for allowing me to use their photographic mounting equipment.

Many people with the Survey and Park Service were involved with the various aspects of the fieldwork and I extend my thanks to all. In particular, many thanks to Jerry DeSanto for logistically accomodating my numerous trips into his district. I am grateful to Sue Johnson for her field assistance and willingness to climb places that most sane geologists would not go. A very special thanks to Sam Dennis who was my field companian for most of the study. His good cheer, hard work, and friendship will always be remembered.

Finally, for her unyielding faith and support, it is to my patient wife, Deb, that I dedicate this thesis.

CHAPTER I

INTRODUCTION

Purpose of Investigation

Studies of Middle Proterozoic Belt terrane have focused primarily on the stratigraphy, structure, and distribution of sedimentary strata. Igneous rocks, both extrusive and intrusive, comprise only a small part of the Belt Supergroup and have received minimal study except for a few of the larger sills (Zartman and others, 1982; Mejstrick, 1975; Mudge and others, 1968). The Purcell Lava is a slightly metamorphosed succession of mafic lava flows well-exposed in the glaciated high country of Glacier National Park. Study of these rocks provides a unique opportunity to better understand Middle Proterozoic volcanic products and processes as well as diagenesis of mafic lava flows. The objectives of this study were to determine the lateral and stratigraphic extent, physical and chemical characteristics, environment of emplacement, and petrogenetic rock type of the Purcell Lava.

The name "Purcell" has been applied to sills and other intrusions inferred to be cogenetic with the extrusive units. In this study, only the extrusive phases were studied in detail. Information regarding certain intrusives is presented for comparative and interpretive purposes.

This investigation is part of a comprehensive geologic study of Glacier National Park begun by the United States Geological Survey (USGS) in 1979.

Location and Geologic Setting

Glacier National Park, which includes 4100 km^2 of glaciated, mountainous terrain in northwestern Montana adjacent to Canada, is located within the northeastern section of Belt terrane (fig. 1).

Purcell Lava crops out in the north-central part of the Park near the crests of the Livingston and Lewis Ranges where seven exceptionally well-exposed sections were chosen for this study (fig. 2). Of these, the Hole-in-the-Wall, Kootenai Peak, Fifty Mountain and Granite Park sections are the best exposed and provided excellent sources of data. Exposures at Mt. Cleveland, Redhorn Peak, and the Apgar Mountains were briefly examined for correlation purposes.

Stratigraphic units in the Park consist primarily of formations of the Middle Proterozoic Belt Supergroup (figs. 3 and 4) within the upper plate of the Lewis thrust fault. Belt strata consist of a thick (15,000+ m total; 5200 m in Glacier Park) sequence of shallow-water red and green argillite and siltite (except for the Prichard Fm., which contains deep water sedimentary facies), minor quartzite, and thick intervals of carbonate (Whipple and others, 1984). In the vicinity of Glacier National Park, Belt rocks have been affected only by low-grade burial metamorphism of the lower greenschist facies (Maxwell and Hower, 1967; Eslinger and Savin, 1973). The age of the Belt Supergroup is bracketed between the 1700-my age of crystalline basement upon which it unconformably rests, and the 850-my age of the unconformably overlying Windermere System, Canada (Harrison, 1972). On the basis of uranium-lead dating of the Crossport C Sill in Idaho, which intrudes the lower to middle parts of the Prichard Formation, Zartman and others (1982) have determined a minimum age of 1433$\pm$ 10 my for lower Belt strata.

Readers interested in a more detailed discussion of Belt terrane are referred to Harrison (1972) and Harrison and Grimes (1970). Additional

stratigraphic and structural data for Glacier National Park and adjacent areas can be found in Ross (1959), Childers (1963), Price (1964), Johns (1970), Mudge (1970, 1977), Harrison and others (1980), Mudge and Earhart (1980), McMechan (1981), Earhart and others (1983, 1984), and Whipple and others (1984).

Previous Work

The first International Boundary Commission (1857-61) was appointed by the British and United States governments to explore and mark the 49th parallel from the Cascade Range to the east flank of the Rocky Mountains (Daly, 1912; Bauerman, 1884). George Gibbs (United States) and Hilary Bauerman (British) of that expedition were probably the first geologists to discover the extrusive lava sequence known today as the Purcell Lava (Gibbs, 1874, p. 385; Bauerman, 1884, p. 28).

George Dawson was attached to the British North American Boundary Commission (1873-74) exploring the 49th parallel from Lake of the Woods, Ontario west to the Rocky Mountains. He too describes an extrusive igneous rock, referred to as "trap" (Dawson, 1875, p. 62.).

In 1901, having been commissioned by the Canadian Minister of the Interior, R. A. Daly began a six-year reconnaissance geological survey of the transmontane section of the 49th parallel (Daly, 1912, p. 1). Daly found a sequence of extensive lava flows that he recognized as an important stratigraphic marker but he did not designate a type locality. Later, he named the unit the "Purcell Lava", having measured the thickest section (142 m, 465 ft) in the McGillivrary Range of the Purcell Mountain System (Daly, 1912, p. 161-163, 207-220). Daly provided the first physical and petrographic descriptions and geochemical analysis of the Purcell.

Also in 1901, reconnaissance surveys along the 49th parallel, including the area that is now Glacier National Park, were led by members of the USGS, notably Bailey Willis (1902). George Finlay (1902) of that party provided the first published description of an extrusive diabase which Daly later examined and determined was the same unit he had named "Purcell Lava" further north.

Soon after the creation of Glacier National Park in 1910, the USGS began extensive geological research under the direction of M. R. Campbell and including W. C. Alden, Eugene Stebinger, E. M. Parks, C. S. Corbett, C. R. Williams, T. W. Stanton, J. R. Hoats, H. R. Bennett, and J. E. Thomas. Their unpublished field notes and maps (located at the USGS Field Records, in Denver, Colorado) provide details of descriptions and localities for the Purcell Lava not included in subsequent publications.

Burling (1916) drew attention to the ellipsoidal base (pillows) of the lowest lava flow at two localities within the Park and concluded that the entire sequence of lava flows was subaqueous in origin. However, he acknowledged that in other localities where the spheroidal masses were seemingly absent and the underlying argillites were ripple-marked and mud-cracked, the flows could have been subaerial. He also listed criteria for determining tops and bottoms for a subaqueous flow.

Fenton and Fenton (1931) gave a brief description of the Purcell Lava in the Park and later (Fenton and Fenton, 1937) presented a more detailed account. They measured stratigraphic thickness, described the flows, and listed the evidence for subaqueous extrusion.

While examining potential dam sites along the Flathead River in the southwest portion of the Park, Erdmann (1947) reported previously unpublished localities for the Purcell Lava.

Ross (1959) published the first comprehensive geologic study of Glacier National Park drawing heavily from the others already mentioned and earlier unpublished data of M. R. Campbell. Ross referred to the unit as "Purcell Basalt", after Wilmarth (1938, p. 1746).

Sweeney (1955), Sommers (1961), Smith (1963), Johns (1970), and Barnes (1963) all briefly describe the Purcell Lava in the Whitefish Range immediately west of the Park. Calkins (1909), Johns (1962, 1970) and Sheldon (1961) describe the succession further to the west, in the Salish Mountains. Recent mapping by Harrison and others (1983) provides many localities for the Purcell Lava west and southwest of Glacier National Park.

A number of Canadian geologists have reported localities and descriptions of the Purcell Lava north of the Park. The most recent list includes Reesor (1958), Leech (1960), Price (1962, 1964), Hoy (1979, 1982, 1984), McMechan (1979, 1981), and McMechan and others (1980).

Hunt (1961, 1962, 1964) provided the first regional petrologic, geochemical, and stratigraphic correlation study of the Purcell Lava, with emphasis on Canadian exposures. He dated the Purcell Lava in Canada at 1075 m.y. by the K-Ar method on hornfels from the lower contact.

During the last decade, detailed stratigraphic and structural studies have advanced the understanding of Belt rocks thus prompting the USGS in 1979 to begin an updated comprehensive geologic study of Glacier National Park, of which this investigation is a part.

Field and Laboratory Methods

Field studies were conducted in three and one-half months during the summers of 1982 and 1983. Sections of the Purcell Lava were measured, sampled, described, and photographed in detail, and the unit was mapped at a scale of 1:24,000 and compiled at 1:50,000 (McGimsey, 1984). Because most exposures of the lava flows are located in remote backcountry areas of the Park, access was either by foottrail, boat, cross-country traverse, or helicopter. All sections were measured using an Abney Level, Jacobs Staff, and steel tape. Over 200 representative samples were collected from which 96 thin-sections were cut and 32 chemical analyses determined. Color photographs were taken with a 35 mm Pentax camera (50 mm lens).

Laboratory methods included staining and polishing of thin-sections and preparation of samples for chemical analysis.

The electron microprobe was used to analyze the composition of altered feldspars, and determination of some trace element contents was by x-ray diffraction methods.

CHAPTER II

DIVISION AND DESCRIPTION OF FACIES

Introduction

The Purcell Lava is a persistent marker in the lower part of the Missoula Group in north-central Glacier National Park (fig. 3). The formation consists of a sequence of lava flow facies that is intercalated with beds of siltite and argillite of the Snowslip Formation (see appendix A for a more complete description of the Snowslip Formation). Despite its antiquity, the Purcell has undergone only low-grade burial metamorphism and consequent diagenetic chemical alteration, therefore, most primary structures and textures are exceedingly well-preserved.

In the Park, the Purcell Lava can be divided into four informal facies distinguished by physical characteristics and occurrence: (1) pillow lava, (2) pahoehoe flow unit sequence, (3) vent rocks, and (4) a hypabyssal diabase sill. The pillowed facies is ubiquitous, and is usually overlain by flow units of the pahoehoe sequence. The vent facies rocks and diabase sill occur locally in the northern parts of the Park (Hole-in-the-Wall, Redhorn Peak) where the succession is thickest. The stratigraphic relationship of the facies is shown diagrammatically in Figure 5. Locations referred to in the text appear on Figure 2 and details of the sections measured at each locality are presented in Appendix B.

Because the Purcell Lava crops out near the crest of the continental divide and is considerably more resistant than the sedimentary strata with which it is intercalated, much of the rock is located in inaccessable cliff faces. Although lichen cover is common on rock surfaces throughout the Park, most of the outcrops examined for this study have relatively fresh, clean surfaces because of the retreat of Neoglacial ice and snowfields. Logistical difficulties limited access to certain sections of the Park; however, most of the best exposures were visited.

The Purcell Lava is divided into facies rather than flows because no evidence was found to delineate individual flows. The pillow lava facies could represent several temporally distinct simple flows, or alternatively, it could be part of a compound flow that includes part or all of the pahoehoe facies. The pahoehoe facies likewise could represent one compound flow, or, several compound flows from separate eruption cycles. Individual lobes and tongues in the pahoehoe facies are referred to as flow units, a term coined by Nichols (1936) and applied to similar Hawaiian flows (Wentworth and Macdonald, 1953, p. 32). In the general case, each flow unit is a separate outpouring of lava (cooling unit), occurring a few hours, days, or weeks apart, during a single eruptive cycle. No evidence was found to indicate whether or not pahoehoe flow units of the Purcell Lava represent more than one eruptive cycle.

Pillow Lava Facies

The basal facies of the Purcell Lava consists of 9 to 15 m of well-developed, variably sized pillows draped with, or surrounded entirely by, a matrix of hyaloclastite breccia. The best exposures are found at Fifty Mountain and Granite Park where in addition to cross-sectional views provided in cliffs, dip slopes containing broad, stair-stepped exposures offer a three-dimensional view of the pillows.

The color of freshly broken surfaces is typically greenish gray to dark greenish gray, and locally, pale reddish purple; brownish olive gray and light reddish brown are characteristic colors on weathered surfaces.

Two-Dimensional Pillow Exposures

Typical two-dimensional exposures exhibit pillows that are broken and truncated as well as those that are unbroken with rounded, outwardly protruding, bulbous ends. The latter produces a distinctive hummocky surface readily identified from a distance (fig. 6a and b). Most pillows appear as individual, circular to elliptical sac-like masses, seemingly floating in a matrix of hyaloclastite breccia (fig. 7). Pillows are typically .07-1.5 m in diameter; large and small pillows alike are randomly distributed throughout the pillowed facies. Many have flat bottoms and smooth, well-rounded, convex upper surfaces; others appear to be entirely rounded. Less commonly, and generally in the lower part of the facies, pillows are stacked one against another with little or no interstitial breccia. They are closely fitted together and have irregular shapes. Generally, the form of the pillows becomes more spherical towards the top of the facies. Flattened or elongate pillows occur locally throughout the facies but are more common in the lower portion. Many of these were probably deformed plastically before cooling by lateral spreading caused either by the weight of overlying pillows or by partial drainage of interiors while the crust was still thin and soft. However, many seemingly flattened pillows are "normal" pillows exposed longitudinally.

Broken pillows with hollow, flat-bottomed cavities at the top are common and are proof that the lava was highly fluid (fig. 8). During formation, these pillows ruptured and partially drained, yet had a strong enough crust to withstand collapse. Modern ana-logs are documented by Ballard and Moore (1977, p. 32-40, 52).

At the basal contact with Snowslip strata, pillows were bulldozed down into the soft sediments extensively deforming the sedimentary beds. As a result, the lower contact is highly irregular. In some cases, sediment was caught between pillows and squeezed into bizarre forms; in other cases, the pillows are entirely buried by sediment (fig. 9). Locally, slabs of sediment, some with relatively undeformed bedding, have been rafted upwards as much as a meter and left stranded amongst surrounding pillows (fig. 10). The most intense soft-sediment deformation was observed at Kootenai Peak and Mt. Cleveland; however, it is common at all sample localities.

At Kootenai Peak, at least five beds of green hyaloclastite tuff (possibly hyalotuff, Fisher and Schmincke, 1984), up to 1 cm thick, are interbedded with Snowslip siltite and argillite (fig. 11). Clasts are angular and have sharp edges (see photomicrograph in Figure 65). The interbeds occur in relatively undisturbed portions of sedimentary strata 1-10 cm below the lowermost pillows. The tuff beds are locally discontinuous due to sediment deformation during pillow emplacement. Whether the tuff was deposited by airfall or current action is unknown; however, fragment imbrication and the presence of intermingled silt and mud particles indicate almost certainly that it was reworked. Silvestri (1963) suggests that water turbulence caused during subaqueous eruption is sufficient to carry small fragments far from an eruption site. However, the angular edges of the clasts suggest that transport by aqueous currents was probably minimal. Whether the hyaloclastite fragments originated from nonexplosive pillow spalling, or from a phreatic or phreatomagmatic explosion remains undetermined.

At or near the base of the Hole-in-the-Wall, Fifty Mountain, and Kootenai Peak sections, pillows grade laterally into and out of massive zones that have irregular, indistinct boundaries; some of these zones have curved, rounded outlines (fig. 12). The massive zones in contact with Snowslip rocks have well-developed pipe vesicles up to 10 cm long extending up from the lower contact and are coarsely vesiculated at their upper and lateral contacts with surrounding pillows. Those at Fifty Mountain and Kootenai Peak are up to 2 m in diameter and probably represent either congealed feeder tubes or exceptionally large pillows. However, they could represent eruption surges during which lava is extruded so voluminously and rapidly that pillows could form only at the outer margins. Larger-scaled, massive zones at Hole-in-the-Wall most likely represent voluminous pulses close to a vent. One such phase is sufficiently large that moderately well-developed columnar joints formed in the interior. The columns are 10-15 cm in diameter and are inclined, at about 45^{o}, to the southwest.

Foreset bedding is common in modern pillow lava (Fuller, 1931; Moore, 1970; Moore and others, 1971; Moore and others, 1973; Ballard and Moore, 1977, p. 26), and usually forms along steep-sided flanks of an advancing flow. The structures can be used as one criterion for determination of flow direction (Waters, 1960). Foreset beds in the Purcell pillowed unit are either absent or so poorly developed that they are unrecognizable.

Interpillow drusy cavities, up to 30 cm long and irregular to elliptical in shape, are located throughout the pillowed facies. They are partially or completely filled with subhedral to euhedral quartz and calcite crystals. Some exhibit calcite, or rarely, barite centers which are surrounded by intergrown quartz; others are mostly hollow with large quartz crystals projecting inward from the walls creating a "dog-tooth" texture. Hargreaves (1976) used laterally continuous zones of interpillow cavities to define possible flow contacts within an Early Precambrian basalt sequence. In the Purcell pillowed facies, however, the cavities are distributed randomly throughout the facies and lack horizontal continuity.

Internal structures and textures are commonly found in many of the pillows. When preserved, the outer crust of the pillows generally is thin (1-3 mm) and consists of concentric laminae of extremely fine-grained, devitrified and altered glass. The laminae are accentuated where preferential weathering has stripped off some or all of the adjacent layers, leading to an appearance similar to that of exfoliating granite boulders.

Certain pillows have crusts thicker than 3 mm that grade outward into the hyaloclastite breccia, thereby producing a poorly defined boundary (fig. 13). The thicker layering could be the result of incomplete spalling during implosions that may have generated the breccia.

Scattered minute laths of quenched plagioclase crystals are visible (with the aid of a hand lens) on weathered pillow surfaces. Also present are very small (about 1 mm) nodular masses that possibly may have been varioles.

Pillows exhibit predominately two types of vesicles: subspherical cavities and/or pipe vesicles. Irregular, subspherical cavities <1 mm to about 15 mm in diameter are either randomly distributed throughout a pillow, or more commonly, arranged in concentric zones along the perimeter (fig. 14a). Pipe vesicles (Waters, 1960) 5-30 mm long radiate out from the center or are also concentrically arranged about the perimeter (fig. 14b). Most larger pillows contain both, with subspherical cavities concentrated in the upper portion of the pillows and pipe vesicles rising from the lower contact, and are very similar to subglacial pillows (Jones, 1970). Many of the vesicles have coalesced near the outer pillow rim, forming large, highly

irregular cavities. The smaller pillows (<15 cm in diameter) are massive and have very few if any vesicles--presumably as a result of rapid quenching.

Nearly all vesicles have amygdaloidal fillings of quartz, calcite, or chlorite, and combinations of all three are not uncommon. Some amygdules are reddish orange (probably because of disseminated hematite); iron and copper sulfide minerals such as pyrite and chalcopyrite are present locally.

Cooling and contraction joints are present in some pillows but are not as common and well-developed as the radial fractures typical of many modern pillow lavas (Wells and others, 1979). Figure 15 illustrates a fractured pillow with hyaloclastite breccia filling the larger cracks. This occurrence is similar to those described by Dimroth and others (1978) of Archean subaqueous basalt flows in Canada.

Although rare, fault slivers (Moore, 1975) and intrapillow selvages (Wells and others, 1979) were found in favorable exposures at several localities. These structures are most visible in longitudinal cross sections. Many pillows are exposed perpendicular to their long axes, a fact that may explain the apparent paucity of the sliver and selvage structures. Also, because precipitous topography prevented close examination of the upper pillowed section at many localities, some of the structures may have gone unnoticed.

Although most pillows appear to be individual, discrete masses, some exposures provide evidence that the pillows are actually interconnected (fig. 16). Three-dimensional exposures are therefore crucial for determining the actual pillow geometry, which in turn provides insight into the process of pillow formation.

Three-Dimensional Pillow Exposures

Three-dimensional exposures reveal that few if any pillows are individual, sac-like entities, rather they are sinuous, tubular, interconnected masses that commonly bifurcate and form multiple branches. Excellent exposures are located at Fifty Mountain and Granite Park. Low in the facies, where the hyaloclastite breccia is least abundant, the pillows are less regular in shape, conformably fitted to irregularities between surrounding pillows (fig. 17). Locally, bulbous and cylindrical pillows are dominant (fig. 18). Higher in the facies, amidst greater quantities of breccia, the pillows are elongate, sinuous bodies, traceable for several meters before disappearing into the tangled, entrail-like conglomeratic pillowed mass (fig. 19). During formation, the pillows typically pinch and swell and abruptly change direction by lateral budding, producing what Ballard and Moore (1977) refer to as "neck and bulb" shapes (fig. 20). Many branch into pillow buds of various size. Fluidal banding parallel to the pillow surface, highlighted by preferential weathering similar to that described by Dimroth and others (1978, p. 906) is not uncommon.

The long axes of many pillows are aligned roughly north-northeast, although locally, highly sinuous, snake-like pillows may have no apparent preferred orientation. However, many of the latter pillows can be traced back to a parent having the common orientation.

Most pillows have slightly hummocky but smooth, rounded outer surfaces and lack corrugations or growth ridges typical of many modern pillows (Moore, 1975; Moore and others, 1973).

Isolated- and Broken-Pillow Breccia

At Fifty Mountain and Granite Park, hyaloclastite breccia is very abundant in the upper part of the facies and pillows are more widely separated

from each other (fig. 21). The term "isolated-pillow breccia" is used by Carlisle (1963) to describe a similar occurrence and is the equivalent of Henderson's (1953) "pillow breccia". The pillows tend to be somewhat smaller in cross section (perpendicular to the long axis) and more irregularly shaped than those lower in the facies. No distinct contact exists between these and the more closely packed lower pillows; instead, the transition is subtly gradational. Isolated-pillow breccia is found only locally. The facies is best exposed at Granite Park and Fifty Mountain where broad stair-stepped dip slopes allow three-dimensional examination of the entire pillowed facies.

Another local subfacies in the uppermost part of the pillow lava facies consists of disaggregated fragments of pillows set in a coarse matrix of hyaloclastite breccia. Carlisle (1963) refers to a similar but more extensive and well-exposed occurrence as "broken-pillow breccia". The fragments are usually less than 25 cm in diameter and many have curved surfaces and concentric zones of subspherical and pipe vesicles. Intermixed with these fragments are angular, massive ones that are probably from pillow interiors.

Broken-pillow breccia is present at Granite Park in small isolated patches and appears to be an autobreccia (fig. 22). At Hole-in-the-Wall, it is not easily distinguished from the vent facies with which it may be genetically associated. A good exposure is located on the southwest flank of Boulder Peak.

Coalesced Pillows and the Upper Contact

The transition from the pillowed facies to the overlying pahoehoe facies is rather abrupt and is marked by a drastic decrease in interpillow hyaloclastite breccia and a pronounced change in pillow morphology. Coherent, tubular masses typical of the isolated-pillow breccia or close-packed lower pillows are replaced by flatter, tongue-like masses similar to pahoehoe toes (fig. 23). In general, the rock is more massive and less vesicular than that in the underlying pillowed facies. Fluidal banding is well-developed and ropy surface textures first become noticeable (fig. 24). The subfacies grades from isolated-pillow breccia or close packed pillows upward into a thin (<1.5 m) massive flow unit having a smooth to ropy top with a pronounced concentration of subspherical and irregularly shaped vesicles near the top. The transition typically occurs within a vertical distance of 1 meter (fig. 25). At Hole-in-the-Wall, the subfacies is characterized by medium-sized (4-20 cm) highly irregular quartz-filled cavities, some with small stringers.

Hyaloclastite Breccia

Figure 26 illustrates the hyaloclastite breccia associated with Purcell pillow lava. The chloritized sub-rounded globules and sharp-pointed, nonvesicular, flake-like shards are up to a centimeter long and are contained in a very fine-grained greenish black matrix. Weathered surfaces are reddish brown to greenish gray with black splotches. Internally, individual fragments contain many tiny concentric, pale olive green bands in a dark green to black sub-matrix. This internal structure is commonly found in ancient hyaloclastite breccias and Moore (1966) suggests that the banding is a relict of chemical zoning associated with palagonitization prior to any subsequent metamorphism. Thus, Purcell hyaloclastite breccia was more than likely altered to palagonite before diagenetic chloritic alteration.

Hyaloclastite breccia associated with pillow lava is usually nonexplosive in origin and is referred to as "aquagene tuff" by Carlisle (1963). The breccia is associated with basaltic lava erupted subaqueously (Schmincke and others, 1979; Lonsdale and Batiza, 1980), subglacially (Peacock, 1926;

Williams and McBirney, 1979, p. 199), or into shallow bodies of water and over wet sediments (Fuller 1931; Moore and others, 1973). In its original form, the breccia consists of irregular fragments of volcanic glass (sideromelane) produced by varying degrees of interaction between water (usually cold) and hot, molten lava. Moore (1975) documented spalling of the outer glassy crust as pillows implode during rapid cooling. Another mechanism is complete in situ globulation and fragmentation of molten lava exposed to extreme quenching (Carlisle, 1963; Walker and Blake, 1966). Lonsdale and Batiza (1980) envision a type of phreatomagmatic eruption in which thermal shock caused granulation of molten lava in the formation of hyaloclastite breccia on seamounts along the East Pacific Rise. Figures 13 and 15 illustrate evidence that both spalling and thermal shock granulation were active processes that formed Purcell Lava hyaloclastite.

Intercalated Sediment

The only intercalated sediment present in the pillowed facies (excepting that forcibly squeezed up around pillows at the basal contact) is very localized accumulations, of volcaniclastic origin, near the vent facies at Hole-in-the-Wall. The volcaniclastic units are less than 12 cm thick and are fine to medium-grained and well-laminated.

In their description of the pillowed lava flow at Granite Park, Fenton and Fenton (1937, p. 1903) write "...the lavas surround detached masses of modified argillite 2 to 12 feet thick...". I found no sediment inclusions larger than 1 m thick in the pillowed facies. However, several sediment bodies of the dimension described by the previous workers are located near the Patrol Cabin at Granite Park, but they are in the uppermost portion of the overlying pahoehoe facies. At least one has been structurally juxtaposed to the flow units; the others are sediment-filled collapse structures discussed in the next section.

Pahoehoe Facies

Above the pillow lava facies lies a pahoehoe flow unit sequence, ranging in thickness from 0-54 m, that is strikingly similar to modern pahoehoe in morphology and structure. The best exposures are located at Hole-in-the-Wall, Boulder Peak and Pass, and Granite Park, where individual flow units are erosionally truncated producing stair-stepped slopes (fig. 27). The rock is fine-grained and distinctly more vesicular and amygdaloidal than that of the underlying pillow lava. Fresh exposures vary in color from medium bluish gray to dark greenish gray and locally are dark gray to grayish black. Flow unit tops are characteristically pale olive green. Weathered surfaces are pale yellowish brown to brownish gray.

Morphology

The pahoehoe facies consists of a number of individual flow units, which as defined by Nichols (1936), are tongue-shaped structures within a flow. Although each flow unit is a separate cooling unit, an entire sequence collectively may represent a single, compound flow (Walker, 1971). Purcell flow units are tabular, lenticular and fan-shaped tongues that complexly overlap one another (fig. 28).

Flow units range in thickness from 10 cm to 6 m and extend laterally as much as several hundred meters. Generally, as the thickness of the entire flow unit sequence increases, the number and thickness of individual flow units likewise increases. Also, flow units close to a vent area (e.g. Hole-

in-the-Wall), are somewhat thicker and more extensive than those located more distally (e.g. Granite Park), although thin pahoehoe lobes and toes are commonly found at both localities.

Flow unit boundaries are distinguished by vesicle patterns, flow tops, and partings along contacts. Characteristically, pipe vesicles extend upward from the base and concentrations of subspherical to irregular vesicles mark the top (Figures 28b and 29). Almost all flow units have pale olive green flow tops several millimeters to 1 cm thick (fig. 30), which most likely represent former subvitric skins that subsequently devitrified and were altered during diagenesis. The coloration is due to the presence of chlorite. Nodular masses reminiscent of varioles cover portions of a few flow tops. Some flow tops are smooth but many exhibit well-developed ropy structures typical of modern pahoehoe flows (fig. 31). The thin olive green flow-top zones resemble fine-grained rocks of the Snowslip and could easily be mistaken for intercalated strata of that formation.

The upper 1 to 5 cm of the uppermost flow units is bleached and oxidized, presumably from prolonged subaerial weathering (fig. 32). The zone occurs exclusively in the highest flow units (i.e. those at the upper contact of Purcell Lava with Snowslip strata); a significant hiatus probably occurred prior to deposition of the overlying Snowslip.

Shape and flow direction of individual flow units was strongly controlled by local surface topography created by coalescence and overlapping of underlying units. Combinations of plan view and cross-sectional exposures reveal that many flow units are irregular in shape (fig. 33). Typically, they thin gradually and pinch out (fig. 34), however, abrupt terminations are not uncommon.

In addition to typically shaped flow units, thin lobes of pahoehoe having smooth, billowy surfaces and protruding toes are also present (fig. 35). Morphologically, these are nearly identical to modern Hawaiian flows as documented by Wentworth and Macdonald (1953, fig. 22, p. 44), Macdonald (1953), and Swanson (1973). Observing the 1969-1971 Kilauea eruptions in Hawaii, Swanson (1973) found that dense, bulbous lobes and toes are formed when tube-fed lava has travelled far from the source, has been largely degassed, and then forced onto the surface by hydrostatic pressure.

Flow directions are normally indicated by downstream convexity of flow-top ropes but exceptions do exist. Figure 36 illustrates the problem of using this criteria to determine regional flow direction, a problem that Macdonald (1953) identified for Hawaiian flows. A few lava coils similar to those documented by Peck (1966) are also present and could possibly be used to determine local flow directions. Although Purcell lava flowed in multiple directions in response to local surface irregularities, enough good exposures of festooned flow units exist at Hole-in-the-Wall, Fifty Mountain, and Granite Park to suggest that flowage was generally in a southward direction; this correlates with the general alignment of pillow axes. Local flow directions to the north are indicated at Hole-in-the-Wall by the orientation of pipe vesicles (discussed later in this chapter).

Current classification of ancient lava flows has not been formalized; existing nomenclature pertains mainly to flows of pillow lava (Dimroth and others, 1978; Wells and others, 1979). Nonpillowed units are commonly referred to only as "massive flows". However, the Purcell pahoehoe facies can be divided into three distinct lava flow types using the classification scheme of Jones (1943) for modern lava flows:

(1) Massive pahoehoe: Flow units possess tumuli and are thick in cross section (> 2m) but thin abruptly producing high surface relief (fig. 37).
(2) Scaly pahoehoe: Thin (< .4 m), tightly overlapping flow units of very local extent that may have bulbous lobes and toes (figs. 35 and 38).
(3) Ropy lava: Any flow unit of average thickness (intermediate between massive and scaly pahoehoe) having a corded or festooned flow top formed by drag of underlying mobile lava (fig. 31).

This classification is applied only in a broad sense because local variations and combinations of lava types are not uncommon as illustrated by Figure 28c.

Internal Structures

Of the variety of internal structures common to nearly all flow units, the most obvious is vesicle zonation (figs. 29 and 38). The first zone contains pipe vesicles that extend upward from the bases of most flow units. Above this lies a massive, vesicle-poor zone that grades upward into a subtly stratified area of hollow, subspherical vesicles. Generally, next above are usually a few larger and more irregular, randomly scattered cavities. The upper portion of each flow unit normally consists of layers of coalesced vesicles oriented parallel to the flow top. The width of individual zones varies with the overall thickness of a flow unit; thicker flow units have wider zones than thinner flows. However, highly vesicular flow units have wider upper zones of vesicle layers than do those of equal thickness and average vesicularity. Although some information on vesicles and their spatial distribution appears in Appendix B, several characteristic types warrant description.

Roughly cylindrical pipe vesicles, 2 to 12 cm long and up to .5 cm in diameter, extend upward from near the lower contacts of most individual flow units (figs. 39, 23a, 28a, 28b, 29, 30a, 35a, and 38). Most rise from the lower few centimeters of a flow unit but some begin 10 to 15 cm up from the base; none extend beyond the lower 30 cm of even the thickest flow units. Although pipes are usually continuous over their entire length, some are segmented and others totally lack a cylindrical shape and are instead linear trains of subspherical vesicles.

In some units the pipes are vertically oriented whereas in others, the vesicles are inclined, as much as 50^{o}, in the direction of flow. Commonly, a large flow unit having inclined pipes will be overlain by a unit with pipes inclined in the opposite direction. This indicates that either lava was supplied from more than one direction, or, that it flowed from one direction but spread laterally as fan-shaped lava tongues advanced and overlapped one another.

Many pipes that rise vertically for most of their length are abruptly bent over at the upper tip. This not only indicates flow direction but proves that the pipes formed prior to cooling of still somewhat mobile, interior lava (DuToit, 1907; Waters, 1960). Using this evidence, it was possible to determine that some flow units (especially at Hole-in-the-Wall) were emplaced from opposite directions. Pipe vesicles in one flow unit are inclined in a certain direction and those in overlying or underlying flow units are inclined in the opposite direction. Indeed, it is not uncommon to find pipe vesicles alternately inclined in opposite directions for a succession of flow units (fig. 40).

Pipe vesicles generally have amygdule fillings of quartz, chlorite, and rarely calcite. Although most flow units have monomineralic pipe amygdules,

some have either polymineralic fillings (e.g. quartz rimmed by chlorite) or intermixed monomineralic fillings (e.g. chlorite amygdules interspersed with a few quartz amygdules).

The upper one-third of nearly all flow units is highly vesicular and in most cases the irregularly shaped vesicles of various sizes are filled with quartz and/or calcite. Vesicles in thinner flows (<1.5 m) appear in cross-section as linear strings or trains; some are joined, forming larger cavities up to 10 cm long that are generally incompletely filled (fig. 38). Thicker flow units have greater concentrations of vesicles. Commonly, these are coalesced into an interconnected network of cavities that were conducive to fluid transport during diagenesis, as shown by the presence of banded, multicolored chalcedony within the voids (fig. 41). Thin-section analysis reveals that the material is internally unlayered, massive cryptocrystalline quartz. The green and orange colors are presumably due to iron impurities present in various quantities and oxidation states. Because of similar color and external banding that resembles sedimentary laminations, the coalesced vesicle horizons are easily mistaken for sediment.

Another internal structure of flow units is represented by lava-filled cracks. In plan view they are tens of meters long, 10-20 cm wide, and may be either straight or sinuous in form (fig. 42a). Rare cross-sectional exposures reveal that some of the cracks extend at least a meter into the flow unit(fig. 42b). The infilled lava is very fine-grained, vesicular along the margins, and similar in color to the pale olive green flow tops. Best exposures are located at Hole-in-the-Wall and in a broad, flat-bottomed valley slightly north of Boulder Peak. It is difficult to determine whether the crack fillings represent linear squeeze-ups of the type described by Nichols (1939), or lava from later flow units that sank into contraction cracks formed during cooling. Squeeze-ups usually form slight topographic highs on a flow unit. Many exposures of Purcell Lava, however, have undergone glacial scouring that would have destroyed these features (fig. 42a). Some fractures in uppermost flow units, which are sediment-filled, obviously resulted from contraction during cooling (fig. 43).

In addition to contraction cracks, the uppermost flow units in many localities also exhibit sediment-filled slump and separation structures (fig. 44). The fractures are larger in scale than those of simple contraction or squeeze-up origin and probably formed by collapse or gravity sliding after the lava had cooled sufficiently. Alternatively, these features could represent former lava channels, the tops and sides of which collapsed after the flow of lava subsided. However, no other large scale flow features (e.g. lava tubes and channels) were found at other localities.

Thin, planar secondary joints, presumably formed during Laramide movement of the allochthonous block along the Lewis Thrust fault, commonly cut the flow units and are generally filled with greenish chalcedonic material very similar to that in the coalesced-vesicle horizons.

Interbedded Pillow Interval

Pillow lava was found in a single, localized interval within the pahoehoe facies and only at the Hole-in-the-Wall locality. It is less than 1 m thick and rests on top of a massive pahoehoe flow unit. The interval consists of small, irregularly shaped pillows surrounded by hyaloclastite breccia that grades abruptly upward into a 1 m thick ropy-topped pahoehoe flow unit, generally lacking basal pipe vesicles (fig. 45a); the transition is similar to that between the pillowed facies and pahoehoe facies. The interval pinches out laterally where the underlying flow unit topographically rises to the

level of transition between pillows and pahoehoe lava (fig. 45b). Thus, the transition probably marks the level of localized ponded water (about 1 m deep) that was overrun by the flow unit (Jones and Nelson, 1970). No other pillow lava was found within the flow units of the pahoehoe facies at any locality. Evidence supporting the subaerial nature of flow units is discussed in a later chapter.

Intercalated Sediments

Only one thin local pocket of sediment was found within the pahoehoe facies. Located at Kootenai Peak in a depression on the upper surface of a flow unit, this lens is 10-15 cm thick, 1 m long, and consists of medium-grained, greenish-brown volcaniclastic material, similar to that found below the pillowed facies at the same locality (see fig. 11).

Vent Facies

In the northern sector of the Park where the Purcell Lava is thickest (77 m), the vent facies consists of a lens-shaped, chaotic breccia containing fragments of various size, color, and origin. Well-exposed accessible sections were found at Hole-in-the-Wall and the southwest flank of Boulder Peak; exposures at Redhorn Peak and Mt. Thunderbird are poorer and not easily accessible. The facies has not previously been identified or described.

In detail, the facies consists of angular and subrounded cognate blocks, bombs, and lapilli intermixed with accidental sediment blocks all set in a fine-grained tuffaceous matrix (fig. 46). Lava blocks, almost all fragments of pillows, are generally equidimensional and 5 to 35 cm across. Nonvesicular clasts are from pillow interiors or massive zones; vesicular ones, some with pipes and others with curved outer edges and concentric bands of vesicles, are from pillow bases and margins, respectively.

Pinkish red, highly vesicular fragments of various size and shape are probably bombs. They are very fine-grained and have small (<2 mm) spherical vesicles filled with clear and milky quartz and black chlorite (fig. 47).

Silicified blocks of Snowslip strata up to 2 m across are distributed randomly throughout the central portion of the lens-shaped unit, becoming less abundant towards the margins. Although most blocks exhibit some degree of internal deformation, a wide range exists. Bedding and primary sedimentary structures are perfectly preserved in some whereas they are contorted and folded in others (fig. 48). Fragments so severely twisted and stretched that all primary structures were destroyed appear as reddish orange blobs and streaks (fig. 49).

The tuffaceous matrix, which contains lava lapilli, is brownish black in fresh exposures, grayish red when weathered. Flow-ribboned textures indicate minor secondary flowage.

In transverse cross section, the vent facies is lens-shaped, has a maximum thickness of about 10 m, and is approximately 3-4 km wide. Stratigraphically, it lies within the pillow lava facies; pillows lap up against the upper margins and a pahoehoe flow unit covers the top (figs. 5b and 50). Pillow lava is 3-4 m thick beneath the central portion of the facies.

On the outer flanks, sediment blocks are absent and lava fragments are smaller and fewer (fig. 51). This may represent a transition to broken-pillow autobreccia although very little hyaloclastite breccia is associated. Alternatively, the fragments could simply be smaller blocks and lapilli ejected to the margins during eruption.

Although no feeder dikes directly associated with the unit were located, the size and lack of sorting of cognate and exotic blocks are strongly indicative of a violent eruption typical of that associated with certain types of vents.

Hypabyssal Diabase Sill

Spatially correlative with vent facies rocks (except at Mt. Cleveland where no vent rocks occur) and located beneath the pillow lava facies is an 18- to 21-meter-thick diabase sill. Excellent exposures occur along the trail from Boulder Pass to Hole-in-the-Wall; the sill is also present at Boulder Peak, Thunderbird, Mountain, Mt. Cleveland, and the Redhorn Peak area.

Generally the sill is separated from the pillow lava facies by 5 m of Snowslip strata. Differences in color and resistance make the interval useful for locating the sill in distant and inaccessible cliff faces (fig. 52).

The sill maintains a fairly constant thickness regionally. However, beneath the vent facies on the west side of Hole-in-the-Wall cirque it thins abruptly to less than 2 m (figs. 50 and 53).

Apophyses and engulfed sediment blocks of various dimension are present along and near the upper contact (fig. 54). Locally, cupolas protrude upward into the Snowslip strata and terminate against the base of, or intrude into, the overlying pillow lava (fig. 55). Deformation along the margins of apophyses indicates that the sediments were unlithified at the time of sill intrusion.

At the head of Hole-in-the-Wall cirque, the sill complexly interfingers with the sediment interval, and intrudes into and along the base of the pillow lava. Orientation of apophyses and imbricated sedimentary rock slabs at the basal contact, indicates that emplacement of the sill was from the north (fig. 56).

Typically, the rock is massive and nonvesicular except for a few sparse spherical and elliptical vesicles (1-2 cm in diameter) near the upper contact. It is dark greenish gray and very fine-grained at the margins (fig. 57). In the center, grain size greatly increases and color changes to medium bluish gray; glomeroporphyritic plagioclase laths up to 5 mm long are megascopically visible on slightly weathered surfaces (fig. 58).

Sedimentary rocks at the lower contact are dense and silicified over a distance of approximately .5 m; they form a distinct contact aureole. At the upper contact, as much as 1 m of the lower portion of the sedimentary rock interval has been affected by contact with sillrock.

The sill is chemically and mineralogically very similar to the pillow lava and pahoehoe flow units (see Chapter 3) and is considered to be part of the Purcell Lava.

Although previous workers (Fenton and Fenton, 1937; Ross, 1959) neither identified nor described the sill, their measured sections of Purcell Lava include both the sill and the interval of sedimentary rock between it and the pillow flow. In all likelihood, the sill was considered to be a thick extrusive flow and the sedimentary strata between thought to be intercalated sediment.

CHAPTER III

PETROGRAPHY AND GEOCHEMISTRY

Petrography

Introduction and General Petrography

The Purcell Lava has been thoroughly altered diagenetically, both chemically and mineralogically. Consequently, little remains of the primary minerals except ghost-like outlines and pseudomorphs. A comprehensive account of the secondary mineralization is beyond the scope of this report. Nonetheless, a few specific minerals and textures are discussed in some detail because they provide insight about the original lithology of the Purcell Lava and the environment into which it was emplaced.

Ninety-six representative thin-sections were examined by means of a Zeiss petrographic microscope. Of these, twenty-nine thin-sections were selected for reflected-light oil-immersion study of the opaque minerals.

Although extensive diagenetic alteration has partially or entirely obliterated most of the primary minerals (fig. 59), it is possible in many cases to determine what they were. Primary minerals, identified optically and by crystal habit, include plagioclase, pyroxene, iron-titanium oxides, and possibly olivine. Because of the extent of alteration, however, mode counting was not attempted. X-ray diffraction was used to identify and/or confirm some of the common alteration products in several samples (e.g. chlorite, clays, albite and potassium mineral phases).

Plagioclase. Plagioclase is the major phenocryst phase still recognizable in the pillows and flow units. Commonly, the arrangement of euhedral to subhedral feldspar laths suggests an initial intergranular to intersertial texture (fig. 60). In many cases, primary interstitial pyroxene has been completely altered to chlorite and iron-titanium oxides. Plagioclase laths are altered to chlorite and other fine-grained clays (fig. 61), and therefore are distinguished only by ghost outlines. All field and petrographic evidence indicates that the Purcell Lava originally was a basalt. Therefore, the primary plagioclase was probably labradorite (An_{50-70}) or bytownite (An_{70-90}). In a few samples in which the feldspars are still present, extinction angles (17^{o}) suggest that albitization has occurred. This was corroborated by electron microprobe analyses (table 1). In many samples, the albite has been pervasively replaced by chlorite (fig. 62). Secondary potassium feldspar is also present.

Pyroxene. No primary pyroxene was identified, as all of the samples have undergone low-grade metamorphism altering pyroxene to chlorite (Deer, Howie, and Zussman, 1966). The presence of chlorite and other alteration products between the plagioclase laths (see Fig. 60) suggests that pyroxene (probably augite) was a major primary constituent, especially in the subaerial flow units. Glass may have been a primary interstitial constituent in the pillows.

Olivine. Rarely, a few grains (now mostly chlorite and other clays) having a shape similar to that of olivine were observed. It would appear, therefore, that olivine was not a major primary phenocryst phase in the basalt.

Iron-titanium oxide minerals. Magnetite is the main iron-titanium oxide mineral present in the Purcell Lava. Primary ilmenite, though rare, is also present. Alteration products include hematite, leucoxene, anatase, ilmenite, and iron hydroxide(?).

Copper-iron sulfide minerals. Rarely, pyrite and chalcopyrite were observed, mainly within vesicle fillings but also as disseminated grains.

The following sections contain specific petrographic information about various facies and minerals of the Purcell Lava.

Pillow Lava

Most pillows typically consist of small phenocrysts of plagioclase suspended in a groundmass of acicular feldspar laths and clay minerals (fig. 63). Feeder tubes and exceptionally large pillows (as much as 2 m in diameter), are somewhat coarser grained. As might be expected, the grain size progressively diminishes towards the margins of the pillows. Pillow rims consist of a few quench crystals of plagioclase in a matrix of fine-grained microlites.

Hyaloclastite Breccia

The hyaloclastite breccia is composed of individual shards and subrounded globules of chloritized, devitrified sideromelane, in a fine-grained, chloritized, microlitic groundmass (fig. 64). Some of the fragments contain quench crystals of plagioclase. The prominent banding, some of which is visible megascopically, is probably a relict feature, the result of chemical zoning during premetamorphic palagonitization of the glass fragments (Moore, 1966).

The hyaloclastite tuff beds located in the Snowslip strata, beneath the pillowed facies at Kootenai Peak, consist of imbricated chloritized hyaloclastite intermixed with grains of silt and mud (fig. 65). The presence of sediment grains indicates reworking of the breccia fragments. However, the preservation of angular edges suggests that the fragments were not carried far from the source area. Possibly, these tuff beds are the airfall product of an explosive phase of Purcell volcanism, perhaps related to the event which produced the vent facies.

Flow Units

The flow units of the compound pahoehoe facies consist of altered plagioclase, pyroxene(?), iron-titanium oxides, and secondary mineral phases, e.g. chlorite, clays, and albite (see previous figs. 60 and 61). The grain size is distinctly larger than that of the pillow lava (including the larger pillows and tubes). Even thin (less than 1 m thick) flow units have grain sizes larger than the centers of most pillows; some of the flow units are thinner than the diameter of average-sized pillows, yet are much coarser grained. This grain-size difference is significant in interpretation of the environments of emplacement of the two facies. Had both the pahoehoe and pillowed facies cooled under similar conditions, the grain size distribution should be about the same. The pillows unquestionably represent extrusion of lava into water, thereby promoting rapid quenching and minimal crystallization. The larger-grained pahoehoe flow units are suggestive of slower cooling, as would be expected in a subaerial environment. For further discussion of these conclusions, see the "Oxide Mineralogy" section of this chapter, and the "Environment of Emplacement" section in Chapter 4.

Vent Facies

Surrounding the cognate and exotic blocks in the vent facies is a tuffaceous matrix of altered microlites and amygdules in an extremely fine-grained mesostasis. A few large quench crystals of plagioclase are scattered randomly, or in some cases, aligned parallel to the general fabric of the rock

(fig. 66). The pilotaxitic texture of the plagioclase microlites in some samples is indicative of flowage (fig. 67). The groundmass probably consisted originally of glass which later devitrified and subsequently was altered during diagenesis. Ubiquitous throughout the vent-rock matrix are web-like cracks filled with cryptocrystalline quartz. In general, the rock is quite vesicular. Vesicles range in shape from perfectly spherical to highly irregular and elongate (refer to fig. 67) and are typically small in size.

Diabase Sill

The largest grain size of all the facies of the Purcell Lava is associated with the hypabyssal diabase sill. Samples from the center of the sill contain large, twinned albitic plagioclase laths (fig. 68). Grain size diminishes towards both the upper and lower contacts. Diagenetic alteration has nearly obliterated all primary minerals (see fig. 68).

Amygdules

The Purcell Lava contains a variety of amygdule-forming minerals. Those identified include quartz, chlorite, calcite, barite, specularite, and potassium feldspar. Rarely, pyrite and chalcopyrite are present.

Oxide Mineralogy

The character of primary iron-titanium oxide minerals in a volcanic rock (e.g. size, shape, degree of development, and state of oxidation) is mainly dependent on the rock's cooling history. Lava flows emplaced into a subaqueous environment generally cool more rapidly than those emplaced subaerially. Consequently, the character of the oxide minerals formed in these two ways will be demonstrably different (see Bleil and Smith, 1980, for reference on the character of magnetite in pillows and massive units known to have been erupted subaqueously; see Larson and others, 1969, and Haggerty, 1976, for a discussion of high-temperature deuteric oxidation). The following preliminary information on opaque minerals in the Purcell Lava is presented in order to substantiate my interpretation of the environment of emplacement for the two main facies (subaqueous pillow lava versus subaerial pahoehoe).

General oxide mineralogy of the Purcell Lava. Magnetite is the prominent primary oxide mineral in both the pillow and pahoehoe facies. In the pillows, the size distribution is bimodal, with a few large and many small (microlitic) grains. A few primary ilmenite grains containing hematite lamellae were observed, as were pyrite and chalcopyrite.

High-temperature deuteric alteration, recognized by the presence of ilmenite lamellae within the magnetite grains, is common only in the pahoehoe flow units.

Low-temperature diagenetic alteration, probably associated with burial metamorphism, has affected the magnetite in both pillowed and massive facies; hematite, leucoxene, anatase, ilmenite, and iron hydroxide(?) are the prominent alteration products. The oxidation state of the opaque grains appears to be at or less than the C4 stage of the seven-stage scale of Haggerty (1976). The pillowed facies is generally more altered than the pahoehoe facies as circulating waters probably had easier access to the pillows along boundary contacts and through interpillow hyaloclastite breccia.

Pillow lava. Most primary magnetite grains in the pillows are small, homogeneous and skeletal-cruciform in shape (fig. 69) as a result of rapid, incomplete growth during quenching. This is the case for even the largest pillows (up to 2 m in diameter). Larger, euhedral to subhedral magnetite grains, exhibiting a secondary skeletal fortress type framework, also occur in

the pillowed facies (figs. 69b and 70). These larger grains probably underwent oxidational exsolution of ilmenite in the melt after their formation. During subsequent diagenesis, the less titanium-rich zones between the ilmenite lamellae dissolved, leaving behind the trellis pattern of Ti-rich lamellae (E. Larson, personal communication).

Flow units. As in the pillow lava, two distinct generations of magnetite grains exist in the pahoehoe flow units. However, there is not a bimodal size distribution as in the pillows.

Euhedral cross-arm type cruciform magnetite (fig. 71) are probably of the same generation as their counterparts in the pillow lava (i.e. grains that grew in the magma chamber and underwent [111] exsolution of ilmenite lamellae).

Primary magnetite grains that grew in the flows units after eruption are euhedral to subhedral and in general are not skeletal. Most grains exhibit what was originally abundant ilmenite lamellae (now hematite due to diagenetic alteration), exsolved along [111] planes during high-temperature, subsolidus deuteric oxidation (fig. 72). The mottled, moth-eaten appearance of the magnetite, and the extent of hematite replacement, are the result of low-temperature diagenesis.

In contrast to the pillow lava, primary magnetite from the pahoehoe flow units are generally much larger, more fully developed and contain evidence of deuteric oxidation. These characteristics are typical of lava flows which cool slowly (subaerially). Even the thinner flow units (those less than 1 meter thick) have large, lamellae-rich primary magnetite--an indication of slower cooling relative to the pillows.

Vent facies. Iron-titantium oxide minerals in the matrix of the vent breccia are typically small but numerous (fig. 73). Most grains are entirely altered to leucoxene and anatase. A red-staining (probably iron hydroxide and/or microcrystalline hematite) gives the rock its characteristic pinkish orange color.

Hypabyssal diabase sill. Magnetite grains in the central portion of the diabase sill are very large and lack ilmenite lamellae (fig. 74). The degree of deuteric oxidation may be related to how efficiently H_2, from dissociated water vapor, is expelled from a flow (Sato and Wright, 1966; Bleil and Smith, 1980). Lack of ilmenite lamellae in the diabase sill may therefore be related to the retention of H_2 in a closed system created by the act of intrusion.

Further detailed study of the opaque minerals (e.g. determination of the probable paragenesis) would contribute towards understanding the complex diagenetic history of the lava flows, as well as the Belt sedimentary rocks in which the Purcell is intercalated.

Geochemistry

Introduction

A geochemical study of the Purcell Lava was undertaken to determine: 1) the primary petrogenetic rock type, 2) the general geochemical effects of diagenetic alteration, and 3) whether the Purcell Lava is related geochemically and petrogenically to a large sill in the Helena Formation (commonly referred to as the Purcell Sill, but called the middle Belt carbonate sill in this report).

The only geochemical study of "Purcell igneous rocks" prior to this investigation is that of Hunt (1961, 1964). Hunt's evaluation was based on the premises that the lava flows and sills were cogenetic and coeval, and that, although the primary minerals had been greatly altered and replaced, the

major elements had been redistributed in a closed system. The present study is based on new chemical data, the recent development of methods to discriminate between tectonically defined magma types using abundances of "immobile" elements (Pearce and Cann, 1973; Floyd and Winchester, 1975), and on the possiblity that the lava flows and sills may neither be coeval nor cogenetic.

Thirty-two representative samples were analyzed for major and minor elements (table 2). Twenty-four samples are from the flows at Granite Park, Fifty Mountain, Red Horn Peak, and Hole-in-the-Wall. Four samples are from the large sill (Earhart and others, 1983) in the Helena Formation (middle Belt carbonate sill). Two samples are from a thick dike that cross-cuts the Purcell Lava and overlying Snowslip strata at Granite Park, that may be related to the middle Belt carbonate sill. Two samples from a 12-m-thick mafic lava flow located in the Mt. Shields Formation (Fenton and Fenton, 1937, p. 1904; Earhart and others, 1983) were also analyzed, for comparative purposes. The flow, referred to here as the Mt. Shields lava flow, is a single cooling unit located 210 m (J. W. Whipple, unpublished data) stratigraphically above the Purcell Lava at Hole-in-the-Wall.

All analyzed samples were prepared in the following manner. Cubes (greater than 18 cm^3) were cut from the interiors of most samples, by means of a diamond saw, to acquire a specimen free of the effects of surface weathering. In some cases, a diamond core drill was used to penetrate into the interior. Only the massive, nonvesicular portions of each sample were used for analysis; care was taken to avoid amygdules and fracture fillings, as well as obvious concentrations of sulfide minerals. Exterior surfaces of the freshly cut cubes and cores were then ground on a flat lap to remove any iron residue left from sawing and drilling.

Major oxides were analyzed by means of x-ray florescence (XRF) (USGS, Lakewood, Colorado). FeO, H_2O+, H_2O-, and CO_2 were also analyzed by the USGS according to standard procedures. Minor elements Be, Co, Cr, Pb, Sc, V, and Yb were analyzed by means of the semiquantitative 6-step spectrographic method (USGS); Ba, Cu, Nb, Ni, Rb, Sr, Y, Zn, and Zr were analyzed by XRF at the University of Colorado.

Table 3 contains previously reported analyses for the Purcell Lava in Canada (Hunt, 1964) and unpublished analyses of the middle Belt carbonate sill in Glacier National Park (Mejstrick, 1975). Table 4 contains chemical analyses, considered to be representative of selected igneous rock types, presented for comparison with analyses of the Purcell Lava.

Determination of Petrogenetic Rock Type

The Purcell Lava has been extensively altered as indicated by comparing its chemistry (table 2) with that of fresh basalts (table 4). The structure and morphology of the Purcell Lava facies are very similar to those of modern basalt flows, suggesting that the Purcell was originally basaltic. However, many major and minor elements are enriched or depleted in quantities far out of the range of typical basalts (table 4), indicating that an open geochemical system existed during alteration processes.

On the basis of ternary plots (AFM) and differentiation indexes, Hunt (1964) separated Purcell igneous rocks (lava flows and sills) into those of eastern and western petrologic provinces. However, many of the chemical elements discussed by Hunt were apparently mobilized and redistributed, in an open system, during alteration of the Purcell Lava. Thus his correlations and interpretations are tenuous.

Methods of classifying fresh, unaltered igneous rocks, (e.g. Irvine and Baragar, 1971; and Jenson, 1976) are not effective when applied to rocks like

the Purcell which have been extensively altered, and in which Fe, K, and Na apparently were geochemically mobile.

Several methods have been devised for determining the original geotectonic setting and petrogenic character of older basic volcanic rocks (Bloxam and Lewis, 1972; Pearce and Cann, 1973; Pearce and others, 1975; Floyd and Winchester, 1975; Pearce, 1975; Garcia, 1978; Hughes, 1982, Chapter 14; Mullen, 1983; Rogers and others, 1984). The methods are based on the comparison of abundances of those elements that are the most immobile during diagenesis and low-grade metamorphism with abundances in modern volcanic rocks in known tectonic settings (Pearce and Cann, 1973).

Elements considered to be the least mobile during low-grade alteration processes are Cr, Ni, Ti, P, Y, Zr, Nb, and Mn; Al and Mg are also somewhat immobile. With this in mind, selected chemical data for the Purcell Lava were plotted on a number of discrimination diagrams (figs. 75-82). These plots collectively illustrate that the data from the various units of the Purcell Lava generally cluster together, an indication that the elements plotted are behaving coherently and that the facies of the Purcell Lava represent a single petrogenic rock type.

All of the plots indicate that the Purcell Lava was originally an alkaline rock. This is further supported by comparison of abundances of several selected major oxides and trace elements in Cenozoic basalts (table 5) with those of the Purcell Lava (table 2). Clearly, the Purcell has concentrations of immobile elements (Ti, Cr, Ni, and Zr) characteristic of alkaline basalts. The thin sheet-like, ropy-topped morphology of the flow units is also consistent with an alkaline affinity (E. Larson, personal communication).

Alkaline lavas are associated with a wide variety of other igneous rock types, felsic to basic, on the continents as well as in the oceans (Carmichael and others, 1974). At best, the various discrimination diagrams only enable differentiation between alkaline, calc-alkaline, and tholeiitic rock types--a continental versus an oceanic setting cannot usually be determined. However, since the Belt Supergroup is underlain by 1700 m.y. crystalline basement rock (Harrison, 1972), a continental tectonic setting is indicated.

Alkaline magmas are thought to originate at depths of 40-100 km and are always associated with regional faulting (Carmichael and others, 1974). The presence of alkaline volcanic rocks within the upper Belt Supergroup suggests the possibility that deep-seated, regional faulting occurred during deposition of early Missoula Group sediments. Regional faulting at this time was also suggested by Whipple and others (1984) as a possible explanation for differences between stratigraphic sequences in Glacier National Park and adjacent areas.

Effects of Diagenetic Alteration on the Geochemistry

To determine the general effects of diagenesis on the Purcell Lava, the present chemical composition must be compared with that of unaltered analogous rocks (tables 2, 4, 5, and 6).

Binary variation diagrams were also plotted to illustrate the range in concentration (i.e. relative mobility) of selected oxides and trace elements. The large range in concentrations of Si, Fe, Ca, and K indicate that these elements have been very mobile, (figs. 83-86); the average concentrations of these elements are also inconsistent with those of average alkaline rocks (table 6).

Although present concentrations of Na_2O are similar to those of average alkaline rocks, plagioclase chemistry (table 1) and petrographic evidence

suggest that the plagioclase was albitized prior to alteration to chlorite; the present level of Na_2O may therefore be fortuitous. Concentrations of Na_2O are shown graphically in Figure 87.

Immobile elements. Ti, Al, Mg, P, and Mn have remained relatively immobile, as judged by the small range in values (figs. 88-92); the average concentrations are also consistent with those of unaltered alkaline basalts.

Trace elements that have been relatively immobile include Co, Cr, Nb, Ni, Y, Yb, and Zr (figs. 93-97). Cr, Nb, and Y were plotted against Ni to emphasize both the immobility of these elements, and the discordance in their abundances in the Purcell Lava and middle Belt carbonate sill and dike (figs. 94-96).

Mobile elements. Si and Ca appear to have been removed during alteration. SiO_2 in the Purcell Lava ranges from 36.9% to 48.7%, averaging 42.9% whereas typical alkaline basalts range from 45 to 47%. Some SiO_2 was utilized to generate the secondary chlorite minerals. However, chlorites are generally lower in SiO_2 than other primary silicate minerals (e.g. pyroxenes and feldspars; Deer, Howie, and Zussman, 1966). During chloritization silica was released, probably during burial metamorphism, and redistributed to vesicles, voids, and possibly into the surrounding sedimentary strata.

CaO in the Purcell Lava ranges from 1.1% to 5.5%, averaging 2.8% (fig. 85, and tables 2 and 6), values far below the range of alkaline basalts (as well as any other basalt!). Although some CaO was redistributed into secondary calcite in vesicles, other cavities, and to a lesser extent the groundmass of the Purcell Lava, much was lost.

The Purcell Lava is enriched with respect to total iron content (tables 4 and 6). Iron mobility is apparent from the wide range of FeO and Fe_2O_3 concentrations shown in Figure 84. Iron was probably introduced into the Purcell Lava (from the surrounding sedimentary strata) during chloritization of primary pyroxenes and feldspars. Chlorites generally contain more iron than do pyroxene and feldspar (Deer, Howie, and Zussman, 1966). Further evidence of the mobility of iron is the presence of orange colored, hematite-stained calcite amygdules.

Also present in above average concentrations is K_2O. Values range from 1.1 to 5.5% for most of the Purcell Lava. Average values are 3.0% and are high even for an alkaline basalt. Two samples of the vent unit matrix have extremely high K_2O contents (10.5 and 10.2%) that may be related to local hydrothermal alteration. Interpillow hyaloclastite breccia (analyses 7 and 8, table 2) have extremely low K_2O contents, possibly resulting from greater penetration of migrating fluids in the breccia. Slabs of the Purcell Lava stained with sodium cobaltinitrite are pervasively yellow, indicating the presence of fine-grained potassium phases.

Also of interest is the K_2O content of the two samples from the Mt. Shields lava flow (analyses 31 and 32, table 2). The concentrations are 7.6% and 5.2%--exceedingly high for any basalt. The Mt. Shields lava flow appears to be of a similar petrogenic origin as the Purcell Lava since its immobile elements generally plot within or near the cluster of Purcell data points. More chemical analyses are needed to interpret the discrepancy.

In light of the wide range and high concentration of K_2O in samples of the Purcell Lava and other igneous rocks in Glacier National Park, caution should be exercised in the application of age-dating techniques in which potassium mineral phases are important.

Trace elements in the Purcell Lava appearing to have been mobile during alteration processes include Ba, Cu, Rb, and Sr (figs. 98-100). Many of the lava flow samples are highly enriched in Ba (tables 2 and 6); exceptions are

the samples of interpillow hyaloclastite breccia (analyses 7 and 8, table 2). Although not as common as calcite and quartz, barite fills a few of the large vugs in the Purcell Lava--another indication of the mobility of Ba. The middle Belt carbonate sill and dike contain lower concentrations of Ba than does the Purcell Lava.

Concentrations of Cu range from below detection levels to 185 ppm (table 2). The higher concentrations probably reflect local copper sulfide mineralization associated with diagenesis.

Rb typically occupies the position of potassium within a crystal lattice, and Sr substitutes for calcium. Therefore, it is not surprising that the mobility of Rb and Sr is closely related to the relative concentrations of K_2O and CaO, respectively. Rb increases directly with K_2O (fig. 98), as does Sr with CaO (fig. 99). Like K_2O, Rb is present in the Purcell Lava in somewhat higher concentrations than it is in the average alkaline basalt (table 6). Concentrations of Sr are low compared with those in alkaline basalts in accordance with the depletion of CaO (table 6).

In light of the mobility of Rb and Sr, any application of Rb-Sr age-dating techniques to the Purcell Lava must be made with caution.

Geochemical Relation of Purcell Lava to the Middle Belt Carbonate Sill and Dike

A large mafic sill (middle Belt carbonate sill) occurs mainly in the Helena Formation and is present throughout Glacier National Park. It ranges in thickness from 9 to 32 m (Mejstrick, 1975) and has been inferred to be coeval with the Purcell Lava (Hunt, 1962). The sill is approximately 29 to 30 m thick near Granite Park (inferred from Mejstrick's data).

At Granite Park, a large dike (27 m thick) cross-cuts the Purcell Lava and overlying Snowslip strata. The sill and dike are both exposed on the steep east side of the Garden Wall below Grinnell Glacier Overlook (see McGimsey, 1984, for location of dike). Unfortunately, the physical relationship between dike and sill is obscured by a perennial snowfield. The dike is not present in Helena strata below the snowfield, nor beyond it, near the Grinnell Glacier.

The possibility exists that the sill and dike are physically connected, a possibility that would demonstrate that the sill is not coeval with the Purcell Lava. Although direct field evidence of a mutual relationship between sill and dike has not been documented, geochemical evidence (this study) supports the theory that the sill is not related geochemically to the Purcell Lava.

In general, the middle Belt carbonate sill and dike have similar geochemical trends that are uniquely different from those of the Purcell Lava (figs. 76, 78-81, and 91 through 100, excluding 97). For example, in Figure 76, Ti, Zr, and Cr are present in the Purcell Lava in similar proportions but occur in different concentrations in the sill and dike. The sill and dike both have similar concentrations of elements considered to be relatively immobile during diagenesis.

Summarizing the diagrams referred to above, the dike and sill have similar concentrations of CaO, Sr, Cr, and Ni that are significantly higher than those in the Purcell Lava. Rb and V concentrations are also somewhat higher on the average. The sill and dike are mutually lower in Ba, Y, Al_2O_3 and P_2O_5 than the lava flows.

Differences in the concentrations of immobile elements, such as Cr, Ni, V, Y, Al, and P, are difficult to explain in terms of variation in diagenesis. Of particular interest is Cr and Ni (fig. 94). Average

concentration of Cr and Ni in the Purcell Lava is significantly lower than that in the sill and dike (table 7). The discrepancy is probably not related to assimilation of country rock by the sill and dike during intrusion since the range of Cr and Ni concentrations in the sill and dike is small; i.e. contamination by assimilation of country rock would not likely be homogeneous. The difference in stable element abundances can be explained easily if the Purcell Lava is not cogenetic with the sill and dike.

Cr and Ni are compatible elements; during melting they are preferentially retained in the residual solid phases (Cox, Bell, and Pankhurst, 1979). Concentrations of compatible elements in a particular parent melt change over time as both melting and crystallization processes progressively enrich or deplete compatible elements in the melt. Since the dike was intruded subsequent to emplacement of the Purcell Lava, and because the dike and sill are geochemically similar, it is likely that the middle Belt carbonate sill, also, is younger than the Purcell Lava.

More chemical data are needed to better define the geochemistry of the igneous rocks in Glacier National Park, as well as those in other areas of Belt terrane. Specifically, rare earth element (REE) geochemistry could prove useful since these elements are rather immobile during low grade metamorphism and are commonly diagnostic of source area chemistry and degrees of melting. Similarly, Nd and Sm isotopic data could prove useful.

CHAPTER IV

DISTRIBUTION, CORRELATION, AND INTERPRETATION OF FACIES

The Purcell Lava generally is discontinuously exposed near the crests of the Lewis and Livingston Ranges, from the International Border south to Granite Park (McGimsey, 1984). The eastern limit of the flows is unknown because of structural displacement of the basin, and deep erosion east of the Lewis Range and along the leading edge of the Lewis Thrust Fault. The only exposures of the Purcell Lava in Glacier Park, west of the Livingston Range, are located on the flanks of Huckleberry Mountain (Apgar Mountains) where the flows thin southward and finally disappear altogether. At Logan Pass, 11 km south of Granite Park, the lava flows are absent from the stratigraphic sequence, apparently having pinched out somewhere in between. The Flathead fault and minor thrust faults structurally separate these exposures from those in the central part of the Park. However, assuming little or no strike slip component on the Flathead fault (R. Earhart, personal communication), a line, projected through the Huckleberry Mountain exposures from the point where the Purcell Lava pinches out to the west in the southern Whitefish Range, passes through the area between Granite Park and Logan Pass; this probably is a good approximation of the former southern limit of Purcell Lava in Glacier Park (fig. 101).

The thickness of the Purcell Lava in the Park ranges from 0 to 77 m. Figure 102 graphically depicts measured sections and shows the thickness of individual facies at each locality; a complete list of all measured sections appears in Table 8 in Appendix B. The total measured thicknesses of the Purcell Lava shown in Figure 102 agree relatively well with those of previous workers (e.g. Fenton and Fenton, 1937), although an important difference exists. Prior to this study, the diabase sill was considered to be an extrusive flow, separated from overlying pillow lava by intercalated sedimentary strata. In this report the diabase sill is included as a facies of the Purcell Lava, and only the extrusive units (e.g. pillow lava, vent rocks, and pahoehoe flow units) are used in the interpretation of thickness variations and geometry. With this in mind, some new and useful information can be extracted from the sections in Figure 102.

Based on the total thickness of all Purcell Lava units, it is evident that the thickness increases from the southeast towards the northwest. If only the extrusive units are considered, a somewhat different thickness trend is apparent. Figure 103 is a fence diagram which shows that Purcell Lava is thickest (65 m) at Kootenai Peak (3) and thins to the southeast (19 m at Granite Park), and northeast (30 m at Mt. Cleveland), and less conspicuously to the northwest (54 m at Hole-in-the-Wall). The subtle northwestward thinning of the Purcell Lava between Kootenai Peak (3) and Hole-in-the-Wall (1), however, does not continue far into Canada. At Sunkist Mountain (about 11 km northwest of Hole-in-the-Wall; Price, 1962), the thickness of the succession increases to 148 m.

Most of the thickness variation of the Purcell Lava is associated with the pahoehoe facies, which increases northwestward from 9 m at Granite Park to 42 m at Hole-in-the-Wall. West, at Huckleberry Mt., the pahoehoe facies thins southward from a maximum thickness of 27 m and eventually pinches out. In contrast to the more variable thickness of the pahoehoe facies, the thickness of pillow lava remains relatively uniform throughout the Park. Sections in the central portion of the Park (except those at Huckleberry Mountain) have pillowed facies thicknesses that range from 9 to 12 m. Pillow lava in the

Huckleberry Mountain sections ranges in thickness from 13 to 15 m. Based on the relatively uniform thickness of the pillowed facies, and evidence for subaerial emplacement of the pahoehoe facies, I interpret the upper limit of pillow lava to mark a paleo-water level; the thickness of pillow lava thereby indicates the former water depth (9-15 m) in this part of the Belt basin at the time of Purcell Lava extrusion. Slight irregularities in the floor of the basin would have produced local variations in water depth, and hence, in the thickness of pillow lava. Similar transitions (pillow lava to massive pahoehoe) have been interpreted as paleo-water levels (Fuller, 1931; Jones and Nelson, 1970). Accordingly, the increase in thickness of pillow lava to the northwest and southwest would indicate that water depth increased in those directions (i.e. the seafloor sloped downward gradually to the northwest and southwest).

The original geometry of the Purcell Lava and its vent system is not easily reconstructed because of extensive erosion, structural complexities, and lack of detailed information on the Purcell west and north of the Park. Moreover, most tectonic structures in this region, which trend northwest-southeast (Harrison, 1972, fig. 1), played a large role in the geomorphological development of landforms (e.g. general orientation of major river valleys, mountain ranges, and glaciers). Because the Purcell Lava is preferentially preserved along this trend, any analysis and correlation of thickness and distribution used to reconstruct paleogeometry contains a bias towards the trend. With these limitations in mind, some general characteristics of the geometry and vent system of the Purcell Lava can nevertheless be inferred from exposures in Glacier Park.

As previously shown, Purcell Lava increases in thickness to the northwest and southwest. Contours on the isolith map (fig. 104) appear to define a lobate, plateau-like body of flows (long axis oriented northwest-southeast and parallel to the trend of vent-rock distribution) that is probably the southeastern margin of Purcell Lava. The slope of the plateau is extremely low: 0.07^{o} from Granite Park to Hole-in-the-Wall, 0.15^{o} from Granite Park to Kootenai Peak, and 0.25^{o} from Mt. Cleveland to Kootenai Peak.

Vent Facies

Vent facies rocks occur at three localities of the Purcell Lava (Hole-in-the-Wall--Boulder Peak, Thunderbird Mountain, and Redhorn Peak), and appear to lie along a narrow linear north-northwest trend (fig. 105). Although exposures of Purcell Lava on the west flank of the Guardhouse (between Hole-in-the-Wall and Redhorn Peak) were not examined, the trend of vent rocks distribution suggests that the vent facies should occur there.

The restricted distribution of vent rocks is evident from the fact that none occur at the Kootenai Peak section which is located only 3 km east of the Redhorn Peak section. West of the trend along which vent rocks occur, there exists in Glacier Park only one outcrop of Purcell Lava, located 5 km west of Boulder Peak near the summit of Kinnerly Peak (Richard Mattson, Park Ranger, personal communication, 1983). The existence of Purcell Lava on Kinnerly Peak is supported by visual projection of the unit from Boulder Pass, by means of an Abney level. However, because of difficult access and the small size of the exposure, this locality was not visited. Nonetheless, the vent unit is only several meters thick in exposures located only several kilometers west of Hole-in-the-Wall (e.g. in the valley immediately north of Boulder Peak, and along the southwest flank of Boulder Peak). The relatively restricted occurrence of vent rocks along the main trend and the apparent westward

thinning of the unit suggests that exposures of Purcell Lava on Kinnerly Peak probably do not contain vent rocks.

The linear distribution trend of vent rocks suggests that the Purcell Lava issued from a fissure(s). The orientation of pillow axes and terminal ends at Hole-in-the-Wall and Boulder Peak (east and west flanks, respectively, of the vent facies) support this theory; they are generally perpendicular to the trend and the terminal ends are distal. Further evidence is found on isolith maps of the Purcell Lava in Glacier Park and Canada that define linear thickness trends which are parallel to the distribution of vent rocks in Glacier Park (figs. 106 and 107), suggesting that the source of lava was a fissure(s).

Several lines of evidence support the hypothesis of multiple fissure vents. First, pillow axes at Fifty Mountain and Granite Park (fig. 2) are generally oriented in the same direction as those at Hole-in-the-Wall, however, the terminal ends indicate that the pillows were emplaced generally from the northeast, towards the vent facies. Therefore, a lava source may have existed east of the Fifty Mountain section. Second, although no feeder dikes were located directly associated with the vent facies, the Glacier Park geologic map of Ross (1959) contains a number of dikes, which could have served as feeders, that are oriented nearly parallel to the distribution trend of vent rocks. At least one large dike located at Grinnell Glacier overlook, near Granite Park, discordantly intrudes the Purcell Lava and overlying Snowslip strata, and therefore postdates lava flow eruption. Finally, based on the inclination of pipe vesicles, overlapping flow units were locally emplaced from opposite directions (fig. 40) suggesting multiple sources.

Based on geologic evidence, explosions from subaqueous basaltic volcanoes can occur when water depth is less than about 100 m (Fisher and Schmincke, 1984, p. 274). It is evident from the thickness of pillow lava, and tidal flat sedimentary structures in the Snowslip rocks underlying the lava flows (see appendix A), that the Purcell Lava was emplaced into a shallow-water environment. The size and lack of sorting of the cognate and exotic blocks contained in the vent facies strongly suggests that a violent eruption, possibly a phreatic or phreatomagmatic explosion, was responsible for creating the deposit. The absence of similar rocks elsewhere in the Park could be the result of erosion. Alternatively, historic fissure eruptions are known to vary in the type of eruptive activity (Williams and McBirney, 1979). Therefore, rocks of the vent facies could have resulted from an isolated violent eruption(s) or explosion(s) along a segment of one fissure, while simultaneously, quiet, nonviolent emission of lava was occurring elsewhere. The unit could also possibly be related to the diabase sill, a point discussed in the next section.

Detailed descriptive studies on the Purcell Lava in Canada (where it is thickest and most extensive) or west of the Park are presently lacking. The real significance of the vent unit awaits further study in these areas. Nonetheless, based on data from in Glacier Park, I hypothesize that the Purcell Lava was erupted from multiple, parallel to sub-parallel, fissure-type vents oriented approximately in a northwest-southeast direction. Point sources that issued greater volumes of lava along a fissure may account for the anomalously thicker succession at Kootenai Peak. Additionally, I conclude that rocks of the vent facies represent the products of explosive activity along one or more fissures or segments of fissures.

Diabase Sill

The diabase sill occurs in the northernmost exposures of Purcell Lava in Glacier National Park (Hole-in-the-Wall, the southwest flank of Boulder Peak,

Thunderbird Mountain, and the northern end of Mt. Cleveland). It may be present at the knob below Red Horn Peak where a poorly exposed massive igneous unit underlies the vent facies.

The sill is generally located about 5 m below the pillow lava section. Locally, it intrudes through the overlying sedimentary interval and into the basal pillows. At one locality, Hole-in-the-Wall, the sill lies intrusively between the pillow lava and Snowslip strata (see fig. 56).

Two lines of evidence tend to indicate that the sill is genetically related to the extrusive units of the Purcell Lava. First, the sill is chemically and mineralogically nearly identical to the pillow and pahoehoe facies (see chapter 3). Had the sill been emplaced at a time subsequent to Purcell Lava eruption, it is unlikely that the chemical composition (specifically, immobile trace elements--see chapter 3) would be so similar. Second, the sill must have been emplaced before lithification of the surrounding sediments because of the near lack of brittle deformation, and the profusion of plastic, soft-sediment deformation along the margins of apophyses.

It is worth noting that the diabase sill is chemically dissimilar from a lava flow (known informally as the Mt. Shields basalt) located 210 m stratigraphically above the Purcell Lava, at Hole-in-the-Wall (J. Whipple, unpublished data). A thick gabbroic sill (middle Belt carbonate sill), located about 600 m (J. Whipple, unpublished data) stratigraphically below the Purcell Lava, in the Helena Formation, also is geochemically distinct from the diabase sill. This suggests that the diabase sill is not related to either of the other igneous bodies.

Field relationships indicate that the diabase sill was emplaced subsequent to the pillowed facies (or at least the lower part of it--see fig. 54); however, there is no evidence from which to determine exactly when, during lava eruption, the sill was emplaced. Possibly it was emplaced during the waning stage when most of the extrusive flow units (collectively up to 54 m thick) had been erupted, providing overburden to contain the intrusion. The answer to the question of whether a sill could be injected and contained at a shallow depth without much overburden is beyond the scope of this study.

Alternatively, the intrusive facies may be an invasive flow, that is, one which initially flowed over soft sediments and then was hydrostatically driven downward to invade the sediments as a sill-like, intrusive body (Beeson and others, 1979; Byerly and Swanson, 1978; and Schmincke, 1964). The shallow depth of intrusion and local emplacement between the pillow lava and Snowslip (figs. 56a and 56b) seem to support such a hypothesis.

Regardless of the mode of emplacement, the sill was probably injected into a shallow, wet environment. It is possible, therefore, that a phreatic or phreatomagmatic explosion related to emplacement of the sill could have created the vent facies; it is perhaps significant that the two facis are geographically distributed over much of the same area.

Broken-Pillow Breccia and Isolated-Pillow Breccia

The localized occurrence of broken-pillow breccia in the Purcell Lava seems to indicate that it resulted from either postemplacement mechanical fracturing, or, isolated incidents of thermal-shock granulation. If the deposit was the product of a hydroexplosion of some type (Fisher and Schmincke, 1984, p. 231), it should probably be more extensive and better sorted and bedded than it is.

The origin of the isolated-pillow breccia is not as straightforward. The subfacies is not as thick or extensive as similar deposits described by

Carlisle (1963), Silvestri (1963), Tazieff (1972), and Dimroth and others (1978). However, it is similar to these deposits in that it occurs near the top of a pillowed section.

Several theories have been formulated to explain the origin of isolated-pillow breccia. Carlisle (1963, p. 69) suggests that the upward increase in hyaloclastite breccia is the result of vigorous globulation associated with an increase in the violent outpouring of lava as an eruption progresses. Tazieff (1972) postulates that hydroexplosions, resulting from the lowering of hydrostatic pressure as a volcanic pile is built upward towards the water surface, produces great quantities of hyaloclastite breccia. Dimroth and others (1978) suggest that isolated- and broken-pillow breccias are created during the waning stage of an eruption when the volume of lava decreases, thereby leading to the formation of smaller-sized pillows that would be more susceptible to thermal strain, and consequently, brecciation. Silvestri (1963) hypothesizes that large quantities of hyaloclastite breccia can form at the onset of submarine eruptions and that succeeding magma is partially intruded, as a sill, between the sea floor and the breccia layer, which acts as an insulative blanket.

The isolated-pillow breccia of the Purcell Lava is similar to deposits described by the aforementioned workers only in that it consists of a high ratio of hyaloclastite breccia to pillows, contains pillows that are few in number and irregular in shape, and occurs near the top of the pillowed facies. Any hypothesis concerning the formation of the Purcell Lava isolated-pillow breccia must account for (1) its thinness and localized extent near the top of the pillows, (2) the irregular shapes of the pillows, and (3) the relatively high proportion of hyaloclastite breccia.

The isolated-pillow breccia is very similar in appearance to the interbedded pillow interval located within a pahoehoe flow unit at Hole-in-the-Wall (i.e. a high ratio of hyaloclastite breccia to pillows and the presence of small, irregularly shaped pillows). I concluded that the interbedded pillow interval probably formed when lava poured into a small, shallow body of ponded water. I envision a similar origin for the isolated-pillow breccia. As the volcanic plateau gradually built upward, it eventually crossed the water-air interface, leading to partial isolation of shallow water ponds on top of the pillowed facies, in depressions between subaerial pahoehoe flow units. As new lava flowed into these ponds, it would trap water under the flows units. Quick conversion from the liquid to steam phase would result in intimate and turbulent interaction. Lava would be shattered and granulated to form the hyaloclastite debris. A few small, scattered pillows would have formed as the activity abated (i.e. when most of the water had been driven off). Quasi-pillows or coalesced pillows (see fig. 23) would have developed between the isolated-pillow breccia and massive pahoehoe flow units, marking the transition from a subaqueous to subaerial environment. The weight of overlying lava probably would result in shifting and settling of the hot mass of breccia and pillows causing the isolated pillows to plastically deform into irregular shapes (see fig. 21).

Pahoehoe Flow Units

Generally, as the thickness of the entire Purcell Lava succession increases (to the northwest and southwest), the number and thickness of individual flow units also increases; there are 5 to 7 flow units at Granite Park, 23 at Kootenai Peak, and 11 to 12 at the Apgar Mountains (see fig. 102). Single flow units could not be traced laterally from site to site, indicating that individual flow units are limited in aerial extent. This

characteristic is also evident from comparison of closely spaced measured sections from the same location. For example, the section of Purcell Lava at the head of Hole-in-the-Wall cirque contains fewer, thicker flow units than that located along the western wall, 1 km south. As is the case with many exposures of Purcell Lava in Glacier Park, a thick lichen cover prevents determination of the exact field relationship between the two sections.

Walker (1972; 1973) theorizes that high rates of effusion tend to form far-reaching, single-unit flows, and low rates are more likely to form localized, compound flows consisting of multiple flow units. If that is true, it would suggest that eruptive rates of the Purcell were relatively low. Thinness and localized extent of the flow units, and the abundance of well-developed ropy flow structures suggests that the lava was very fluid and was extruded in relatively small volumes. The lack of lava tubes and channels suggests that the lava was surface-fed, probably spilling out of fissures in pulses and flowing in sheets, guided by the gentle topography of previously emplaced flow units.

The fact that none of the pahoehoe flow units grade laterally into aa is consistent with the lack of channelized transport of lava away from the vent. Surface channels or tube-fed flows (e.g. those described by Macdonald, 1953, and Swanson, 1973) cool during transport and usually attain a critical degree of crystallinity while still in motion, thereby changing from pahoehoe to aa (Swanson, 1973). Sheet flows like those of the Purcell Lava, flowing over gentle topography, probably came to rest before the lava cooled sufficiently to develop the crystallinity necessary for conversion to aa.

The time interval between emplacement of successive flow units was long enough for the earlier flow units to cool sufficiently and to attain enough rigidity to maintain their form (i.e. there is no visible deformation due to loading from overlying flow units). Also, the presence of contraction cracks, many that penetrate deep into the flow units, indicates significant cooling occurred before successive flow units covered and filled the cracks. Yet, the interval was short enough so that no weathering, surface erosion, or deposition of sediment occurred.

There is no evidence to indicate that Purcell volcanism, in the area of Glacier National Park, represents more than one eruptive episode or cycle; there are no intercalated sediments, erosional unconformities, or interflow weathered horizons. However, sequences of intercalated sediments within the Purcell in Canada (McMechan and others, 1980) are indicative of multiple eruptive events separated by significant hiatuses. Therefore, the Purcell Lava in Glacier Park probably represents only one of several events. The apparent subaerially weathered zone at the top of the uppermost flow units most likely represents a significant hiatus between the eruption of Purcell Lava and deposition of overlying Snowslip sediments.

The pillowed and pahoehoe facies of the Purcell Lava are very similar in structure and morphology to modern basalts emplaced under broadly similar conditions; compare the photographs and descriptions in this report with those in Fuller (1931), Macdonald (1953), Green and Short (1971), and Swanson (1973). Using a uniformitarian approach, the volcanic processes that produced the Purcell Lava during the Middle Proterozoic were probably very similar to processes active today. Likewise, the character of the ancient lava (i.e. temperature, composition, volatile content, viscosity, etc.) is inferred to have been similar to its modern counterparts.

The environment in which basaltic volcanism occurs can play an important role in determining the style of eruption. The style of eruption in turn controls the morphology of the products. For example, extrusion of basalt at

great depth on the ocean floor would probably produce pillow basalt and thin sheet flows, whereas eruption of the same basalt in a shallow-water or glacial environment might be explosive, producing large quantities of hyaloclastite breccia. It follows that stratigraphic and morphological differences between ancient and modern flows (Wells and others, 1979) probably are a reflection of differences in environmental conditions in which volcanism occurred, and not necessarily the nature of the volcanic processes and products.

Environment of Emplacement

Prior to this study, the Purcell Lava in Glacier National Park was generally thought to have been extruded entirely within a subaqueous environment (Burling, 1916; Fenton and Fenton, 1937). This interpretation was based on the presence of pillow lava, steam tubes, what were thought to be primary sediment inclusions, banded amygdule fillings mistaken for sediment, olive-colored flowtops mistaken for intercalated sediment, and the fact that the lava flows occur within a thick succession of miogeosynclinal sedimentary strata.

The pillowed facies was undoubtedly extruded subaqueously. However, evidence from this study strongly suggests that the upper facies (the pahoehoe flow unit sequence) was emplaced subaerially. This evidence is:

(1) Pillow lava beneath the pahoehoe facies is of uniform thickness and grades abruptly upward into massive, unpillowed pahoehoe. There is no interlayering of pillowed and massive facies such as that shown to occur in basalt successions known to have been erupted subaqueously (Donnelly and others, 1980, p. 9; Flower and others, 1980, p. 950; Robinson and others, 1980; Baragar, 1984, p. 784). Nor are there any lateral transitions from pahoehoe to pillows as is the case with subaqueous sheet flows (Ballard and others, 1979). The underlying pillowed facies does have transitions from massive, unpillowed zones to pillowed zones. Had the pahoehoe flow units been emplaced under water, pillows would probably have formed at the distal margins as the flows slowed and cooled sufficiently to allow globulation. More information on subaqueous sheetflows is available in Lonsdale (1977), Lonsdale and Batiza (1980), and Hekinian (1984).

(2) Except for a few thin, isolated patches of volcaniclastic material, there are no intercalated sediments between flow units; also, no sediment fills the cooling cracks and surface irregularities of flow units (except in the case of the uppermost flow units that were eventually covered by Snowslip sediments as the basin filled). What was previously thought to be primary intercalated sediment and considered proof of the subaqueous nature of the flows has proven to be pale-green flow-tops (1-2 cm thick), coalesced vesicles with banded amygdules, and structurally juxtaposed blocks of sedimentary strata.

(3) The highest flow units in the succession have a 1- to 5-cm-thick oxidized zone at their top surface (see Figure 32), indicative of prolonged subaerial exposure (K. Pierce, personal communication).

(4) Vesicles in the pahoehoe flow units are large and commonly so numerous that they are coalesced into trains and layers; in contrast, vesicles in the pillow lava are fewer and much smaller. Rapid quenching inhibits vesiculation by increasing the viscosity and solubility of the lava, thus preventing volatiles from fully exsolving (Fisher and Schmincke, 1984, p. 77).

(5) Grain size of the pillow lava is much smaller than that in the overlying flow units; some flow units, only .3 to .5 m thick, have a much larger grain size than even the largest pillows (diameters as much as 2 m). This suggests that the flow units cooled more slowly than the pillow lava, as would be the case in subaerial exposure.

(6) Magnetite grains in the pillow lava exhibit no trace of ilmenite lamellae, whereas magnetite in the pahoehoe flow units contain abundant ilmenite lamellae. Magnetite in subaerial pahoehoe commonly contains ilmenite lamellae, an indication of relatively slow cooling (E. Larson, personal communication). Had the Purcell Lava flow units been emplaced subaqueously, formation of ilmenite lamellae would probably not have occurred (see Bleil and Smith, 1980).

(7) Finally, water depth in the basin (in the area now Glacier Park) was probably very shallow as indicated by sedimentary structures (e.g. mudcracks, mudchip breccia, oscillation ripples, cross-bedding, see appendix A), and the presence of stromatolites in rocks of the Snowslip Formation directly underlying the basal lava flow. The Purcell Lava (extrusive units only) is up to 65 m thick in Glacier Park. It seems unlikely that sedimentary structures typically formed in a shallow, often high-energy environment, would be developed in water deep enough to contain the entire thickness of Purcell Lava.

A one-meter-thick, thinly laminated, argillite of the Snowslip Formation directly overlies the uppermost flow units of the Purcell Lava in several localities. Argillite is generally indicative of a quiet water depositional environment in which clay-sized sediment was deposited from suspension in thin layers. If the pahoehoe flow units were emplaced subaerially (which the preceding evidence demonstrates), then where is the evidence for the marine transgression (e.g. tidal flat or high energy beach-type facies), which eventually covered the lava flows? It is perfectly conceivable if not probable that areas of quiet water, essentially cut-off from pre-eruption sediment sources could have been created by emplacement of the lava flows. Also, the slope of the basaltic plateau is so low that a definable shoreline would be hard to identify; slight inundation would submerge large areas of basalt, which due to the low slope would have protection from high-energy wave and current action.

The true relationship between the sediments and the underlying lava flows may be ascertained only by systematic study of the sedimentary and volcanic units in areas outside of Glacier Park.

Age of the Purcell Lava and its Relationship to Intrusives

Hunt (1962) dated the hornfelsed strata beneath the Purcell Lava at 1075 m.y. by the K-Ar method using biotite. He also dated the large gabbroic sill in the Helena Formation (middle Belt carbonate sill) at 1110 m.y. by the same method using amphibole. Similarity of the dates, along with the general similarity in major oxide chemistry and mineralogy, and the paucity of dikes and sills in the strata overlying the Purcell Lava, have led to the inference that the Purcell Lava and the sill are coeval and cogenetic (Ross, 1959, p. 57). However, similarity of the ages of the two may be fortuitous since the validity of using the K-Ar method for altered, thermally overprinted rocks is questionable (Kulp, 1963).

Recently, granophyric bodies within the gabbroic sill (sampled during this study) have been dated by the Rb/Sr isochron method at 605 to 717 m.y., which is interpreted to be the age of a thermal event (Z. Peterman, unpublished data).

The degree of diagenetic alteration nearly precludes dating the Purcell Lava directly using current methods, except possibly by the Sm-Nd method which has not yet been attempted. No unaltered, differentiated samples of the Purcell Lava were discovered in Glacier National Park. Nonetheless, during the course of this study, several interesting points surfaced that may provide some insight into the relative age of the Purcell Lava.

A large dike (27 m thick), in Granite Park and crossing the Garden Wall at Grinnell Glacier overlook (see McGimsey, 1984, for location), was discovered to have cut through the Purcell Lava and overlying Snowslip strata. The dike, which can be traced from the overlook westward across Granite Park and through the southern tip of Flattop Mountain, obviously postdates the Purcell Lava.

Several unsuccessful attempts were made late in two field seasons to see the contact between sill and dike but the relationship is obstructed by a perennial snowfield below Grinnell Glacier Overlook. Nonetheless, the dike is not present in the rocks exposed beneath the sill, in front of Grinnell Glacier, nor on line at Allen Mountain further to the east. Chemically, the sill and dike are very similar to each other; yet, they are different from the Purcell Lava, especially in the content of certain trace elements (see chapter 3). Although the evidence is circumstantial, it appears reasonable that the sill and dike are genetically related. Additionally, because of the cross-cutting field relationship between the dike and the Purcell Lava, I conclude that the middle Belt carbonate sill and Purcell Lava are not coeval. The dike and sill would then represent a younger igneous event. Possibly, therefore, the 605 to 717 m.y. age of the sill does not represent a thermal overprint but rather the time of intrusion of the sill and dike. This age is close to the 750 ± 25 my age determined for similar sills in Belt rocks to the south of Glacier Park (Mudge and others, 1968).

Clearly, in order to better define the geochronology of the Belt Supergroup established by Obradovich and Peterman (1968), further isotopic studies must be conducted on the igneous rocks. The Sm-Nd system remains a possible alternative to classic methods which have produced tenuous results thus far.

CHAPTER V

CONCLUSIONS

The Purcell Lava in Glacier National Park is divisible into four informal facies. Lowermost is a 9- to 15-m-thick, subaqueously emplaced, pillow lava facies that consists of variably sized (20 cm to 2 m in diameter), interconnected pillows and associated hyaloclastite breccia. Two subfacies--isolated- and broken-pillow breccia--are also distinguishable. The transition from the pillowed facies to the overlying pahoehoe facies defines a former water level; therefore the thickness of the pillow lava facies represents the water depth (9-15 m) in this part of the Belt basin at the time of lava extrusion.

Overlying the pillowed facies is a subaerially emplaced pahoehoe flow sequence consisting of multiple flow units (10 cm to 6 m thick) that extend laterally for as much as several hundred meters. The unit ranges in thickness from 0-54 m; the number and thickness of individual flow units generally increases from southeast to northwest. The flow units are morphologically and structurally very similar to modern pahoehoe flows.

Locally, a vent facies occurs within the upper part of the pillowed facies in the northernmost part of the Park. The facies, a chaotic breccia of variably sized cognate fragments and accidental blocks of Snowslip strata set in a fine-grained tuffaceous matrix, is probably the product of a phreatic or phreatomagmatic explosion. Erosionally discontinuous exposures extend from Hole-in-the-Wall south to at least Red Horn Peak; transverse cross sections are lens shaped and approximately 3-4 km wide. Based on the geographic distribution of the vent facies, orientation of pillow axes, and emplacement directions of pahoehoe flow units, the vent system for the Purcell was probably northwest-oriented fissures.

A hypabyssal diabase sill is spatially correlative with the vent facies near the northern Park boundary and is located generally 5 m below the pillow lava facies. The sill, which is as much as 21 m thick and complexly intrudes the surrounding Snowslip sedimentary strata and the lowermost part of the pillowed facies, is mineralogically and geochemically identical to the other facies of the Purcell Lava. Intrusion was subsequent to eruption of the lowermost part of the pillow lava facies.

The Purcell Lava has been extensively altered mineralogically and geochemically as a result of low-temperature diagenesis related to burial. The original mineralogy consisted primarily of calcic plagioclase, pyroxene, and Fe-Ti oxides. Alteration of these primary minerals has resulted in chlorite, and other clay minerals, leucoxene and anatase. Major oxides determined to have been particularly mobile include SiO_2, Fe_2O_3, FeO, CaO, Na_2O, K_2O and H_2O; SiO_2, CaO, and Na_2O were apparently removed from the system, and Fe_2O, FeO, K_2O and H_2O were enriched. Mobile trace elements include Ba, Cu, Rb, which are enriched in the Purcell, and Sr, which was depleted. TiO_2, Al_2O_3, MgO, P_2O_5, MnO, Co, Cr, Nb, Ni, Y, Yb, and Zr were relatively immobile during diagenesis.

Based on the concentration of certain immobile elements (e.g. Cr, Ni, Zr, and Ti), the Purcell Lava appears to have originally been an alkaline basalt.

The Purcell Lava is probably neither cogenetic nor coeval with the conspicuous gabbroic sill (middle Belt carbonate sill) located mainly in the Helena Formation.

Except for thickness measurements, very little detailed information has been gathered on sections of Purcell Lava that occur north and west of Glacier

National Park. If the character of the Purcell is to be more fully understood (i.e. geometry, physical and chemical characteristics, timing and environment of emplacement) these localities must be closely examined and described.

REFERENCES

Ballard, R. D., Holcomb, R. T., and van Andel, T. H., 1979, The Galapagos rift at 86° W: Sheet flows, collapse pits, and lava lakes of the rift valley: Journal of Geophysical Research, v. 84, no. B10, p. 5407-5422.

Ballard, R. D., and Moore, J. G., 1977, Photographic atlas of the Mid-Atlantic Ridge rift valley: New York, Springer-Verlag, 114 p.

Baragar, W. R. A., 1984, Pillow formation and layered flows in the Circum-Superior Belt of eastern Hudson Bay: Canadian Journal of Earth Science, v. 21, p. 781-792.

Barnes, W. C., 1963, Geology of the northeast Whitefish Range, northwest Montana: Unpublished Ph.D. Thesis, Princeton University, 102 p.

Bates, R. L., and Jackson, J. A., eds., 1980, Glossary of geology (2nd ed.): Virginia, American Geological Institute, 749 p.

Bauerman, Hilary, 1884, Geology of the country near the forty-ninth parallel of north latitude west of the Rocky Mountains: Geological and Natural History Survey of Canada, Report of Progress 1882-83-84, pt. B, p. 5-42.

Beeson, M. H., Perttu, R., and Perttu, J., 1979, The origin of the Miocene basalts of coastal Oregon and Washington: An alternative hypothesis: Oregon Geology, v. 41, no. 10, p. 159-166.

Bleil, U., and Smith, B., 1980, Petrology of magnetic oxides at site 417, in Donnelly, T., and others, Initial Reports of the Deep Sea Drilling Project, v. 51, 52, 53, Part 2: Washington (U.S. Government Printing Office), p. 1411-1428.

Bloxam, T. W., and Lewis, A. D., 1972, Ti, Zr, and Cr in some British pillow lavas and their petrogenetic affinities: Nature Physical Science, v. 237, p. 134-136.

Burling, L. D., 1916, Ellipsoidal lavas in the Glacier National Park, Montana: Journal of Geology, v. 24, p. 235-237.

Byerly, G. R., and Swanson, D. A., 1978, Invasive Columbia River basalt flows along the northwestern margin of the Columbia Plateau, north-central Washington: Geological Society of America Abstracts with Programs, v. 10, no. 3, p. 98.

Calkins, F. C., 1909, A geological reconaissance in northern Idaho and northwestern Montana: U.S. Geological Survey Bulletin 384, p. 7-91.

Carlisle, D., 1963, Pillow breccias and their aquagene tuffs, Quadra Island, British Columbia: Journal of Geology, v. 71, p. 48-71.

Carmichael, I. S. E., Turner, F. J., and Verhoogan, J., 1974, Igneous petrology: New York, McGraw-Hill, 739 p.

Childers, M. O., 1963, Structure and stratigraphy of the southwest Marias Pass area, Flathead County, Montana: Geological Society of America Bulletin, v. 74, p. 916-938.

Cox, K. G., Bell, J. D., and Pankhurst, R. J., 1979, The interpretation of igneous rocks: London, George Allen and Unwin, 450 p.

Daly, R. A., 1912, Geology of the North American Cordillera at the forty-ninth parallel: Geological Survey of Canada Memoir 38, pt. 1, 546 p.

Dawson, G. M., 1875, Report on the geology and resources of the region in the vicinity of the forty-ninth parallel from the Lake of the Woods to the Rocky Mountains: British North American Boundary Commission, New York, B. Westermann and Co., 379 p.

Deer, W. A., Howie, R. A., and Zussman, J., 1966, An introduction to the rock forming minerals: London, John Wiley, 528 p.

Dimroth, E., Cousineau, P., Leduc, M., and Sanschagrin, Y., 1978, Structure and organization of Archean subaqueous basalt flows, Rouyn-Noranda area, Quebec, Canada: Canadian Journal of Earth Sciences, v. 15, p. 902-918.

Donnelly, T., Francheteau, J., Bryan, W., Robinson, P., Flower, M., Salisbury, M., and others, 1980, Initial Reports of the Deep Sea Drilling Project, v. 51, 52, 53, Part 1: Washington (U. S. Government Printing Office), 718 p.

DuToit, A. L., 1907, Pipe-amygdaloids: Geological Magazine, v. 4, p. 13-17.

Earhart, R. L., Mudge, M. R., and Connor, J. J., 1984, Belt Supergroup lithofacies in the northern disturbed belt, northwest Montana: Montana Geological Society 1984 Field Conference and Symposium Guidebook, p. 51-66.

Earhart, R. L., Raup, O. B., Conner, J. J., Carrara, P. E., McGimsey, D. H., Constenius, K. N., and Van Loenen, R. E., 1983, Preliminary geologic map and cross sections of the northwest part of Glacier National Park, Montana: U.S. Geological Survey Map MF-1604-A.

Engel, A. E. J., Engel, C. G., and Havens, R. G., 1965, Chemical characteristics of oceanic basalts and the upper mantle: Geological Society of America Bulletin, v. 76, p. 719-734.

Erdmann, C. E., 1947, Geology of dam sites on the upper tributaries of the Columbia River in Idaho and Montana, Part 3, Miscellaneous dam sites on the Flathead River upstream from Columbia Falls, Montana: U.S. Geological Survey Water-Supply Paper 866-C, p. 37-116.

Eslinger, E. V., and Savin, S. M., 1973, Oxygen isotope geothermometry of the burial metamorphic rocks of the Precambrian Belt Supergroup, Glacier National Park, Montana: Geological Society of America Bulletin, v. 84, p. 2549-2560.

Fenton, C. L., and Fenton, M. A., 1931, Algae and algal beds in the Belt series of Glacier National Park: Journal of Geology, v. 39, p. 670-686.

Fenton, C. L., and Fenton, M. A., 1937, Belt series of the north: Stratigraphy, sedimentation, paleontology: Geological Society of America Bulletin, v. 48, p. 1873-1970.

Finlay, G. I., 1902, Igneous rocks of the Algonkian series of the Lewis and Livingston Ranges, Montana: Geological Society of America Bulletin, v. 13, p. 349-352.

Fisher, R. V., and Schmincke, H.-U., 1984, Pyroclastic rocks: New York, Springer-Verlag, 472 p.

Flower, M. F. J., Ohnmacht, W., Robinson, P. T., Marriner, G., and Schmincke, H.-U, 1980, Lithologic and chemical stratigraphy at Deep Sea Drilling Project sites 417 and 418, in Donnelly, T., and others, Initial Reports of the Deep Sea Drilling Project, v. 51, 52, 53, Part 2: Washington (U.S. Government Printing Office), p. 939-956.

Floyd, P. A., and Winchester, J. A., 1975, Magma type and tectonic setting discrimination using immobile elements: Earth and Planetary Science Letters, v. 27, p. 211-218.

Fuller, R. E., 1931, The aqueous chilling of basaltic lava on the Columbia River plateau: American Journal of Science, ser. 5, v. 21, p. 281-300.

Garcia, M. O., 1978, Criteria for the identification of ancient volcanic arcs: Earth-Science Reviews, v. 14, p. 147-165.

Gibbs, George, 1874, Physical geography of the northwestern boundary of the United States: Journal of the American Geographical Society of New York, v. 4, p. 298-392.

Gill, J. G., 1981, Orogenic andesites and plate tectonics: New York, Springer-Verlag, 390 p.

Green, J., and Short, N. M., 1971, Volcanic landforms and surface features, a photographic atlas and glossary: New York, Springer-Verlag, 522 p.

Haggerty, S. E., 1976, Oxide minerals: Mineralogical Society of America Short Course Notes, Chapter 4, p. Hg1-Hg28, and Chapter 8, p. Hg101-Hg135, and Hg-176.

Hargreaves, R., 1976, Early Precambrian basalt flows, Utik Lake, Manitoba: Center of Precambrian Studies, University of Manitoba, Annual Report, p. 52-55.
Harrison, J. E., 1972, Precambrian Belt basin of northwestern United States: It's geometry, sedimentation, and copper occurrences: Geological Society of America Bulletin, v. 83, p 1215-1240.
Harrison, J. E., Cressman, E. R., and Whipple, J. W., 1983, Preliminary geologic and structure maps of part of the Kalispell 1^{o} X 2^{o} quadrangle, Montana: U.S. Geological Survey Open-File Report 83-502.
Harrison, J. E., and Grimes, D. J., 1970, Mineralogy and geochemistry of some Belt rocks, Montana and Idaho: U.S. Geological Survey Bulletin 1312-O, 49 p.
Harrison, J. E., Kleinkopf, M. D., and Wells, J. D., 1980, Phanerozoic thrusting in Proterozoic Belt rocks, northwestern United States: Geology, v. 8, p. 407-411.
Hekinian, R., 1984, Undersea volcanoes: Scientific American, v. 251, p. 46-55.
Henderson, J. F., 1953, On the formation of pillow lavas and breccias: Transactions of the Royal Society of Canada, ser. 3, v. 47, sec. 4, p. 23-32.
Hoy, T., 1979, Geology of the Estella-Kootenay King area: British Columbia Ministry of Energy, Mines, and Petroleum Resources, Preliminary Map 36.
Hoy, T., 1982, The Purcell Supergroup in southeastern British Columbia; sedimentation, tectonics, and strataform lead-zinc deposits: in Hutchinson, R. W., and others, eds., Precambrian sulphide deposits, H. S. Robinson Memorial Volume, Geological Association of Canada Special Paper 25, p. 127-147.
Hoy, T., 1984, The Purcell Supergoup near the Rocky Mountain trench, southeastern British Columbia: Montana Bureau of Mines and Geology, Special Publication 90, p. 36-38.
Hughes, C. J., 1982, Igneous petrology: New York, Elsevier Scientific Publishing Company.
Hunt, G. H., 1961, The Purcell eruptive rocks: Unpublished Ph.D. Thesis, University of Alberta, 139 p.
Hunt, G. H., 1962, Time of Purcell eruption in southeastern British Columbia and southwestern Alberta: Journal of the Alberta Society of Petroleum Geologists, v. 10, p. 438-442.
Hunt, G. H., 1964, Chemical correlation of the Purcell igneous rocks: Bulletin of Canadian Petroleum Geology, v. 12, Field Conference Guide Book, p. 544-555.
Hyndman, D. W., 1972, Petrology of igneous and metamorphic rocks: New York, McGraw-Hill, 533 p.
Irvine, T. N., and Baragar, R. A., 1971, Guide to the chemical classification of the common volcanic rocks: Canadian Journal of Earth Sciences, v. 8, p. 523-548.
Jenson, L. S., 1976, A new cation plot for classifying subalkalic volcanic rocks: Ontario Division of Mines, Miscellaneous Paper 66, 22 p.
Johns, W. M., 1962, Belt Series in Lincoln and southwest Flathead Counties, Montana: American Institute of Mining Engineers Transactions, v. 223, p. 184-192.
Johns, W. M., 1970, Geology and mineral deposits of Lincoln and Flathead Counties, Montana: Montana Bureau of Mines and Geology Bulletin 79, 182 p.
Jones, A. E., 1943, Classification of lava surfaces: American Geophysical Union, Transactions for 1943, pt. 1, p. 265-268.

Jones, A. E., and Nelson, P. H. H., 1970, The flow of basalt lava from air into water--its structural expression and stratigraphic significance: Geological Magazine, v. 107, no. 1, p. 13-19.
Jones, J. G., 1970, Intraglacial volcanoes of the Laugarvatn region, southwest Iceland: Journal of Geology, v. 78, p. 127-140.
Kulp, J. L., 1963, Potassium-Argon dating of volcanic rocks: Bulletin of Volcanologique, ser. 2, v. 26, p. 247-258.
Larson, E., Ozima, M., Ozima, M., Nagata, T., and Strangway, D., 1969, Stability of remanent magnetization of igneous rocks: Geophysical Journal of the Royal Astronomical Society, v. 17, p. 263-292.
Leech, G. B., 1960, Geology of the Fernie, Kootenai district, British Columbia: Geological Survey of Canada Map 11-1960.
Lonsdale, P., 1977, Abyssal pahoehoe with lava coils at the Galapagos Rift: Geology, v. 5, p. 147-152.
Lonsdale, P., and Batiza, R., 1980, Hyaloclastite and lava flows on young seamounts examined with a submersible: Geological Society of America Bulletin, v. 91, pt. 1, p. 545-554.
Macdonald, G. A., 1953, Pahoehoe, aa, and block lava: American Journal of Science, v. 251, p. 169-191.
Maxwell, D. T., and Hower, J., 1967, High-grade diagenesis and low-grade metamorphism of illite in the Precambrian Belt Series: The American Mineralogist, v. 52, p. 843-857.
McGimsey, R. G., 1984, Map showing the distribution of the Purcell Lava in Glacier National Park, Montana: U.S. Geological Survey Open-File Report 84-0853.
McMechan, M. E., 1979, Geology of the Mount Fisher-Sand Creek area: British Columbia Ministry of Energy, Mines, and Petroleum Resources, Preliminary Map 34.
McMechan, M. E., 1981, The Middle Proterozoic Purcell Supergroup in the southwestern Rocky and southeastern Purcell Mountains, British Columbia and the initiation of the Cordilleran Miogeocline, southern Canada and adjacent United States: Bulletin of Canadian Petroleum Geology, v. 29, p. 583-621.
McMechan, M. E., Hoy, T., and Price, R. A., 1980, Van Creek and Nichol Creek Formations: A revision of the stratigraphic nomenclature of the Middle Proterozoic Purcell Supergroup, southeastern British Columbia: Bulletin of Canadian Petroleum Geology, v. 28, no. 4, p. 542-558.
Mejstrick, P. F., 1975, Petrogenesis of the Purcell Sill, Glacier National Park, Montana: Unpublished M.S. Thesis, University of Montana, 74 p.
Moore, J. G., 1966, Rate of palagonitization of submarine basalt adjacent to Hawaii: U.S. Geological Survey Professional Paper 550-D, p. D163-D171.
Moore, J. G., 1970, Pillow lava in a historic lava flow from Hualalai volcano, Hawaii: Journal of Geology, v. 78, p. 239-243.
Moore, J. G., 1975, Mechanism of formation of pillow lava: American Scientist, v. 63, no. 3, p. 269-277.
Moore, J. G., and Reed, R. K., 1963, Pillow structures of submarine basalts east of Hawaii: U.S. Geological Survey Professional Paper 475-B, Article 40, p. B153-B157.
Moore, J. G., Cristofolini, R., and Lo Giudice, A., 1971, Development of pillows on the submarine extension of recent lava flows, Mount Etna, Sicily: U.S. Geological Survey Professional Paper 750-C, p. C89-C97.
Moore, J. G., Pillips, R. L., Griggs, R. W., Peterson, D. W., and Swanson, D. A., 1973, Flow of lava into the sea, 1969-1971, Kilauea volcano, Hawaii: Geological Society of America Bulletin, v. 84, p. 537-546.

Mudge, M. R., Erickson, R. L., and Kleinkopf, D., 1968, Reconnaissance geology, geophysics, and geochemistry of the southeastern part of the Lewis and Clark Range, Montana: U.S. Geological Survey Bulletin 1252-E, 35p.

Mudge, M. R., 1970, Origin of the disturbed belt in northwestern Montana: Geological Society of America Bulletin, v. 81, p. 377-392.

Mudge, M. R., 1977, General geology of Glacier National Park and adjacent areas, Montana: Bulletin of Canadian Petroleum Geology, v. 25, p. 736-751.

Mudge, M. R., and Earhart, R. L., 1980, The Lewis thrust fault and related structures in the disturbed belt, northwestern Montana: U.S. Geological Survey Professional Paper 1174, 18 p.

Mullen, E. D., 1983, $MnO/TiO_2/P_2O_5$: A minor element discriminant for basaltic rocks of oceanic environments and its implications for petrogenesis: Earth and Planetary Science Letters, v. 62, p. 53-62.

Nichols, R. L., 1936, Flow-units in basalt: Journal of Geology, v. 44, p. 617-630.

Nichols, R. L., 1939, Squeeze-ups: Journal of Geology, v. 47, p. 421-425.

Nockolds, S. R., 1954, Average chemical compositions of some igneous rocks: Geological Society of America Bulletin, v. 65, p. 1007-1032.

Obradovich, J. D., and Peterman, Z. E., 1968, Geochronolgy of the Belt Series, Montana: Canadian Journal of Earth Sciences, v. 5, p. 737-747.

Peacock, M. A., 1926, The geology of Videy, S. W. Iceland: A record of igneous action in glacial times: Transactions of the Royal Society of Edinburgh, v. 54, p. 441-465.

Pearce, J. A., 1975, Basalt geochemistry used to investigate past tectonic environments on Cyprus: Tectonophysics, v. 25, p. 41-67.

Pearce, J. A., and Cann, J. R., 1973, Tectonic setting of basic volcanic rocks determined using trace element analyses: Earth and Planetary Science Letters, v. 19, p. 290-300.

Pearce, T. H., Gorman, B. E., and Birkett, T. C., 1975, The TiO_2-K_2O-P_2O_5 diagram: A method of discriminating between oceanic and non-oceanic basalts: Earth and Planetary Science Letters, v. 24, p. 419-426.

Peck, D. L., 1966, Lava coils of some recent historic flows, Hawaii: U.S. Geological Survey Professional Paper, 550-B, p. 148-151.

Price, R. A., 1962, Fernie map-area, east half, Alberta and British Columbia: Geological Survey of Canada, Paper 61-24, 65 p.

Price, R. A., 1964, The Precambrian Purcell System in the Rocky Mountains of southern Alberta and British Columbia: Bulletin of Canadian Petroleum Geology, v. 12, p. 399-426.

Reesor, J. E., 1958, Dewer Creek map-area with special emphasis on the White Creek batholith, British Columbia: Geological Survey of Canada Memoir 292, 78 p.

Robinson, P. T., Flower, M. F. J., Swanson, D. A., and Staudigel, H., 1980, Lithology and eruptive stratigraphy of Cretaceous oceanic crust, western Atlantic ocean: in Donnelly, T., and others, Initial Reports of the Deep Sea Drilling Project, v. 51, 52, 53, Part 2: Washington (U.S. Government Printing Office), p. 1535-1555.

Rogers, J. J. W., Suayah, I. B., and Edwards, J. M., 1984, Trace elements in continental-margin magmatism: Part IV. Geochemical criteria for recognition of two volcanic assemblages near Auburn, western Sierra Nevedas, California: Geological Society of America Bulletin, v. 95, p. 1437-1445.

Ross, C. P., 1959, Geology of Glacier National Park and the Flathead Region, northwestern Montana: U.S. Geological Survey Professional Paper 296, 125 p.

Sato, M., and Wright, T. L., 1966, Oxygen fugacities directly measured in magmatic gases: Science, v. 153, p. 1103-1105.

Schmincke, H.-U., 1964, Petrology, paleocurrents, and stratigraphy of the Ellensburg Formation and interbedded Yakima basalt flows, south-central Washington: Unpublished Ph.D. dissertation, Johns Hopkins University.

Schmincke, H.-U., Robinson, P. T., Ohnmacht, W., and Flower, F. J., 1979, Basaltic hyaloclastites from Hole 396B, DSDP Leg 46, in Dmitriev, L., Heirtzler, J., and others, eds., Initial Report of the Deep Sea Drilling Project, v. 46: Washington (U.S. Government Printing Office), p. 341-355.

Sheldon, A. W., 1961, Geology of the northwest 15-minute Ural quadrangle, Lincoln County, Montana: Unpublished M.S. Thesis, Montana State College, 65 p.

Shervais, J. W., 1982, Ti-V plots and petrogenesis of modern and ophiolitic lavas: Earth and Planetary Science Letters, v. 59, p. 101-118.

Silvestri, S. C., 1963, Proposal for a genetic classification of hyaloclastites: Bulletin Volcanologique, ser. 2, v. 25, p. 315-321.

Smith, A. G., 1963, Structure and stratigraphy of the northwest Whitefish Range, Lincoln County, Montana: Unpublished Ph.D. Thesis, Princeton University, 151 p.

Sommers, D. A., 1961, Geology of the Ural northeast 15-minute quadrangle, Lincoln County, Montana: Unpublished M.S. Thesis, University of Rochester, 52 p.

Swanson, D. A., 1973, Pahoehoe flows from the 1969-1971 Mauna Ulu eruption, Kilauea Volcano, Hawaii: Geological Society of America Bulletin, v. 84, p. 615-626.

Sweeney, G. L., 1955, A geologic reconnaissance of the Whitefish Range, Flathead and Lincoln Counties, Montana: Unpublished M.A. Thesis, Montana State University, 43 p.

Tazieff, H., 1972, About deep-sea volcanism: Geologische Rundschav, v. 61, p. 470-480.

Walker, G. P. L., 1972, Compound and simple lava flows and flood basalts: Bulletin Volcanologique, ser. 2, v. 35, p. 579-590.

Walker, G. P. L., 1973, Lengths of lava flows: Philosophical Transactions of the Royal Society of London, v. 274, p. 107-118.

Walker, G. P. L., and Blake, D. H., 1966, The formation of a palagonite breccia mass beneath a valley glacier in Iceland: Quarterly Journal of the Geological Society of London, v. 122, p. 45-61.

Waters, A. C., 1960, Determining direction of flow in basalt: American Journal of Science, v. 258-A, p. 350-366.

Wells, G., Bryan, W. B., and Pearce, T. H., 1979, Comparative morphology of ancient and modern pillow lavas: Journal of Geology, v. 87, p. 427-440.

Wentworth, C. K., and Macdonald, G. A., 1953, Structures and forms of basaltic rocks in Hawaii: U.S. Geological Survey Bulletin 994, 98 p.

Whipple, J. W., Conner, J. J., Raup, O. B., and McGimsey, R. G., 1984, Preliminary report on the stratigraphy of the Belt Supergroup, Glacier National Park and adjacent Whitefish Range, Montana: Montana Geological Society 1984 Field Conference and Symposium Guidebook, p. 33-50.

Williams, H., and McBirney, A. R., 1979, Volcanology: San Francisco, Freeman, Cooper and Co., 397 p.

Willis, Bailey, 1902, Stratigraphy and structure, Lewis and Livingston Ranges, Montana: Geological Society of America Bulletin, v. 13, p. 305-352.

Wilmarth, M. G., 1938, Lexicon of geologic names of the United States: U.S. Geological Survey Bulletin 896, pt. 2, M-Z, p. 1245-2396.

Zartman, R. E., Peterson, Z. E., Obradovich, J. D., Gallego, M. D., and Bishop, D. T., 1982, Age of the Crossport C Sill near Eastport, Idaho: in Reed, R. P., and Williams, G. A., eds., Society of Economic Geologists 1977 Cordillera Field Conference, Idaho, Idaho Bureau of Mines and Geology Bulletin 24, p. 61-69.

APPENDICES

APPENDIX A

Snowslip Formation

The Snowslip Formation is the lowest member of the Missoula Group (fig. 4) and in Glacier National Park consists mainly of alternating successions of pale-maroon and grayish-green siltites, argillites, arenites and minor stromatolite limestone beds. The unit is 490 m (1606 ft.) thick at the type section in southern Glacier Park (Childers, 1963, p. 146) and thins northward to 358 m (1172 ft.) thick at Hole-in-the-Wall near the International Boundary (Whipple and others, 1984, p. 41).

In Glacier National Park, the Snowslip is divided into six informal members (Whipple and others, 1984). The Purcell Lava is located conformably within the uppermost member (6) in the northern half of the Park.

The first few meters of Snowslip strata directly beneath the pillow lava facies consists of green and red siltite and argillite that contains abundant sedimentary structures (e.g. dessication cracks, ripple marks, mudchip breccias, cross-beds, and cross-laminations). A pinkish-red stromatolite limestone bed (as much as 1 m thick) occurs locally at, or as much as 8 m below the contact with pillow lava. A conspicuous 40 to 50-meter-thick interval of red siltite and argillite lies beneath the stromatolite bed and contains abundant sedimentary structures indicative of tidal flat deposition (e.g. oscillation ripples, dessication cracks, rip-up breccias, and raindrop imprints). This interval has also been interpreted as representing a distal fluvial environment (sheet flood deposits in a braided stream system) by J.W. Whipple (personal communicaton). In general, the sedimentary structures in strata beneath the Purcell Lava are indicative of a marine transgression (well-laminated, fine-grained sediments containing stromatolites overlying tidal flat and/or fluvial sediments) with a water depth consistent with the thickness of the pillow lava flow facies.

Overlying the Purcell Lava are alternating beds of red and green siltite, argillite, and arenite. At Fifty Mountain and Kootenai Peak, a very fine-grained, dark grayish-green argillite, about 1 m thick, rests directly on the uppermost flow unit, filling cracks and surface irregularities. Snowslip strata overlying the Purcell is approximately 16 m thick at Hole-in-the-Wall, 27 m thick at Kootenai Peak, and about 40 m thick at Granite Park.

Snowslip Sedimentary Rock Below and Above Purcell Lava, Glacier National Park, MT (From northern to southern sections)

Hole-in-the-Wall Section

--Five-meter-thick layer of sedimentary rock between base of pillow lava facies and upper contact of hypabyssal sill is green and red siltite and argillite (predominantely green beds); outer margins are silicified and form a distinct contact aureole.

--Hypabyssal diabase sill lies in contact with a zone of red and green argillite 2-3 m thick with small (9 mm) limonitic pyrite cubes; below this lies primarily red siltite and argillite; the "baked" zone of the contact aureole is 40-50 cm thick.

--There is 16.5 m of Snowslip strata above the highest lava flow unit, using the criteria of Whipple (unpublished data: the contact between Snowslip and overlying Shepard is placed at the "top of the uppermost grayish-green siltite and argillite sequence that contains thin laminae of white quartz arenite, and very little carbonate"). The top of the Snowslip is picked at the last green argillite bed above which lies a buff colored carbonate bed and is 16.5 m from top of the last flow unit to the Shepard Formation.

--On Thunderbird Mountain, finely laminated, massive, green beds rest on uppermost flow unit, the surface of which is pinkish red and scoriaceous. Above, lie beds of siltite and argillite with reworked sand-size and larger fragments, of volcanic rock. Sedimentary structures in the first .5 m of strata above the uppermost flow unit include oscillation ripple marks and cross-laminations.

Mt. Cleveland

--Predominately red siltite and argillite at the base of the hypabyssal sill; green beds directly above uppermost flow unit.

Kootenai Peak

--An 8-10 m sequence of red siltite and argillite with a few greenish cross-bedded sand layers lies beneath the pillow lava facies. Sedimentary structures include abundant dessication cracks, ripple marks (normal and oscillation types), some flaser bedding, raindrop pits, and mudchip breccias. The rock is deep purplish red to lavender in color.

--Thin (1 cm) beds of sand-size, reworked hyaloclastite tuff occurs locally in the first 10 cm beneath the pillows.

--The first meter of Snowslip below the pillows contains fine-grained, finely laminated (wavy) siltite and argillite with fluid escape structures, rip-up breccias, and fluted and cross-bedded sand lenses. Sedimentary structures are absent in the 15-20 cm interval directly below the pillow lava facies. Pale green siltite and argillite with reddish-brown oxidation stains extend down to a brown stromatolitic limestone zone about 1 m thick and 8.5 m below the base of the pillow lava facies.

--Below the stromatolitic zone is a 30-40 m interval of red siltite and argillite.

--Snowslip strata between the Purcell Lava and Shepard Formation is sandy siltite and argillite with a few 1-meter-thick, cross-laminated sand layers containing limonitic pyrite. A massive, fine-grained, dark green argillite occurs locally at the top of the uppermost flow unit. A similar rock occurs at the Fifty Mountain section. There is 21 m of Snowslip strata above the

highest flow unit, measuring up to the first thick bed (2 m) of buff colored carbonate. A thinner stromatolitic zone lies 3 m below and may be more appropriate to establish the upper contact.

Fifty Mountain Area

--Snowslip strata beneath lava flows consists of alternating red and green argillite and siltite with abundant mudchip breccia, dessication cracks, and oscillation ripples. The .5 m interval below the basal contact with pillows contains limonite-coated pyrite cubes as much as 1 cm large. Locally, a pinkish-red stromatolite zone (.5 m to 20 cm thick) lies either directly in contact with, or as much as .5 m below, the pillow lava. The first few meters of Snowslip strata beneath the pillow lava consists predominately of green beds; a 40-50 m interval of red argillite and siltite occurs below this.

--Snowslip strata above the uppermost flow unit at the measured section is a greenish-black (fresh, medium bluish-gray when weathered), very fine-grained siltite. The interval is less than 1 m thick, weathers out into massive blocks, and has very fine bedding visible only in thin-section. It contrasts markedly from the argillaceous rock above it. Locally, it fills cracks and irregularities in the upper surfaces of the uppermost flow unit(s). The same rock occurs at the Kootenai Peak section.

Granite Park

--Fine-grained green argillite and siltite occurs at the basal contact with the pillow lava. Below the contact (30-40 cm) is a buff colored calcareous arenite bed, as much as 10 cm thick, with cross-laminations. The exposure is discontinuous and at the measured section is about 5 m long.

Swiftcurrent Peak (southeast face)

--Snowslip strata immediately below the pillow lava is finely laminated, alternating red and green beds; the interval has a dominantly green color due to the greater abundance of green beds.

--A thick sequence (about 50 m) of red siltite and argillite with shallow-water sedimentary structures (i.e. dessication cracks, mudchip breccia, oscillation ripples, cross-ripples, and well-developed cross-laminations in the arenite layers) occurs below the overlying green and red beds.

Apgar Mountains

--The pillow lava rests on green argillite with a 30-40 m interval of predominantly red siltite and argillite below. The upper contact of flow units with Snowslip strata is not well-exposed.

--Occurring at the top of lava flow sequence on Huckleberry Mountain, above the bridge crossing the Northfork of the Flathead River, are many well-rounded cobbles representing a range of lithologies (e.g. quartzite, arkosic arenite, diabase, and volcaniclastic) nearly identical to those occurring in the stream bed below. The clasts are most likely of glacio-fluvial origin and should not be mistaken for the pebble-cobble conglomerate that occurs directly above the Purcell Lava in the Shepard Formation in the Whitefish Range to the west.

APPENDIX B

Measured Sections of the Purcell Lava

Twelve sections of the Purcell Lava were measured in Glacier National Park (table 8). Of these, three were described in detail; the others were measured to correlate thicknesses and facies. Those sections not described in detail are located at (1) Hole-in-the-Wall, east and north walls; (2) the southwest face of Boulder Peak, above Pocket Lake; (3) the west face of Mt. Cleveland; (6) along the trail up the southern end of Flattop Mountain; (7) Trapper Peak (thickness measured by computerized photogrammetric plotter); and (8) the north flank of Huckleberry Mountain, up from the bridge over the North Fork, and 2 sections along the southwest flank of the Apgar Mountains where the lava flow(s) pinch out (see McGimsey, 1984, for location).

Sections measured at Granite Park, Fifty Mountain and Hole-in-the-Wall (west wall) were described in detail and appear on the following pages. The descriptions include the number and location of selected rock samples collected at each section.

Measured Section of Purcell Lava at Granite Park

The section of Purcell Lava at Granite Park was measured on the south flank of Swiftcurrent Peak, immediately west of Swiftcurrent Pass (fig. 108). Granite Park is a misnomer coined by early prospectors (J. Holterman, unpublished information) upon finding the coarse granophyric zone of the middle Belt carbonate sill that crops out in the basin.

The Granite Park section is arranged such that flow unit 1 is the first massive flow overlying the pillow lava facies. Flow unit 8 is in contact with the overlying Snowslip strata.

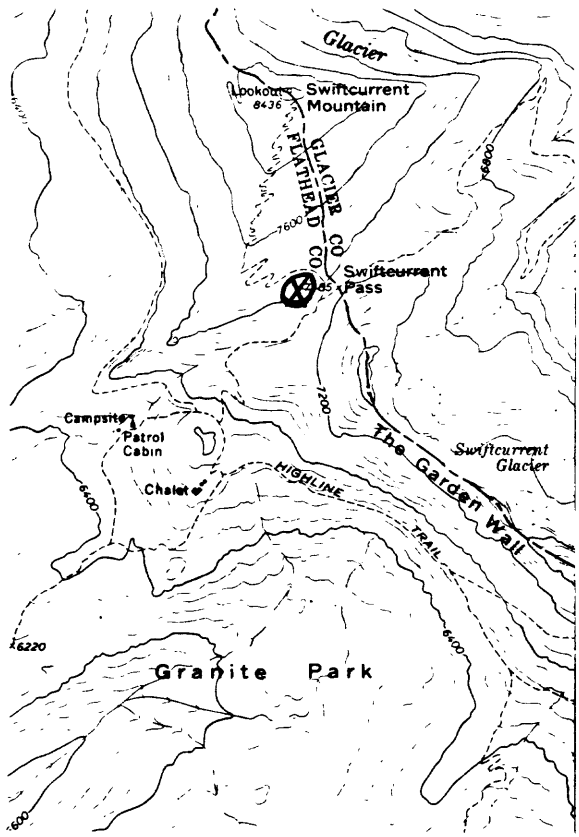

Figure 108. Location map for the section of Purcell measured at Granite Park. Map is from the USGS Ahern Peak 1:24,000 quadrangle.

Measured section of Purcell Lava at Granite Park

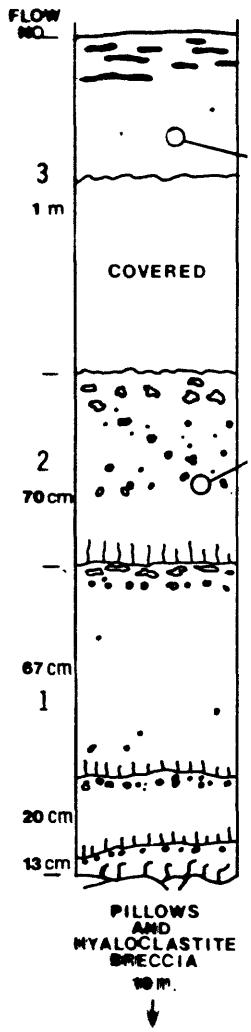

upper 0.4 m—large elongate cavities up to 10 cm in length, smaller ones are quartz-filled, larger cavities are quartz-lined, scattered spherical chlorite-filled vesicles (<5 mm)
82M-36 - sulfides present

flow of variable thickness
chlorite amygdules becoming smaller upward, quartz-filled cavities becoming larger and more abundant
82M-35 - dark grayish-green, very vesicular, irregular-shaped amygdules of quartz with a black rim and an olive-green halo around the perimeter
20 cm above base - zone of spherical to subspherical vesicles (< 5 mm) filled with chlorite, some intermixed irregular-shaped quartz-filled vesicles up to 1 cm in length with a black chloritized rims

pipe vesicles filled with quartz or chlorite
variably sized hollow cavities and irregular, elongate quartz-filled and/or lined vesicles
multiple flow toes
pipe vesicles—chlorite-filled, inclined towards the southwest

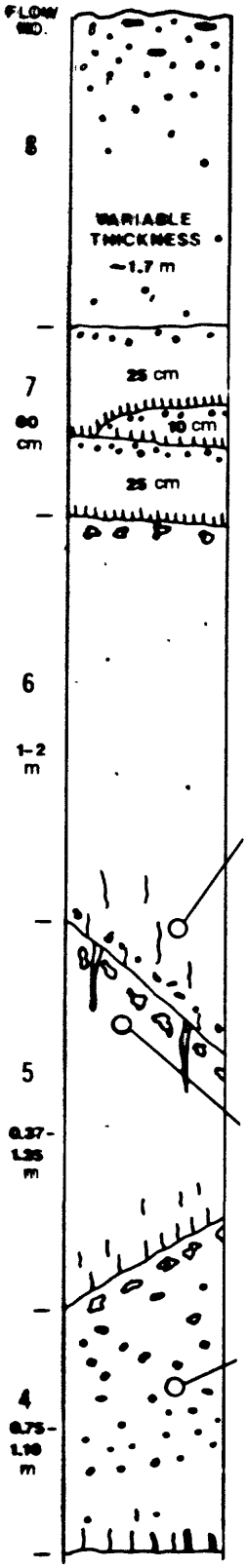

contact with overlying Snowslip Fm.; sediment conformably filled the highly irregular upper surface
vesicles are larger and some are coalesced, banded cryptocrystalline quartz is present in some cavities
upper 0.85 m—very vesicular, hollow vesicles

mostly massive with subspherical chlorite amygdules (< 5 mm)
spherical chlorite-filled vesicles at the top of each toe
each cooling unit or toe has an olive-green skin, pipe vesicles at the base are generally hollow

top-ropy with thin (1 - 3 mm) olive-green skin, large quartz-lined vesicles with some cryptocrystalline quartz-fillings

82M-39 - dark gray with a slight purple hue, small (< 1 mm) chlorite-filled irregular vesicles, calcite and quartz amygdules (1 - 2 mm)
some pipe vesicles extend up into the inner zone
a few pipe vesicles at the base with a layer of irregularly shaped, chlorite-filled vesicles
flow unit 5 thins greatly

large irregular quartz-filled vesicles, cooling cracks infilled with lava from the upper flow
82M-38 - medium dark gray with a slight purple hue, large (as much as 1 cm) milky and clear quartz- and colored calcite-filled vesicles, chalcopyrite abundant
concentration of very large (up to 3.5 cm) irregularly-shaped hollow vesicles with quartz linings
variable thickness

82M-37 - dark greenish gray, quartz and calcite amygdules up to 1 cm—some very irregular; chalcopyrite abundant

center of flow - massive with large subspherical, black chlorite-filled vesicles
quenched base with chlorite- and quartz-filled micro-vesicles and pipe vesicles

Measured Section of Purcell Lava at Fifty Mountain

In reality, there is no "Fifty Mountain". The area is so named because from the Fifty Mountain campsite, fifty mountains are supposedly visible (J. Holterman, unpublished information). Figure 109 shows the location of the section measured on the south flank of Mt. Kipp.

In the Fifty Mountain sections, flow unit 1 rests on the pillow lava; flow unit 12 is highest in the section and is in contact with overlying Snowslip strata.

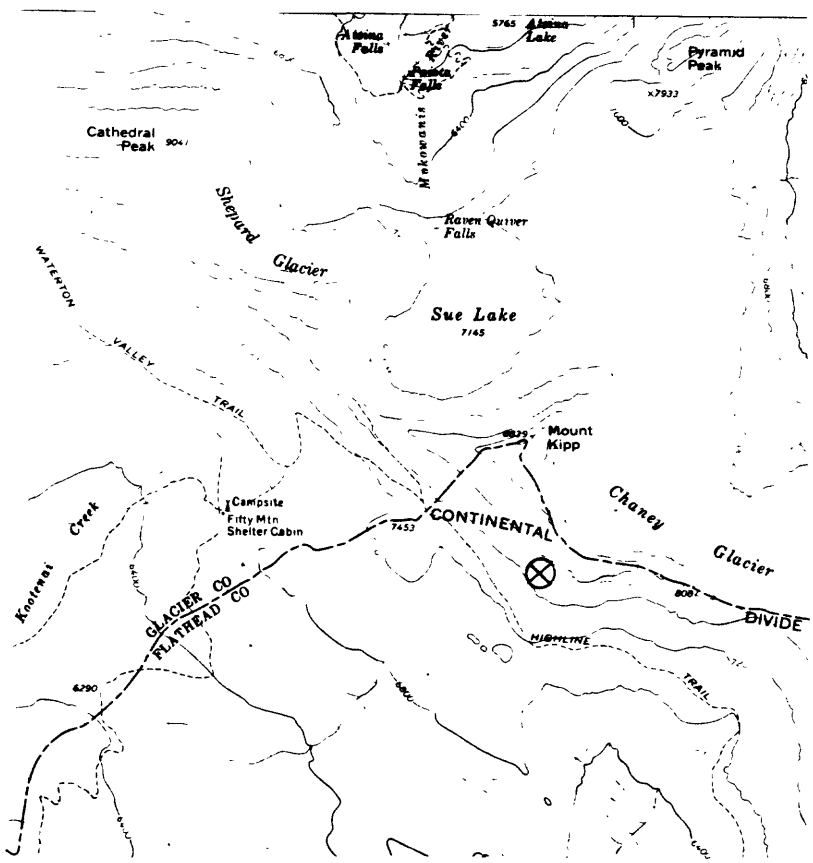

Figure 109. Location map for the section of Purcell Lava measured at Fifty Mountain. Map is from the USGS Ahern Pass 1:24,000 quadrangle.

Measured section of Purcell Lava at Fifty Mountain

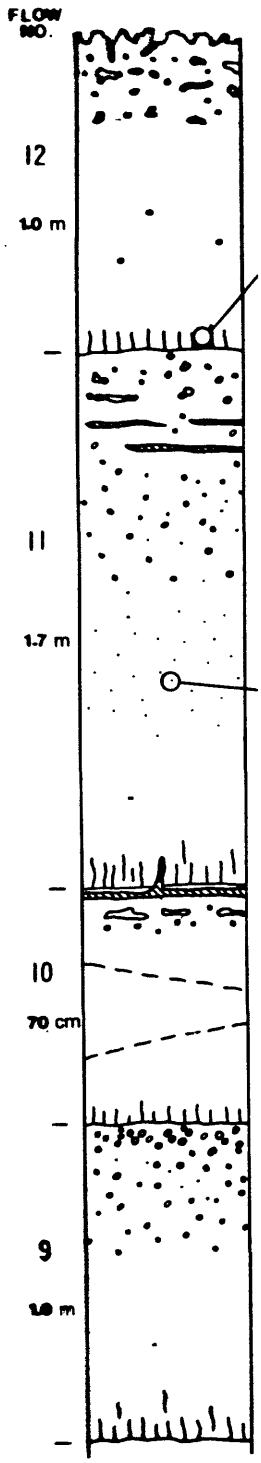

top of flow unit—a few amygdules and several large irregular quartz- and calcite-filled drusy cavities, 1-5 cm-thick weathered zone
upper 30 cm—very vesicular; vesicles are hollow and irregular, some are interconnected
center - massive with a few scattered quartz-filled vesicles
82M-57 - dark greenish-gray on weathered surface, chlorite amygdules with disseminated sulfides

small (< 2 mm) spherical vesicles intermixed with pipe vesicles (up to 4 cm in length) with orange calcite- and black chlorite- and/or black quartz-filling—some hollow; chalcopyrite present
5-10 mm olive-green skin; large drusy quartz-lined cavities; some removal of quartz-fillings by recent weathering
coalesced vesicle horizons - elongate lenses filled with cryptocrystalline quartz, typically 4 cm thick and up to 1 m long
upper 60 - 80 cm—very vesicular with a few irregular quartz and chlorite amygdules

82M-59 - fine-grained, dark greenish-gray, containing black chlorite amygdules 1 mm in diameter

numerous spiracles(?) and pipe vesicles
1.5 cm olive-green zone (cryptocrystalline quartz)
82M-60 - 2 cm thick horizon of cryptocrystalline quartz
large, hollow, irregular cavities, some are 10 - 15 cm long
2 or 3 cooling units or flow toes

concentration of subrounded vesicles at top of flow unit

upper 50 cm - vesicular, underlying 30 cm is massive

flow unit "9" pinches out as flow unit "10" thickens

good pipe vesicles occur in lower 20 cm near the base of the flow unit

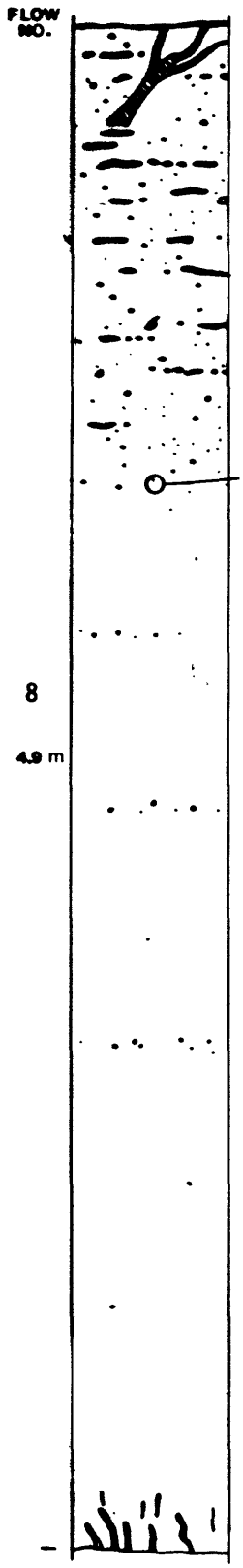

smooth olive-green flow-top overlain by 1 - 4 cm of banded cryptocrystalline quartz

crack infilled with cryptocrystalline quartz

upper 80 cm - cherty lenses prevalent

upper 1.5 m - large elongate vesicles and trains of vesicles up to 5 cm in length

spherical and irregular chlorite amygdules that appear as black blebs on weathered surfaces

82M-62 - dark gray with a slight reddish hue, amygdules of quartz and chlorite, one containing disseminated chalcopyrite

center of flow unit is primarily massive with several zones of vesicles

lower 10 cm. - quartz-filled or -lined pipe vesicles

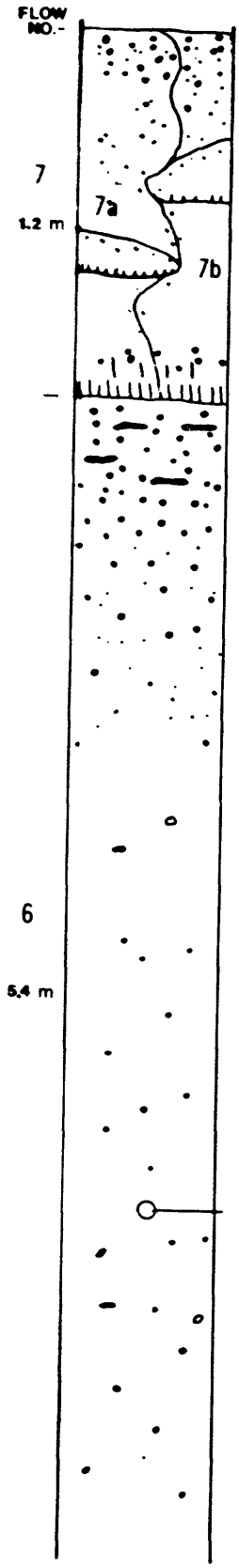

smooth olive-green flow-top 2 - 3 mm thick

flow unit "7a" comes in as flow-unit "7b" pinches out, both are about the same thickness and occupy the same stratigraphic horizon

several smaller toes of limited lateral extent with olive-green flow-tops are present in both flow units

amygdules common toward the base
1 - 2 mm thick olive green zone at top of flow unit
cherty lenses also present

top 1 m of flow - irregular quartz amygdules

amygdaloidal, purple hue to the rock

82M-63 - dark grayish-red purple, glassy and milky quartz amygdules up to 5 mm in diameter

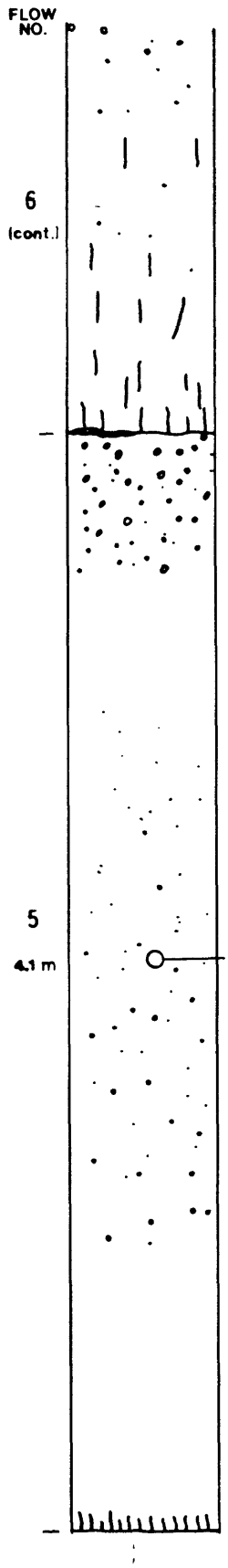

pipes vesicles present up to 1 m from basal contact

numerous quartz-filled pipe vesicles up to 3 cm in length
local patches of basal breccia
ropy flow top of flow unit 5 with olive green altered zone

vesicular zone near top

82M-64 - grayish-red purple, multicolored amygdules of quartz and calcite and black to dark green chlorite amygdules

massive, with chlorite amygdules averaging 5 mm in size, some quartz and calcite amygdules present, as well as chalcopyrite

pipe vesicles

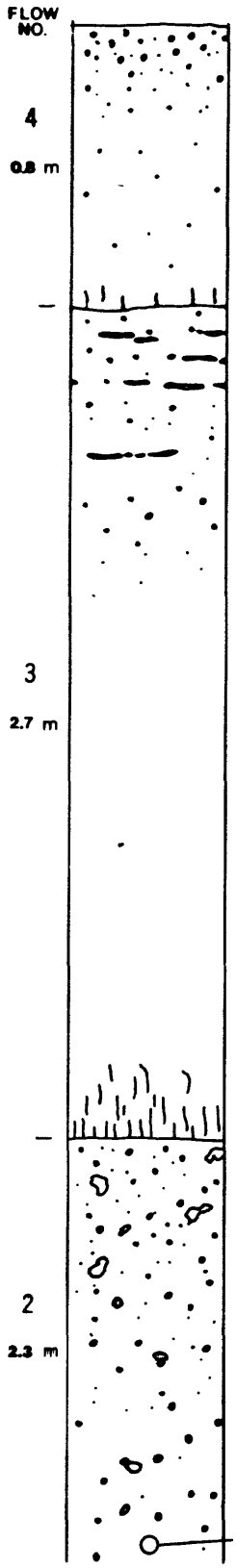

smooth, olive-green flow top

amygdaloidal

base not well-exposed
smooth olive-green flow-top

upper 0.5 m - horizontal trains of amygdules

very fine-grained, massive

numerous pipe vesicles at the base of the flow unit
smooth olive green flow-top

upper 1 m - very vesicular and amygdaloidal, some large drusy cavities filled or lined with calcite and/or quartz

very dark green in color

82M-65 - dark gray with a slight reddish hue on fresh surface, dark greenish-gray chlorite amygdules

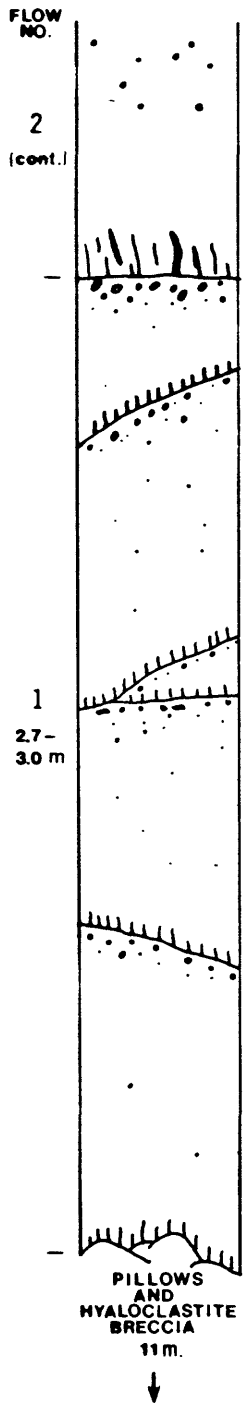

3–4 individual flow toes of limited lateral extent

coalesced pillows

Measured Section of Purcell Lava at Hole-in-the-Wall

Hole-in-the-Wall cirque is named after the falls that issue out of a cave in the Helena limestone high above Bowman Creek (J. Holterman, unpublished information). Sections of the Purcell Lava were measured on the east, north and west walls (fig. 110) of the cirque; only the west wall section is described in detail.

Flow units are numbered 1-23 with 1 resting on pillows; 23 is the highest flow unit in the section and is in contact with overlying Snowslip strata.

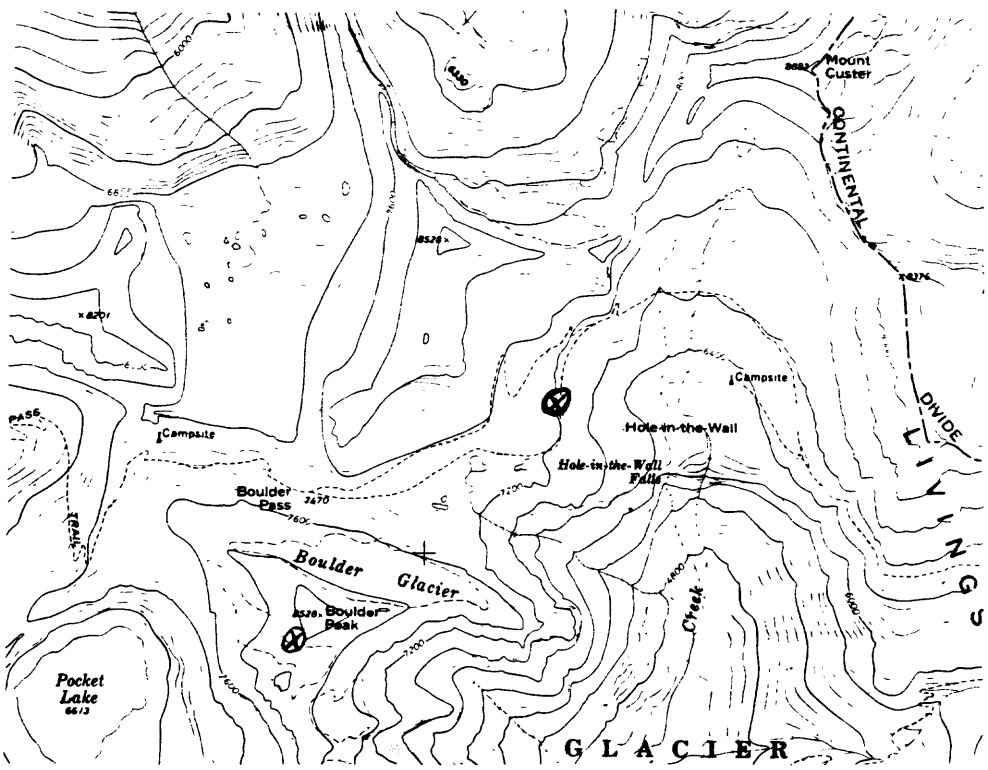

Figure 110. Map showing the location of the measured section of Purcell Lava at Hole-in-the-Wall. The Boulder Peak section locality is also shown. Map is from the USGS Mt. Carter 1:24,000 quadrangle.

Measured section of Purcell Lava
at Hole-in-the-Wall

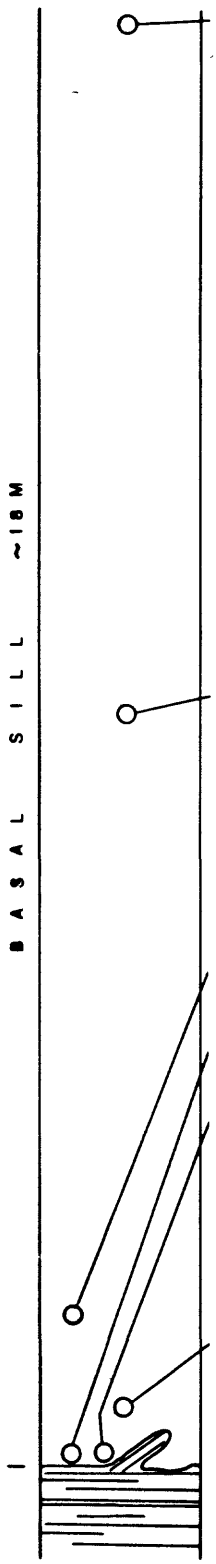

82M-110 - dark gray, feldspar laths (1 mm) visible on fresh as well as weathered surfaces, rock is massive and nonvesicular

82M-109 - med. dark gray with slight purple hue, sulfide mineralization disseminated throughout, diabase texture easily visible on weathered surfaces with some feldspar laths up to 1 mm long

82M-108 - dark gray with slight purple hue, massive, non-vesicular, fine-grained, diabase, feldspar laths visible only on weathered surface with the aid of a hand lens

82M-106 - from basal 0.8 m, rock is massive grayish green, calcite film on joint surfaces

82M-105 - collected at the basal contact; very fine-grained, grayish green to dk. greenish gray, sprinkled with fine-grained sulfides (chalcopyrite); and quenched, altered plag. laths present, calcite film on joint surfaces; no pipes, vesicles, or voids, except for where local concentrations of sulfides weather out and leave subspherical or ellipsoidal cavities, no soft-sediment deformation except for one small slab of the Snowslip Fm. swung up out of place

82M-104 - dark greenish-gray, a few very tiny (< 1 mm) chlorite amygdules (?) which appear as black splotches on weathered surfaces, cut surface has tiny light-colored speckles lower 1 m weathers out in angular blocks and appears very massive

Snowslip Fm. - approximately 0.5 m of hornfelsed and silicified sediment, red and green with limonite coated pyrite cubes (up to 1 cm)

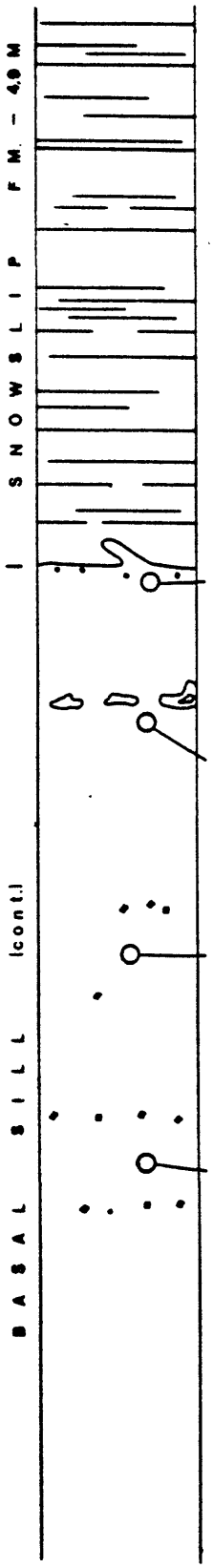

sediment interval varies in thickness laterally from 0 - 5 m

Snowslip Fm. in contact with sill - sediment is slightly hornfelsed and silicified

upper contact of basal sill—apophyses, scattered small (< 5 mm) amygdules, thin (< 1 cm) granophyric intergrowths

82M-114 - med. dk. gray, very fine-grained, massive

zone, traceable laterally, of large (6-60 cm) cavities filled or lined with euhedral quartz crystals, occasionally the smaller cavities (5-20 cm) are calcite-filled, cavity shapes vary from circular and ellipsoidal to irregular

82M-113 - fine-grained, med. bluish gray, sulfides present, feldspar laths are not megascopically visible

rock is finer grained toward upper contact

a few zones containing pyrite are still present

82M-112 - medium dk. gray with purple hue, black splotches on surface give false impression that the rock is vesicular, these are irregular patches of chlorite in the matrix

zone of limonite-coated cubes of pyrite (up to 4 cm wide)

82M-111 - medium-grained, dark gray, massive

zone containing pyrite cubes (up to 4 cm wide)

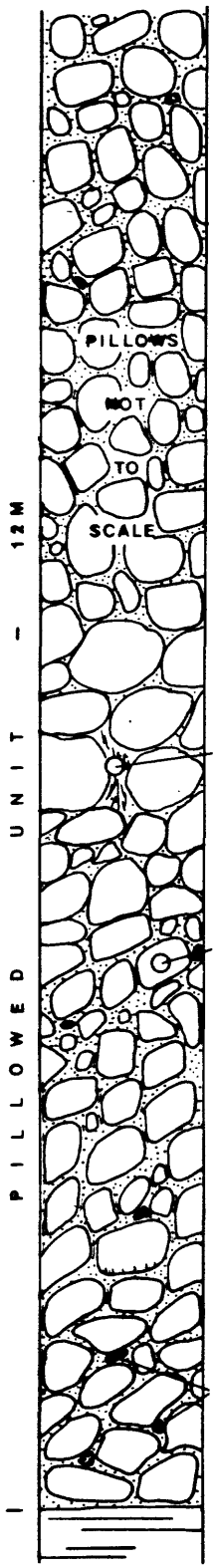

82M-118 - zone of dike or vein like bodies within the lava that are accentuated by weathering, splotches of chlorite amygdules (1 mm) and a light olive green color set the zone apart from the adjacent pillows; these bodies may be either alteration zones or spiracles

82M-117 - nodular masses resembling varioles are present on some surfaces and are up to 1 cm in size; pillow interiors are mostly massive except for a few quartz amygdules, 1 - 2 cm large

some pillows are ellipsoidal, others are highly irregular in shape, at least one example of fault slivers was observed

some pillows are not as well developed as those at other localities; here, pillows grade in and out of massive zones

pillows are interconnected; many are flatbottomed with quartz- or chlorite-filled pipe vesicles at the base

hyaloclastite breccia and cherty lining between pillows; cherty lenses between pillows can be up to 20 cm thick, green and red in color

drusy interpillow cavities

top of sediment interval separating pillows from diabase sill

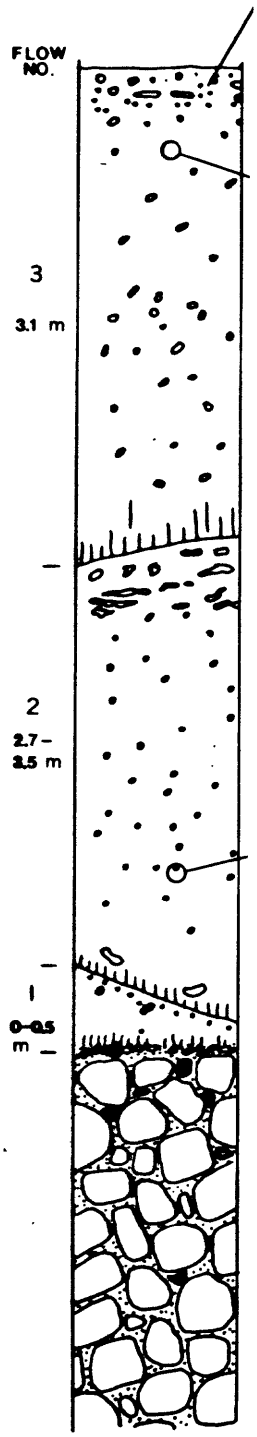

upper 20 cm - medium-sized (up to 5 cm) quartz, calcite, and chlorite amygdules of irregular shape, quartz amygdules have intergrowths of chlorite, chlorite amygdules are smaller and become more abundant in the upper 10 cm, quartz and calcite amygdules are roughly horizontally layered

82M-120 - medium dark gray with a slight purple hue, amygdaloidal—mostly quartz (both milky and clear), amygdules are very irregular in shape, up to 1 cm in diameter

hollow, spherical, vesicles (1 cm in diameter) in center with amygdules above and below

base not well-exposed

quartz and calcite amygdules are irregular in shape and roughly aligned in horizontal layers or trains, some are interconnected, many amygdules have quartz stringers

flow is very vesicular, and has nearly spherical, open vesicles (up to 1 cm) in center, and amygdules at top and bottom

82M-119 - med. dark gray with purple hue, fine- to medium-grained, feldspar laths are macroscopically visible, amygdules of calcite (1 mm) are very common, quartz amygdules (up to 1 cm) are generally irregular in shape and rimmed with calcite pipes vesicles, mostly quartz-filled, and a few large drusy cavities at the base of the flow unit

many quartz- and chlorite-filled vesicles near top of flow, quartz-filled vesicles (5 mm) are generally larger than the chlorite-filled vesicles (1-3 mm), some medium-sized (up to 20 cm) drusy cavities with quartz linings occur locally, pipe vesicles are predominantly quartz-filled

top of pillowed facies—isolated pillow breccia grading downward into coalesced pillows

medium-sized (4-20 cm) quartz-filled cavities, some with small stringers attached

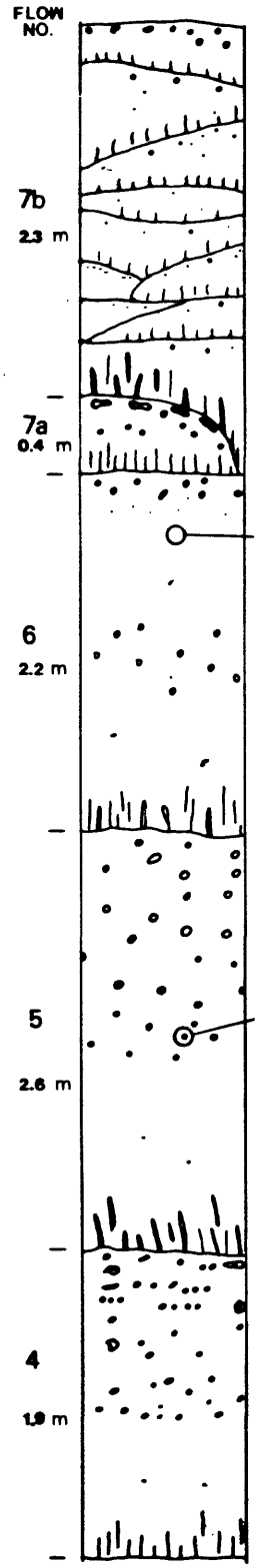

flow unit is made up of multiple lobes or toes with pipe vesicles at the base of each, amygdaloidal throughout

hollow pipe vesicles at the base

hollow cavities (up to 10 cm long) at the top, some of which are quartz-lined
hollow vesicles in center, pipe vesicles at base
calcite and quartz amygdules (3-5 mm) are present in quantity only at upper contact

82M-122 - med. dark gray, irregularly shaped pink quartz and white calcite amygdules (1-3 mm)

vesicular but not strongly amygdaloidal
hollow, spherical vesicles

pipes at base
ropy, olive green flow top
no horizontal layering of vesicles
vesicles - primarily quartz-filled, some are chlorite-filled or lined, a few are filled with orange-colored calcite

82M-121 - med. bluish gray, fine- to med.-grained diabase containing sulfides, orange calcite-filled vesicles (some lined with chlorite) up to 0.5 cm, and smaller quartz amygdules
rock is fairly massive for lowermost 1 m with hollow, spherical vesicles abundant above
dusky green in color
hollow pipe vesicles at base
horizontal trains of amygdules
some of the larger cavities (approx. 3 cm) are hollow
amygdules - quartz-filled or lined, becoming more numerous toward the top
hollow vesicles

above pipe vesicles, rock is massive for a few ten's of cms
well developed pipe vesicles, quartz- and chlorite-filled, up to 5 cm in length

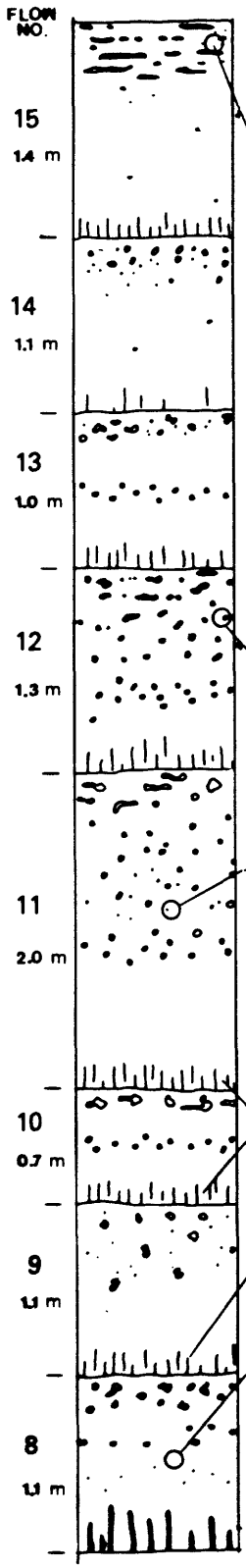

upper 50 cm—strongly amygdaloidal with very strung out amygdules, some composed of massive green-colored cryptocrystalline quartz, horizontal layering is prevalent

82M-126 - typical of this zone, some spherical quartz amygdules with intermingled chlorite, others are very irregular in shape

center—massive, nonvesicular

pipe vesicles at base

upper part amygdaloidal

center—massive, nonvesicular

only a few scattered pipes at base

irregular quartz amygdules at top

hollow vesicles in center

pipes at base

amygdaloidal to the top, quartz amygdules are larger, more irregular and strung out towards the top, interconnected amygdules with horizontal layering prevalent at the top

82M-125 - fine-grained, dk. gray with a purple hue, irregular quartz amygdules up to 1.5 cm in diameter

approx. 25-cm-thick zone of hollow ves., 45 cm up from the base

well-developed pipe vesicles at base

larger quartz amygdules of irregular shape, strung out

20 - 30 cm below top, spherical quartz amygdules

82M-124 - med. bluish-gray; quartz amygdules up to 1 cm, some with chlorite halo, chlorite amygdules weather in a black "splotchy" pattern

hollow vesicles, 10 - 20 cm zone

pipe vesicles at base

large (approx. 5 cm) quartz-filled or lined cavities, some strung-out horizontally

hollow vesicles in a narrow zone in center

pipe vesicles

irregular, quartz amygdules randomly scattered at and near top, fine-grained disseminated sulfide in some amygdules, chlorite disseminated in some amygdules

well-developed pipe vesicles at base

amygdaloidal zone with irregular quartz-filled vesicles

zone of hollow vesicles

82M-123 - med. dk. gray, fine-grained, massive, with a few small, scattered calcite amygdules, chalcopyrite present in 1 - 3 mm concentrates

rock is somewhat coarser grained than lower flow units

30 cm above pipe vesicles rock is very massive with a few black, chlorite-filled vesicles

well-developed pipe vesicles at base

strongly amygdaloidal at the top (both quartz and calcite fillings)

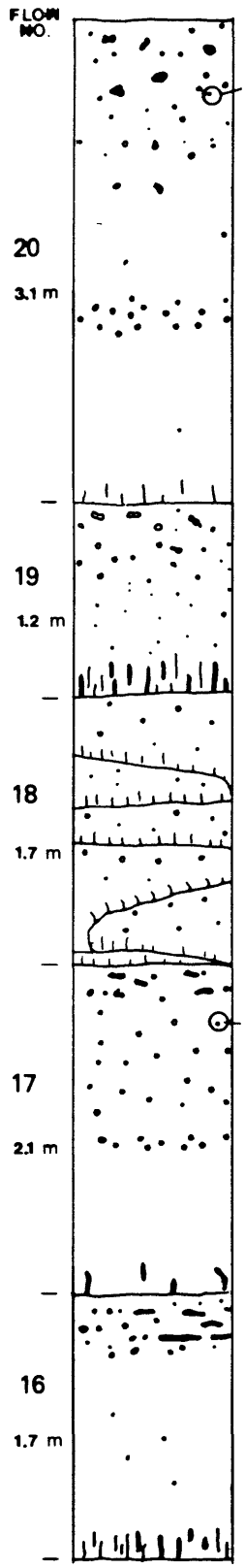

82M-128 - med. dk. gray with a pronounced purplish hue, very fine-grained, quartz amygdules with speckled chlorite rims, calcite amygdules with green quartz rims, some cavities are drusy (up to 1.5 cm) filled with brown colloidal material

hollow vesicles in center of flow unit
several lobes coalescing into one at this point

poorly developed pipe vesicles at base

amygdaloidal throughout; however, amygdules increase in size with smaller vesicles intermixed and are only partially filled with quartz and/or calcite near the top
well developed pipe vesicles

composed of several thin flow toes that pinch out locally, each has pipe vesicles at the base and scattered amygdules upwards

irregular amygdules, roughly layered, larger than below
82M-127 - med. bluish-gray, fine- to med.-grained, orange quartz and calcite amygdules (1-5 mm)
quartz and calcite amygdules which are somewhat smaller than in lower flows, few are interconnected and layering is not obvious
zone of hollow vesicles

only a few pipe vesicles at base

strongly amygdaloidal at top, amygdules are irregular, strung out and horizontally layered

pipe vesicles

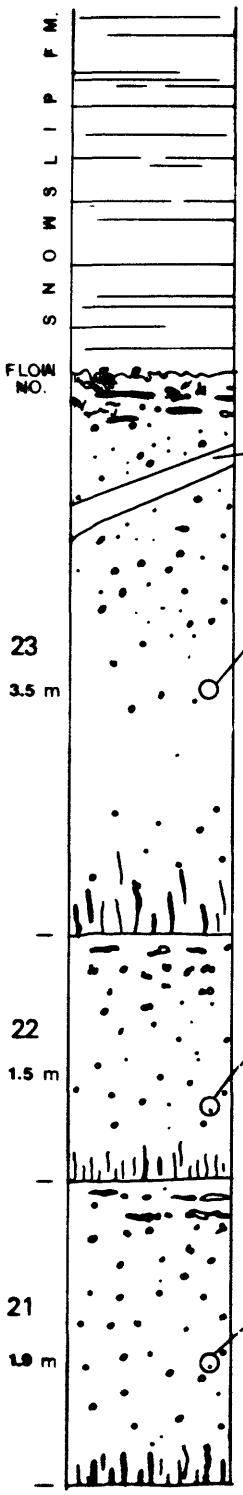

approximately 16.5 m of Snowslip Fm. above the Purcell Lava, contact with the Shepard Fm. picked at the top of the last green argillite bed underlying a buff colored carbonate bed

top is scoriaceous and/or smooth and ropy with a 1 - 5 cm pinkish-red oxidized horizon

banded cryptocrystalline quartz filling coalesced vesicles

late-stage, very fine-grained, massive, oxidized intrusive, presumably associated with the vent facies, 4 - 5 m long and about 30 cm thick (82M-130, -131)

82M-132 - fresh surface is med. bluish gray, weathers light brownish gray, fine-grained, very vesicular—vesicles are irregular, up to 0.5 cm dia., and filled with calcite and chlorite, some with associated quartz

1.5 m above base—rock is very vesicular; vesicularity increases upward making the rock nearly scoriaceous; vesicles are hollow

well-developed quartz-filled pipe vesicles with a few scattered quartz-filled vesicles above

mixed quartz-filled and hollow vesicles, some with green cherty cryptocrystalline quartz-filling, roughly layered

82M-133 - medium bluish-gray, fine- to med.-grained, amygdaloidal, hollow vesicles on weathered surfaces, vesicles are small (1 - 3 mm) quartz- and chlorite-filled with disseminated sulfides

approx. 1-m-thick zone of hollow vesicles

very well-developed pipe vesicles

mixed hollow vesicles and quartz amygdules in upper portion of the flow unit, some are interconnected and layered, some are only partially filled

82M-129 - medium bluish-gray, fine-grained, orange-stained quartz amygdules—subspherical

1-m-thick zone of hollow vesicles

very well-developed pipe vesicles at the base of the flow unit

APPENDIX C

Chemical analyses of middle Belt carbonate sill in Glacier National Park from Mejstrick (1975). "Analyses are by x-ray florescence, except for Na_2O which are by atomic absorption. Each analysis represents the average of two analyses from separate fractions of the handspecimen". Analyses 1-9 are from Mejstrick's Siyeh Pass section. Analyses 10, 11, and 12 are from the chill zone of the sill at Siyeh Pass, Dawson Pass, and Yarrow Creek, respectively. Total iron is reported as FeO.

	1	2	3	4	5	6	7	8	9	10	11	12
	Major oxides (weight percent)											
SiO_2	48.9	48.7	48.9	49.4	48.8	51.1	50.7	50.7	52.3	48.9	48.8	49.0
TiO_2	4.3	4.2	3.7	3.9	4.4	3.8	3.6	4.2	3.4	4.3	4.0	4.3
Al_2O_3	12.5	12.1	11.9	10.8	10.3	14.6	14.6	14.4	13.7	12.5	12.4	12.6
FeO	11.9	12.1	13.9	11.7	12.4	12.3	12.9	12.2	12.6	11.9	12.5	12.3
MgO	7.7	7.6	9.2	9.5	10.0	4.7	4.7	5.1	4.5	7.7	8.2	7.8
CaO	10.0	10.2	8.9	10.8	10.9	7.6	7.4	8.4	8.2	10.0	9.0	9.2
Na_2O	4.9	4.1	4.1	3.2	3.2	5.8	5.1	4.8	4.6	4.9	4.5	5.2
K_2O	1.0	1.3	.74	1.0	1.3	1.8	1.8	1.5	1.9	1.0	1.7	1.5
Total	101.2	100.3	101.3	101.3	101.4	101.7	100.8	101.3	101.2	101.2	101.1	101.9

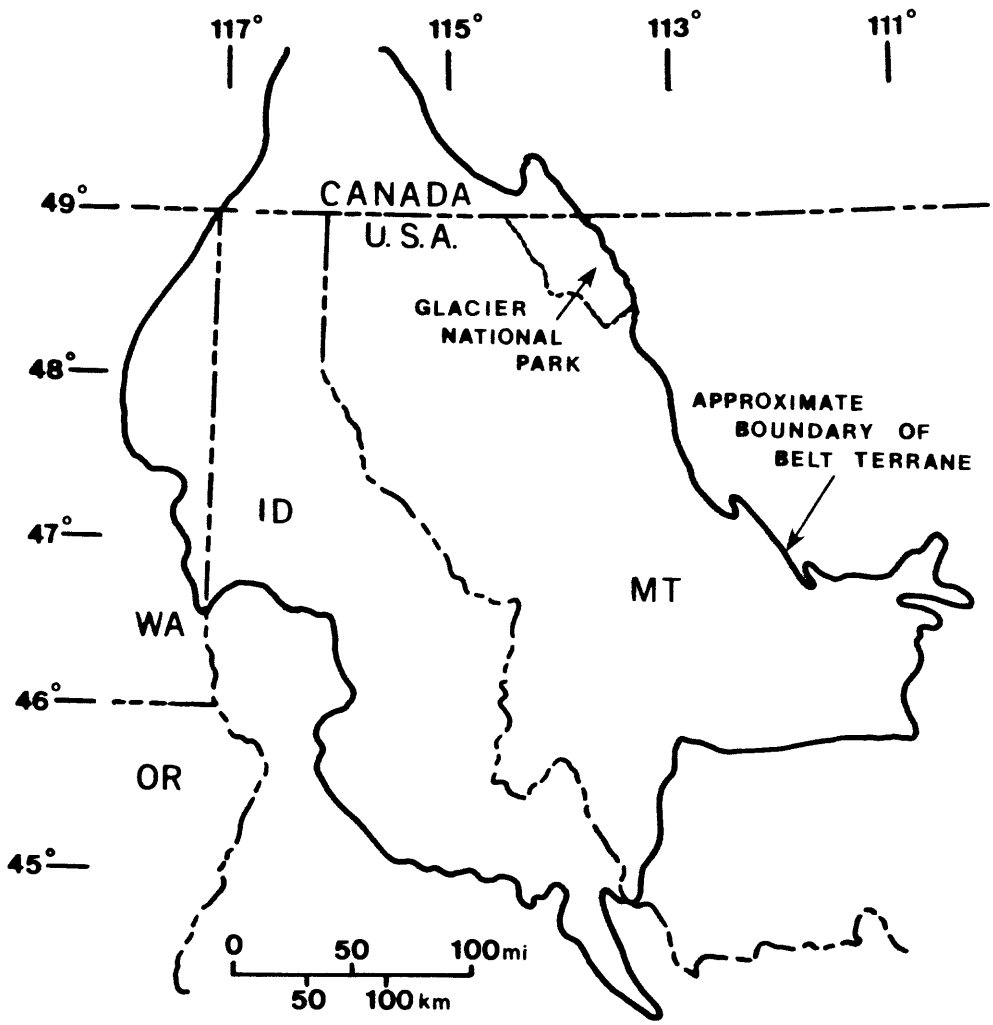

Figure 1. Location of Glacier National Park within the present boundaries of Belt terrane. (Modified after Harrison, 1972).

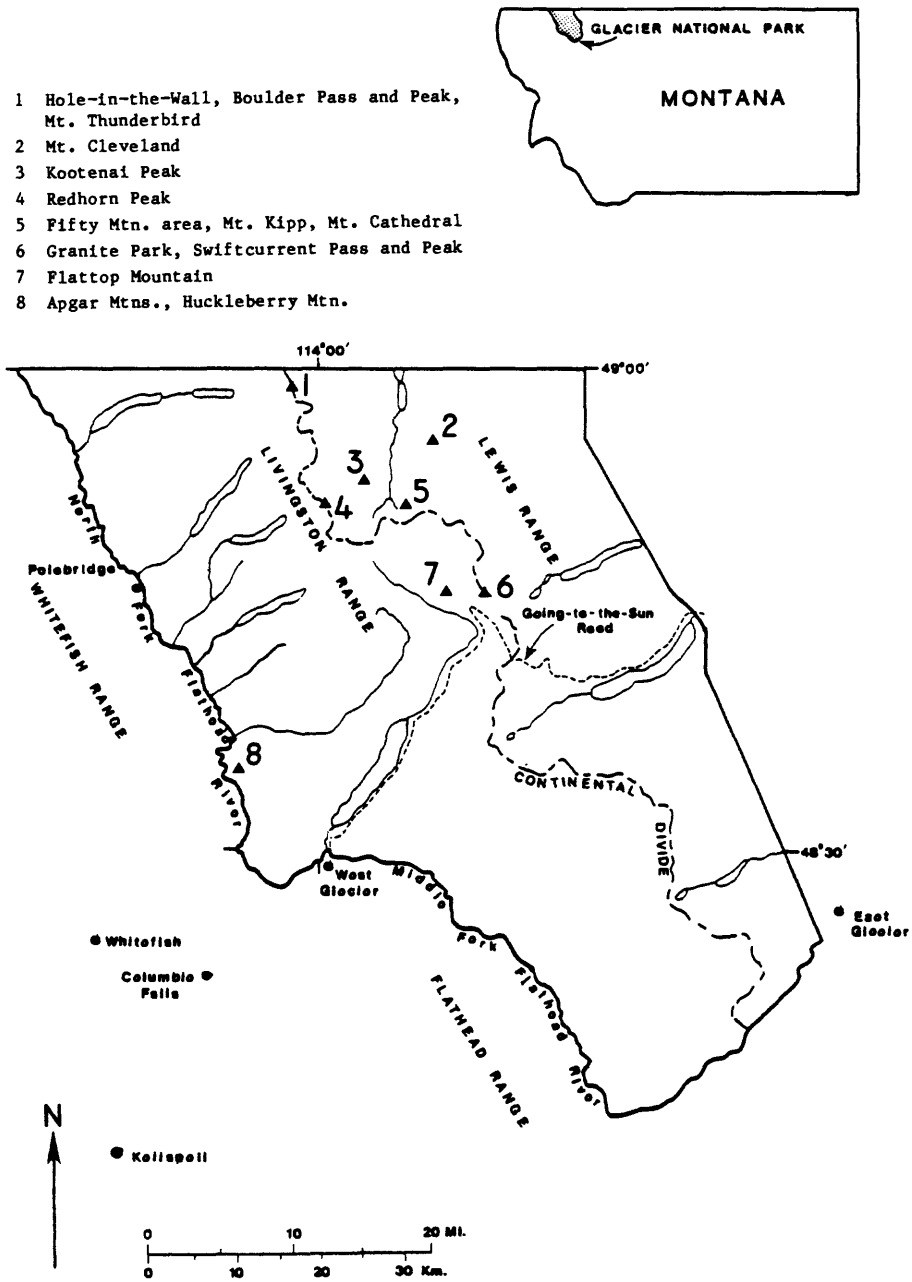

Figure 2. Physiographic map of Glacier National Park showing location of Purcell Lava exposures examined in this study.

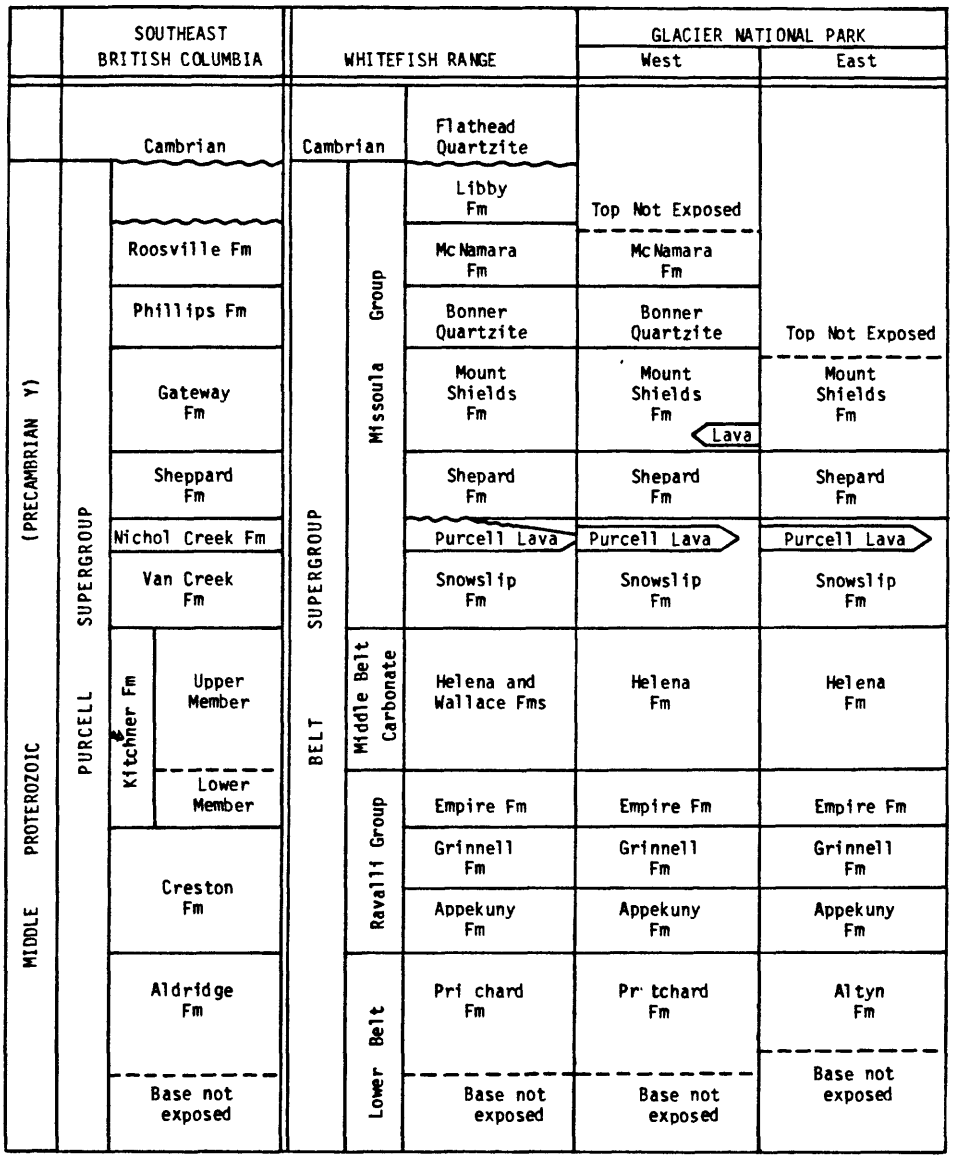

Figure 3. Generalized correlation chart for the Belt and Purcell Supergroups in Glacier National Park, Whitefish Range, and southeastern British Columbia. Modified after Whipple and others (1984).

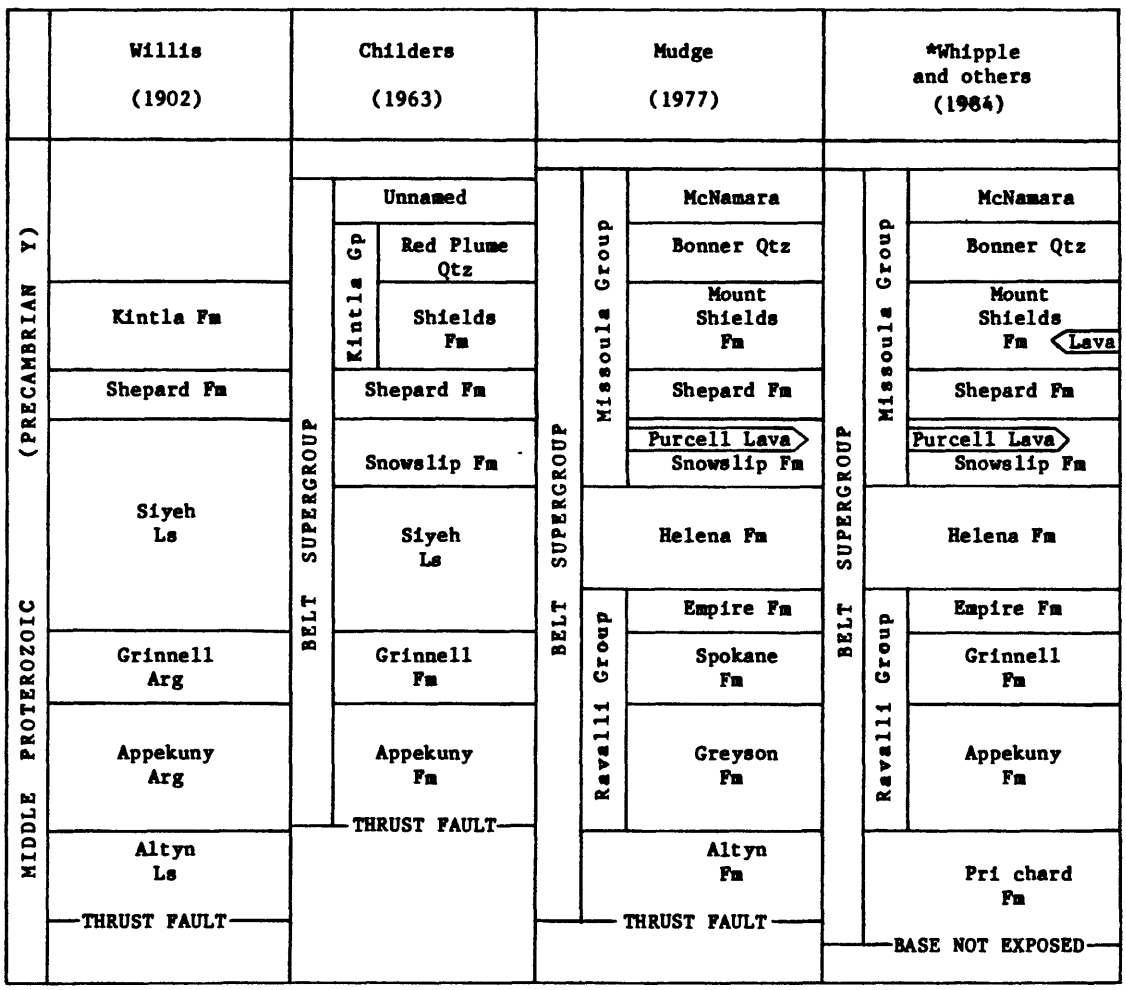

Figure 4. Correlation of past and present stratigraphic terminology within Glacier National Park. *Stratigraphic column for the portion of Glacier National Park west of the continental divide, modified after Whipple and others (1984).

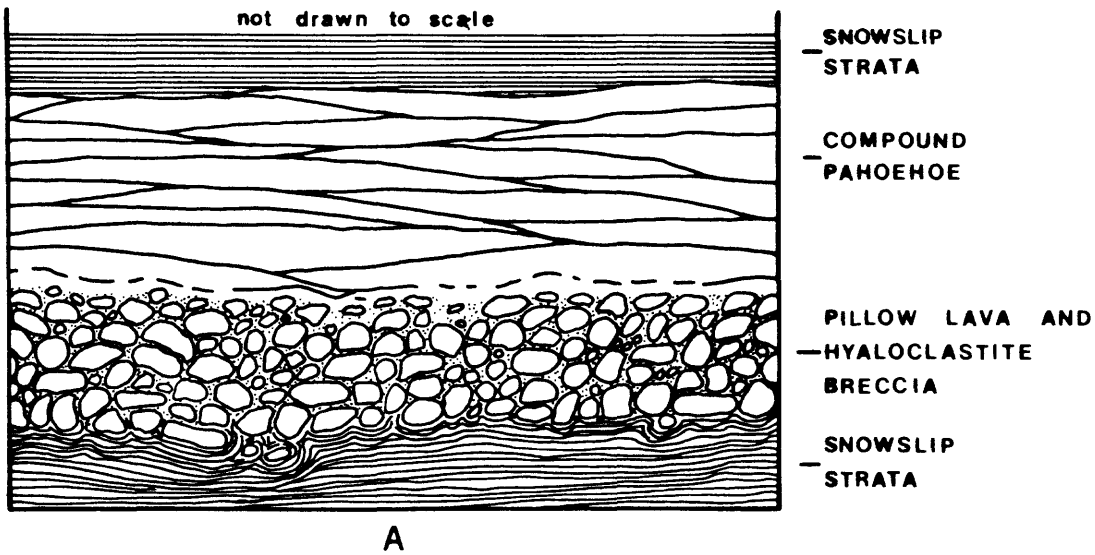

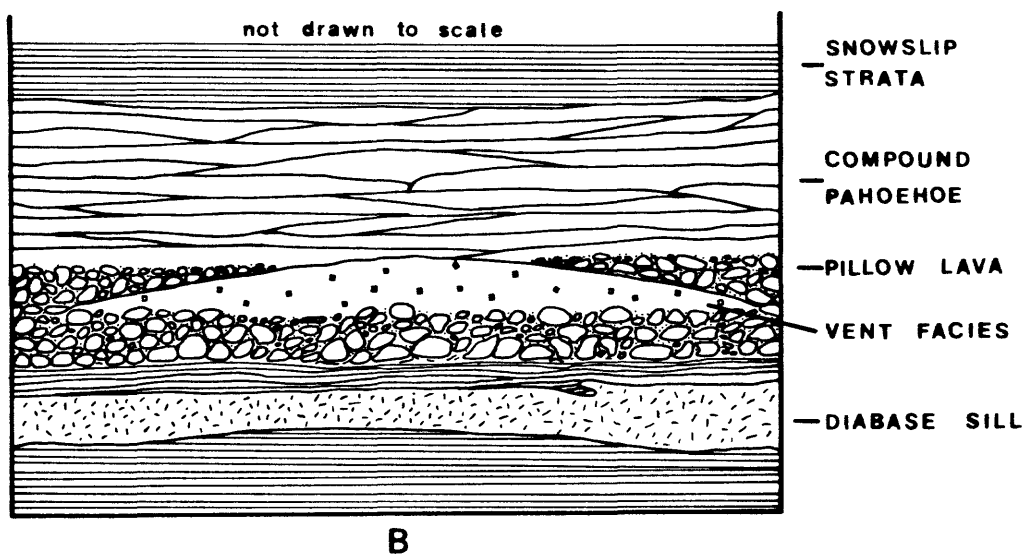

Figure 5. Cross-sectional sketches showing the general stratigraphic relationship of Purcell Lava facies: (A) normal succession of pillow lava overlain by pahoehoe flow-units, (B) pillow lava and pahoehoe flow units with local vent rocks and diabase sill. Not drawn to scale.

Figure 6a. Outwardly protruding pillows such as this produce the hummocky outcrop shown in (b).

Figure 6b. Distinctive hummocky outcrop produced by outwardly protruding, bulbous pillows. Located at Mt. Kipp in the Fifty Mountain area.

Figure 7. Matrix (hyaloclastite) supported pillows, Fifty Mountain.

Figure 8a. Ruptured and partially drained pillow at Granite Park. Dog-toothed quartz crystals line the cavity wall.

Figure 8b. Ruptured and partially drained pillow at Fifty Mountain. The flat-bottomed cavity marks the former lava level.

(a)

(a)

Figure 10. Relatively undeformed sediment slabs that were displaced upwards as much as 1 m during emplacement of pillow lava, Kootenai Peak. Jacobs staff is set at 1 m in photograph (b).

Figure 9a. At the base of the pillowed facies, some pillows were forcibly emplaced into the soft Snowslip sediment. Not only was bedding deformed, but sediment was squeezed up between and around pillows. Exposure is located at Fifty Mountain.

Figure 9b. Intense soft-sediment deformation produced during pillow emplacement, Granite Park. Note that the pillow in the lower right corner is entirely buried. The basal contact of the Purcell Lava with the Snowslip Formation is thus locally very irregular.

Figure 11. Hyaloclastite tuff beds, about 1 cm thick, interlayered with Snowslip sediment at basal contact with pillow lava, Kootenai Peak. The mass in upper right corner is the edge of a pillow.

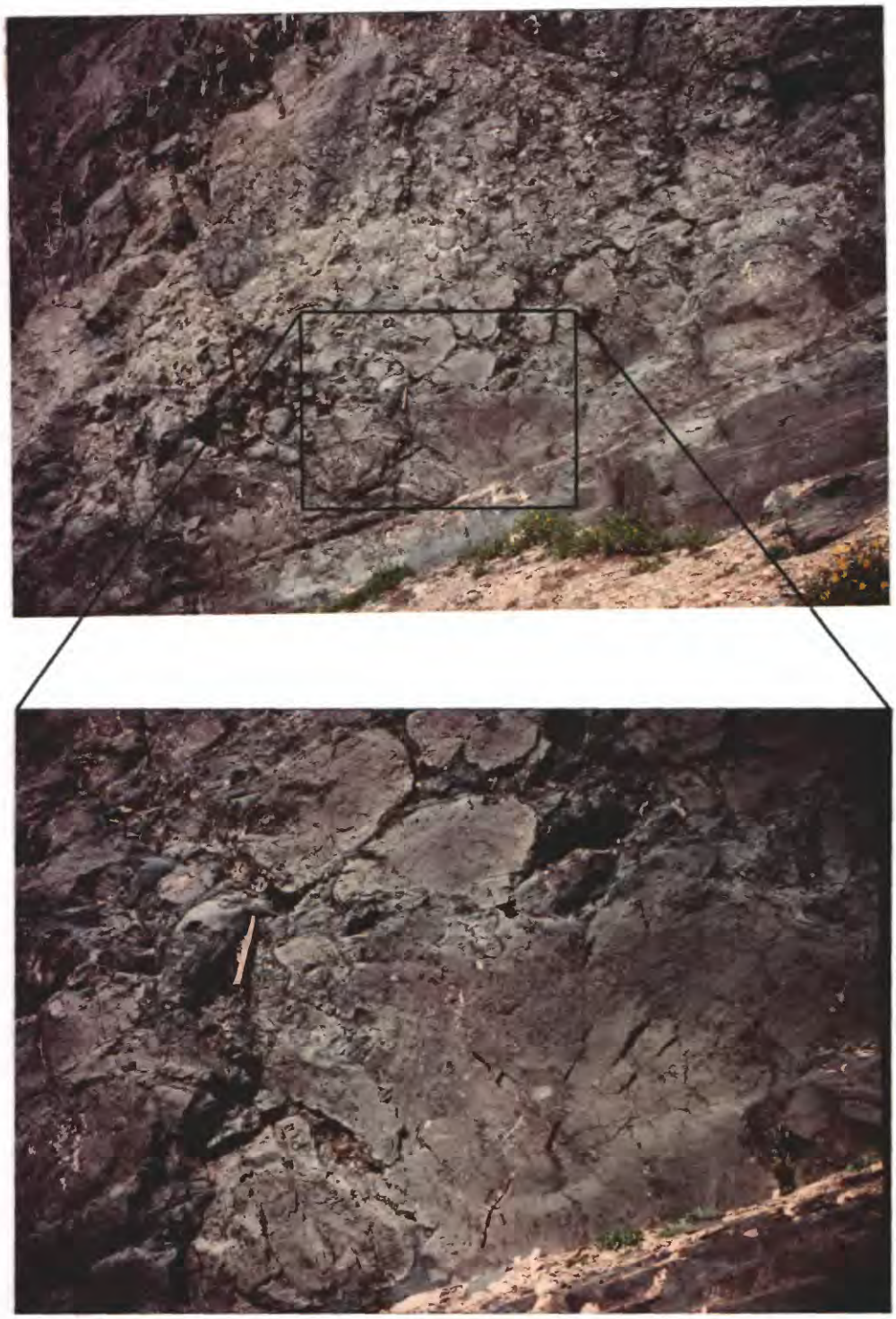

Figure 12a. Large (greater than 2 m) massive zone in the pillowed facies, Kootenai Peak. The zone has slightly rounded borders and lies amid pillows that are, in general, less than 1 m in diameter. Massive zones in the pillow lava facies represent either congealed feeder tubes or exceptionally large pillows.

Figure 12b. Massive zone, 2 m in diameter, with well-rounded borders, Kootenai Peak. Note the well-developed pipe vesicles at the base.

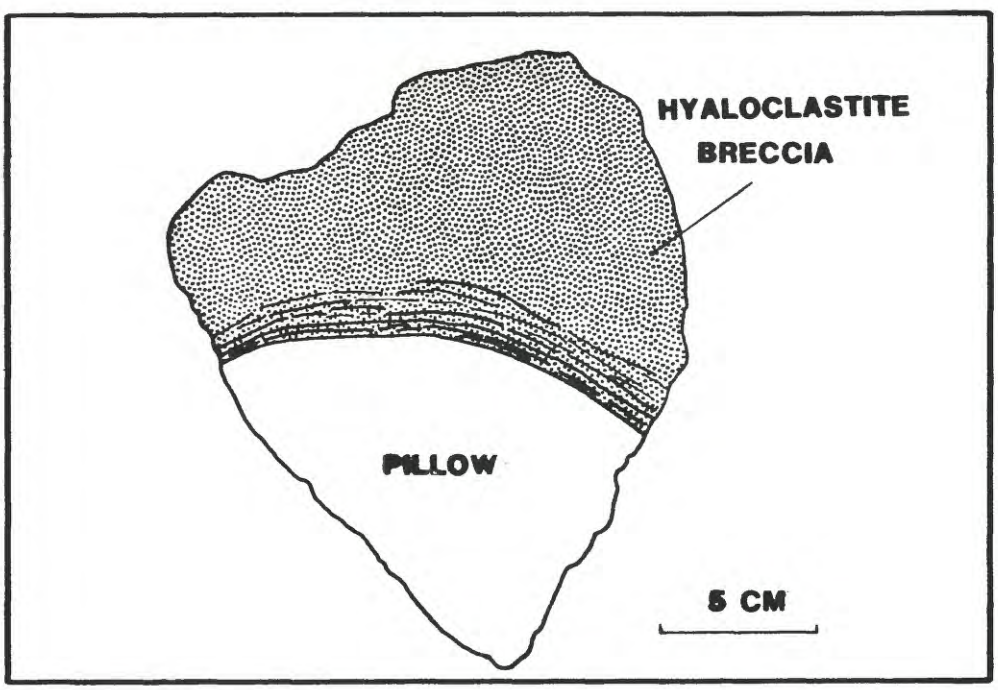

Figure 13. Cross section of a pillow showing thick, concentrically layered, hyaloclastite breccia that probably formed from incomplete spalling during pillow implosion. Collected from the Apgar Mountain section.

Figure 14a. Subspherical vesicles concentrically arranged about the perimeter of a small pillow, Granite Park. Note the radial cooling cracks.

Figure 14b. Pipe vesicles concentrically arranged about the perimeter of a pillow at Granite Park. Pillow is surrounded by hyaloclastite breccia.

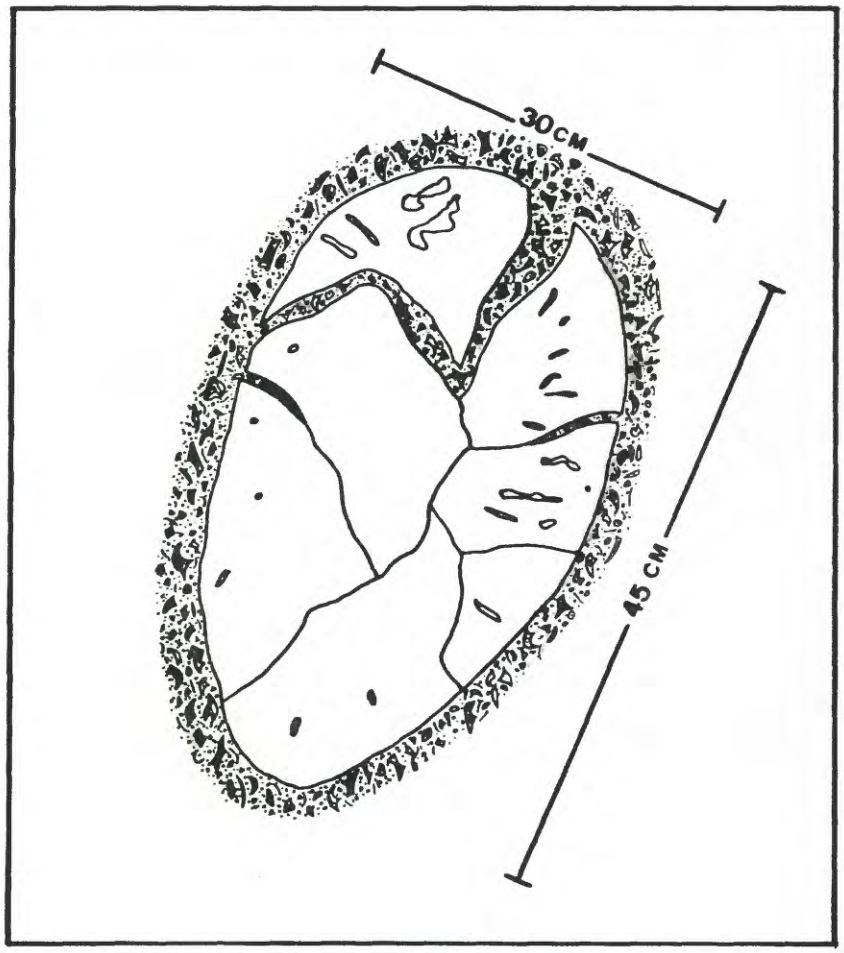

Figure 15. Cross section of fractured pillow, Granite Park. Hyaloclastite breccia fills some of the larger cracks and probably formed in situ by thermal shock granulation.

Figure 16. Cross-sectional view of interconnected pillows, Hole-in-the-Wall.

Figure 17a. Tightly-packed pillows with little interstitial hyaloclastite breccia, Hole-in-the-Wall. The pillows are slightly irregular in shape; note the flat tabular pillow draped over one that is tubular in form.

Figure 17b. Elongate, closely-packed, tubular pillows at Granite Park.

Figure 18. Bulbous and cylindrical pillows at Hole-in-the-Wall. For comparison with modern analogs, see Figure 40.2-A of Moore and Reed (1963), and p. 20-23 of Ballard and Moore (1977).

Figure 19a. Elongate, sinuous pillow at Fifty Mountain section. The material between pillows is hyaloclastite breccia.

Figure 19b. Elongate, sinuous pillow at Granite Park partially surrounded by hyaloclastite breccia. The slightly flattened top is due to glacial scour.

Figure 19c. Elongate, sinuous pillows that form a tangled, entrail-like mass. Individual pillows are traceable for up to 2 m before disappearing into the conglomeratic mass. Location is a dipslope less than 1 km south of the campground at Fifty Mountain.

Figure 20a. Pinching and swelling of pillows during lateral budding produced the "neck and bulb" shape. The "neck" is left of the hammer. Exposure is located at Fifty Mountain area.

Figure 20b. Elongate, sinuous pillow that abruptly changed direction during budding; Fifty Mountain area.

Figure 21a. Isolated-pillow breccia that occurs locally in the upper part of the pillowed facies. The subfacies is characterized by irregularly shaped, widely spaced pillows that are surrounded by voluminous hyaloclastite breccia. Outcrop pictured above is located at Granite Park.

Figure 21b. Isolated-pillow breccia in the upper portion of the pillowed facies at Granite Park.

Figure 22. Broken-pillow breccia within the pillowed facies at Granite Park. Pillow fragments rest in a matrix of hyaloclastite breccia.

Figure 23a. Tongue-like pillow in the coalesced pillow zone near the top of the pillowed facies at Hole-in-the-Wall. The coalesced pillow zone marks the transition from the pillowed facies to the pahoehoe facies.

Figure 23b. Coalesced pillows at the transition from pillowed facies to pahoehoe facies. The hammer rests on a small, isolated patch of hyaloclastite breccia, the presence of which suggests that the mass was emplaced under or into water. How far underwater? Note the fluidal banding and flow structures. The lava that formed these pillow masses was not quickly chilled but instead remained hot and fluid long enough to spread laterally and coalesce with adjacent masses. This suggests that the lava was emplaced at or near the water surface.

Figure 24. Ropy texture of pahoehoe toes at the transition from the pillowed facies to the pahoehoe facies, Fifty Mountain.

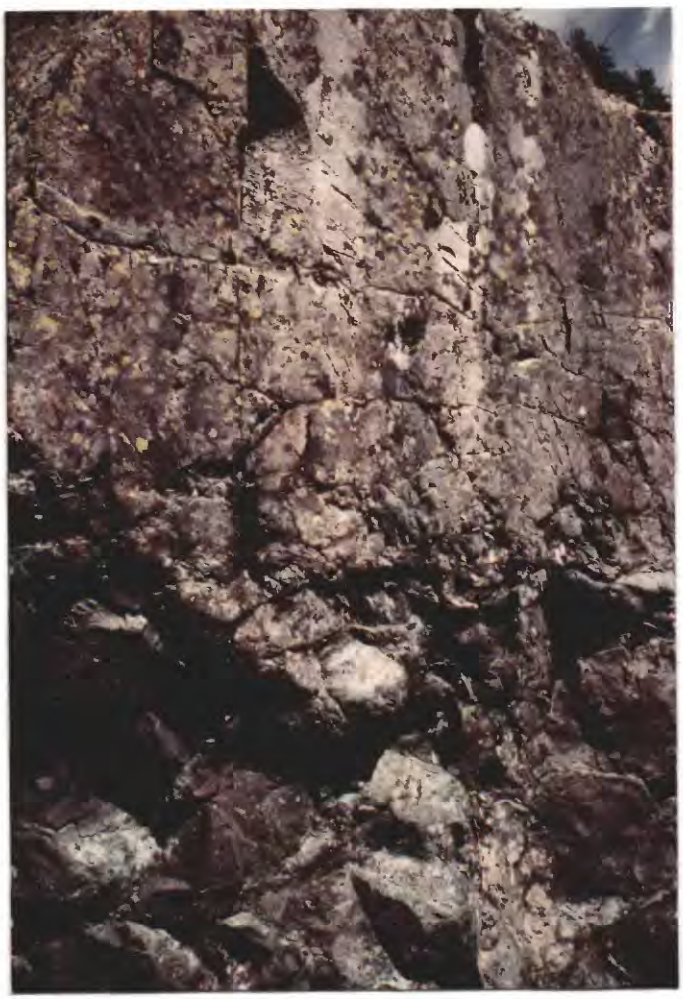

Figure 25a. Cross-sectional view of the transition from the upper pillow facies to the pahoehoe facies, Fifty Mountain. Zone in the center of photograph is the coalesced pillow subfacies.

Figure 25b. Cross-sectional view of the transition from the upper pillow facies to the pahoehoe unit, Fifty Mountain.

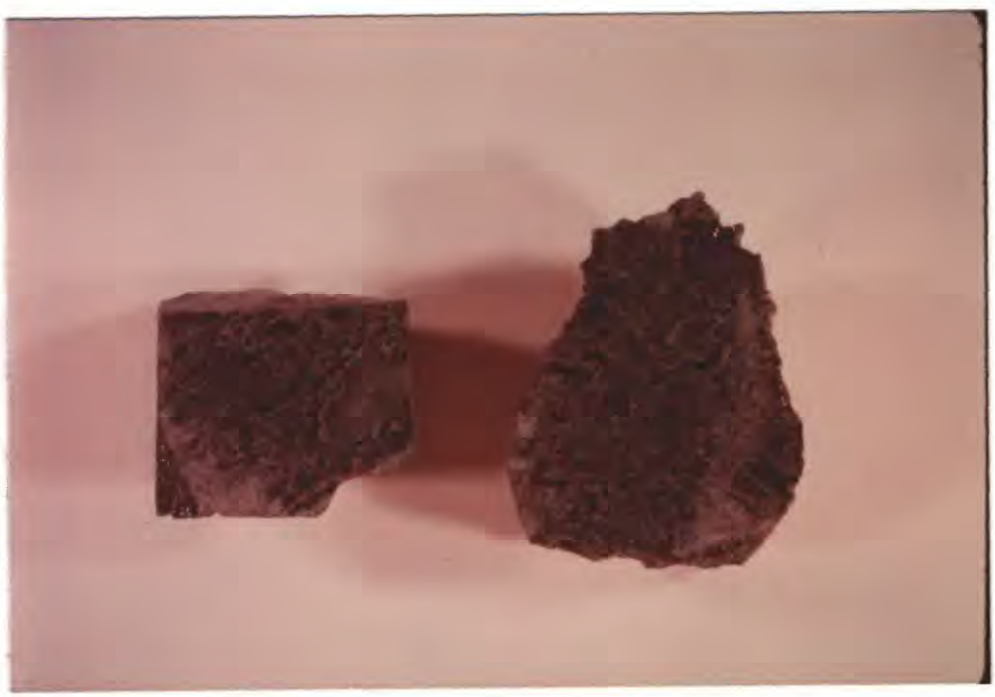

Figure 26. Interpillow hyaloclastite breccia. Fragments are chloritized sub-rounded globules and angular shards. For scale, sample on left is 5 cm across.

Figure 27. Erosionally truncated flow units form a stair-stepped slope, Hole-in-the-Wall. The Purcell Lava was referred to only as "trap" by early workers like Dawson (1875, p. 62) and Bauerman (1884, p. 26), a term used to describe any dark-colored, fine-grained, nongranitic hypabyssal or extrusive rock. The term originated from the Swedish word trappa, meaning "stair-stepped" (Bates and Jackson, 1980).

Figure 28a. Tabular flow unit in the pahoehoe facies of the Purcell Lava, Granite Park.

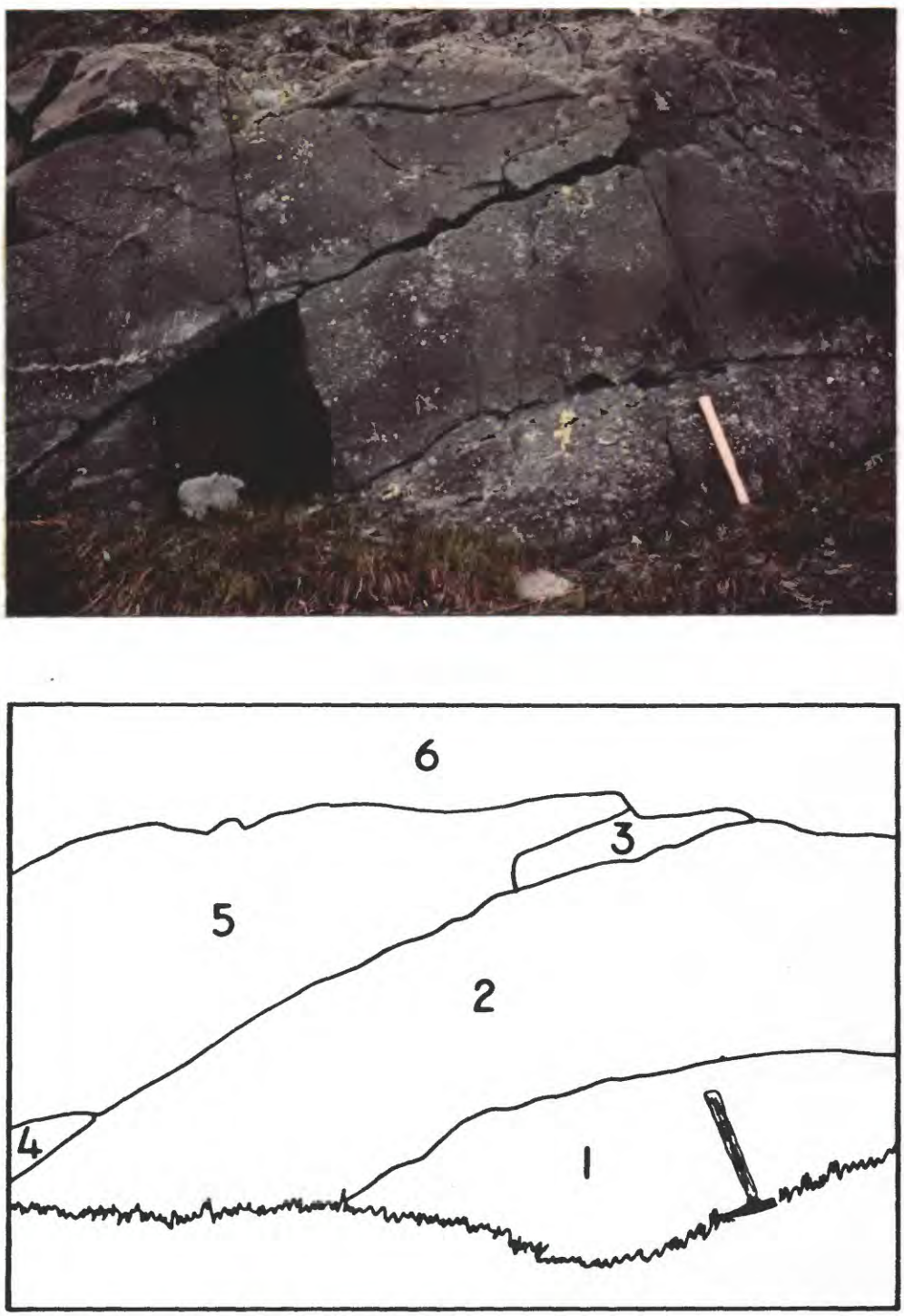

Figure 28b. Lenticular flow units at Granite Park. Tracing shows location of flow units. Regional dip of the strata at Granite Park is 15° to 20° towards the left side of the photograph.

Figure 28c. Fan-shaped lava tongues of the pahoehoe facies, Fifty Mountain. Note that the small fan of ropy pahoehoe in foreground spilled from the side of the larger fan to the upper right.

Figure 29. Three flow units at Hole-in-the-Wall. Hammer rests at the contact between the lower two flow units; pipe vesicles are visible extending up from near the base of the middle flow unit. Note the concentration of subspherical cavities in the upper part of the lower flow unit (below hammer). The upper and lower boundaries of nearly all flow units are easily discernable on the basis of pipes near the base and concentrations of subspherical cavities near the top.

(a)

(b)

Figure 30. Thin (less than 1 cm thick), pale-olive flow tops are characteristic of many flow units. The flow-unit in (a) is located on the southeast flank of Kootenai Peak; the outcrop shown in (b) is located at Hole-in-the-Wall. Note the pipe vesicles extending upwards from the base of the upper flow unit in (b).

Figure 31a. Ropy texture of pahoehoe flow unit, Fifty Mountain.

Figure 31b. Ropy flow textures on the upper surfaces of pahoehoe flow units at Hole-in-the-Wall.

Figure 31c. Ropy pahoehoe, southwest flank of Boulder Peak, about .5 km south of the Boulder Pass campground.

Figure 32. Bleached and oxidized zone at the top of an uppermost flow unit at Thunderbird Mountain. The zone probably represents weathering (subaerial) prior to depostion of the overlying sediments of the Snowslip Formation.

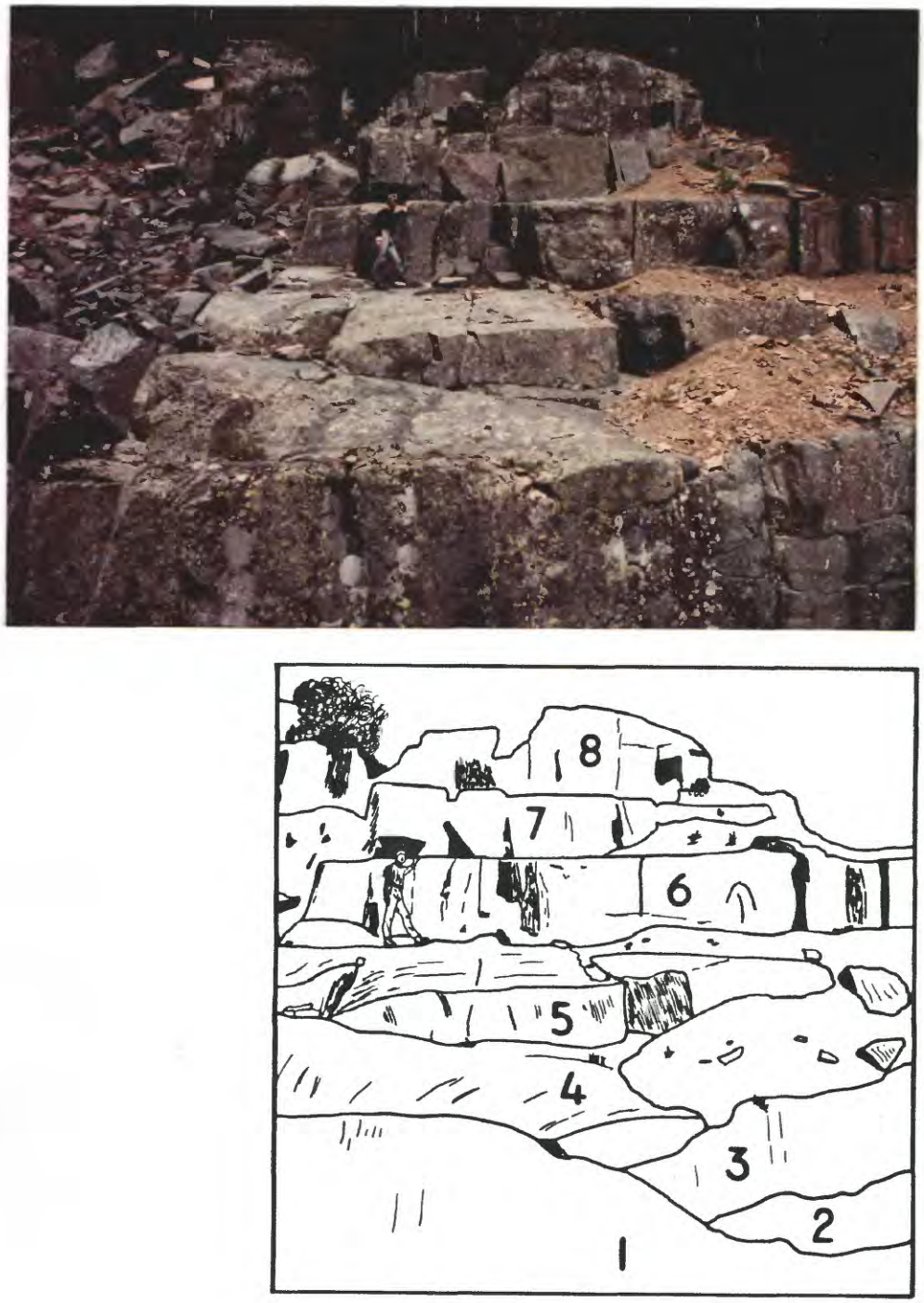

Figure 33. Typical flow units of the Purcell Lava. Most are irregular in shape having conformed to the surface topography of underlying flow units. Area in photograph is located on the southwest flank of Swiftcurrent Peak, about 1 km north of the Granite Park Chalet. Lower sketch is of the photograph and indicates flow units and the order of emplacement.

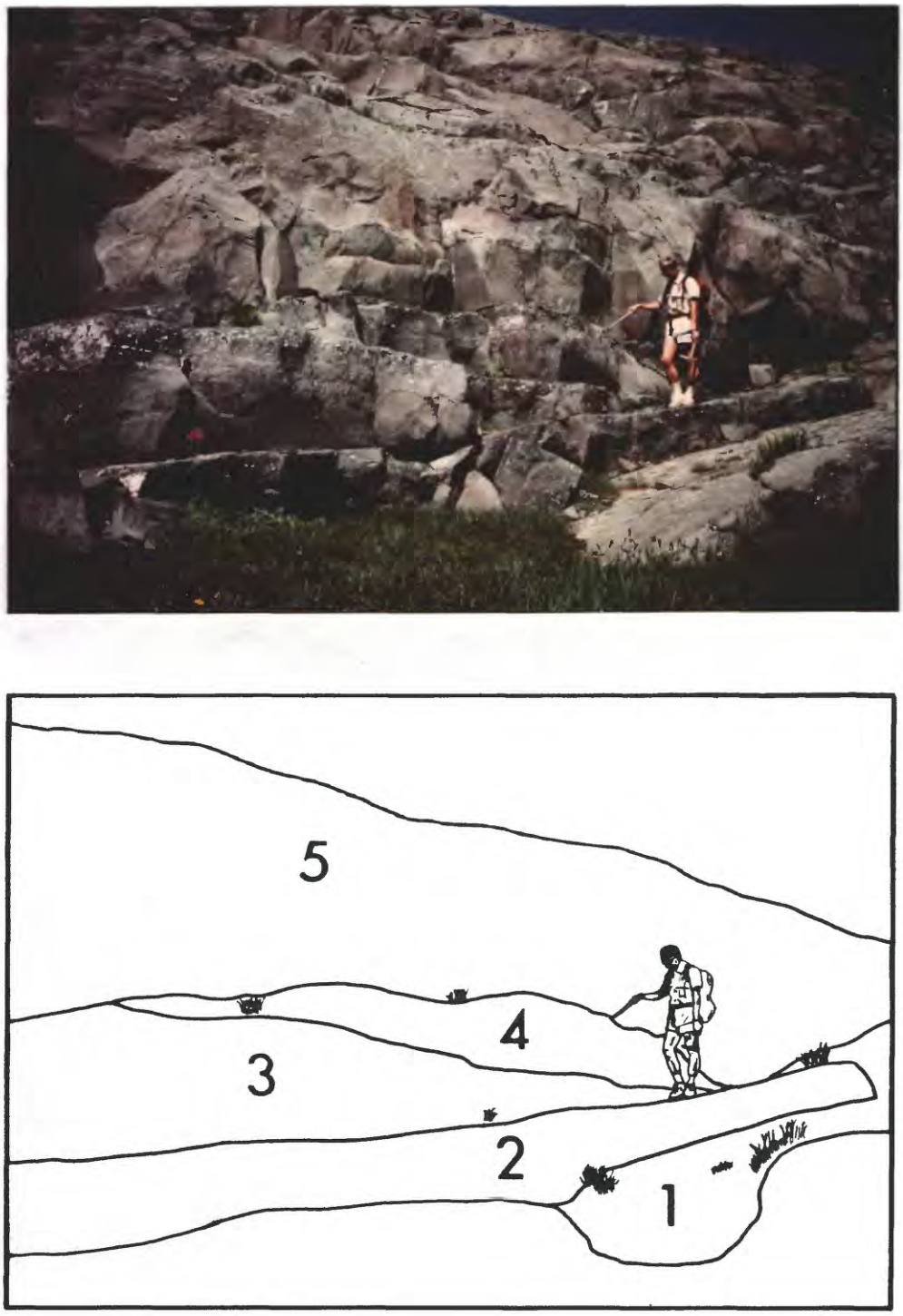

Figure 34. Flow units of the Purcell Lava typically thin gradually and pinch out. The exposure shown above is located at Hole-in-the-Wall and consists of several overlapping flow units. Lower sketch is from the photograph and indicates the flow units and the order in which they were emplaced.

(a)

(b)

Figure 35. Thin lobes of scaly pahoehoe that have smooth, billowy surfaces and protruding toes. Location of (a) is the southwest flank of Boulder Peak; (b) is from the flat-bottomed valley north of Boulder Peak. Pahoehoe toes can look very much like flattened pillows. However, nearly all pillows in the Purcell Lava are associated with hyaloclastite breccia. The breccia is not found in conjunction with pahoehoe lobes and toes.

Figure 36. Top of a flow unit at Hole-in-the-Wall that has adjacent surface ropes convex in opposite directions. Flow of lava could have been towards the bottom of the photograph as suggested by the convexity of the flow structure on the right, or, using the flow structure to the left, flow could have been towards the top of the photograph. This illustrates that caution must be used when attempting to determine regional flow direction using the convexity of pahoehoe ropes, especially in partially exposed terrain.

Figure 37. Cross-sectional exposure of massive pahoehoe with tumulus at Hole-in-the-Wall. The flow unit is thick (as much as 2 m) at the center but thins abruptly at the outer margins. Photo by Ed Larson.

Figure 38. Thin, tightly overlapping flow units of scaly pahoehoe at Hole-in-the-Wall. Hammer rests at the contact of two flow units. Note the well-developed pipe vesicles at the bases, and the coalesced vesicles in horizontal layers near the tops of the flow units.

Figure 39. Amygdaloidal pipe vesicles at the base of a flow unit at Hole-in-the-Wall. Amygdules are quartz. Photo by Ed Larson.

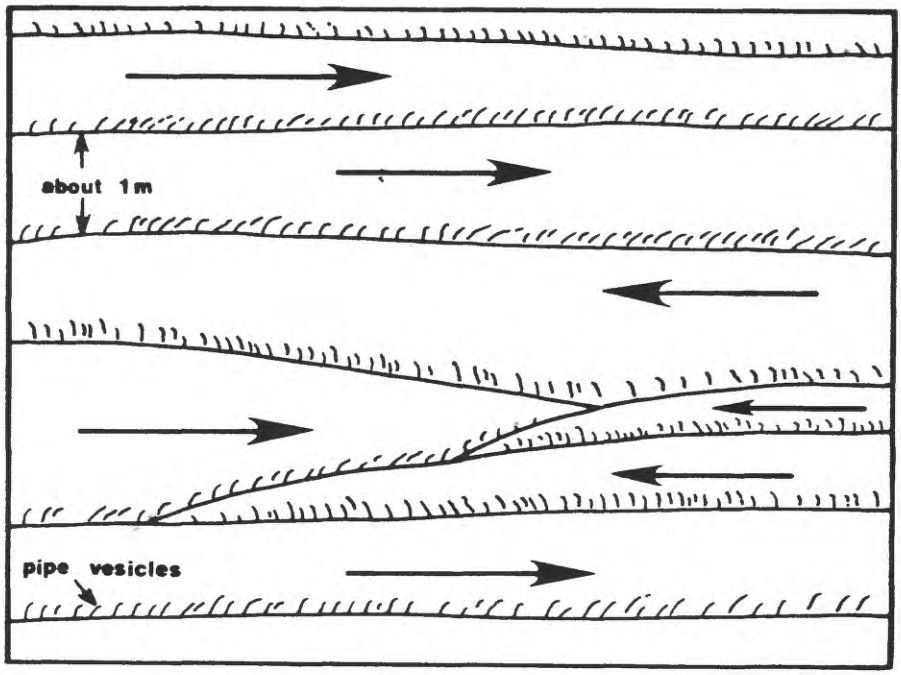

Figure 40. Some flow units were clearly emplaced from opposite directions as indicated by the inclination of pipe vesicles. The sketch above is based on exposures at Hole-in-the-Wall where flow units were emplaced generally from the north and south. This may indicate the presence of multiple sources for the lava, an idea elaborated in Chapter 4. Pipe vesicles are not drawn to scale.

Figure 41. Layers of coalesced vesicles in flow units at Boulder Pass campground. The vesicle layers are generally concentrated in the upper one-third of a flow unit. The base of the flow unit shown is not exposed. The outcrop in is approximately 2 m high.

Figure 42a. Lava-filled crack in a flow unit located in the flat-bottomed valley slightly north of Boulder Peak. Because the surface has been glacially scoured, it is difficult to determine whether the feature represents a linear squeeze-up (Nichols, 1939), or contraction crack formed during cooling that was filled with lava from the succeeding flow.

Figure 42b. Cross-sectional view of lava-filled crack at Hole-in-the-Wall. Because it tapers downwards, the crack probably does not represent a squeeze-up, but instead formed by contraction during cooling and subsequently was filled by lava from the overlying flow unit. The rock within the crack is very fine-grained and lighter green in color than the wall rocks. Note the vesicles aligned near the outer margins of the filling.

Figure 43. Cooling crack in the ropy top of an upper flow unit at Granite Park. Snowslip sedimentary rock has been erosionally removed from the flow-top except for what remains in the crack and in the troughs between some of the ropes.

(a)

(b)

Figure 44. Primary slump and separation structures in uppermost flow units at Granite Park. Snowslip sediments were deposited conformably into the surface irregularities. Photograph (b) shows sediments that were deposited under an overhanging slab thus giving the appearance that the sediments were intercalated with the flow unit. The structures could represent collapsed lava channels.

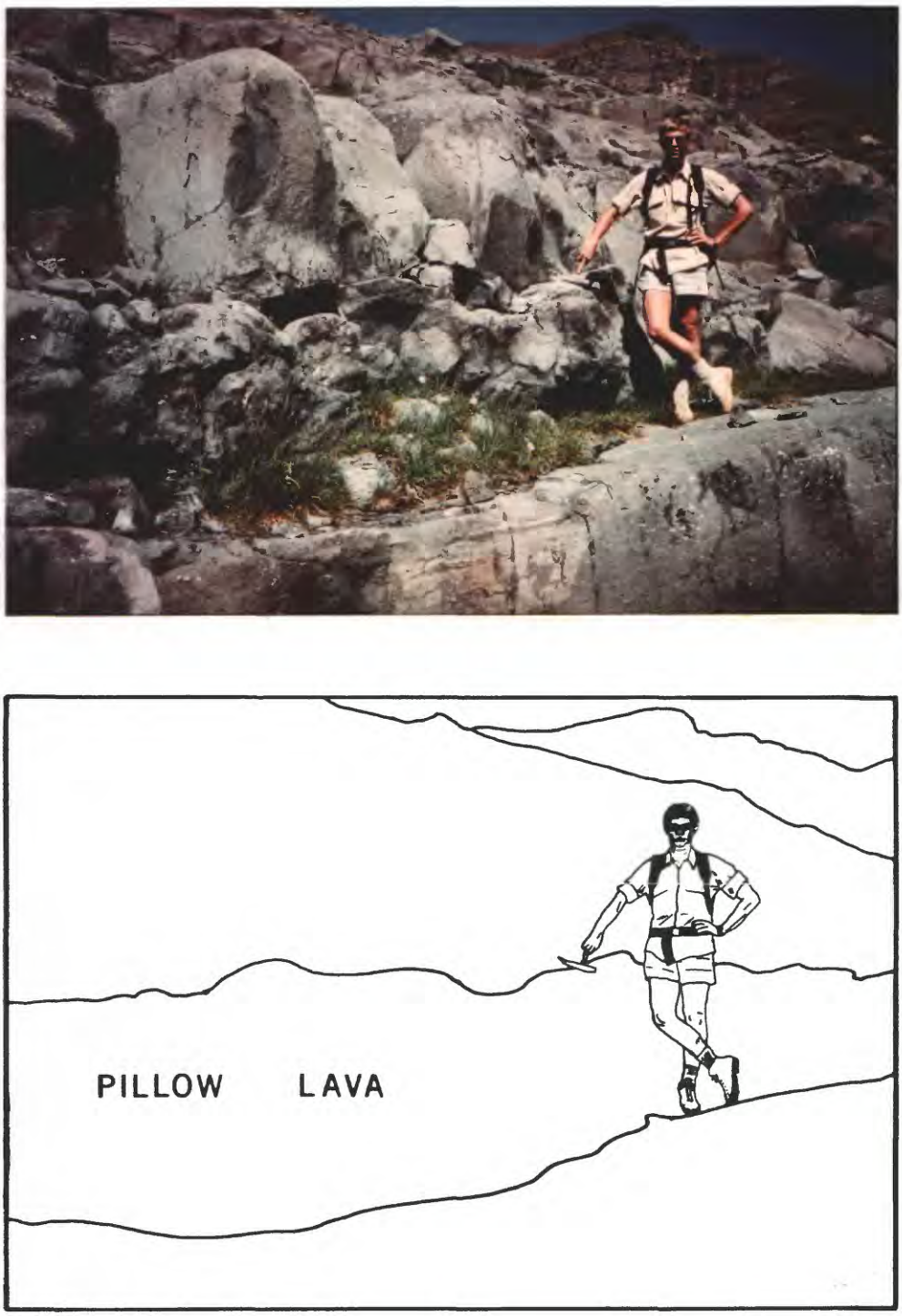

Figure 45a. Pillow lava interval within a pahoehoe flow unit at Hole-in-the-Wall containing small, irregularly shaped pillows surrounded by hyaloclastite breccia. The interval is less than 1 m thick, rests on top of a massive, ropy-topped flow unit, and grades upward into a 1-meter-thick ropy pahoehoe flow unit.

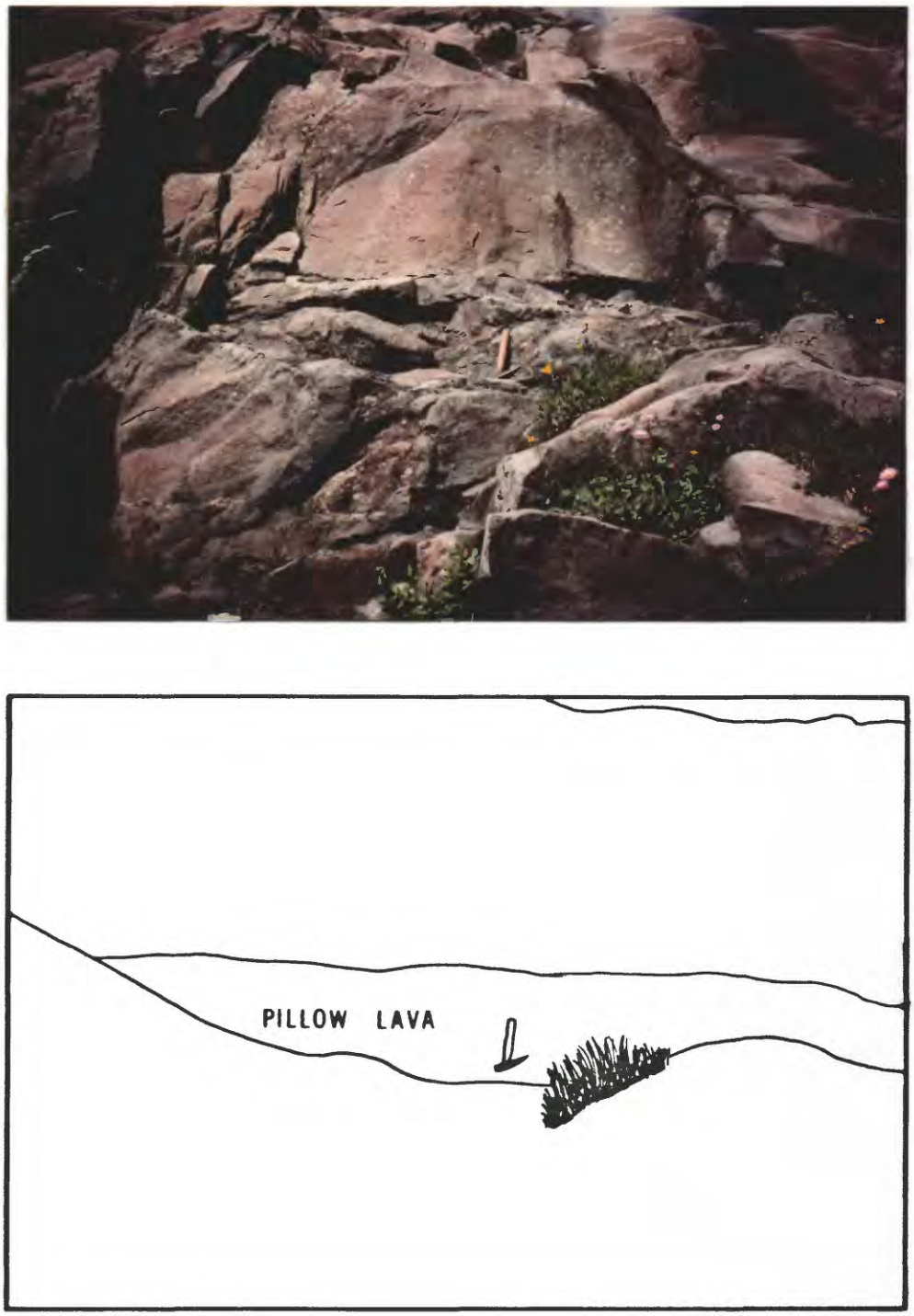

Figure 45b. Traced laterally, the pillow interval shown in Figure 43a terminates against a surface high point in the underlying flow unit. The pillows probably formed when a flow unit entered a localized body of ponded water. No other pillows or pillow intervals were found in the pahoehoe facies.

(a)

(b)

Figure 46. The vent facies is a chaotic breccia consisting of cognate blocks, bombs, and lapilli intermixed with accidental sediment blocks in a fine tuffaceous matrix. Photographs are from Hole-in-the-Wall, where the vent facies is best exposed. In (a), Ed Larson stands to the left of a large block of Snowslip sedimentary rock. Photograph (b) shows cognate blocks (note the pipe vesicles) in the vent facies.

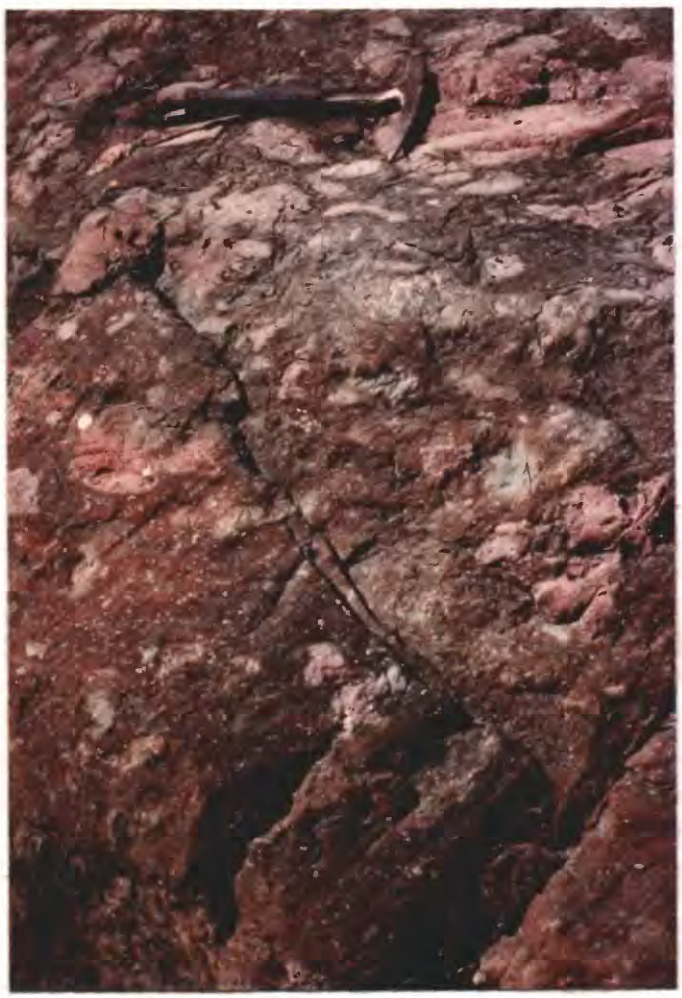

Figure 47a. Highly vesicular fragments in the vent facies unit are probably bombs and cinders; they are pinkish in color. Those above are located at Hole-in-the-Wall. Amygdule fillings are quartz and chlorite. Photograph by Ed Larson.

Figure 47b. Close-up view of pinkish-red, highly vesicular fragment from the vent facies at Hole-in-the-Wall. The dark amygdules are chlorite and the white ones are quartz. Photograph by Ed Larson.

(a)

(b)

Figure 48. Blocks of Snowslip sedimentary rock in the vent facies. In (a), primary bedding is nearly undisturbed; Redhorn Peak. Photograph (b) shows a larger block at Hole-in-the-Wall with intensely deformed sedimentary bedding indicating that the sediments were not well indurated when transported to the surface and ejected.

Figure 49a. Some blocks of Snowslip sediments were intensely deformed during the eruption that brought them to the surface. Sedimentary bedding is barely recognizable in the above pictured block.

Figure 49b. Reddish-orange blobs and streaks such as those in the vent facies pictured above near Redhorn Peak, presumably were chunks of Snowslip sediments that were broken apart and intensely deformed during the eruption.

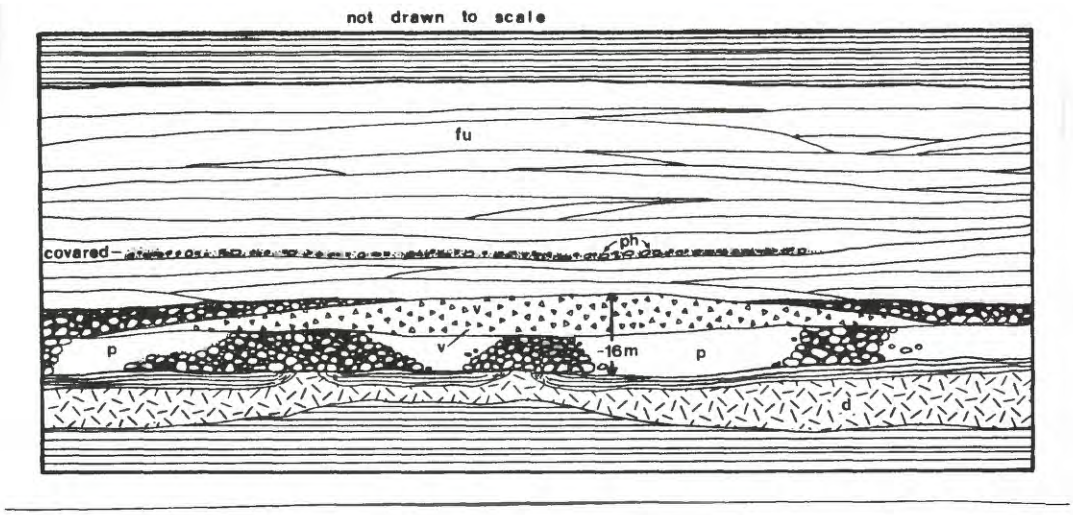

Figure 50. Schematic diagram showing the stratigraphic position of the vent facies at Hole-in-the-Wall. Symbols: d = diabase sill; p = pillow lava and gradational massive zones; ph = pilllow interval in a pahoehoe flow unit; fu = pahoehoe flow units. Strata above flow units, and below the pillow lava is Snowslip sedimentary rock.

Figure 51a. Cognate blocks in the outer margins of vent facies at Hole-in-the-Wall. Sediment blocks are absent. At this locality the unit looks very similar to broken-pillow breccia because of the abundance of pillow fragments.

Figure 51b. Small cognate blocks in the outer margin of the vent facies, Hole-in-the-Wall. Sediment blocks are absent and fragment size smaller than that located in the central portion of the facies.

Figure 51c. Cognate blocks in the vent facies, southwest flank of Boulder Peak. The block beneath hammer is a partial pillow.

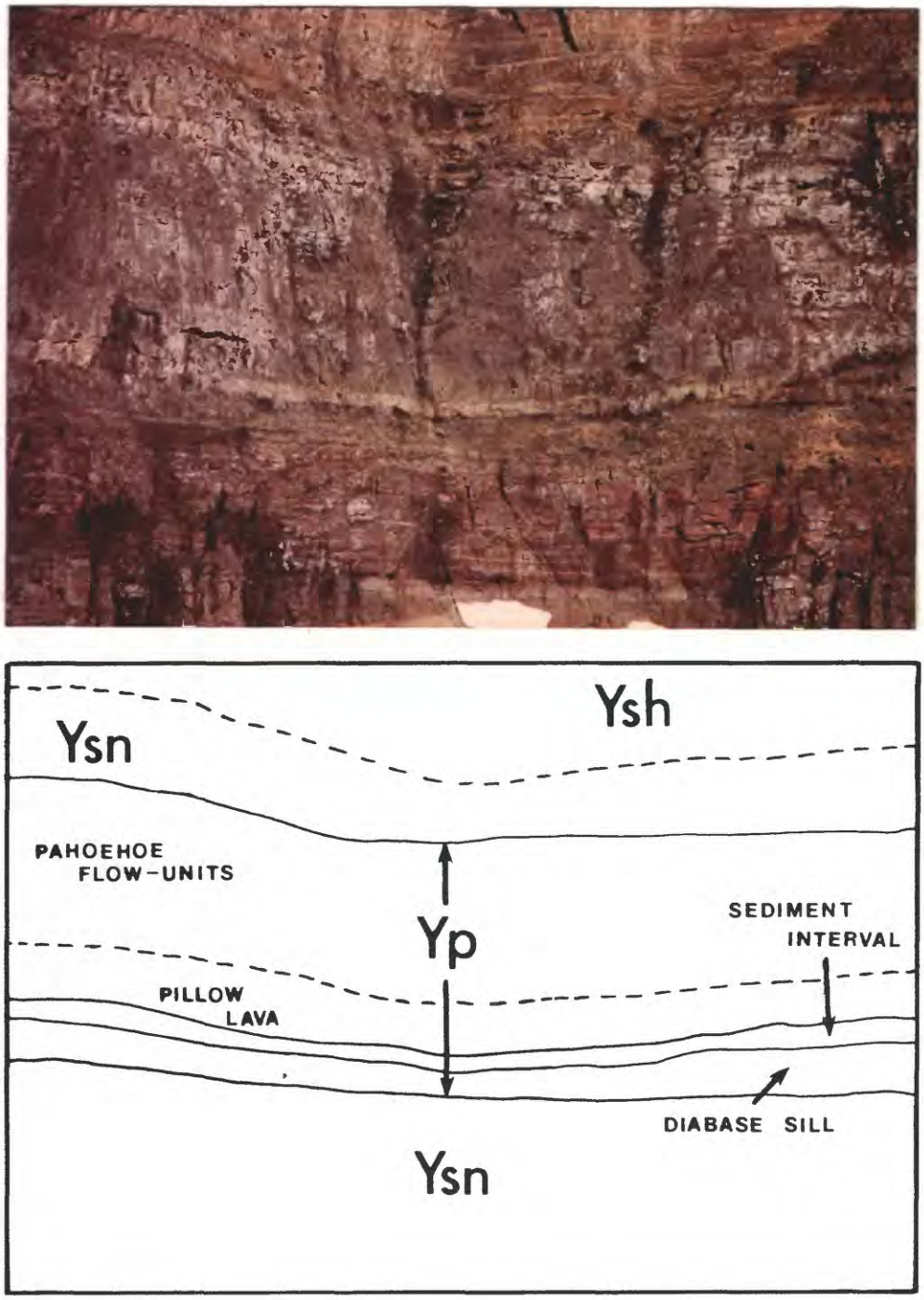

Figure 52. (a) View from Hole-in-the-Wall of the east flank of Boulder Peak where the Purcell Lava is exposed. (b) Tracing of the view shown in (a) indicating the location of specific units. Symbols: Ysn = Snowslip Formation, Yp = Purcell Lava, Ysh = Shepard Formation. The diabase sill is approximately 18 to 20 m thick; the sediment interval is about 5 m thick; the pillowed facies is about 12 m thick; and the pahoehoe flow units collectively are approximately 42 m thick. Because the cliff is lichen covered and inaccessable, the presence of the vent facies could not be varified. The measured section at Hole-in-the-Wall is about 1 km off to the right of view.

Figure 53. Abrupt thinning of diabase sill at Hole-in-the-Wall from a general thickness of about 18 to 20 m to less than 2 m occurs beneath the thickest part of the vent facies.

Figure 54. Apophysy of the diabase sill intruding into the Snowslip sediment interval at the upper contact of the sill at Hole-in-the-Wall. The apophysy was injected from a northerly direction (from right to left in the photograph). Such features are proof that the rock is intrusive rather than extrusive as previously interpreted (Fenton and Fenton, 1937; Ross, 1959).

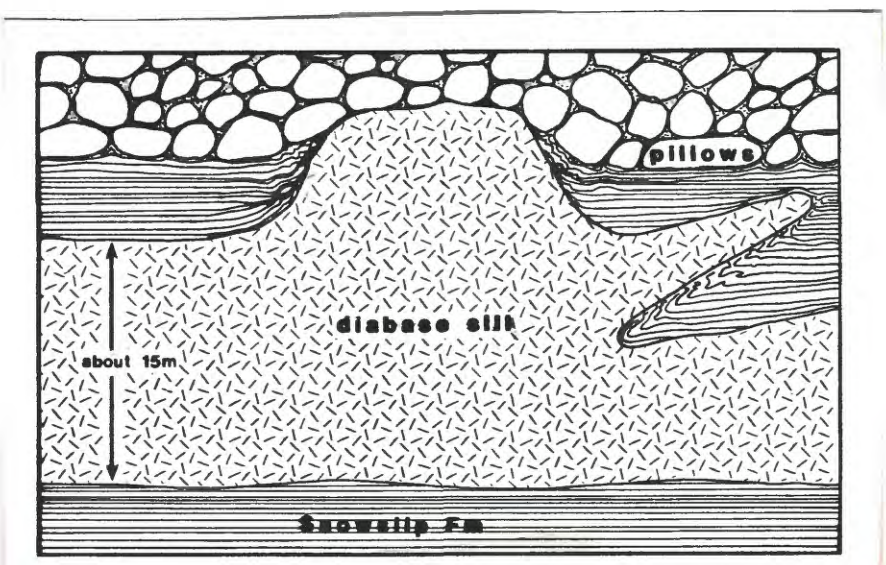

Figure 55. Schematic illustration of a cupola of the diabase sill breaching the Snowslip sediment interval and terminating against the base of overlying pillow lava. Cupolas of this type are located at the Hole-in-the-Wall section (along trail to Boulder Pass) and the southwest flank of Boulder Peak. Because the cupolas terminate against or intrude into pillow lava, the diabase sill must have been emplaced subsequent to emplacement of at least the lowermost pillows. Not drawn to scale.

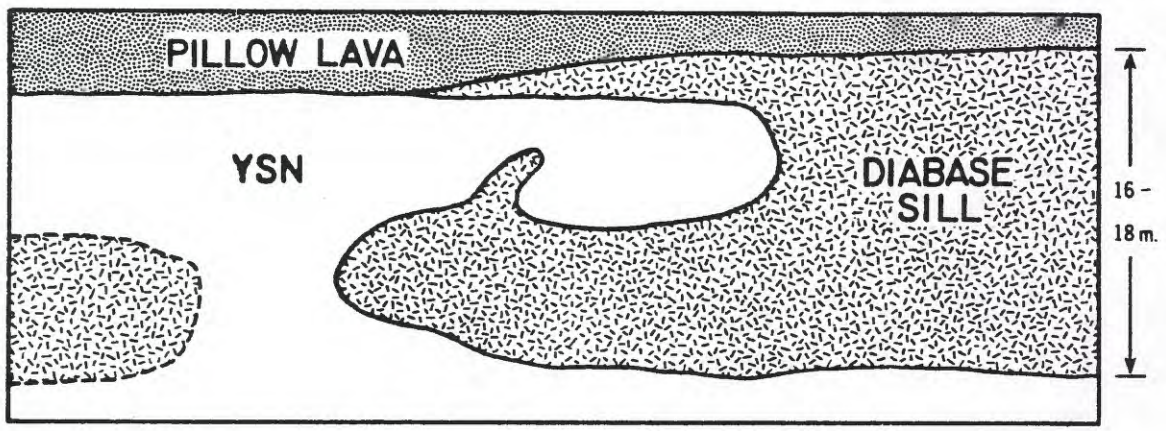

Figure 56a. Sketch showing intrusive relationship of the diabase sill at the head of Hole-in-the-Wall cirque. "Ysn" is the symbol for Snowslip sedimentary rock. North is into the page. Not drawn to scale.

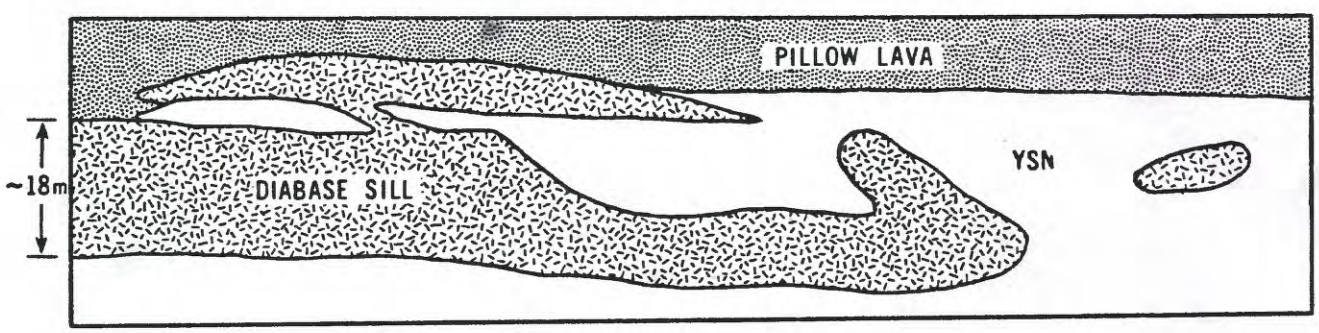

Figure 56b. Sketch showing the intrusive relationship of the diabase sill at the head of Hole-in-the-Wall cirque. "Ysn" is Snowslip sedimentary rock. Not drawn to scale. North is into the page.

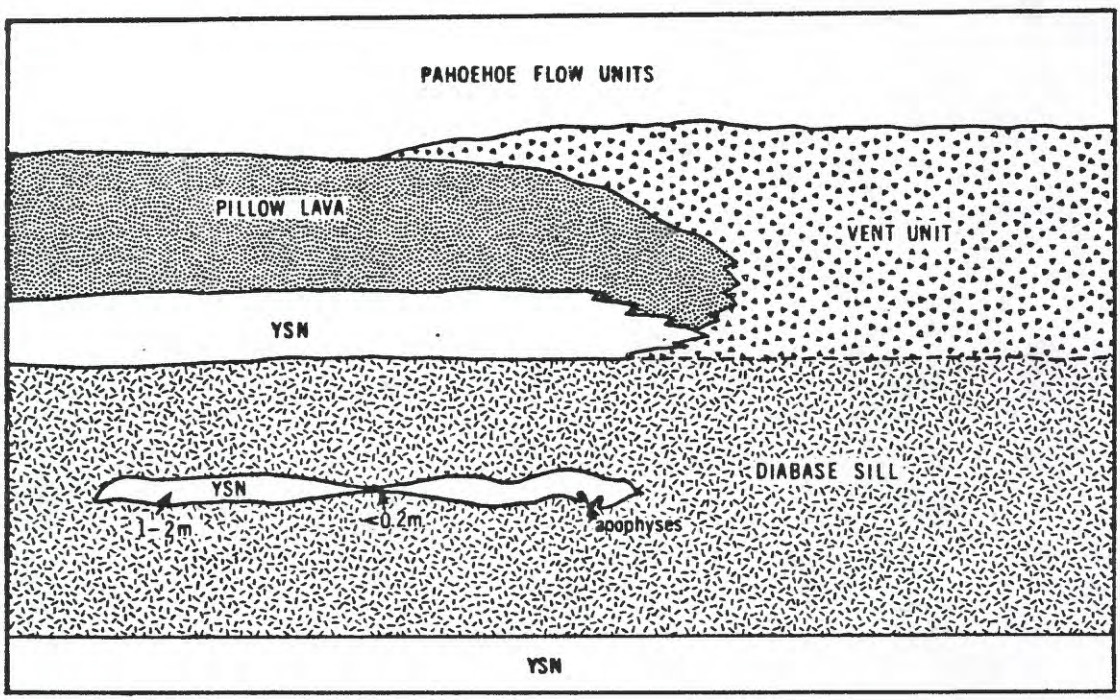

Figure 56c. Sketch showing the intrusive relationship of the diabase sill at the head of Hole-in-the-Wall cirque. Note the interval of sedimentary rock (Ysn) entirely engulfed within the sillrock. The relationship between the sill and vent facies is not clear since the outcrop is partially obscured by heavy lichen cover. North is into the page. Not drawn to scale.

Figure 57. Base of the diabase sill at Hole-in-the-Wall (along trail to Boulder Pass). The rock is very fine-grained and weathers into massive blocks.

Figure 58. Close-up view of diabasic texture in the center of the hypabyssal sill at Hole-in-the-Wall. The texture is most visible on slightly weathered surfaces. Photograph by Ed Larson.

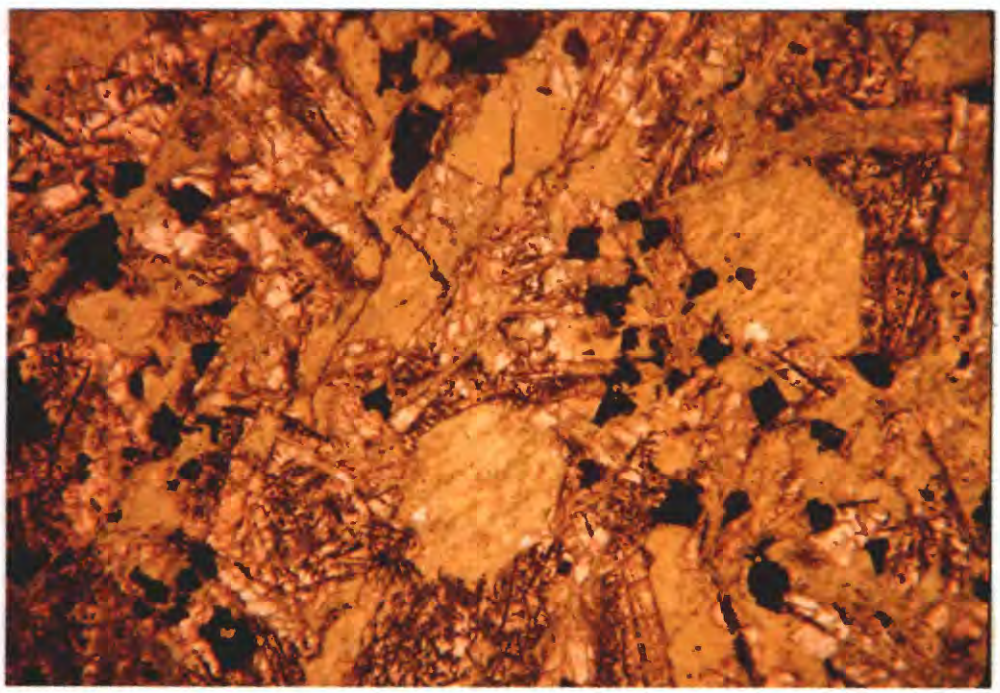

Figure 59. Photomicrograph (plain light) showing partial and entire replacement of primary minerals by chlorite. Sample is from the coalesced pillow zone of the pillow lava facies. Magnification is 24x.

Figure 60. Photomicrograph (crossed nichols) showing diabase texture typical of most facies. Sample is from a flow-unit at Hole-in-the-Wall. Note that any pyroxene that may have existed between the feldspar laths has been entirely replaced. Magnification is 24x.

Figure 61. Photomicrograph (crossed nichols) showing the near total replacment of plagioclase by chlorite and other fine-grained clay minerals. Magnification is 24x.

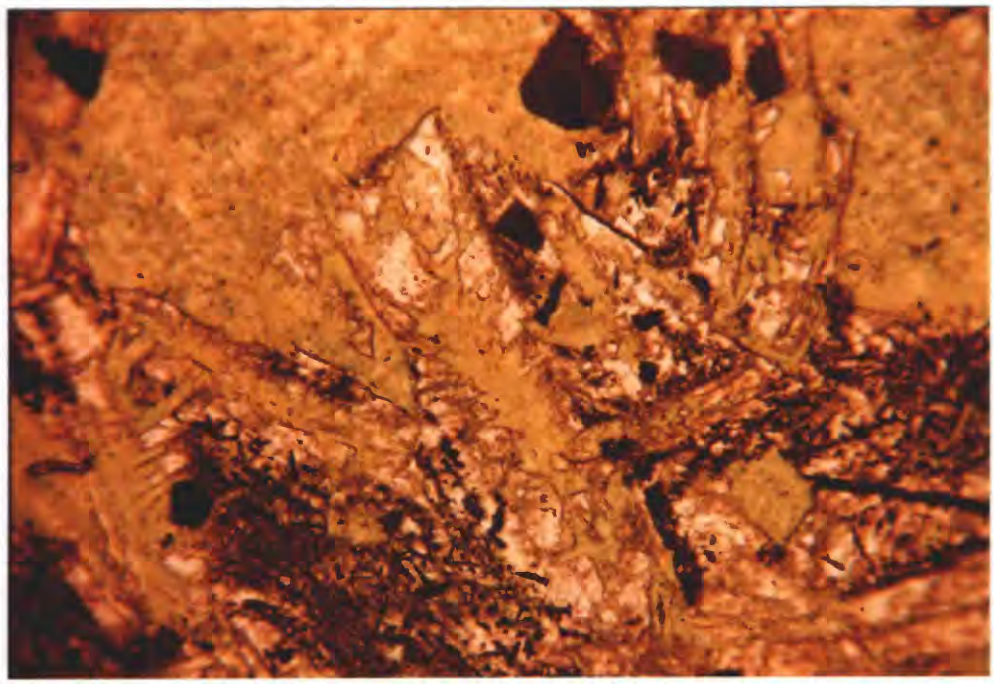

Figure 62. Photomicrograph (plain light) showing the pervasive chloritization of albitized plagioclase, suggesting multiple episodes of alteration. Magnification is 80x.

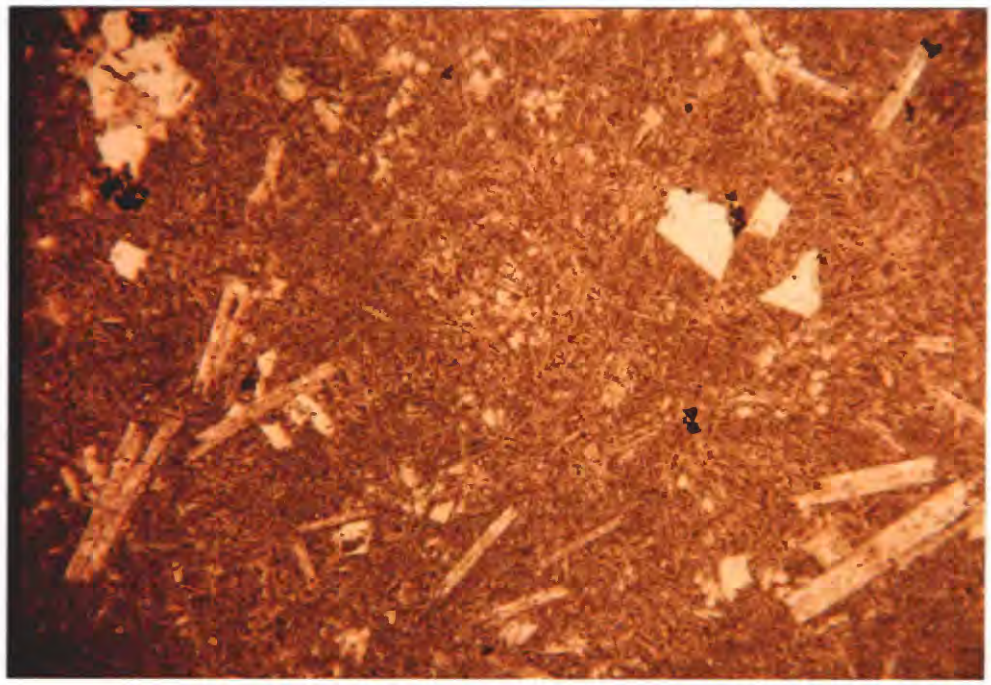

Figure 63. Photomicrograph (plain light) showing the typical grain size of the pillow lava. Magnification is 24x.

Figure 64. Photomicrograph (plain light) of the interpillow hyaloclastite breccia. Magnification is 24x.

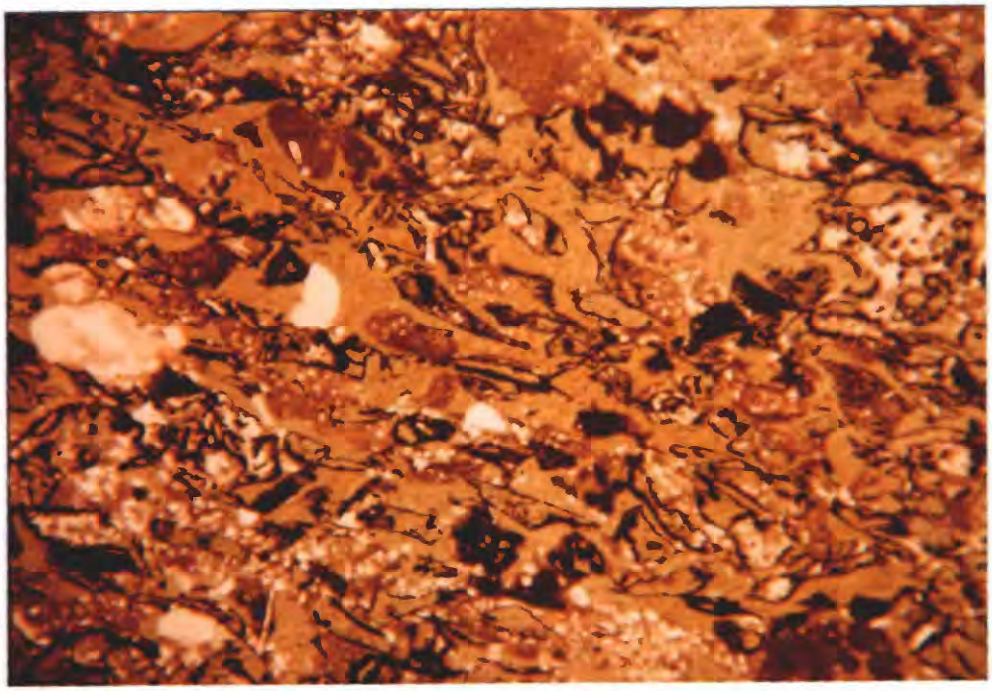

Figure 65. Photomicrograph (plain light) of a reworked hyaloclastite tuff bed located in the Snowslip strata directly beneath the pillow lava at Kootenai Peak. Magnification is 24x.

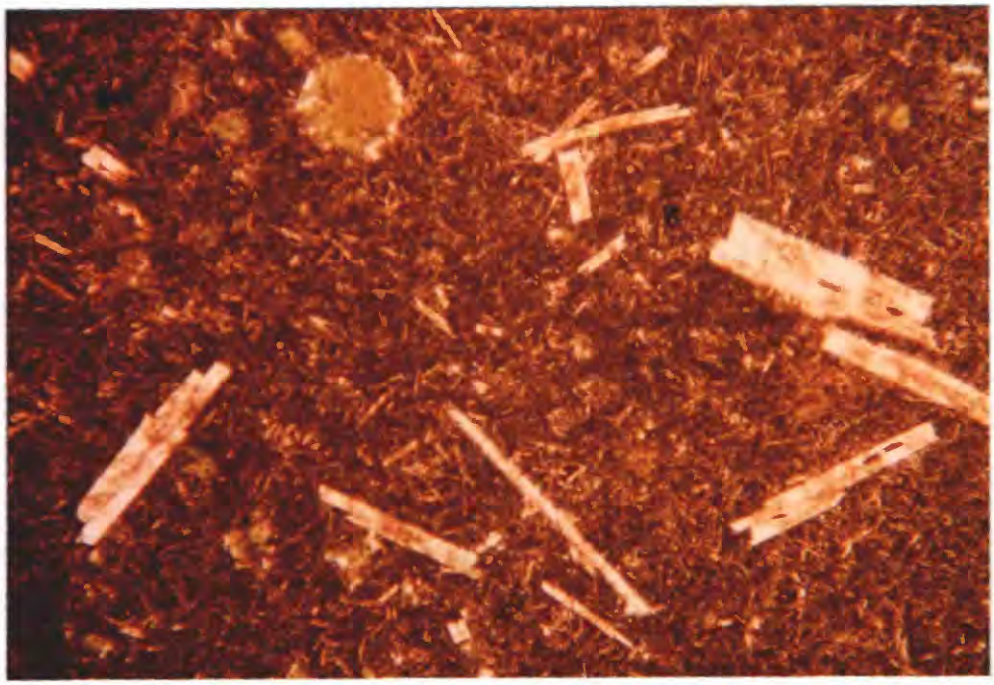

Figure 66. Photomicrograph (plain light) of the vent facies matrix. Note the similarity in grain size between the vent facies matrix and the pillow lava of Figure 63. Both are quenched phases. Magnification is 24x.

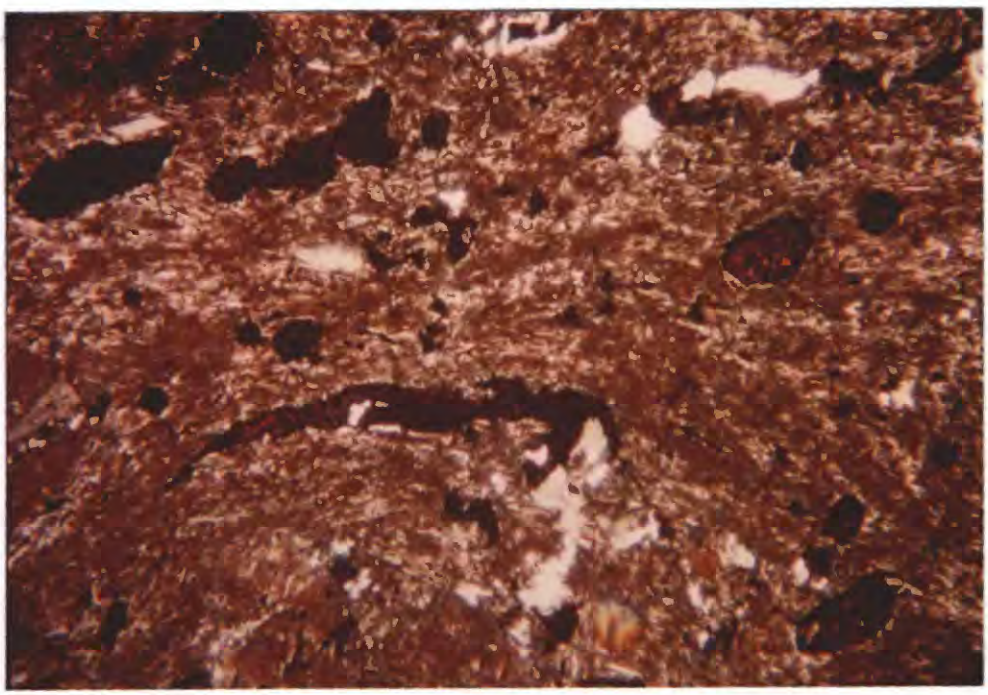

Figure 67. Photomicrograph (crossed nichols) of the vent facies matrix. Note the alignment of plagioclase microlites and amygdules (former pumices?) wrapping around the larger lens-shaped amygdule in the center of photograph. The up-turned end indicates flow was from the left to right side. Dark blebs and lenses are probably amygdules. Magnification is 24x.

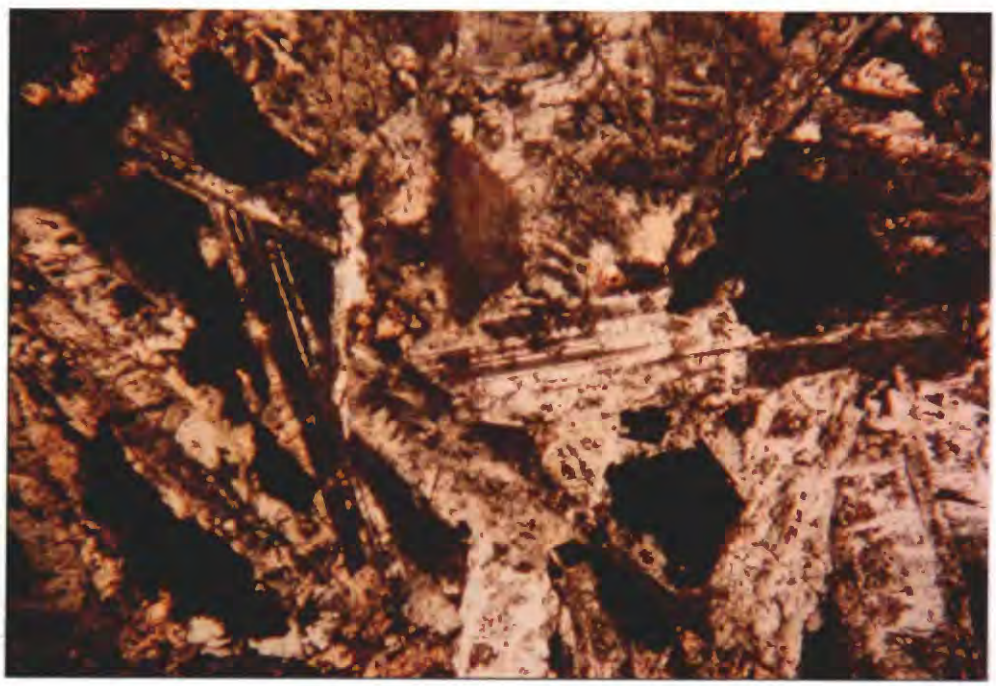

Figure 68. Photomicrograph (crossed nichols) showing large diagenetically altered plagioclase grains in the center of the hypabyssal diabase sill. Magnification is 24x.

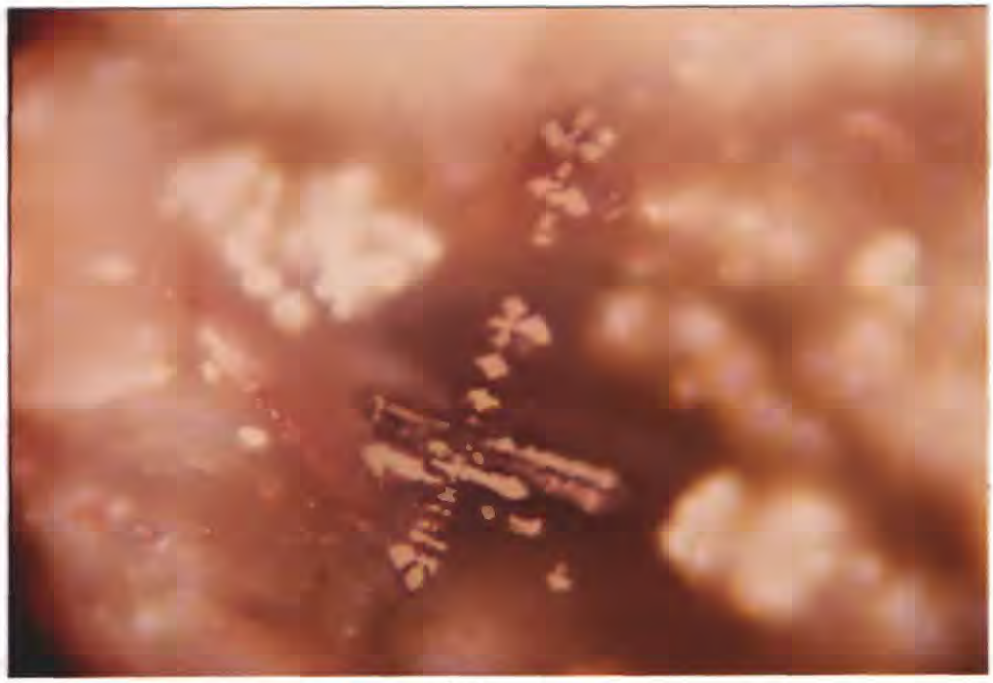

(a)

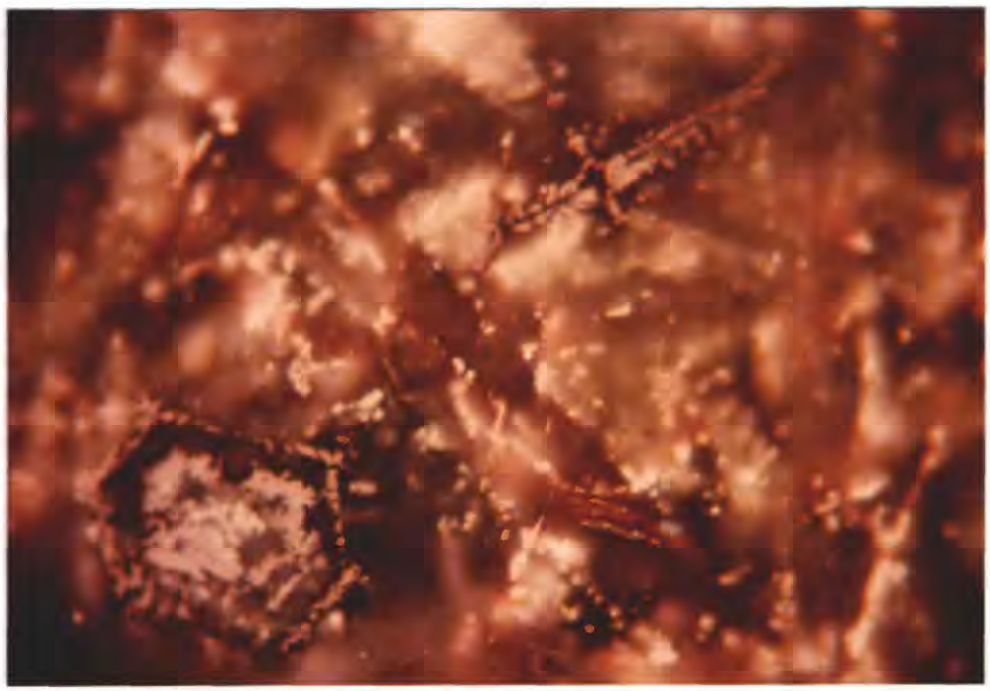

(b)

Figure 69. Photomicrograph (plain reflected light) of primary magnetite microlites typical of the pillow lava. (a) Homogeneous skeletal cruciform type magnetite (partially altered to hematite) under high power (1200x). (b) Skeletal cruciform type magnetite in upper right corner and early generation fortress type magnetite in lower left corner. See text for explanation. Magnification in (b) is 480x.

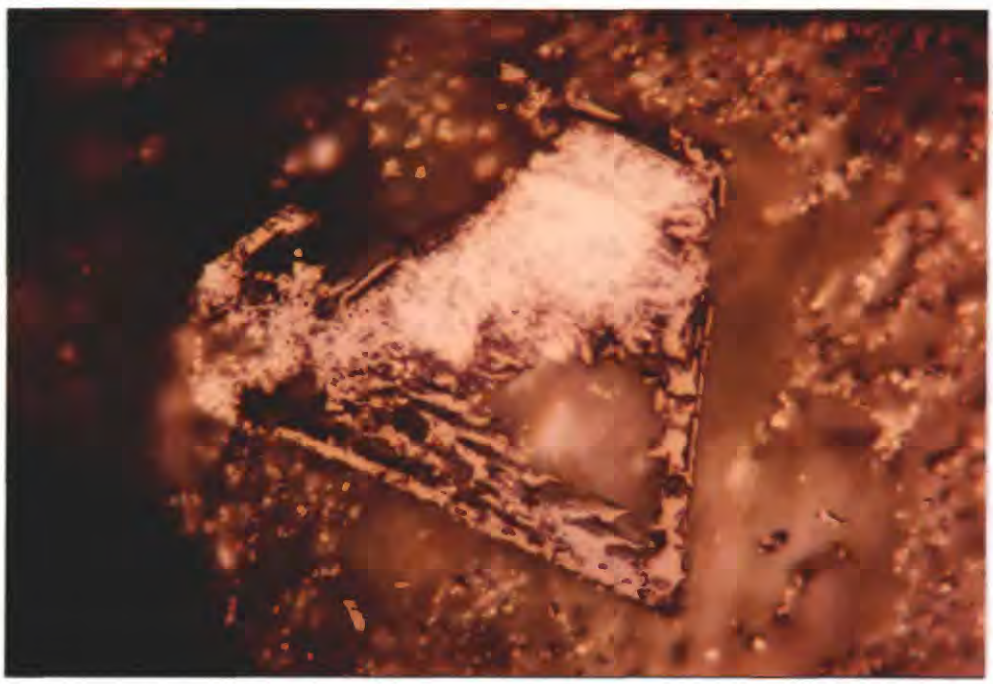

Figure 70. Photomicrograph (plain reflected light) of early-generation magnetite in pillow lava. Bright yellow mineral in upper portion of grain is leucoxene. Note the smaller, bimodal primary magnetite grains surrounding the larger grain. Magnification is 480x.

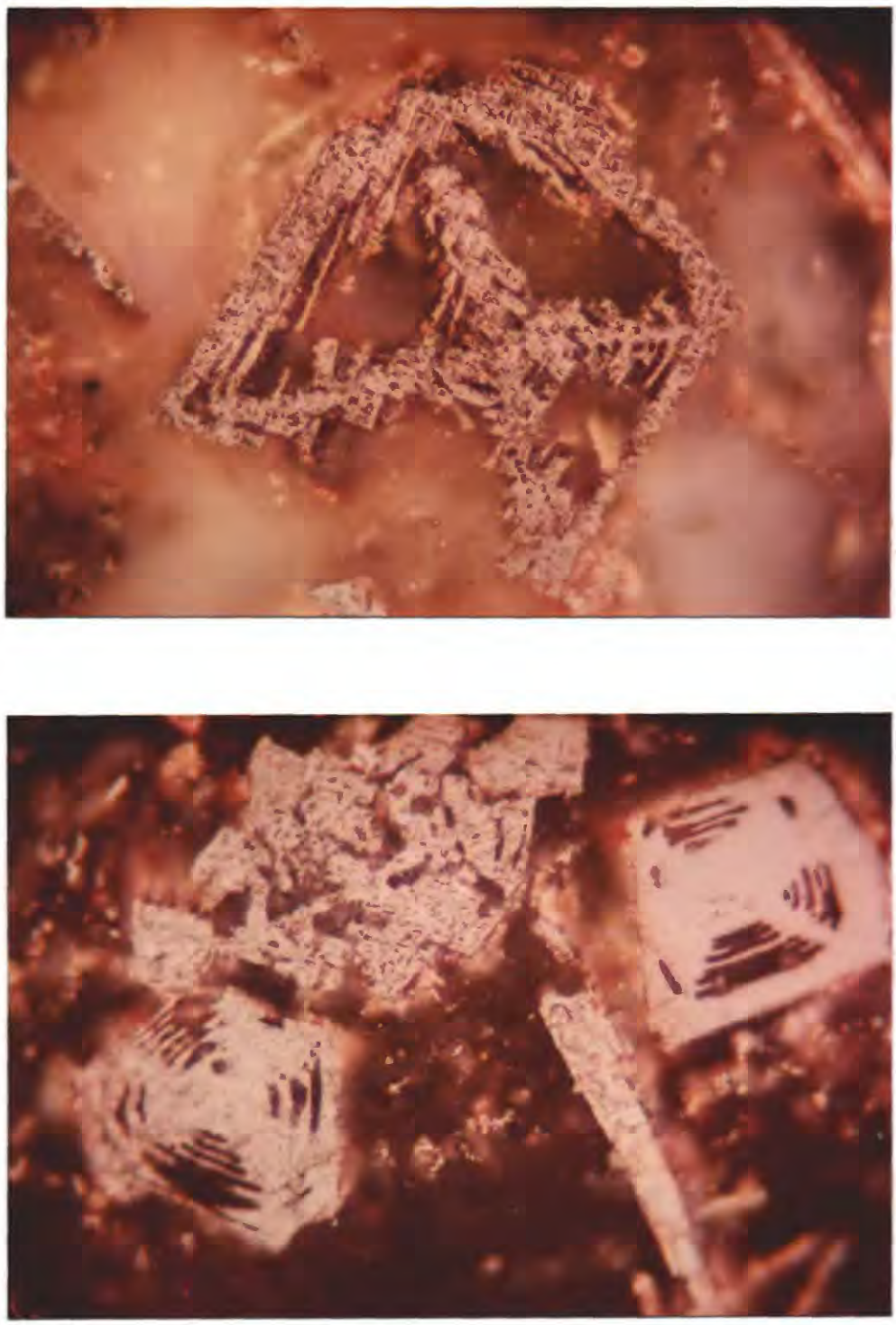

Figure 71. Photomicrographs (plain reflected light) of euhedral cross-arm, cruciform type magnetite in pahoehoe flow units. These grains probably grew in the magma chamber and were carried in the melt. Diagenesis has preferentially redistributed the titanium-poor zones. Magnification is 480x.

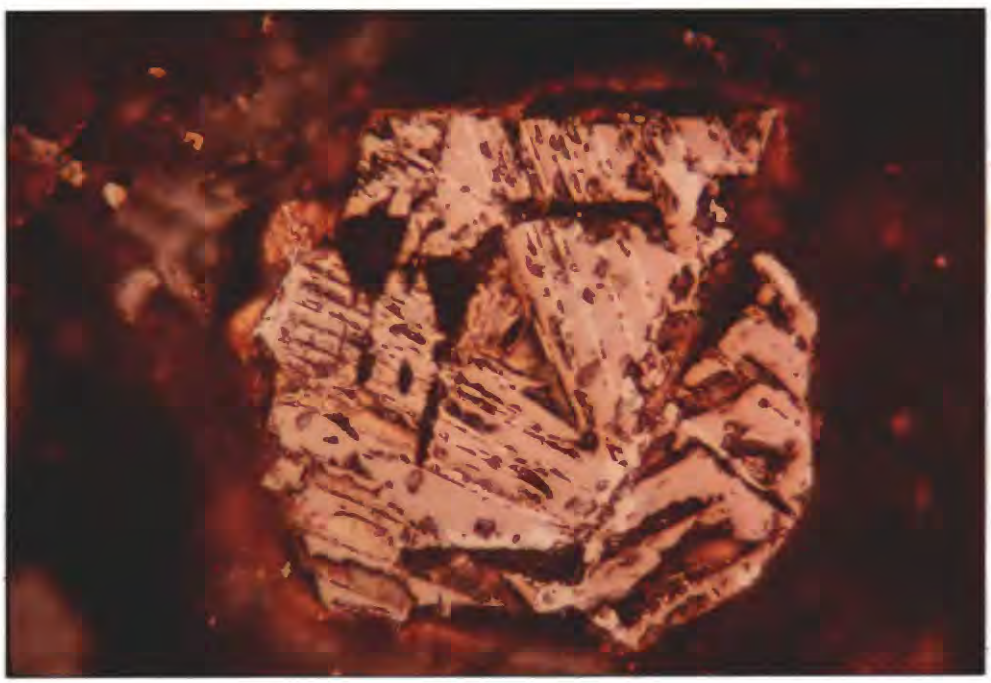

(a)

Figure 72. Photomicrographs (plain reflected light) of euhedral to subhedral magnetite grains of the pahoehoe flow units. Note that all show evidence of having had ilmenite lamellae. (a) Large composite magnetite with hematite lamellae (after ilmenite). (b) Side by side magnetite grains. Grain on the right has abundant trellis-type lamellae. Grain on left has fewer lamellae probably due to differences in the microenvironment in which each grain grew. (c) Large, euhedral, partly moth-eaten magnetite with abundant trellis type lamellae (formerly ilmenite). Magnification is 480x.

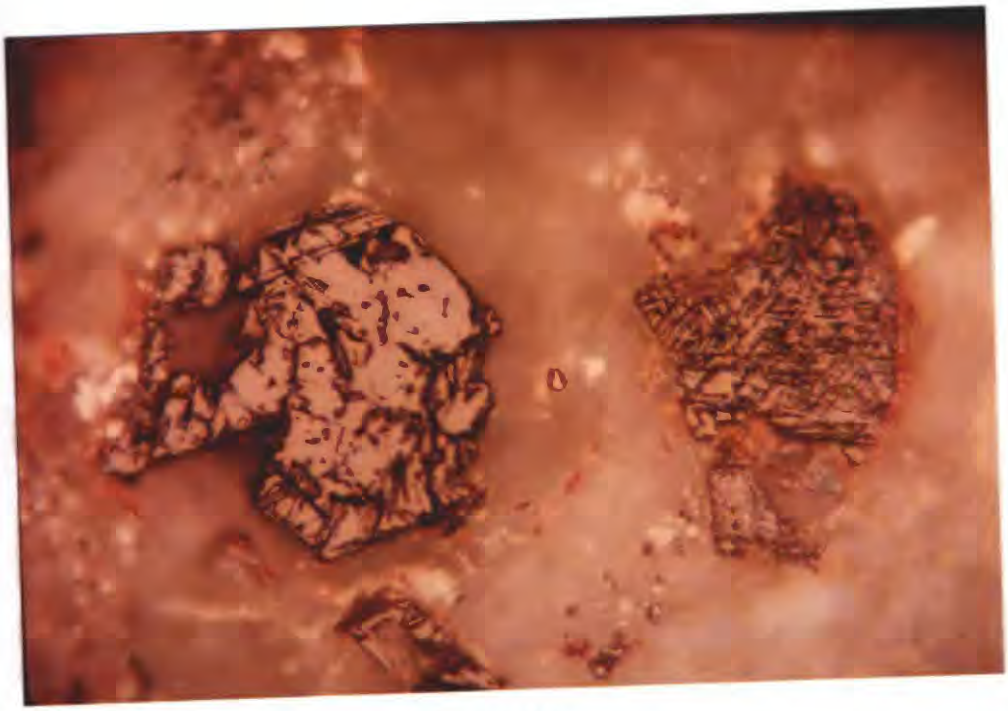

Figure 72b.

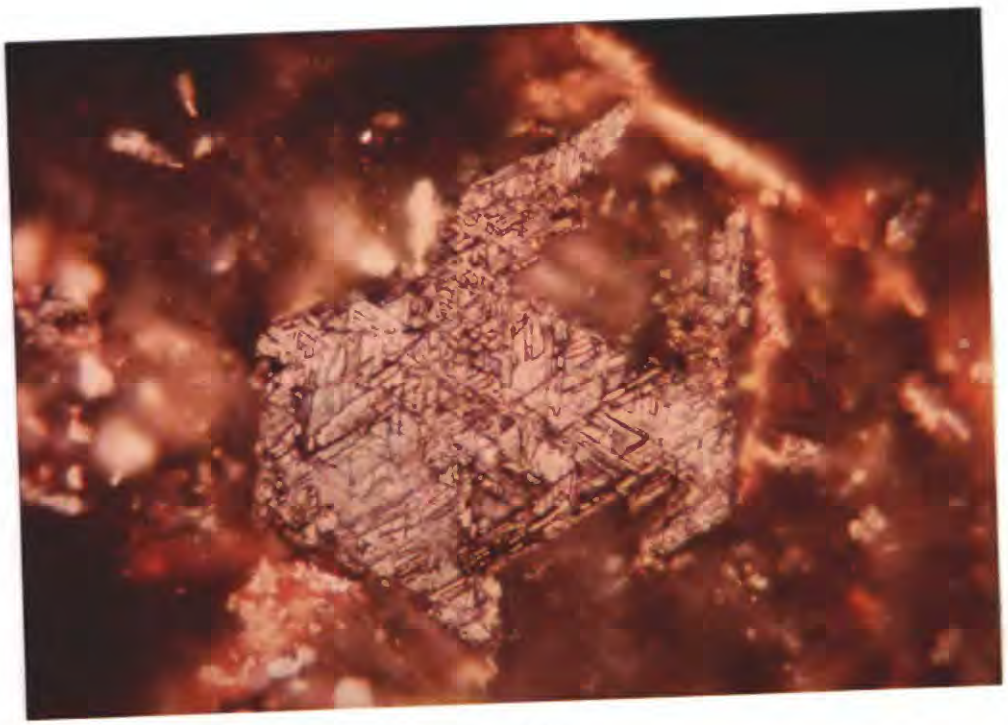

Figure 72c.

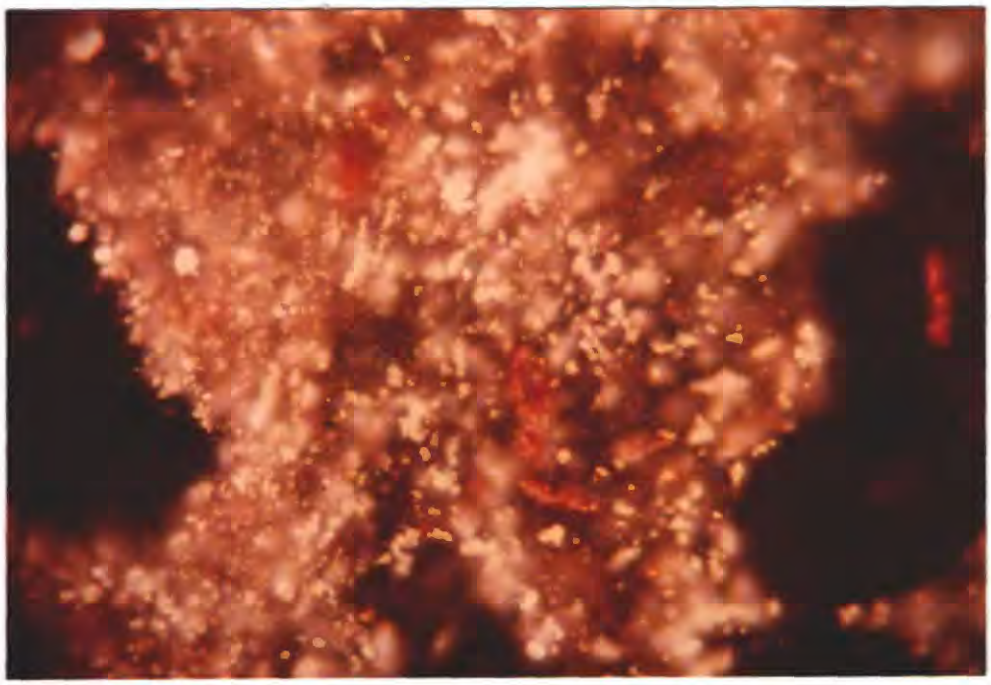

Figure 73. Photomicrograph (plain reflected light) of the vent facies matrix. Iron-titantium oxide minerals are numerous but small, and are completely oxidized. Red portions may be iron hydroxide or microcrystalline hematite. Magnification is 480x.

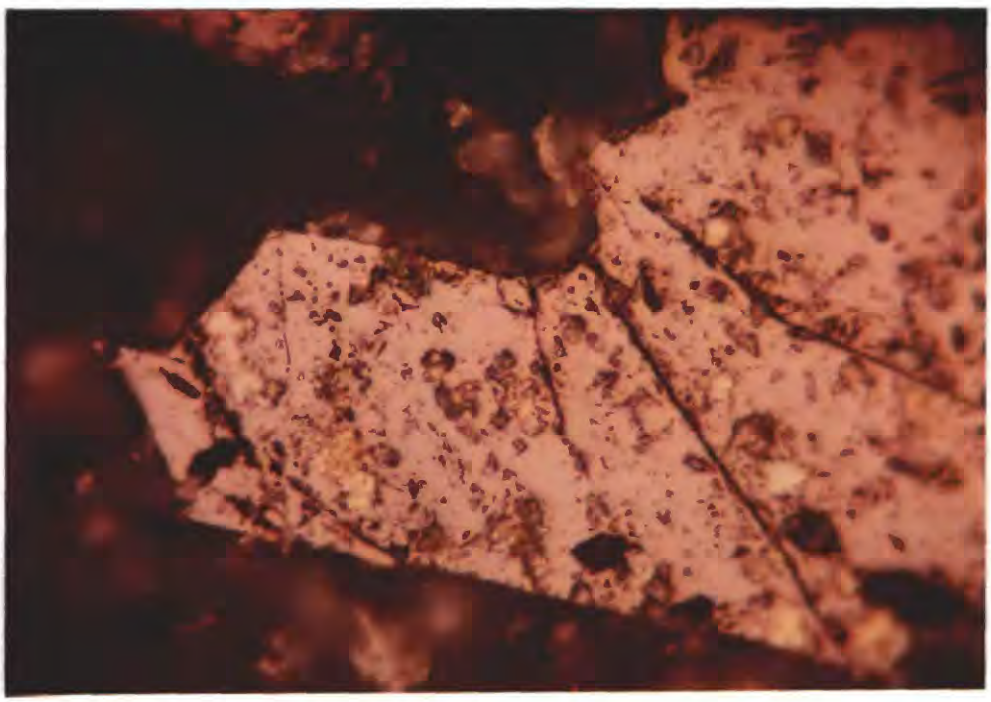

Figure 74. Photomicrograph (plain reflected light) of large, mottled, euhedral magnetite grain from the center of the hypabyssal diabase sill. Magnification is 480x.

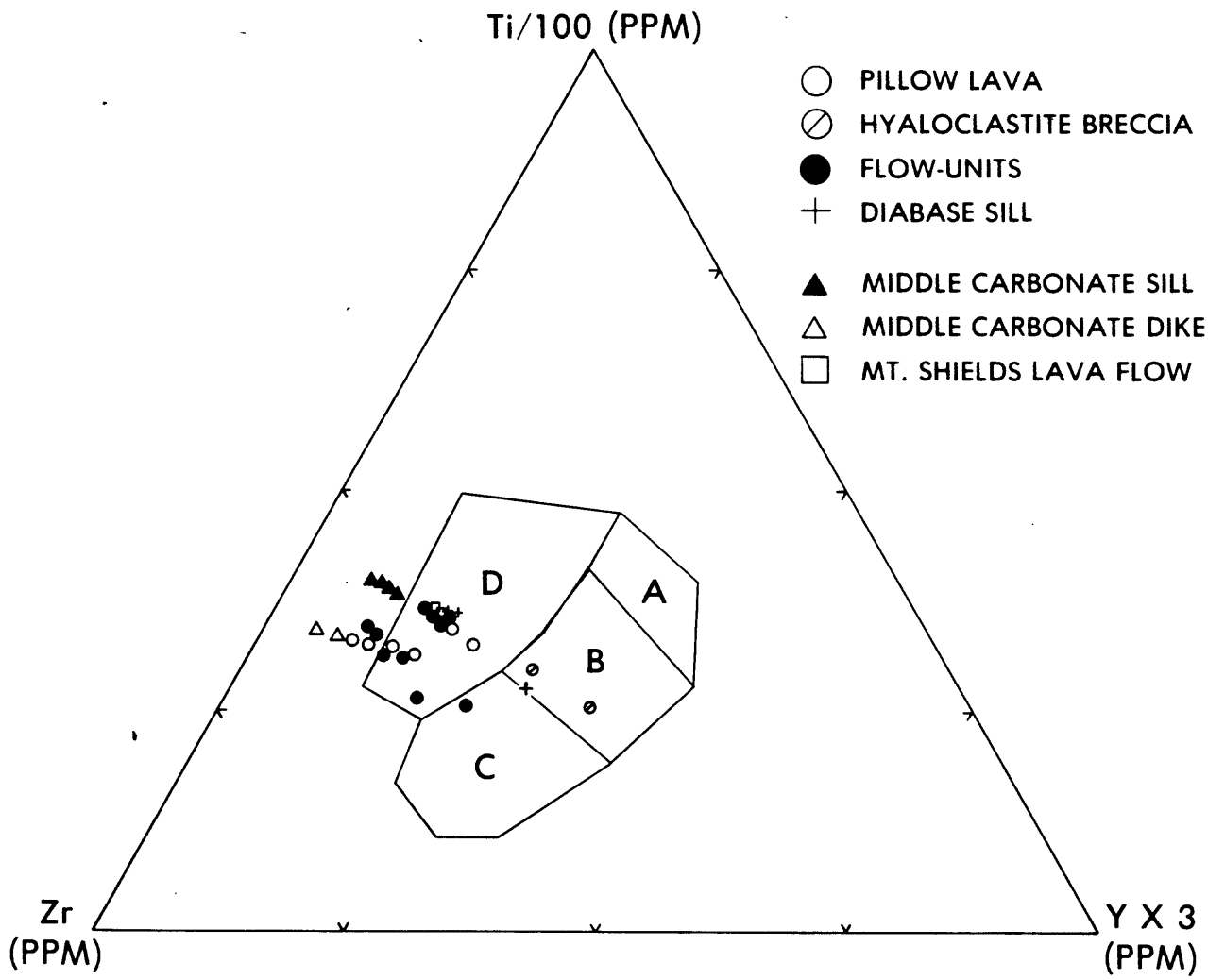

Figure 75. Ti - Zr - Y diagram of Pearce and Cann (1973). "Within-plate" basalts (i.e. ocean island or continental) plot in field D, ocean-floor basalts plot in field B, low-potassium tholeiites plot in fields A and B, and calc-alkaline basalts plot in fields B and C. Most of the Purcell Lava data points plot in the D field suggesting an intra-plate tectonic setting. Samples of the hyaloclastite breccia, and a flow unit that was in close proximity to the vent unit plot far out of the general cluster of other Purcell Lava values. This is a common occurrence on most of the diagrams and reflects the extreme effects of alteration (palagonitization and possibly hydrothermal alteration, as well as diagenesis and metamorphism related to burial). Note that the middle Belt carbonate sill and dike plot out of the main cluster of the Purcell Lava.

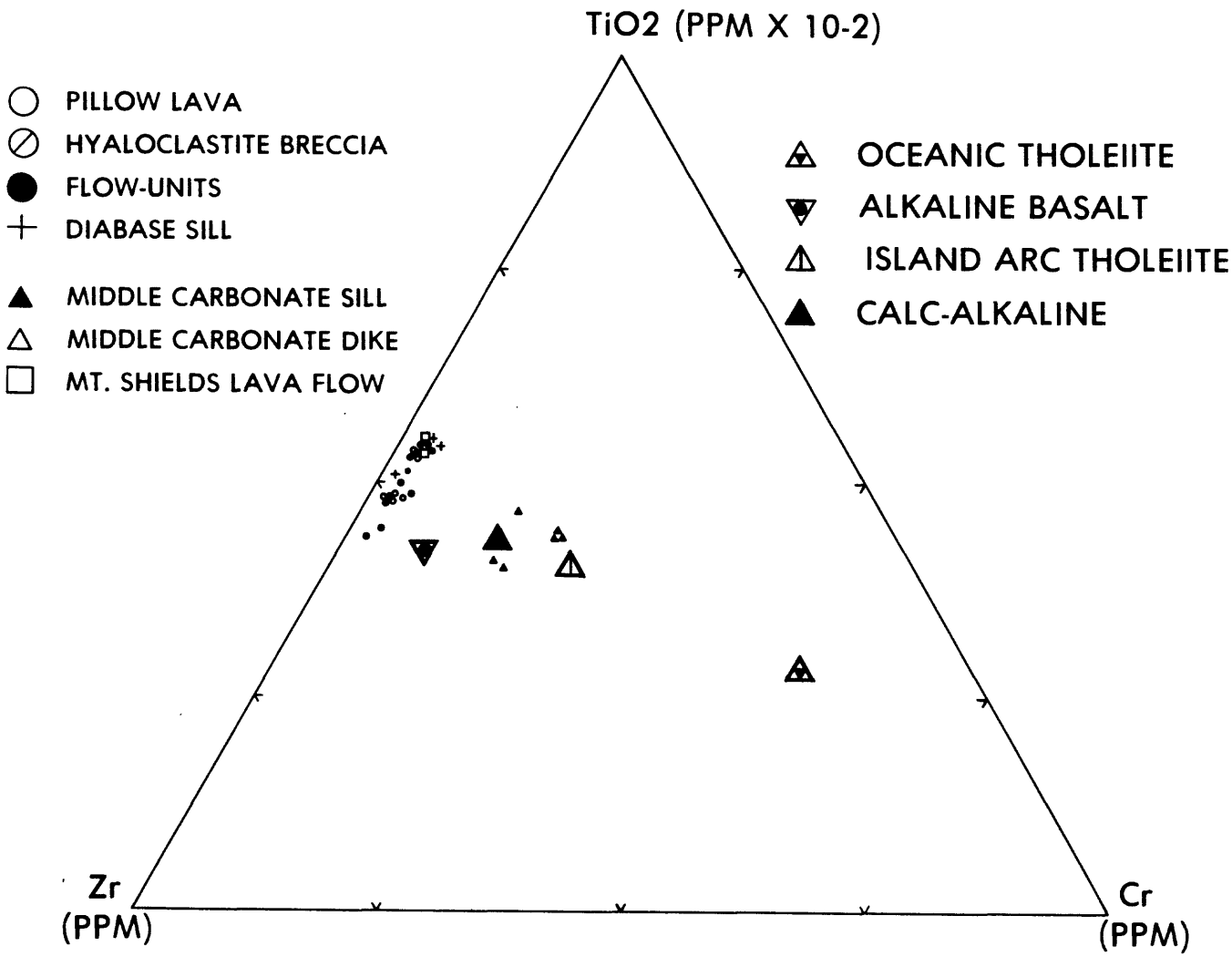

Figure 76. TiO_2 - Zr - Cr discriminant plot from Bloxam and Lewis (1972). A linear trend defines alkaline, tholeiite, and calc-alkaline rock types. The Purcell Lava plots entirely within the alkaline field along this trend. Ti and Cr are believed to be the most immobile elements. Comparison of Zr concentrations in the Purcell Lava with those of Cenozoic alkaline basalts shown in Table 5, suggests that Zr has also been rather stable during alteration processes. Note that data from the middle Belt carbonate sill and dike do not plot concordantly with those of the Purcell Lava.

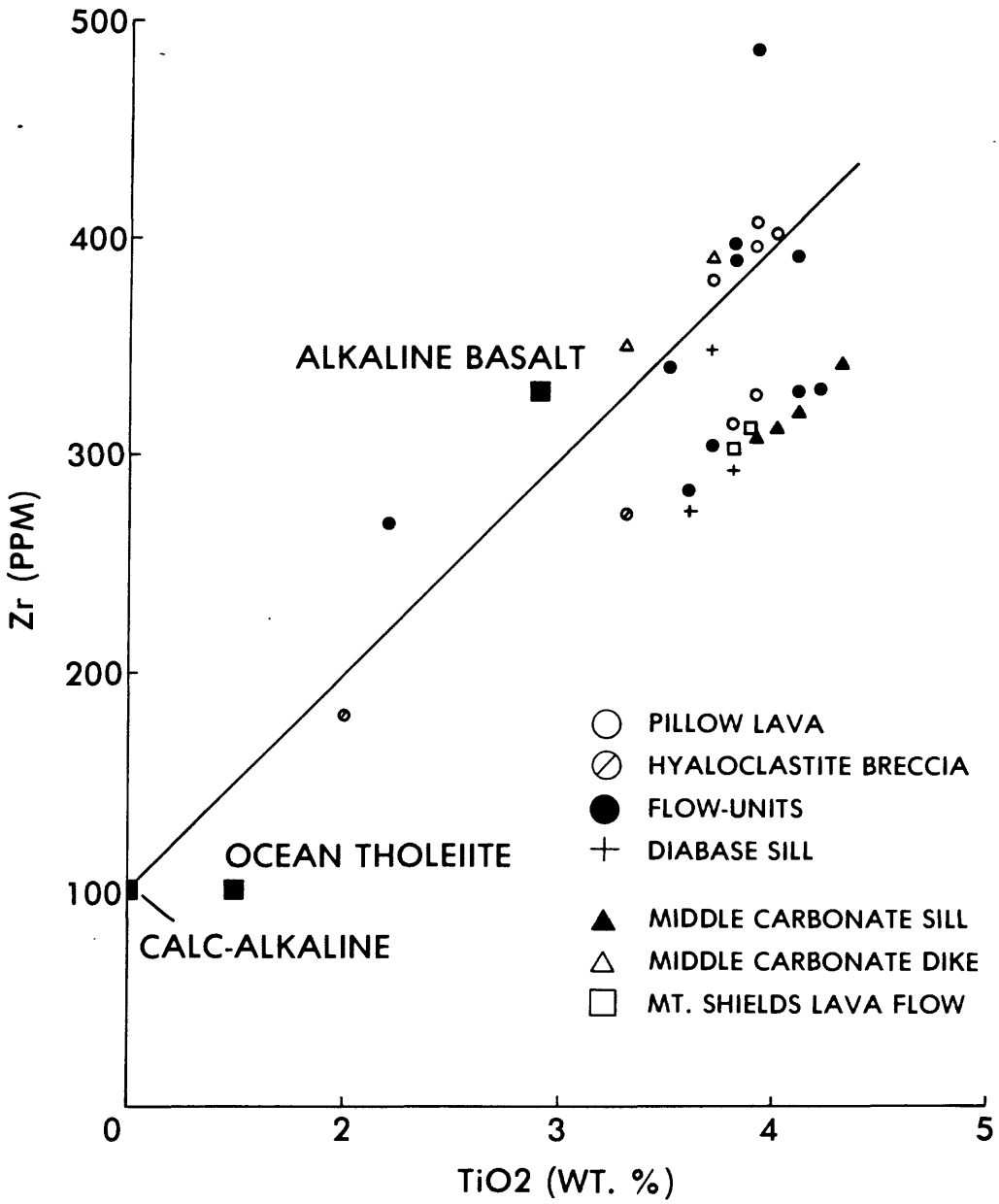

Figure 77. TiO_2 - Zr binary plot. Bloxam and Lewis (1972) found a high degree of covariance between Ti (as TiO_2) and Zr from different petrogenic rock types. With the exception of samples from the hyaloclastite breccia and a flow unit located in close proximity to the vent facies, all data points for the Purcell Lava plot in the alkaline field.

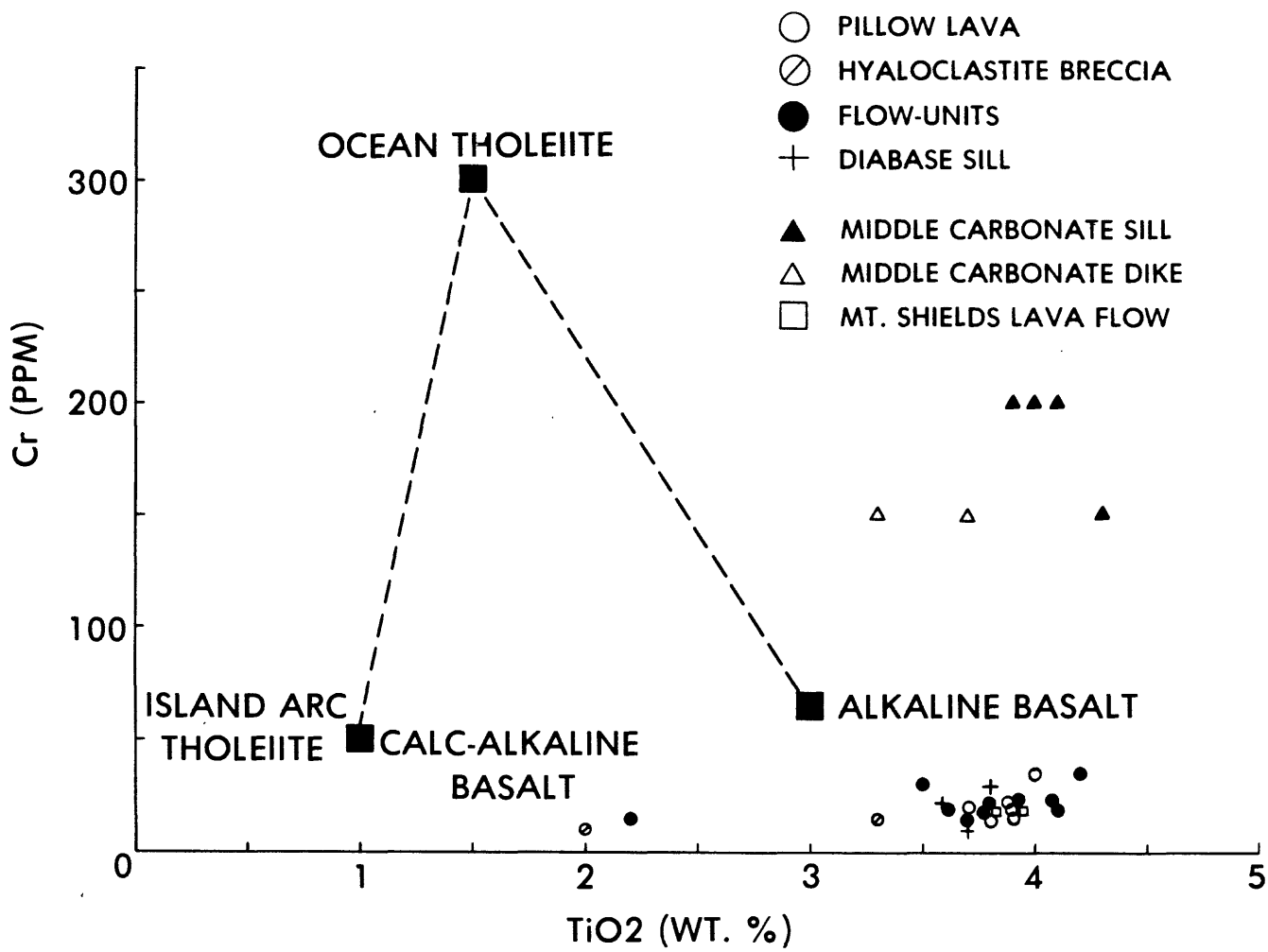

Figure 78. Cr - TiO_2 binary discriminant plot from Bloxam and Lewis (1972). The Purcell Lava data points plot in a fairly tight cluster in the alkaline basalt field with the exception of the extremely altered samples of hyaloclastite breccia and a flow unit(?) at Red Horn Peak. Note that the middle Belt carbonate sill and dike plot together and out of the field of the Purcell Lava.

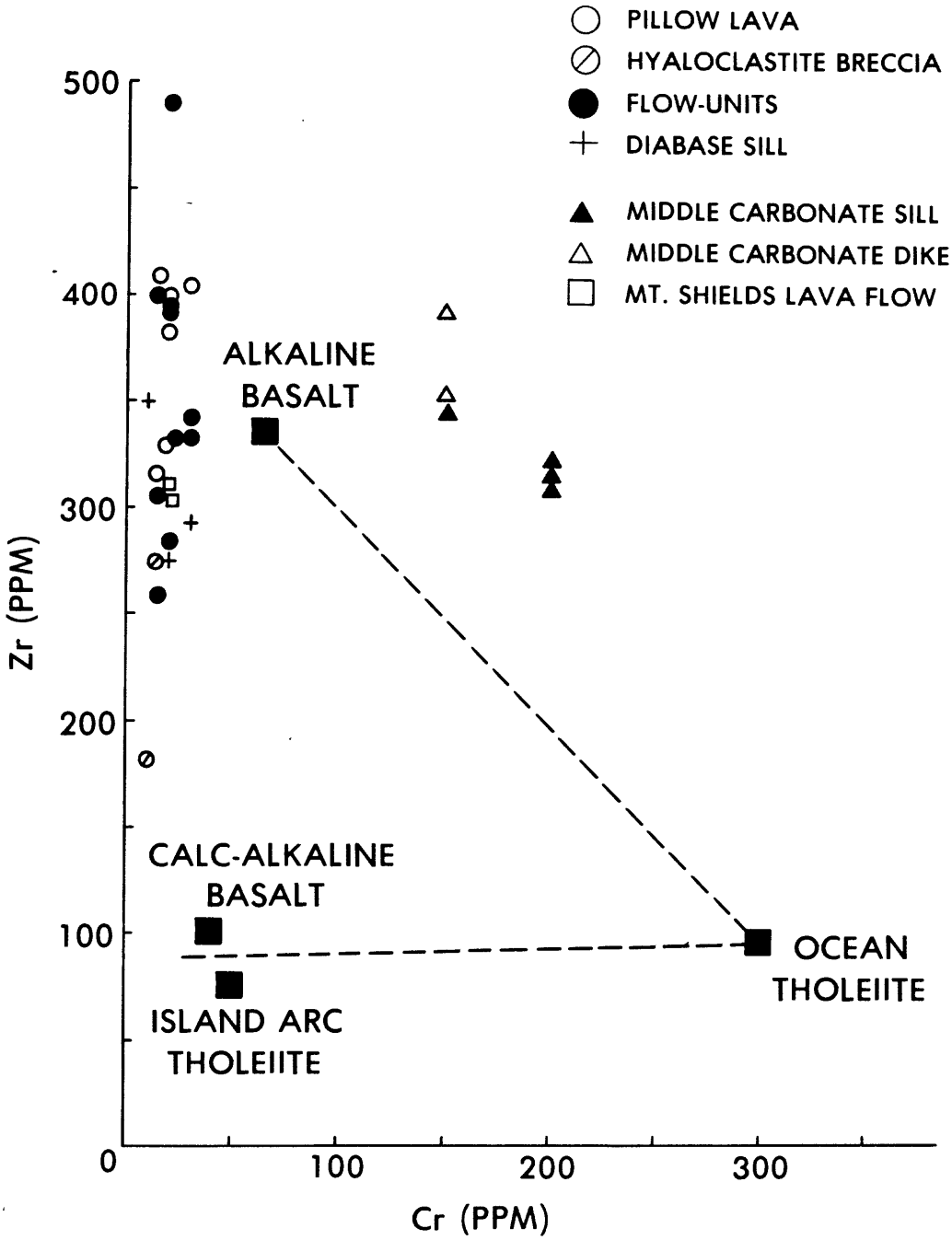

Figure 79. Zr - Cr binary discriminant plot from Bloxam and Lewis (1972). The Purcell Lava plots in the alkaline basalt field, having low Cr and high Zr concentrations consistant with alkaline basalts (Table 5). Note that the middle Belt carbonate sill and dike plot together and away from the Purcell Lava data points. The sill and dike have much higher Cr values than the Purcell, inconsistent with normal differentiation trends and the notion that the sill and lava flows are cogenetic and coeval.

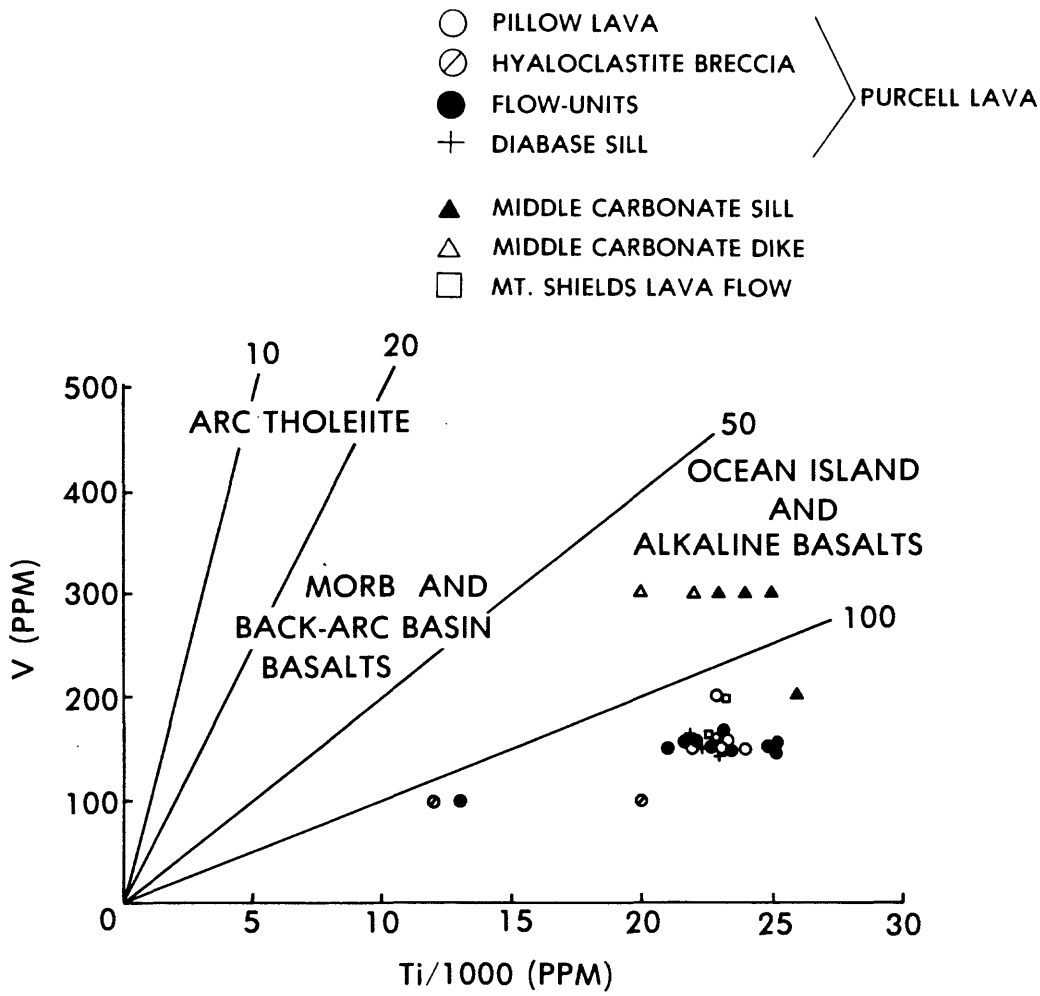

Figure 80. V-Ti discrimination diagram of Shervais (1982). Data points of the Purcell Lava and middle Belt carbonate intrusions plot in the alkaline basalt field.

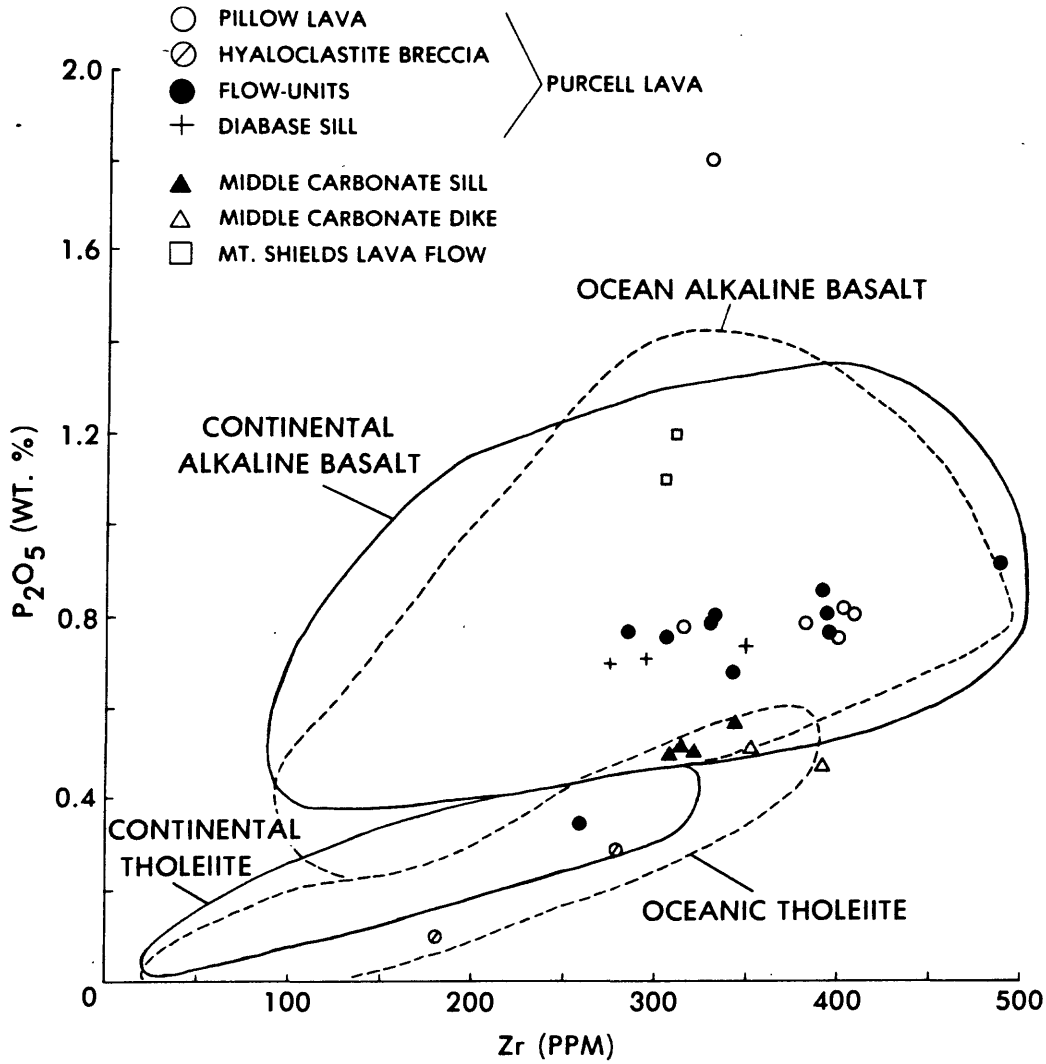

Figure 81. P_2O_5 - Zr binary plot from Floyd and Winchester (1975). Figures 75-80 have all shown that the Purcell Lava has alkaline affinities. However, many continental tholeiites are similar to alkaline basalts in terms of some major and minor element chemistry. The previous figures discriminate between oceanic and calc-alkaline type tholeiites, but do not separate out continental tholeiites. The diagram above does separate oceanic/continental tholeiites and alkaline basalts. The Purcell Lava plots nicely within the overlapping continental and oceanic alkaline basalt fields, with exception of the two extremely altered samples mentioned previously (fig. 75). This P_2O_5 - Zr diagram therefore leaves little doubt of the alkaline affinity of the Purcell Lava. Note that the middle Belt carbonate sill and dike plot together and separate from the Purcell Lava.

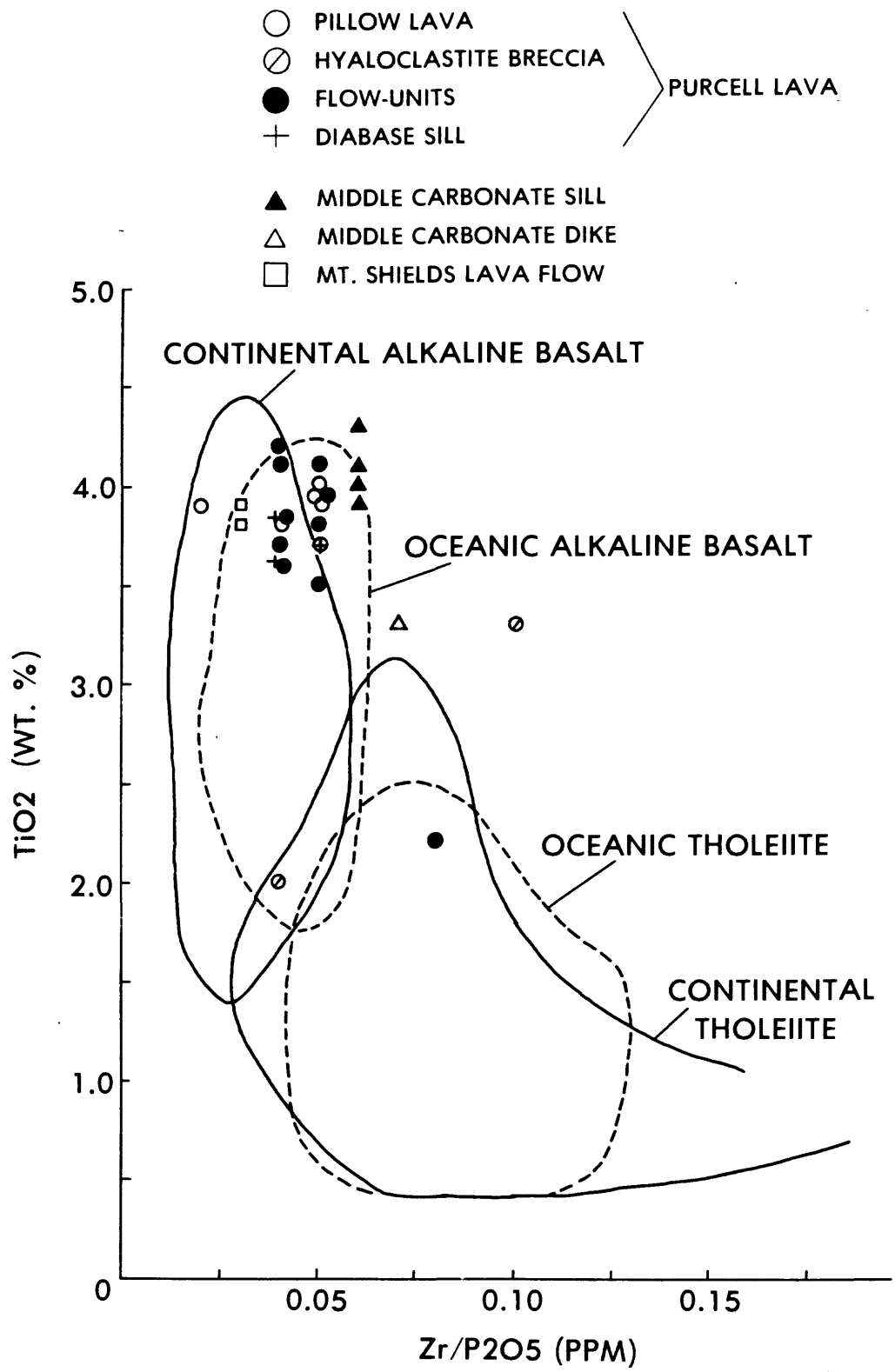

Figure 82. TiO_2 - Zr/P_2O_5 binary plot of Floyd and Winchester (1975) that discriminates between alkaline and tholeiite petrogenic rock types. Continental and oceanic analogs of any one basalt type cannot be separated. However, field relationships indicate that the Purcell Lava was erupted through a continental plate. The diagram above, like the previous diagrams, indicates that the Purcell Lava is alkaline in nature.

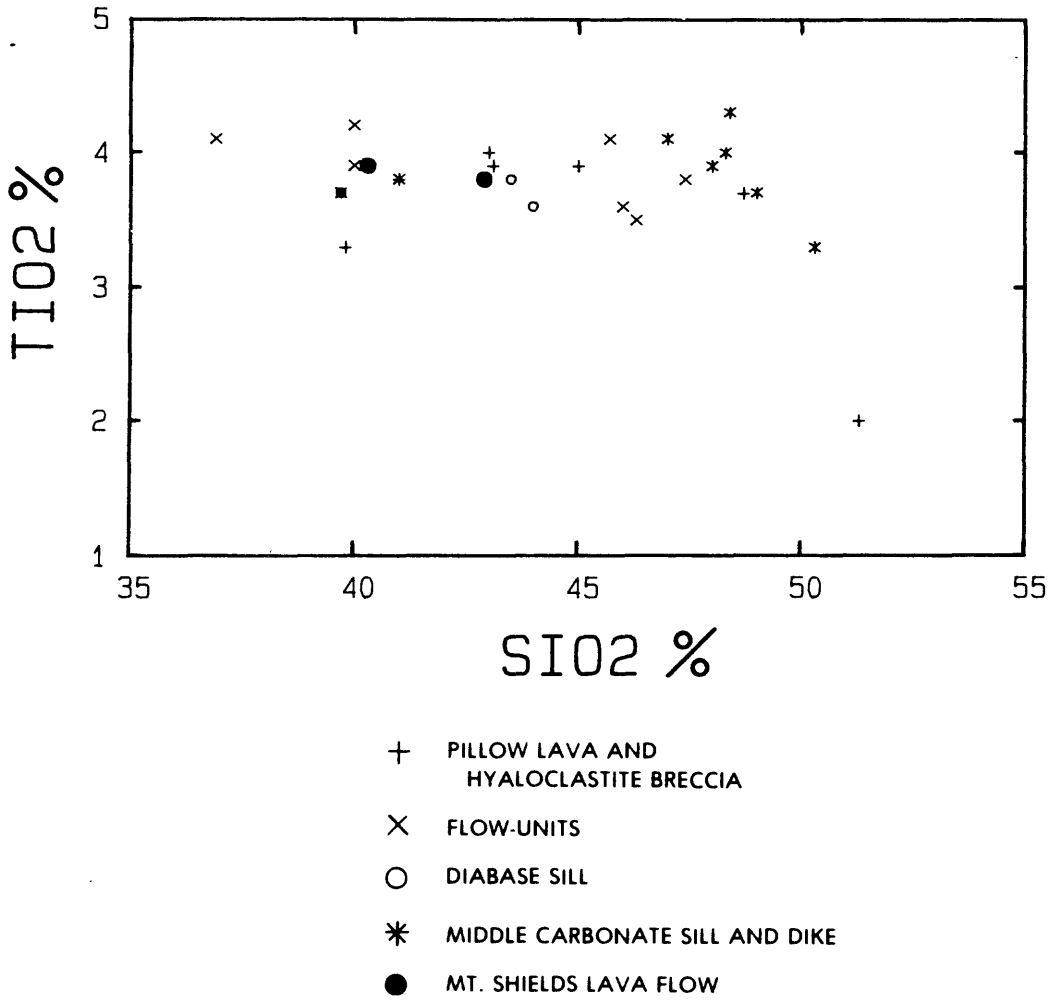

Figure 83. SiO_2-TiO_2 variation diagram illustrating the concentration range of SiO_2 in the Purcell Lava, Mt. Shields lava flow, and middle Belt carbonate sill and dike. The large range indicates that SiO_2 has been very mobile during diagenesis.

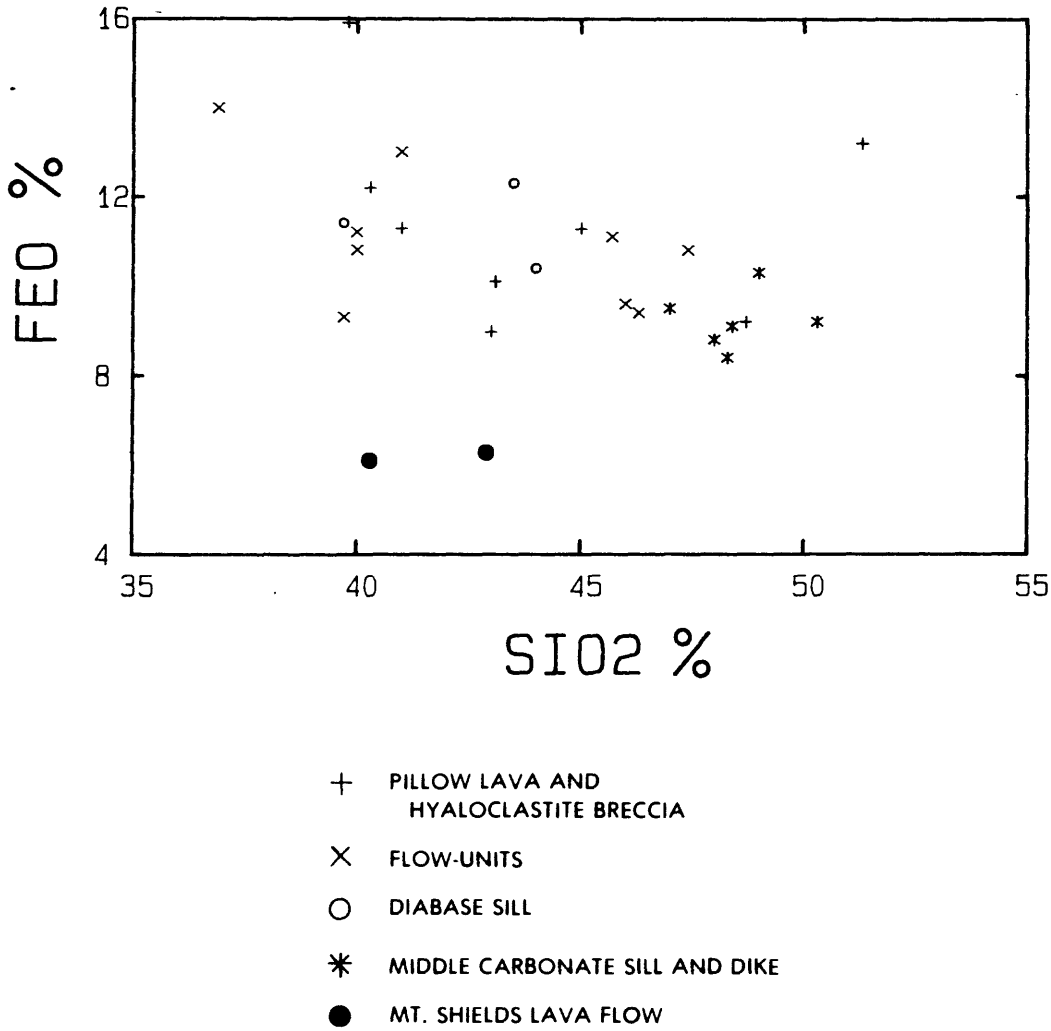

Figure 84a. SiO_2-FeO variation diagram. The large range in iron concentration (as well as silica) indicates that these elements were mobile during diagenesis and concentrated heterogeneously in the rocks.

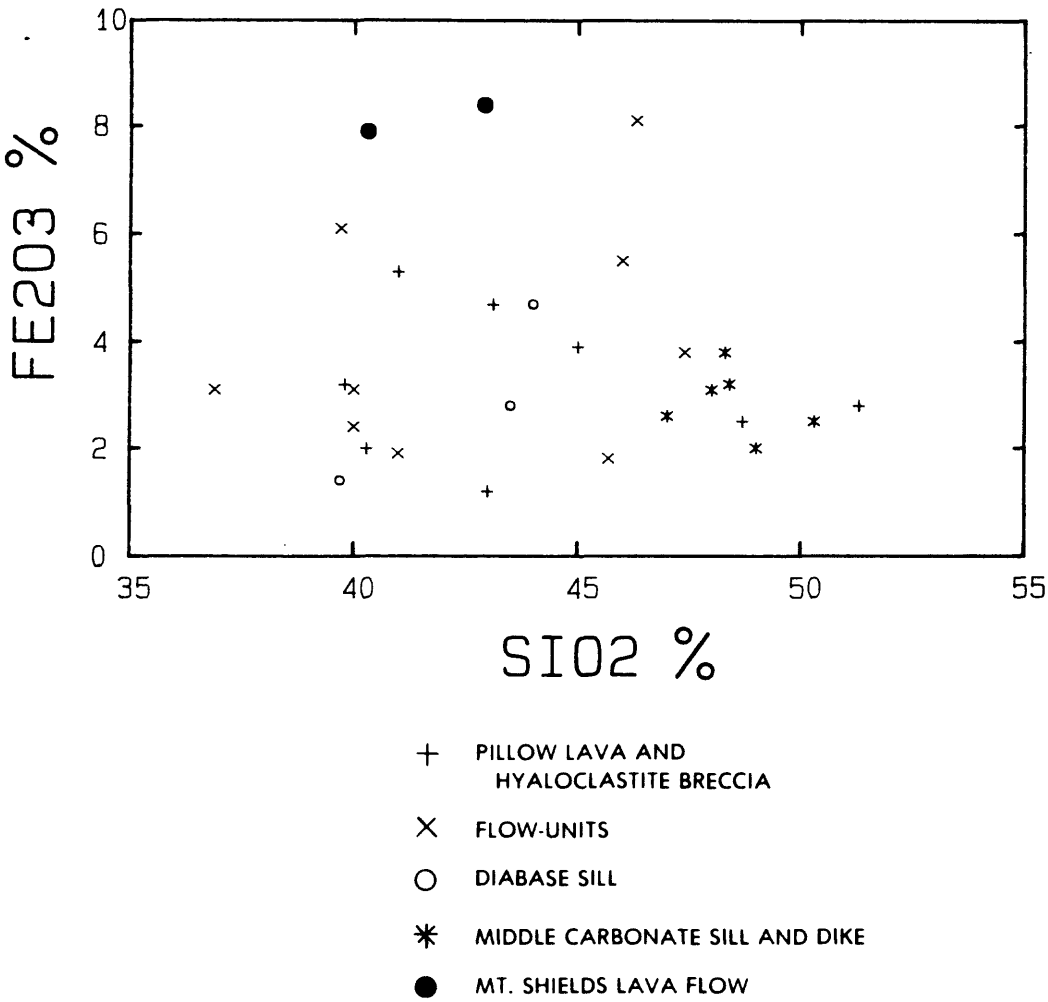

Figure 84b. SiO_2-Fe_2O_3 variation diagram. The large range in iron concentration (as well as silica) indicates that these elements were mobile during diagenesis and concentrated heterogeneously in the rocks.

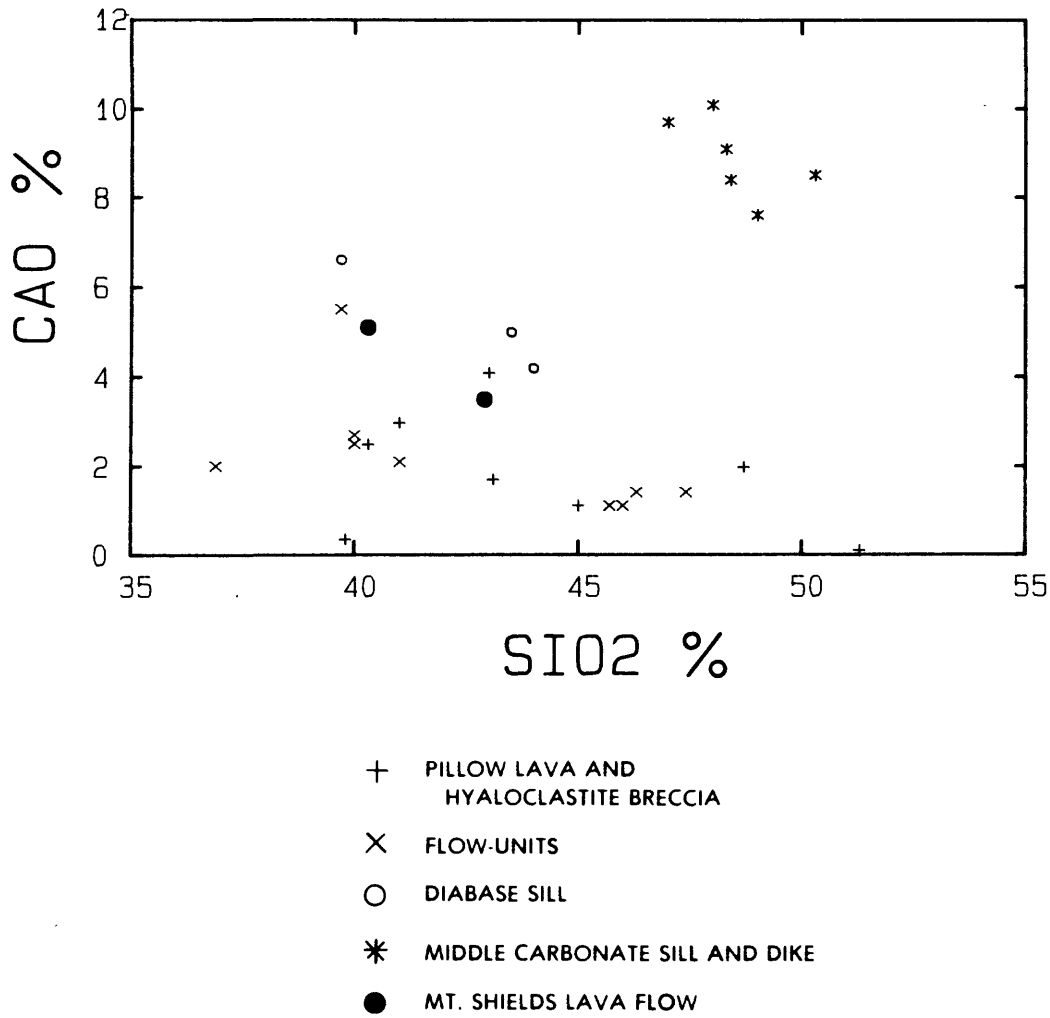

Figure 85. SiO_2-CaO variation diagram. CaO concentrations range widely, and all values for the Purcell Lava are lower than that of most basalts (compare with CaO in Table 4). Note that the data points of the middle Belt carbonate sill and dike cluster together and are segregated from those of the Purcell Lava. The range in CaO values in the sill and dike is much smaller than that of the lava flows, and is similar to that of unaltered basalts. This suggests that calcium has not been as mobile in the sill and dike as in the Purcell Lava.

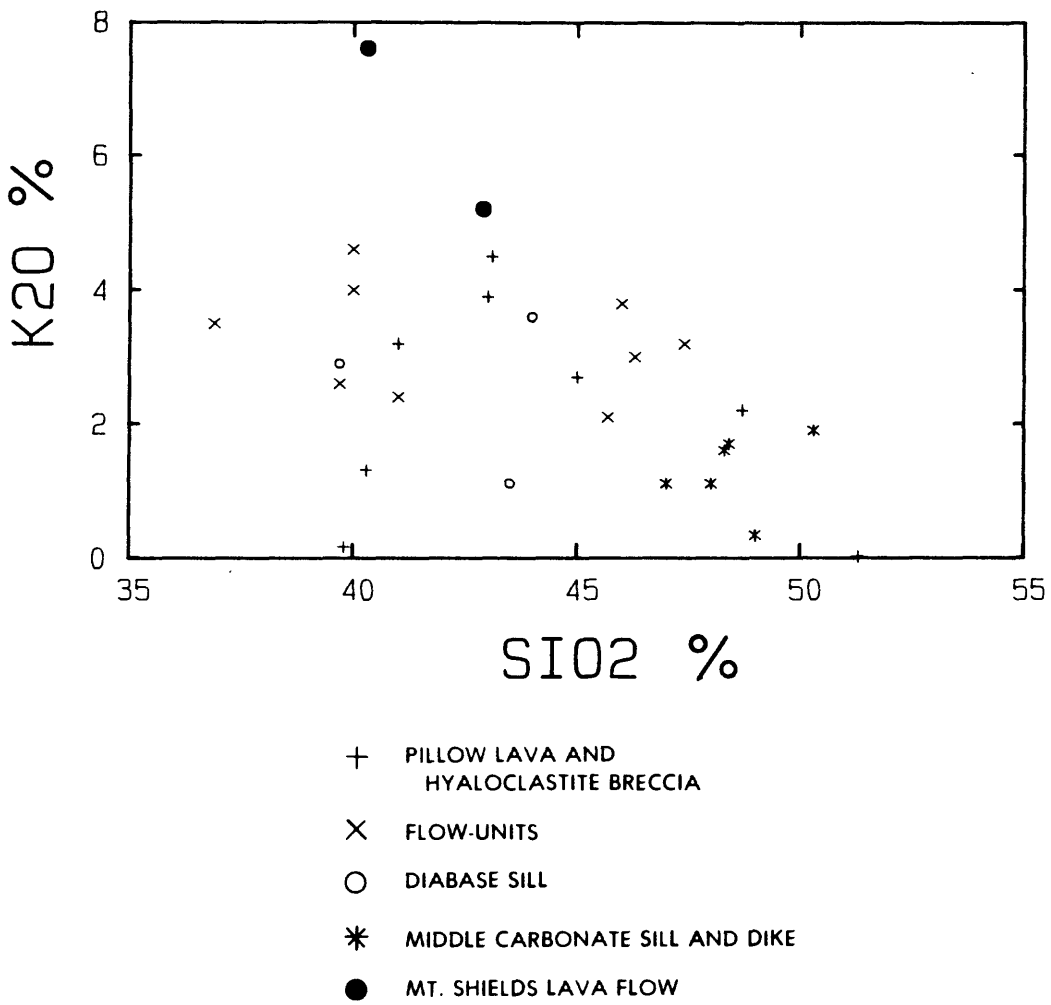

Figure 86. SiO_2-K_2O variation diagram. The plot illustrates the wide range of K_2O concentrations present in the Purcell Lava and lack of any systematic variation with SiO_2. Both K_2O and SiO_2 have been very mobile in the Purcell Lava during diagenesis. Data points of the middle Belt carbonate sill and dike plot together and have a smaller range of values than those of the Purcell. K_2O was less mobile in the dike and sill probably because of the more massive, coarser-grained character of the rock.

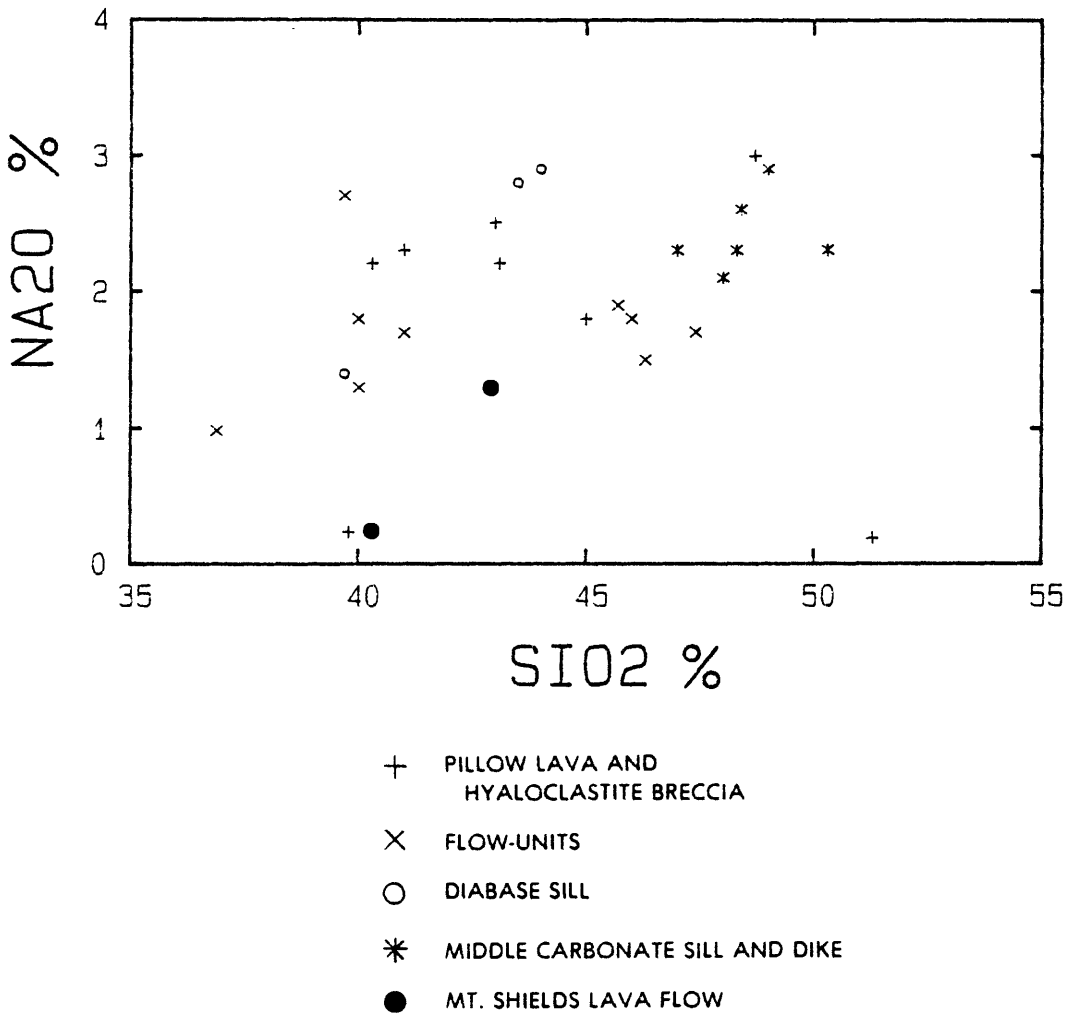

Figure 87. SiO_2-Na_2O variation diagram. Although the average concentration of Na_2O in the Purcell Lava is not inconsistent with that of average basalts, the wide range of values suggests that Na_2O was mobile during diagenesis. Petrographic and electron microprobe analyses of rarely preserved plagioclase indicates that the feldspar was albitized prior to chloritization. Since albitization typically increases the Na_2O content, the low Na_2O values of the Purcell Lava may be a fortuitous consequence of alteration.

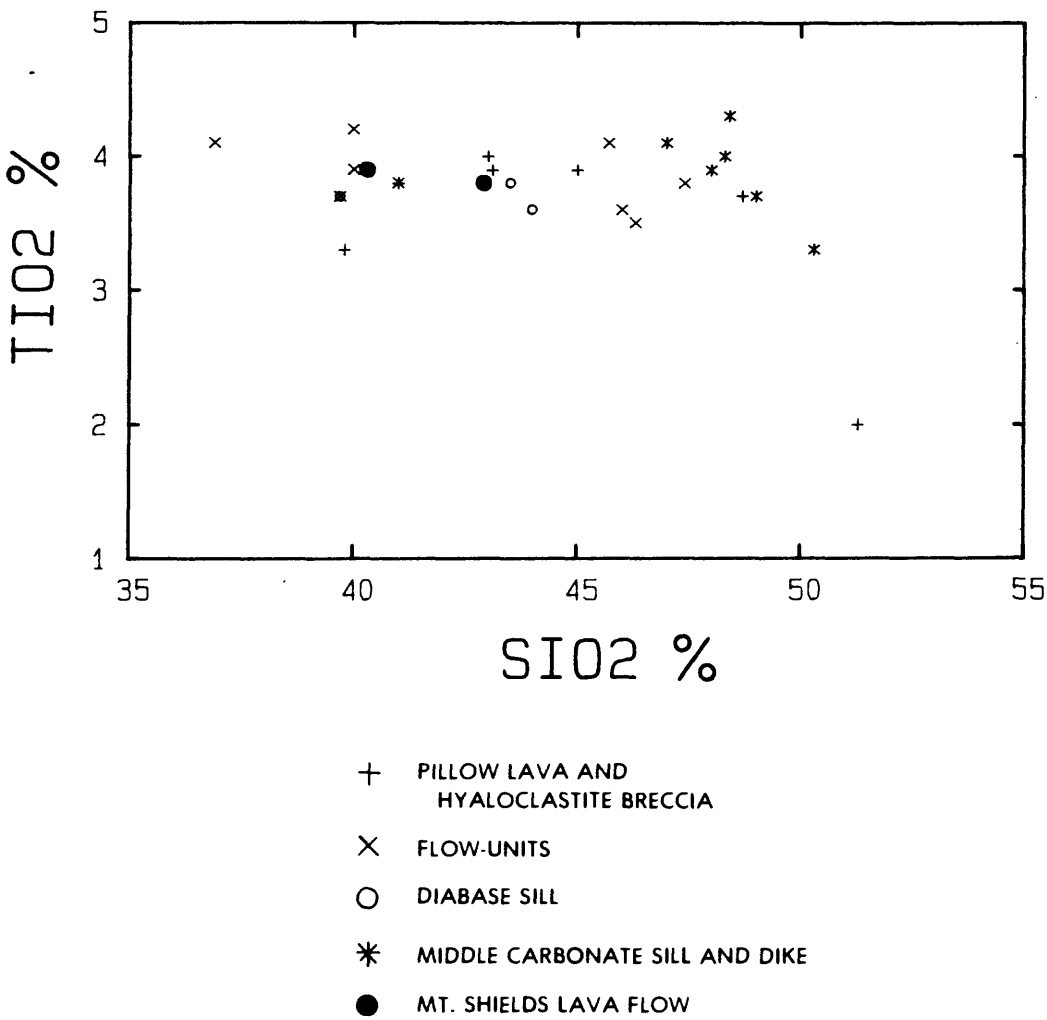

Figure 88. SiO_2-TiO_2 variation diagram. With only a few exceptions, TiO_2 concentrations are relatively constant over the wide range of SiO_2 contents. This indicates that TiO_2 was stable during diagenetic alteration. Present concentrations of TiO_2 are therefore close to that originally present in the rocks and are suitable for comparison with TiO_2 concentrations in unaltered basalts.

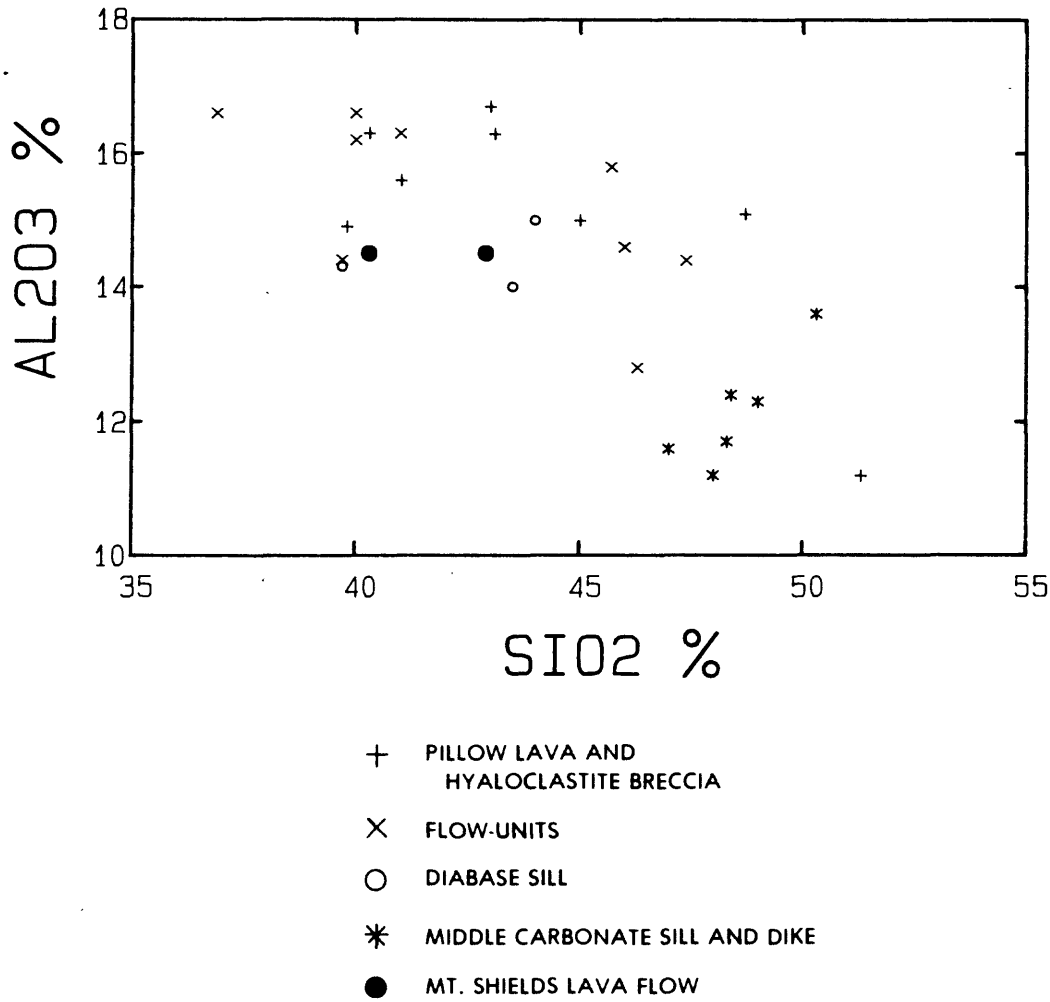

Figure 89. SiO_2-Al_2O_3 variation diagram. Except for a few intensely altered samples, values of Al_2O_3 in the Purcell Lava fall within the 14-17% range. Data points of the middle Belt carbonate sill and dike plot together and are generally lower in Al_2O_3 than those of the Purcell.

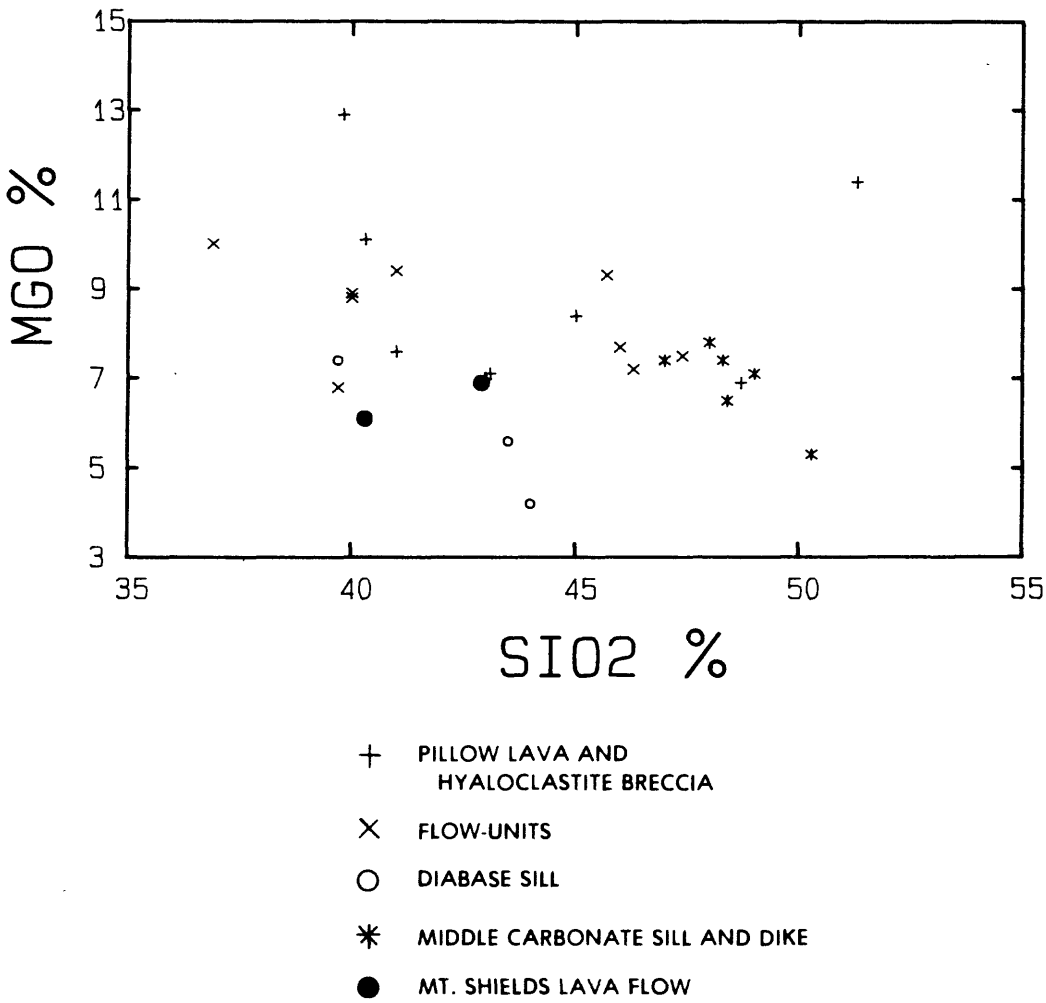

Figure 90. SiO_2-MgO variation diagram. The wide range of MgO values in the Purcell Lava indicates the apparent mobility of MgO during alteration. Data points of the middle Belt carbonate sill and dike form a tighter cluster, more in the range of typical basalts, an indication that MgO has not been as mobile in the sill and dike.

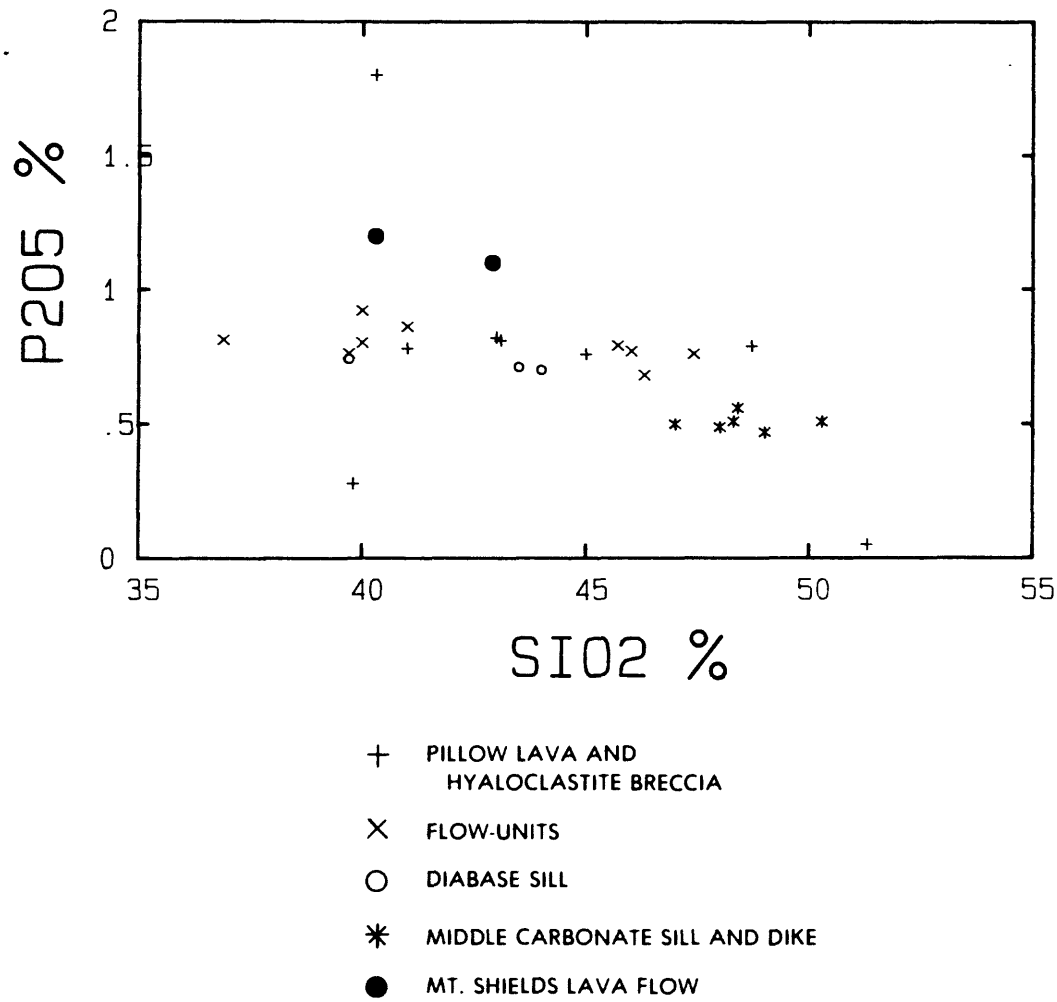

Figure 91. SiO_2-P_2O_5 variation diagram. P_2O_5 concentrations are nearly constant in the Purcell Lava as well as the middle Belt carbonate sill and dike. The lack of much deviation from the mean concentrations indicates that P_2O_5 has remained immobile during diagenesis. Note, however, that the concentrations of P_2O_5 in the Purcell are consistently higher than that of the middle Belt carbonate sill and dike. This may be an indication that the sill and dike are not related chemically to the Purcell Lava.

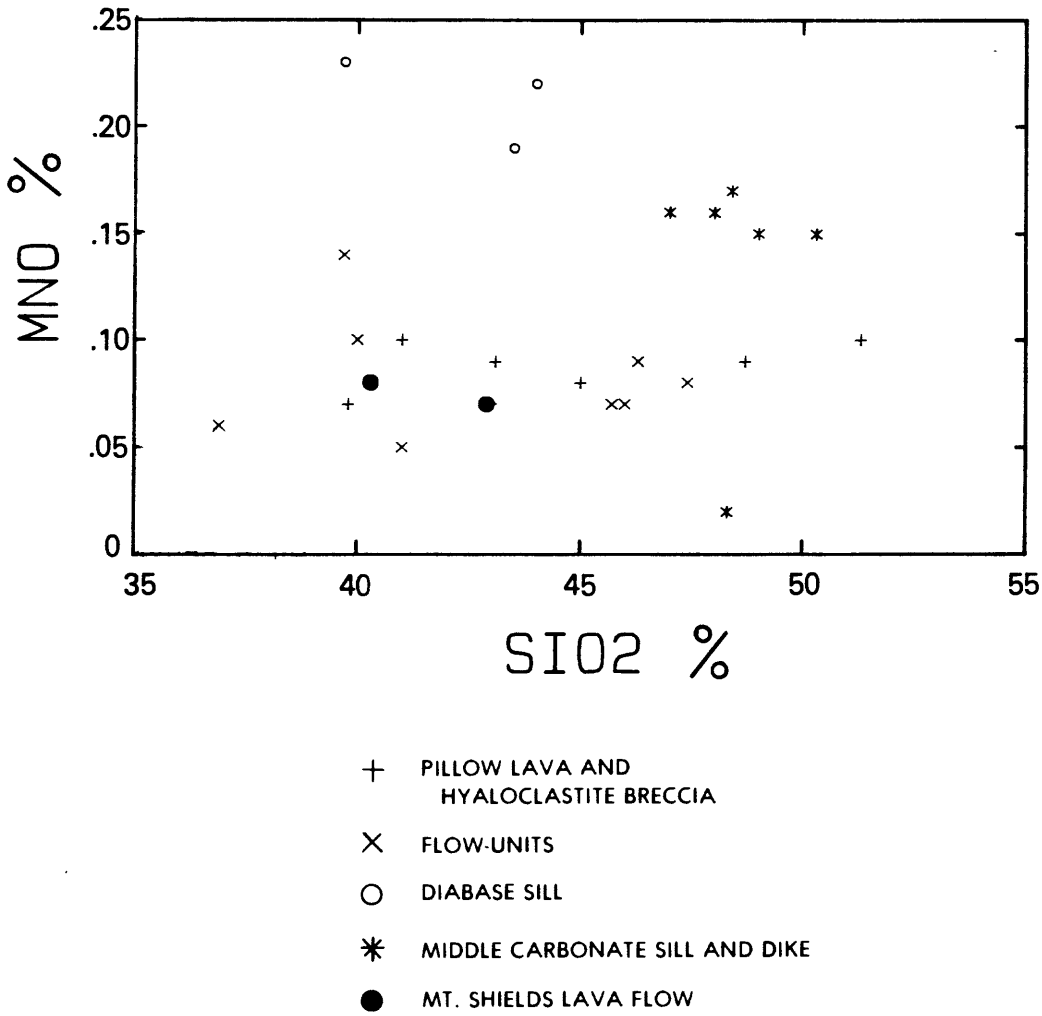

Figure 92. SiO_2-MnO variation diagram. Although concentrations of MnO occur over a substantial range, data points of the middle Belt carbonate sill and dike cluster around .15-.17%; those of the Purcell cluster loosely around .08-.10% MnO.

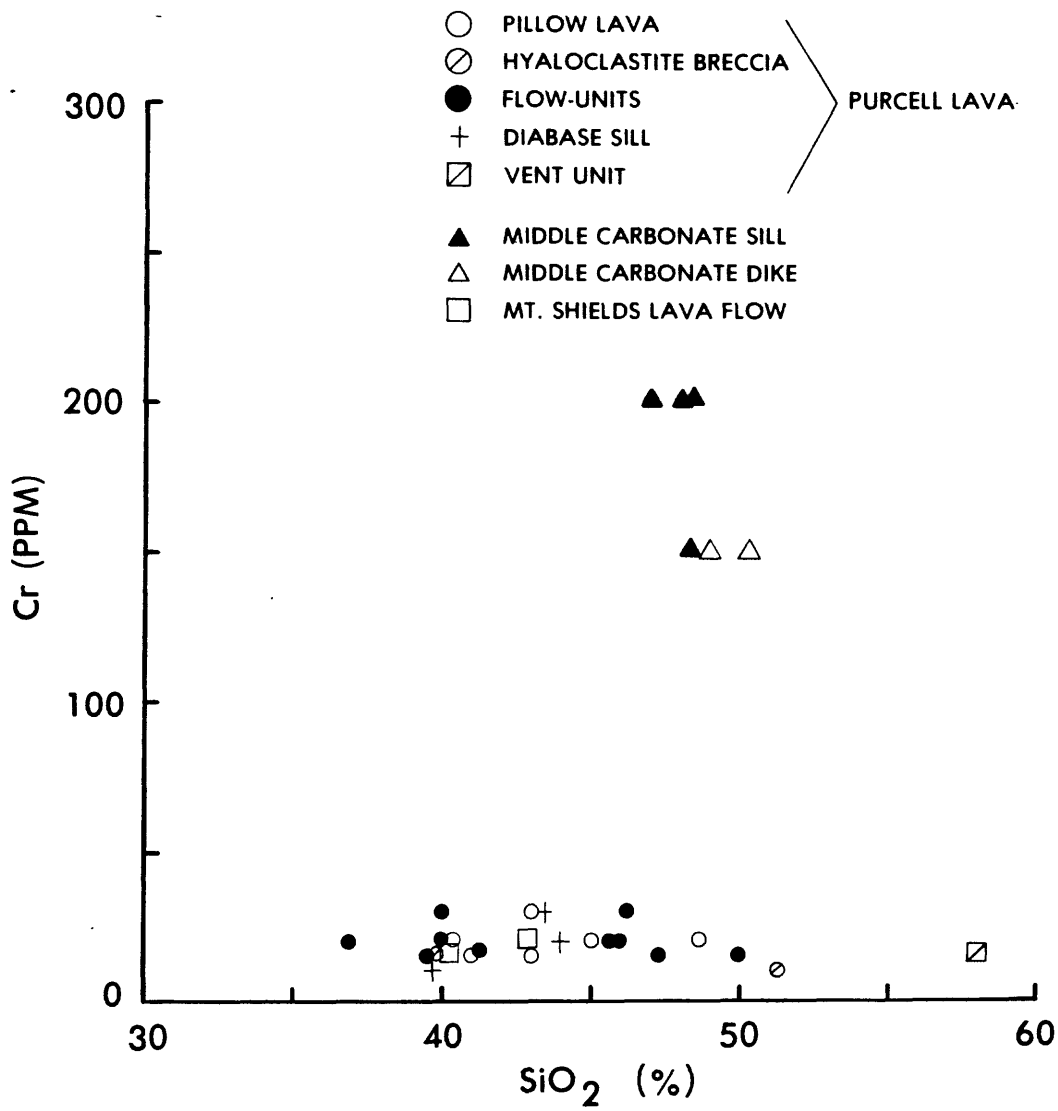

Figure 93. SiO_2-Cr variation diagram. Although the percent SiO_2 ranges widely for the Purcell Lava (due to secondary alteration), the concentration of Cr is rather uniform. This is an indication of the immobility of Cr during diagenesis. Note that concentrations of Cr in the middle Belt carbonate sill and dike are significantly higher than that in the Purcell Lava.

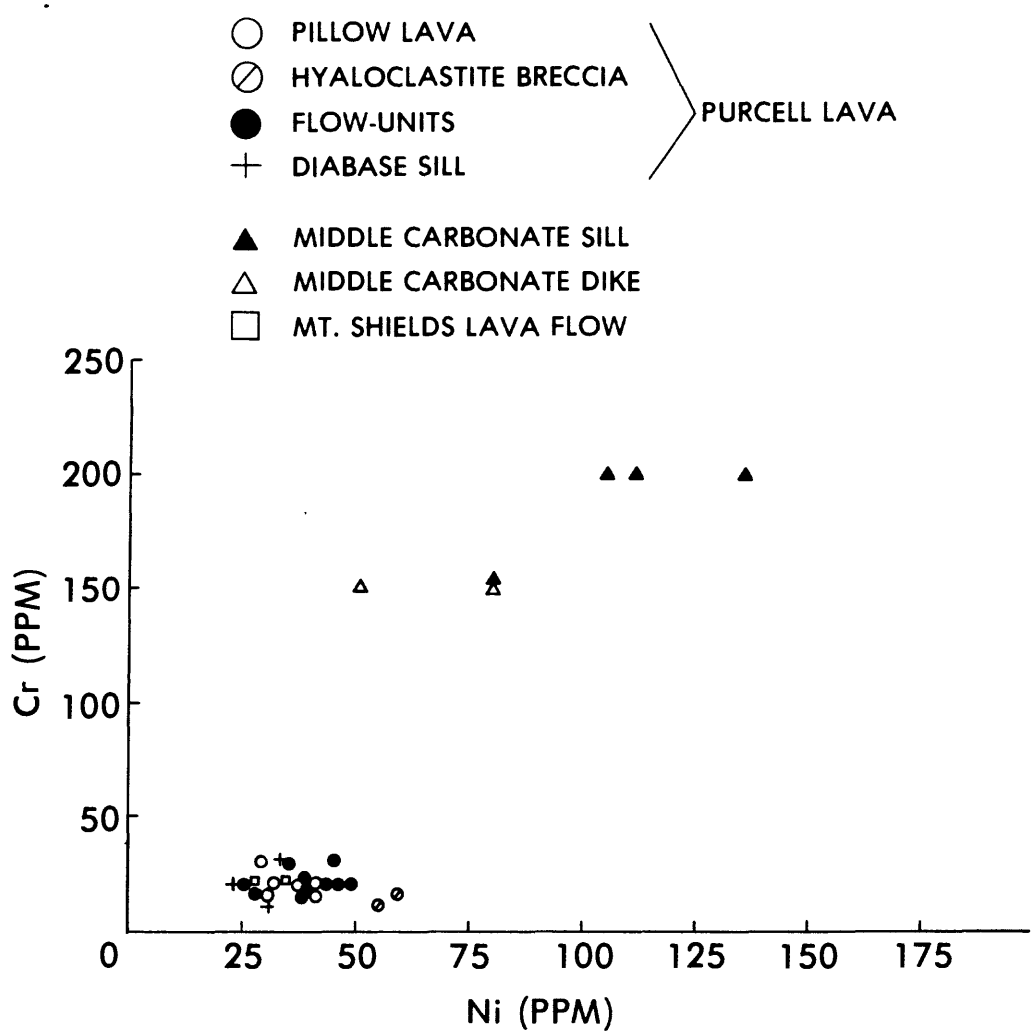

Figure 94. Cr-Ni variation diagram. The tight cluster of data points of the Purcell Lava and the Mt. Shields lava flow are indicative of the immobility of Cr and Ni in these flows. The middle Belt carbonate sill and dike have similar concentrations of Cr and Ni that are strikingly dissimilar from those of the Purcell.

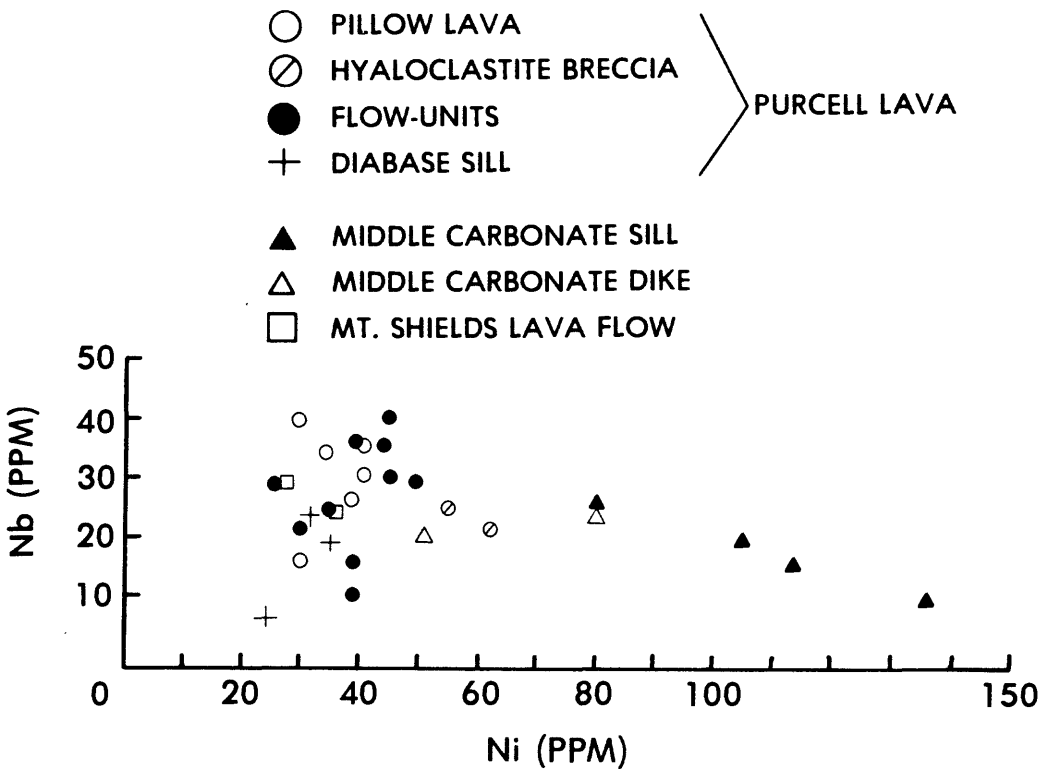

Figure 95. Nb-Ni variation diagram. Clustering of data points of the Purcell Lava indicates that Nb and Ni were immobile elements during alteration. The middle Belt carbonate sill and dike have significantly higher concentrations of Ni.

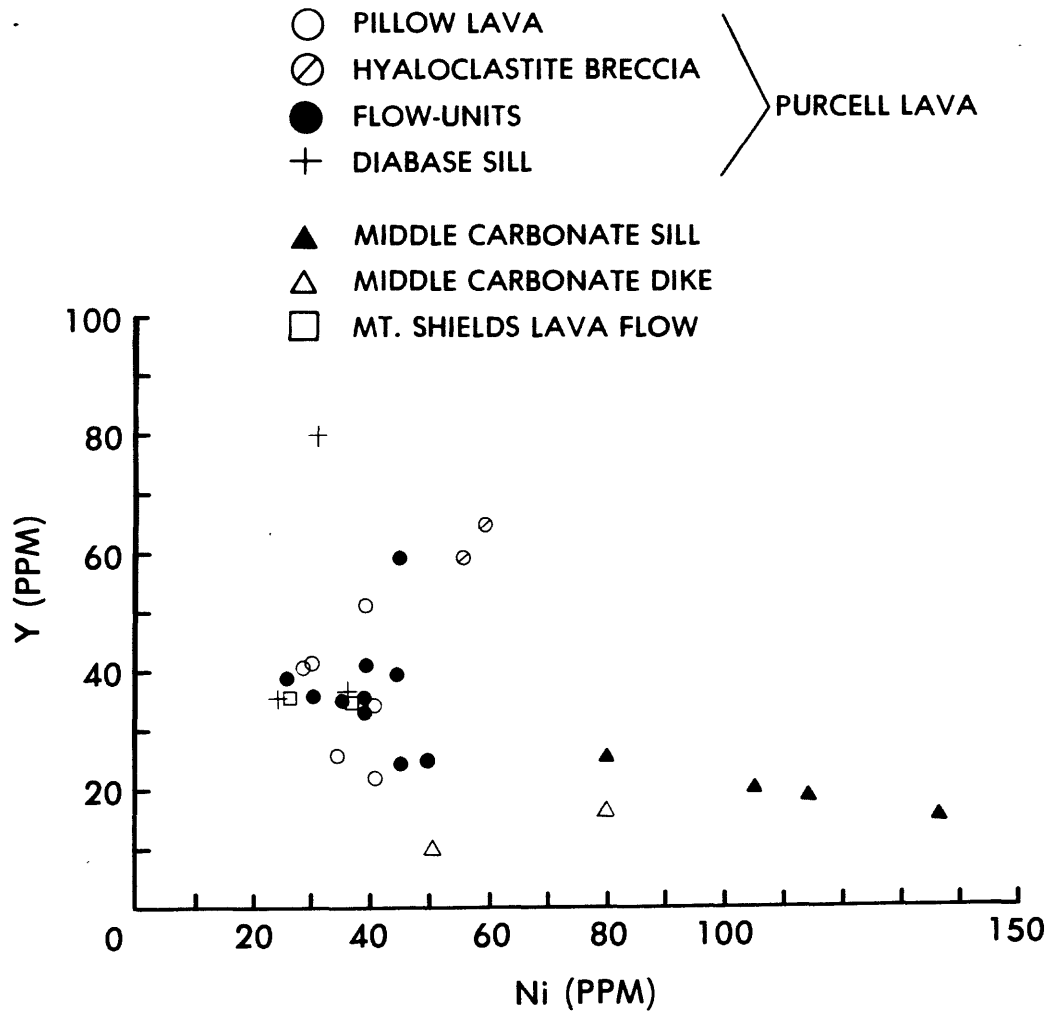

Figure 96. Y-Ni variation diagram. Generally, Y data points of the Purcell Lava cluster around 30-40 ppm. The scattering of some data points indicates that Y was mobilized to some extent during diagenesis. The middle Belt carbonate sill and dike have concentrations of Y and Ni that are distinctly different from the those of the Purcell Lava and Mt. Shields lava flow.

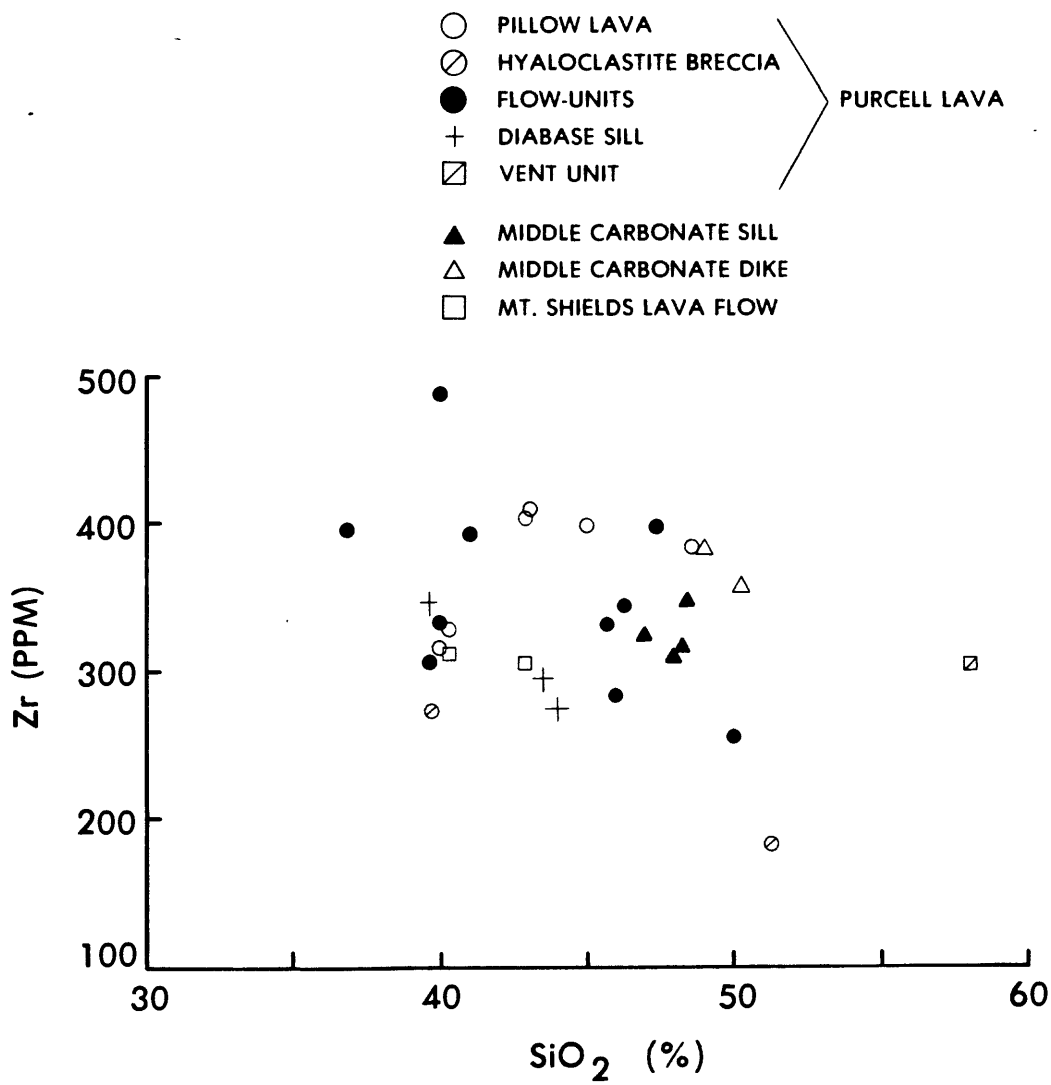

Figure 97. Zr-SiO_2 variation diagram. This plot illustrates the general range of Zr concentrations (300-400 ppm) in the Purcell Lava, Mt. Shields lava flow, and middle Belt carbonate sill and dike. The average Zr content in alkaline rocks is 333 ppm (Bloxam and Lewis, 1972). The average Zr content in the Purcell Lava and middle Belt carbonate sill and dike is 339 and 338 ppm, respectively, which closely approximates concentrations in average alkaline basalts.

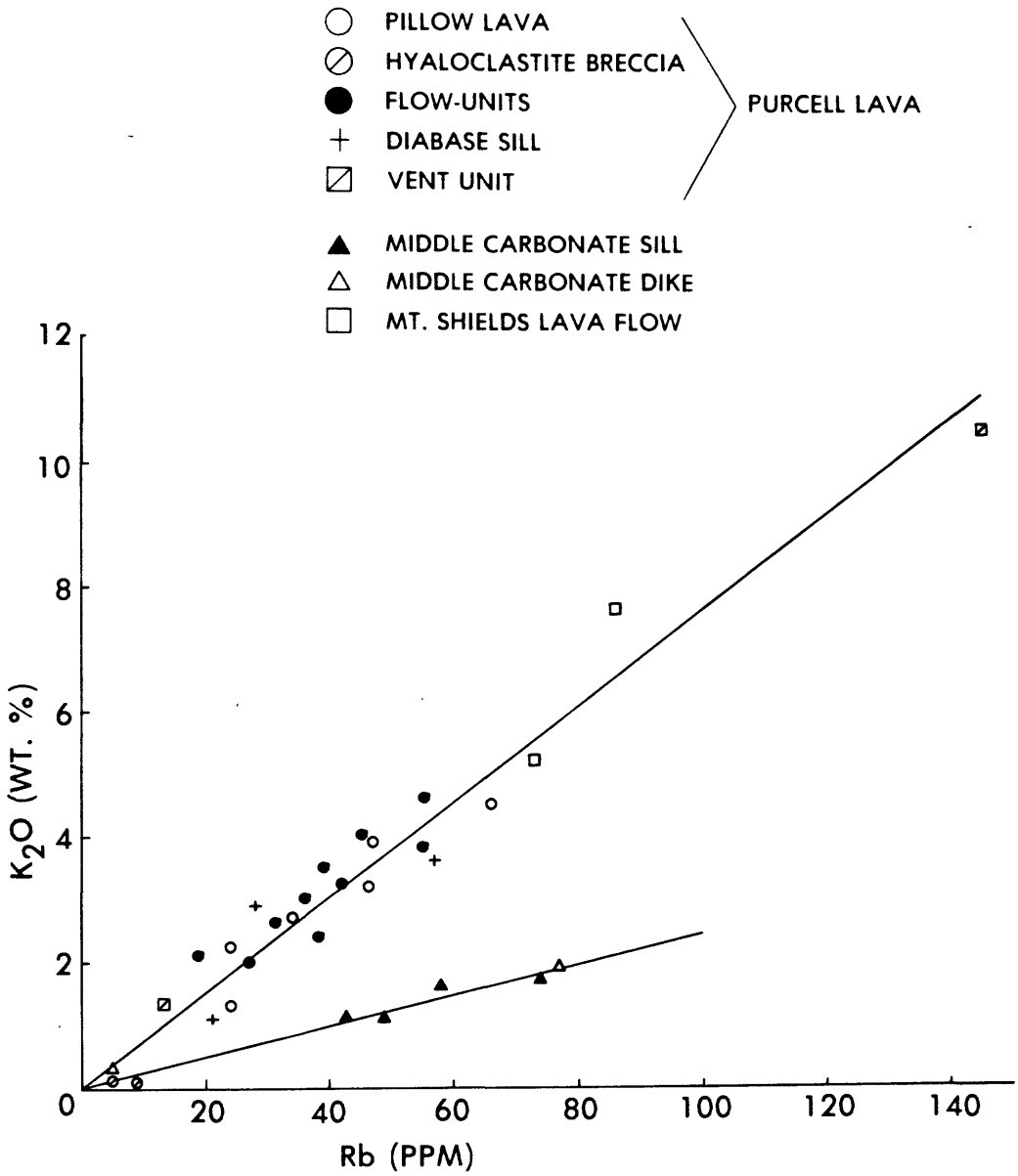

Figure 98. K_2O-Rb variation diagram. K_2O varies linearly with Rb in the Purcell Lava as well as in the middle Belt carbonate sill. The range values is a reflection of the movement of K_2O during diagenesis and the proportional movement of Rb. Data points of the middle Belt carbonate sill and dike lie along a line indicating that the sill and dike are geochemically similar; data points of the Purcell Lava lie along a separate line. This suggests that the Purcell is geochemically not related to the sill and dike.

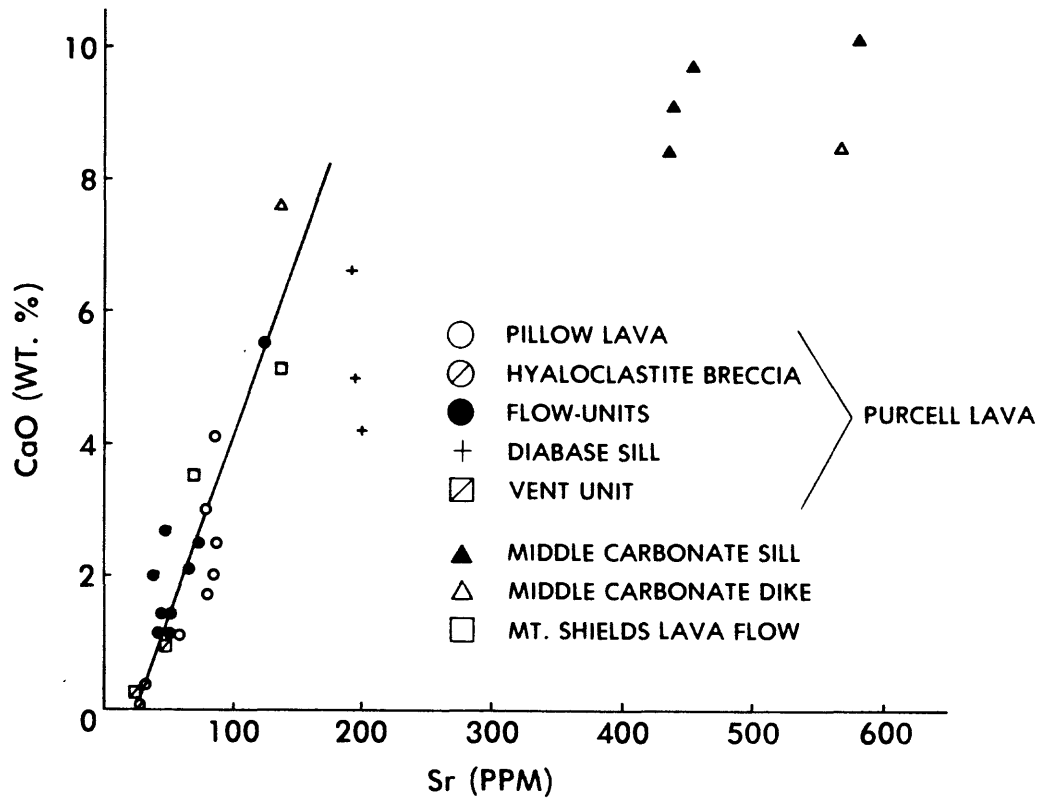

Figure 99. CaO-Sr variation diagram. CaO generally varies colinearly with Sr in the Purcell Lava. The range of CaO contents reflects the mobility of calcium during diagenesis. Note that data points of the middle Belt carbonate sill and dike plot separately from those of the Purcell Lava, which suggests that geochemically, the lava flows are distinct from the sill and dike.

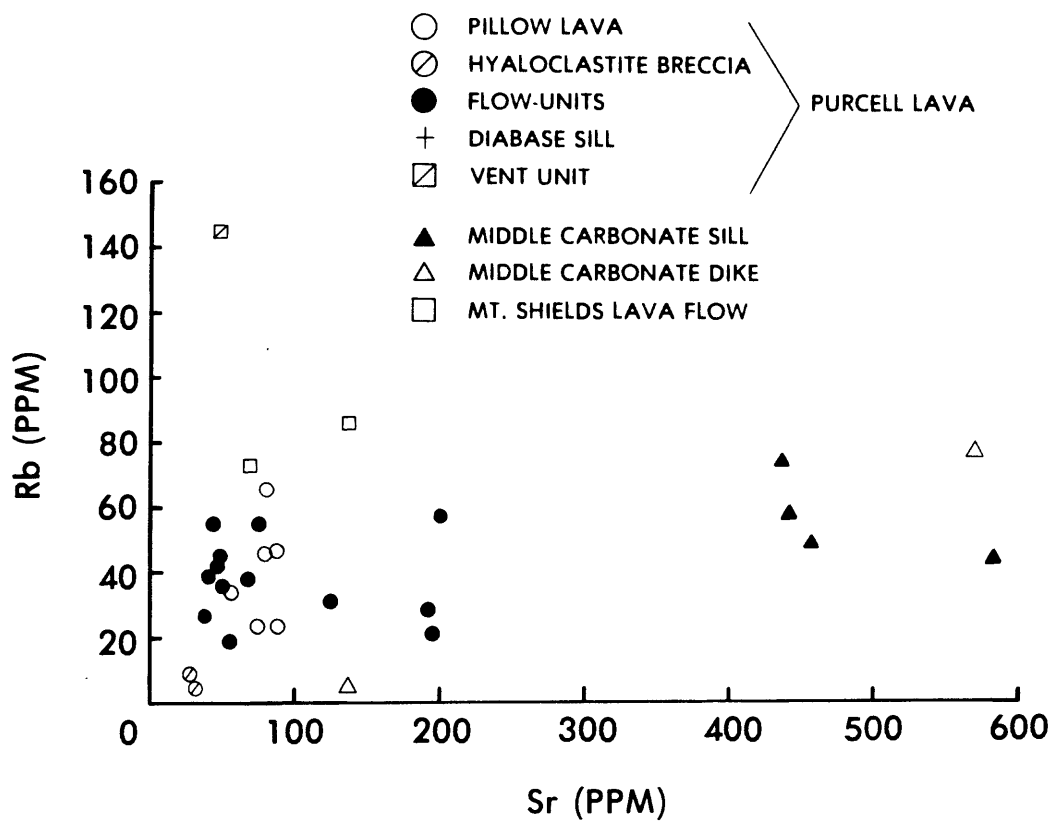

Figure 100. Rb-Sr variation diagram. This diagram illustrates that the Purcell Lava is geochemically different from the middle Belt carbonate sill and dike with respect to Rb and Sr contents.

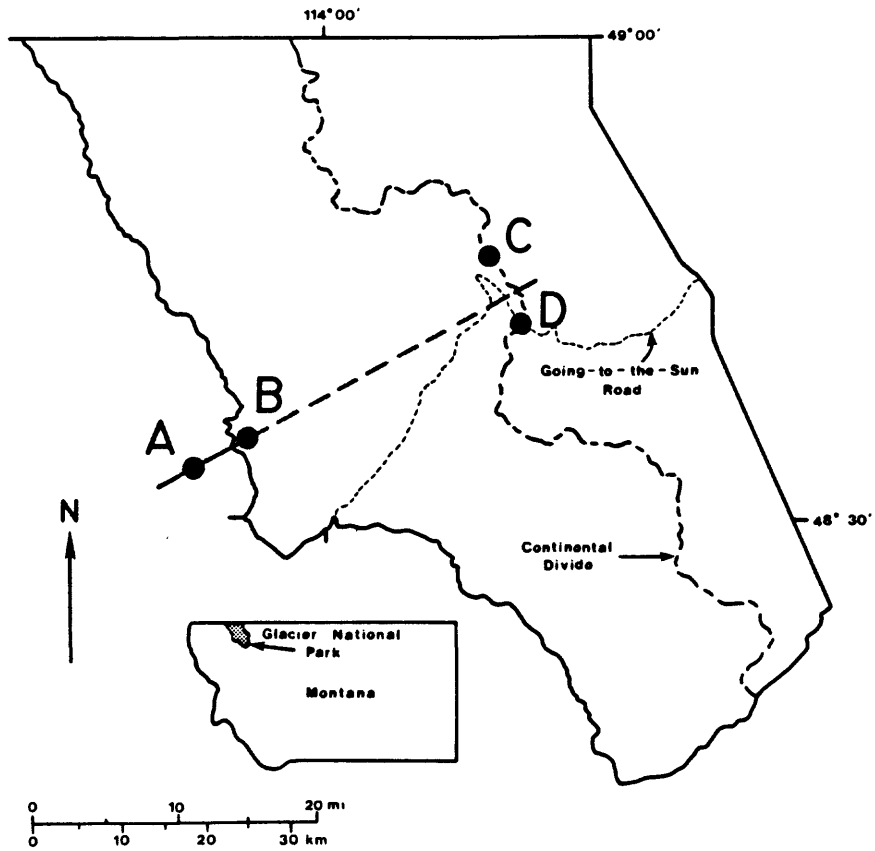

Figure 101. Map showing the probable former southern limit of Purcell Lava in Glacier National Park. Point A is where the Purcell Lava thins to zero thickness in the Whitefish Range (Harrison and others, 1983); B is where the Purcell Lava thins to zero in the Apgar Mountains; C is Granite Park where the Purcell Lava is 19 m thick; and D is Logan Pass where the Purcell Lava is absent from the stratigraphic succession.

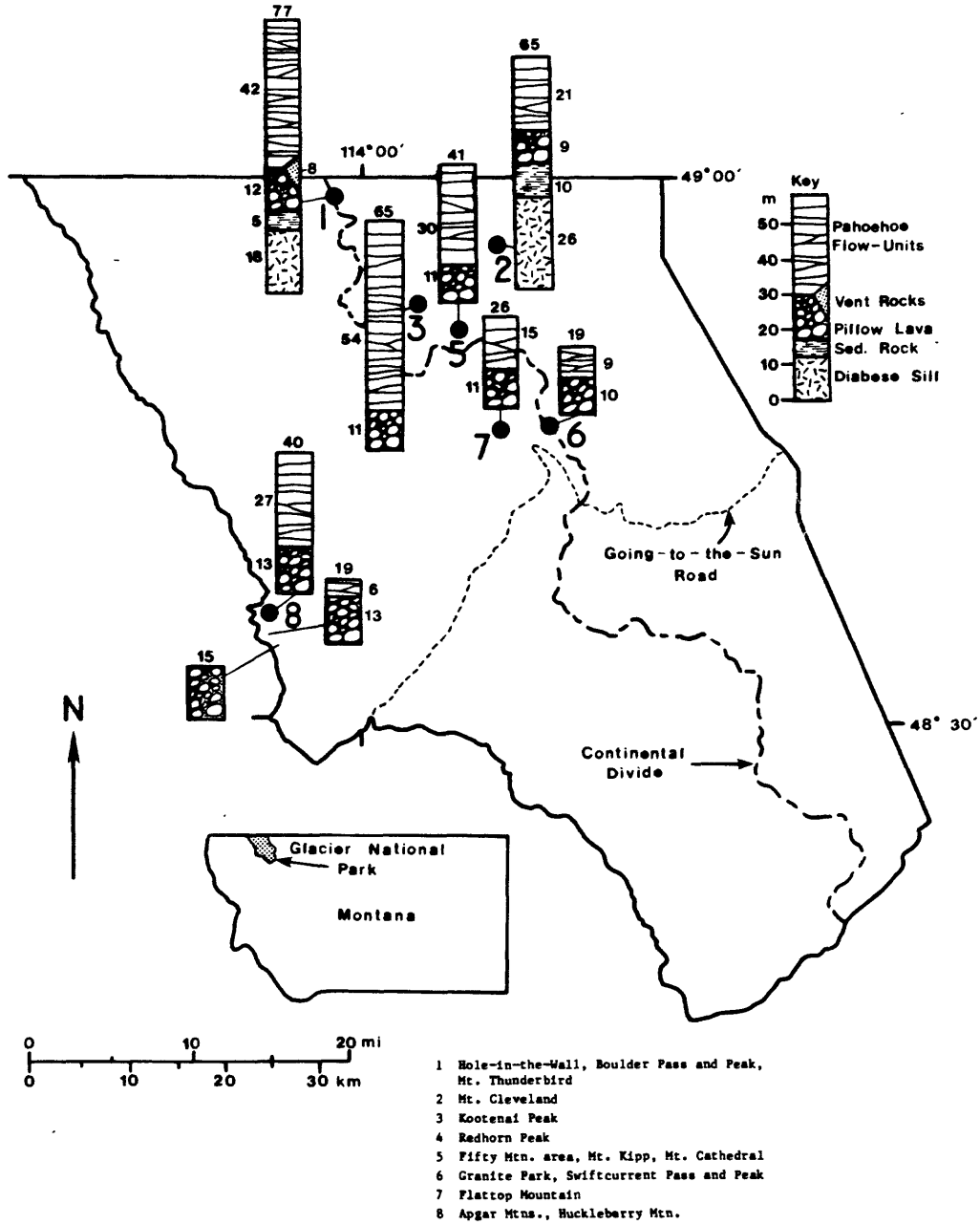

Figure 102. Graphic plot of measured sections of Purcell Lava in Glacier National Park. Locality 4 is not shown because the section there is incomplete and not well exposed; all other sections are complete and bounded by strata of the Snowslip Formation. Depiction of pillow diameters and the thickness of individual flow units is not drawn to scale. Each column shows the approximate number of flow units identified at that locality. Thickness units are in meters; total thickness appears at the top of each section and the thickness of individual facies is shown along the side margins. All sections were measured at least twice with an Abney Level, Jacobs staff, and steel tape.

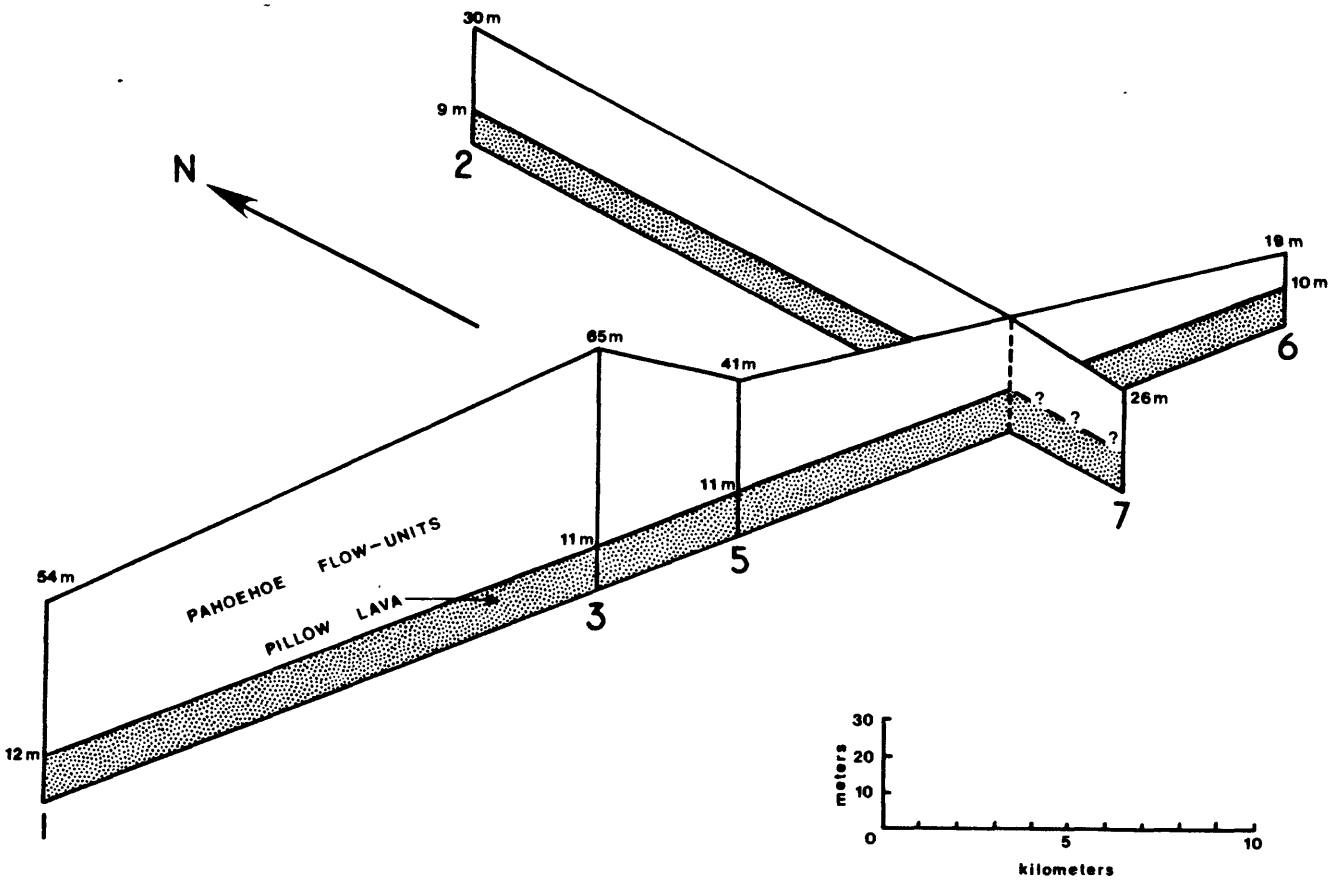

Figure 103. Fence diagram depicting thickness variations of Purcell Lava in Glacier National Park. Thicknesses exclude the hypabyssal diabase sill and sedimentary rock interval between it and the pillowed facies. Thickness of the pahoehoe facies generally increases to the north. The uniformity of pillow lava thickness suggests that the upper limit of pillow lava marks the paleo-waterline, and thickness represents paleo-water depth. Location numbers are keyed to Figure 101. Sections of Purcell Lava at Huckleberry Mountain are not included because of structural complexities and lack of exposures in between the localities. Also evident from the diagram is that the thickness of pillow lava increases to the northwest and southwest, indicating that the seafloor sloped downward in those directions (i.e. water depth increased). Note that if thickness of the diabase sill and sediment interval were included (refer to Figure 101), the northward thickening trend would still apply.

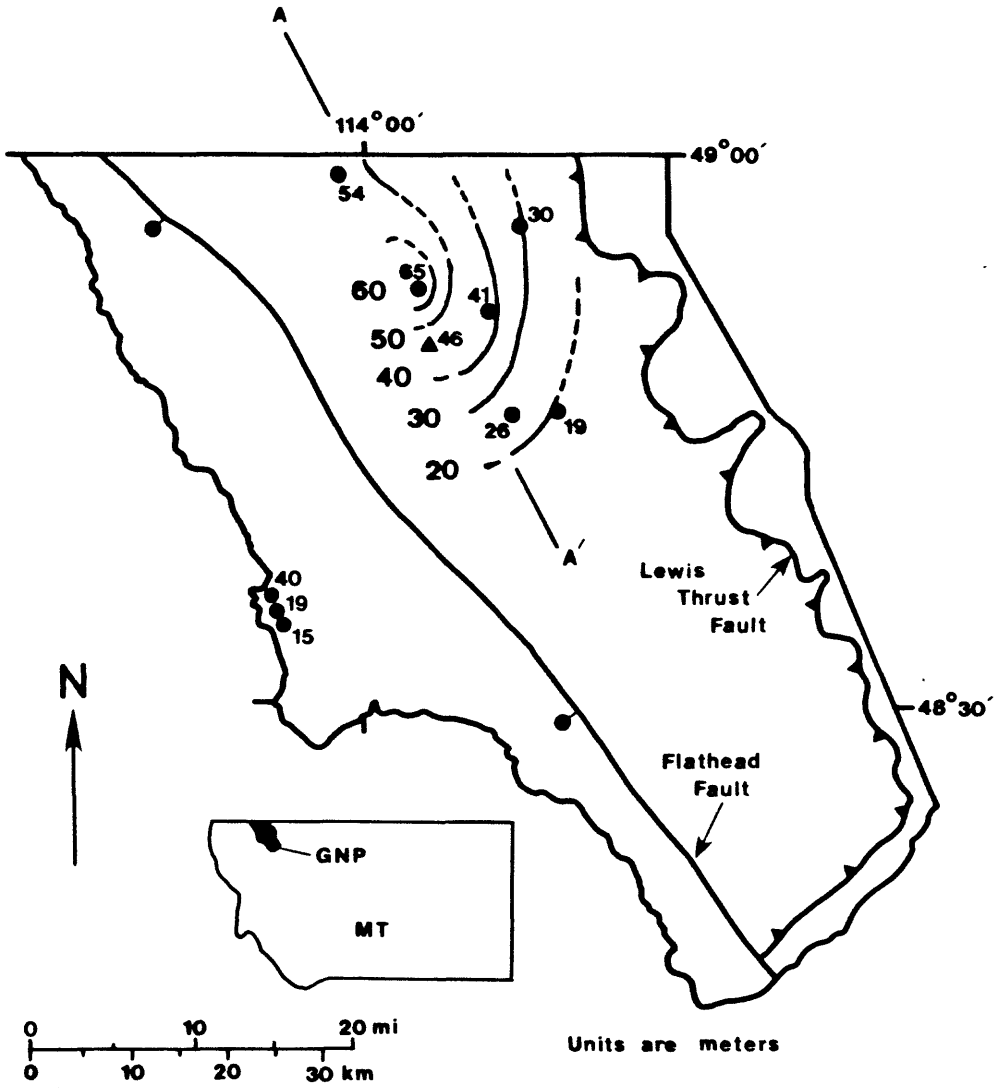

Figure 104. Isolith map of Purcell Lava in Glacier National Park (GNP). The configuration of the isoliths defines a trend (A-A') that is similar to that formed by isoliths of the Nichol Creek Lavas (Purcell Lava equivalent) in Canada (Hoy, 1984); compare with Figures 106 and 107. Solid circles mark the location of measured sections and the triangle marks the location of Purcell Lava at Trapper Peak where the thickness was calculated using a computer assisted photogrammetric mapping system. The section located at Huckleberry Mountain (on the west side of Flathead Fault) were not contoured because of the lack of data points across the fault.

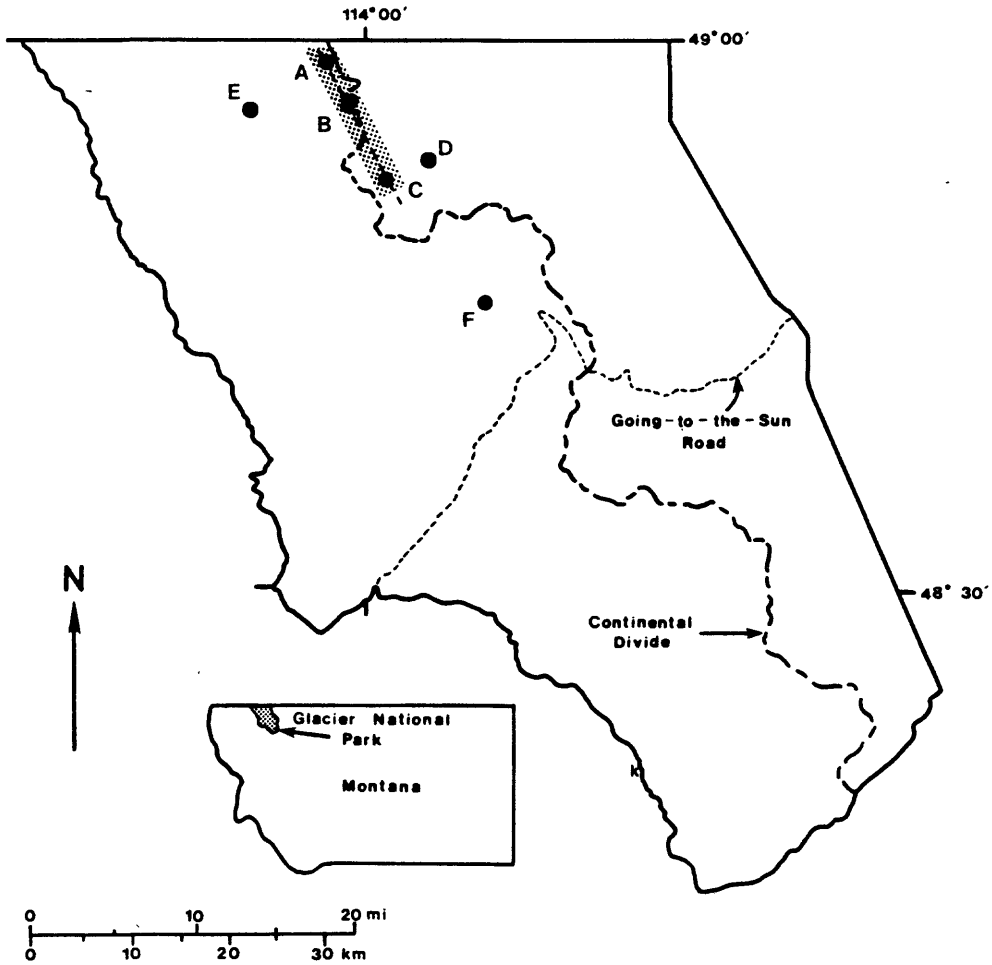

Figure 105. Rocks of the vent facies occur at three localities of Purcell Lava examined in this report: Hole-in-the-Wall and Boulder Peak (A), Mt. Thunderbird (B), and the 6784-ft. knob 3 km northeast of Redhorn Peak (C). The exposures lie along a linear north-northwest trend (about 3 km wide) indicated by the stipled pattern. At the Kootenai Peak section (D), only 3 km northeast of 6784 knob, no vent rocks occur. Along the main trend, but 15 km southeast, the Flattop Mountain section (F) likewise contains no rocks of the vent facies. The only exposure of Purcell Lava preserved west of the three localities that define the trend is near the summit of Kinnerly Peak (E) and probably does not contain vent rocks (see text for explanation).

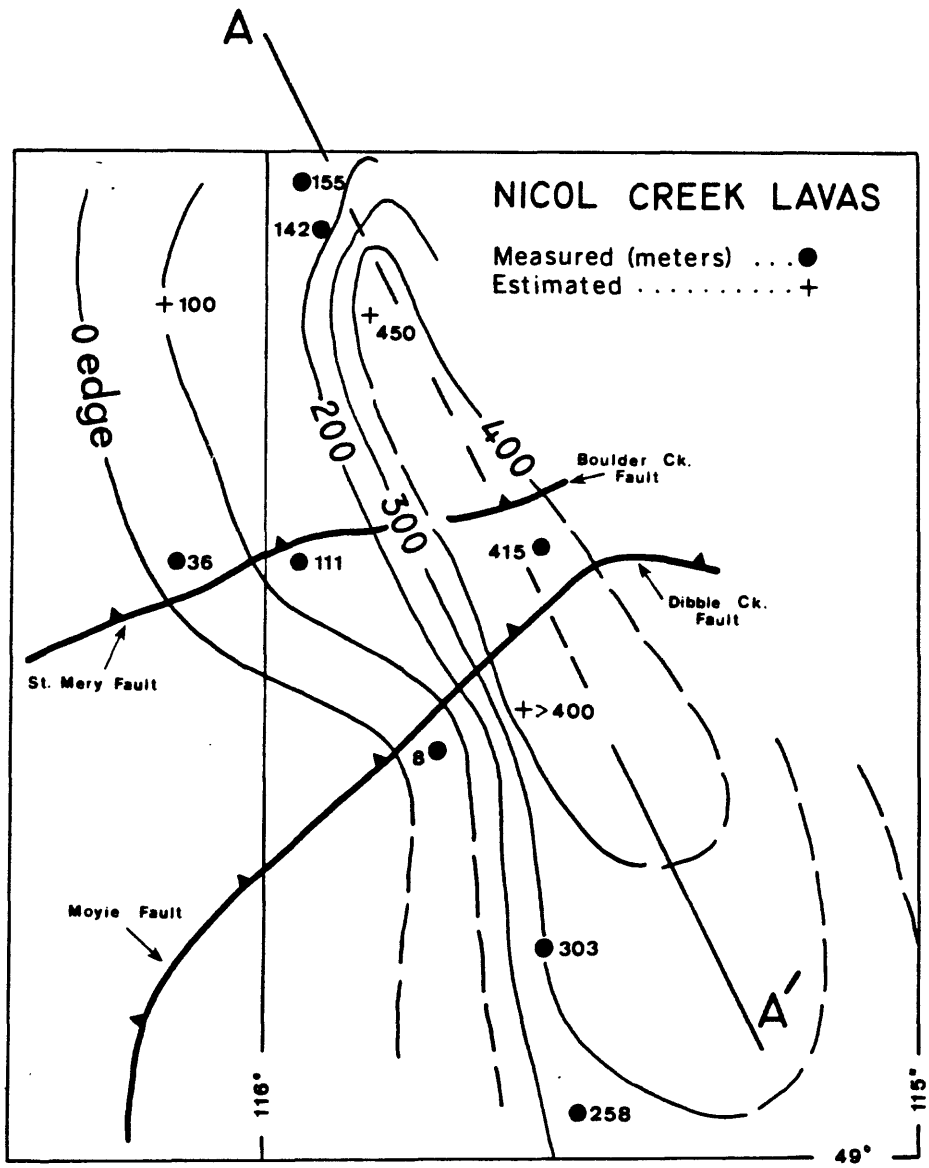

Figure 106. Isolith map from Hoy (1984) of the Nicol Creek Formation of Canada (Purcell Lava equivalent of McMechan and others, 1983). Isoliths form a linear trend (A-A′) oriented north-northwest, similar to that defined by the Purcell Lava isolith map (Figure 104), and distribution of vent rocks in Glacier National Park (Figure 102). The Nichol Creek Formation is restored for movement along the St. Mary, Moyie, Dribble Creek, and Boulder Creek faults.

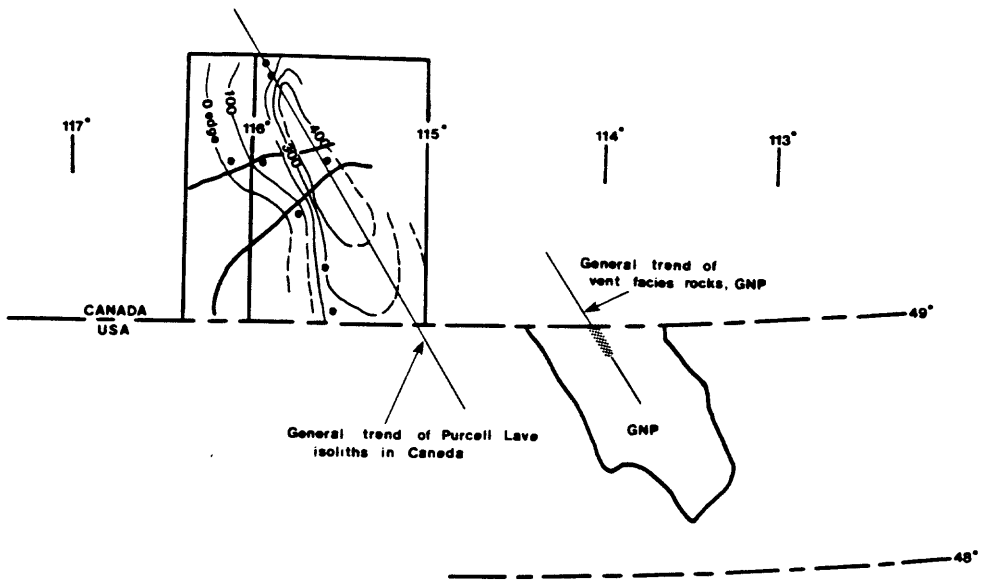

Figure 107. Sketch map showing the similarity between the trends of vent rock distribution in Glacier National Park (this study) and isoliths of the Nichol Creek Formation (Purcell Lava equivalent in Canada)(Hoy, 1984). Similar orientation of the two trends supports a hypothesis of a fissure-type vent system. Geographical offset of the trends is probably not primary. Also, similarity of the trends could be fortuitous since a number of large tectonic structures exist west of Glacier Park and in the southern part of the Canadian exposures, the movement along which has not been adequately documented to palinspastically reconstruct basin geometry (J. Harrison, personal communicantion, 1984). Refer to Figure 106 for details of the Canadian isolith map.

Table 1. Plagioclase chemistry of a few selected samples of Purcell Lava. Analyses were performed by John Drexler by means of Energy Dispersive Microprobe, University of Colorado. %Ab = (Na/Na+K) X 100; %Or = (K/Na+K) X 100.

Sample	Oxide Formula	Oxide Percent	Number of Cations	%Ab	%Or
	Na_2O	6.38	0.5538	64	
1	Al_2O_3	21.90	1.1558		
(82M-111)	SiO_2	65.12	2.9164		
	K_2O	5.48	0.3132		36
	Na_2O	6.43	0.5609	59	
2	Al_2O_3	19.68	1.0436		
(82M-49)	SiO_2	66.23	2.9791		
	K_2O	6.83	0.3922		41
	Na_2O	10.39	0.8674	99	
3	Al_2O_3	20.55	1.0430		
(82M-49)	SiO_2	69.63	2.9980		
	K_2O	0.21	0.0113		1
	Na_2O	10.59	0.8791	99	
4	Al_2O_3	20.50	1.0345		
(82M-49)	SiO_2	70.13	3.0024		
	K_2O	0.15	0.0080		1
	Na_2O	3.80	0.3494	34	
5	Al_2O_3	18.58	1.0391		
(82M-49)	SiO_2	62.53	2.9669		
	K_2O	11.00	0.6658		66
	Na_2O	10.26	0.8617	99	
6	Al_2O_3	20.22	1.0326		
(82M-120)	SiO_2	69.41	3.0072		
	K_2O	0.21	0.0117		1
	Na_2O	10.37	0.8769	98	
7	Al_2O_3	20.34	1.0452		
(82M-119)	SiO_2	68.61	2.9917		
	K_2O	0.37	0.0206		2
	Na_2O	9.52	0.8125	91	
8	Al_2O_3	21.74	1.1273		
(82M-119)	SiO_2	66.62	2.9317		
	K_2O	1.40	0.0786		9

Table 2.--Chemical analyses of the Purcell Lava and other selected igneous rocks in Glacier National Park. NA = sample was not analyzed for the specified element; numbers in parantheses indicate limits of detection (ppm); * total iron; LOI = lost on ignition. Analysts: A. Bartel, K. Stewart, and J. Taggart (major oxides); C. Stone, H. Neiman, and G. Mason (FeO, H_2O+, H_2O-, and CO_2); M. Malcolm (Be, Co, Cr, Pb, Sc, V, and Yb); John Drexler (Ba, Cu, Nb, Ni, Rb, Sr, Y, Zn, and Zr.

Sample	1	2	3	4	5	6	7
	Purcell Lava						
Rock type	Pillow lava						Breccia
Field No.	82M-117	82M-174	82M-52	82M-49	82M-29	82M-151	82M-146
Lab No.	D252252	D252263	D252239	D252236	D252232	D252260	D252259
	Major oxides (weight percent)						
SiO_2	41.0	43.1	45.0	48.7	43.0	40.3	39.8
TiO_2	3.8	3.9	3.9	3.7	4.0	3.9	3.3
Al_2O_3	15.6	16.3	15.0	15.1	16.7	16.3	14.9
Fe_2O_3	5.3	4.7	3.9	2.5	1.2	2.0	3.2
FeO	11.3	10.1	11.3	9.2	9.0	12.2	15.9
MgO	7.6	7.1	8.4	6.9	7.0	10.1	12.9
CaO	3.0	1.7	1.1	2.0	4.1	2.5	.35
Na_2O	2.3	2.2	1.8	3.0	2.5	2.2	.23
K_2O	3.2	4.5	2.7	2.2	3.9	1.3	.16
H_2O+	5.1	4.7	5.6	4.6	4.5	6.7	8.6
H_2O-	.21	.27	.36	.26	.24	.26	.57
P_2O_5	.78	.81	.76	.79	.82	1.8	.28
MnO	.10	.09	.08	.09	.07	.08	.07
CO_2	.29	.33	.03	.69	2.3	.04	.02
Total	99.58	99.80	99.93	99.73	99.33	99.68	100.28
	Selected minor elements (parts per million)						
Ba (6)	824	1907	615	315	776	334	39
Co (3)	20	20	50	30	20	50	30
Cr (1)	15	15	20	20	30	20	15
Cu (10)	37	44	7	4	6	21	18
Nb (11)	17	32	36	34	39	27	22
Ni (4)	30	42	42	34	29	38	59
Pb (10)	<10	<10	<10	<10	<10	<10	<10
Rb (2)	46	66	34	24	47	24	5
Sc (5)	20	15	15	15	15	15	10
Sr (2)	79	79	56	74	87	88	32
V (7)	200	150	150	150	150	150	100
Y (7)	42	23	34	26	42	52	64
Yb (1)	3	2	2	3	3	3	2
Zn (4)	298	208	285	235	206	415	514
Zr (5)	315	408	398	382	403	329	273

Table 2 (continued);

Sample	8	9	10	11	12	13	14
	Purcell Lava						
Rock type	Breccia	Pahoehoe flow units					
Sample No.	82M-51	82M-119	82M-126	82M-133	82M-85	82M-65	82M-62
Lab No.	D252237	D252253	D252254	D252256	D252246	D252243	D252242
	Major oxides (weight percent)						
SiO_2	51.3	39.7	46.0	40.0	50.0	46.3	47.4
TiO_2	2.0	3.7	3.6	4.2	2.2	3.5	3.8
Al_2O_3	11.2	14.4	14.6	16.2	13.7	12.8	14.4
Fe_2O_3	2.8	6.1	5.5	3.1	2.4	8.1	3.8
FeO	13.2	9.3	9.6	10.8	12.2	9.4	10.8
MgO	11.4	6.8	7.7	8.8	9.5	7.2	7.5
CaO	.09	5.5	1.1	2.7	.44	1.4	1.4
Na_2O	.19	2.7	1.8	1.8	.46	1.5	1.7
K_2O	<.02	2.6	3.8	4.0	2.0	3.0	3.2
H_2O+	7.0	4.4	4.8	5.7	6.3	4.5	5.0
H_2O-	.58	.23	.25	.28	.43	.25	.31
P_2O_5	<.05	.76	.77	.80	.34	.68	.76
MnO	.10	.14	.07	.10	.10	.09	.08
CO_2	.01	3.4	.01	1.2	<.01	.36	.33
Total	99.87	99.73	99.60	99.68	100.07	99.08	99.68
	Selected minor elements (parts per million)						
Ba (6)	170	400	502	414	200	486	546
Co (3)	30	30	30	50	20	30	30
Cr (1)	10	15	20	30	15	30	15
Cu (10)	21	22	7	17	17	8	23
Nb (11)	25	22	16	24	10	30	37
Ni (4)	56	30	38	35	38	45	38
Pb (10)	15	<10	<10	<10	<10	<10	<10
Rb (2)	9	31	55	45	27	36	42
Sc (5)	10	15	15	15	15	15	15
Sr (2)	28	124	44	49	38	51	47
V (7)	100	150	150	150	100	150	150
Y (5)	59	37	36	35	42	24	33
Yb (1)	2	3	3	3	2	3	3
Zn (4)	358	251	271	288	533	238	228
Zr (5)	181	305	284	332	258	342	398

Table 2 (continued);

Sample	15	16	17	18	19	20
	Purcell Lava					
Rock type	Pahoehoe flow units				Hypabyssal sill	
Field No.	82M-59	82M-35	82M-39	82M-155	82M-108	82M-110
Lab No.	D252241	D252233	D252234	D252261	D252250	D252251
	Major oxides (weight percent)					
SiO_2	40.0	41.0	36.9	45.7	43.5	44.0
TiO_2	3.9	3.8	4.1	4.1	3.8	3.6
Al_2O_3	16.6	16.3	16.6	15.8	14.0	15.0
Fe_2O_3	2.4	1.9	3.1	1.8	2.8	4.7
FeO	11.2	13.0	14.0	11.1	12.3	10.4
MgO	8.9	9.4	10.0	9.3	5.6	4.2
CaO	2.5	2.1	2.0	1.1	5.0	4.2
Na_2O	1.3	1.7	.98	1.9	2.8	2.9
K_2O	4.6	2.4	3.5	2.1	1.1	3.6
TiO_2	3.9	3.8	4.1	4.1	3.8	3.6
H_2O+	5.9	6.4	6.9	6.0	4.5	3.5
H_2O-	.45	.28	.40	.16	.13	.14
P_2O_5	.92	.86	.81	.79	.71	.70
MnO	.10	.05	.06	.07	.19	.22
CO_2	1.0	.69	.68	.05	2.9	2.1
Total	99.77	99.88	100.03	99.97	99.33	99.26
	Selected minor elements (parts per million)					
Ba (6)	1600	1012	547	671	405	2705
Co (3)	30	50	50	30	50	30
Cr (1)	20	20	20	20	30	20
Cu (10)	185	<10	<10	24	42	25
Nb (11)	40	35	29	28	18	<11
Ni (3)	30	30	30	20	30	30
Pb (10)	<10	<10	<10	<10	<10	<10
Rb (2)	55	38	39	19	21	57
Sc (5)	15	15	15	15	15	15
Sr (2)	75	67	40	55	195	200
V (7)	150	150	150	150	150	150
Y (5)	58	39	25	38	36	36
Yb (1)	3	3	3	3	3	3
Zn (4)	270	282	271	373	234	224
Zr (5)	488	391	393	330	293	275

Table 2 (continued);

Sample	21	22	23	24	25	26
			Purcell Lava			
Rock type	Sill	Intrusion	Vent breccia		Mid. Belt carb. sill	
Field No.	82M-87	82M-131	82M-86a	82M-86b	82M-102	82M-82
Lab No.	D252248	D252255	D252247	D250980	D252249	D252245
			Major oxides (weight percent)			
SiO_2	39.7	74.8	58.0	57.9	48.0	47.0
TiO_2	3.7	.38	2.9	3.1	3.9	4.1
Al_2O_3	14.3	7.0	15.4	15.1	11.2	11.6
Fe_2O_3	1.4	1.7	.75	*5.6	3.1	2.6
FeO	11.4	5.7	4.3		8.8	9.5
MgO	7.4	4.8	3.3	3.4	7.8	7.4
CaO	6.6	.16	.99	1.0	10.1	9.7
Na_2O	1.4	.27	.20	.15	2.1	2.3
K_2O	2.9	1.3	10.5	10.2	1.1	1.1
H_2O+	5.3	3.2	2.4	—	2.1	2.3
H_2O-	.21	.12	.14	—	.13	.18
P_2O_5	.74	.15	.77	.81	.49	.50
MnO	.23	.04	.02	.03	.16	.16
CO_2	4.4	<.01	<.01	—	.32	.02
LOI	—	—	—	2.1	—	—
Total	99.68	99.62	99.67	99.39	99.13	99.66
			Selected minor elements (parts per million)			
Ba (6)	588	160	1092	NA	207	204
Co (3)	30	20	15	NA	30	30
Cr (1)	10	15	15	NA	200	200
Cu (10)	67	21	22	NA	74	70
Nb (11)	23	—	28	NA	<11	19
Ni (4)	32	16	19	NA	137	105
Pb (10)	1000	<10	<10	NA	<10	<10
Rb (2)	28	13	145	NA	44	49
Sc (5)	15	7	15	NA	15	20
Sr (2)	192	28	48	NA	583	457
V (7)	150	50	70	NA	300	300
Y (5)	80	<5	32	NA	16	21
Yb (1)	2	1	2	NA	2	2
Zn (4)	295	162	132	NA	158	148
Zr (5)	349	178	301	NA	308	321

Table 2 (continued);

Sample	27	28	29	30	31	32
	Mid. Belt carb. sill		Dike		Mt. Shields basalt	
Field No.	82M-75	82M-164	82M-41	82M-42	82M-138	82M-139
Lab No.	D252244	D252262	D252238	D252235	D252257	D252258
	Major oxides (weight percent)					
SiO_2	48.3	48.4	49.0	50.3	40.3	42.9
TiO_2	4.0	4.3	3.7	3.3	3.9	3.8
Al_2O_3	11.7	12.4	12.3	13.6	14.5	14.5
Fe_2O_3	3.8	3.2	2.0	2.5	7.9	8.4
FeO	8.4	9.1	10.3	9.2	6.1	6.3
MgO	7.4	6.5	7.1	5.3	6.1	6.9
CaO	9.1	8.4	7.6	8.5	5.1	3.5
Na_2O	2.3	2.6	2.9	2.3	.24	1.3
K_2O	1.6	1.7	.33	1.9	7.6	5.2
H_2O+	2.0	2.0	3.4	2.2	3.6	3.9
H_2O-	.23	.15	.36	.25	.12	.20
P_2O_5	.51	.56	.47	.51	1.2	1.1
MnO	.16	.17	.15	.15	.08	.07
CO_2	.02	<.01	.06	.02	2.7	1.5
Total	99.52	99.46	99.67	100.03	99.34	99.57
	Selected minor elements (parts per million)					
Ba (6)	292	391	118	551	1893	400
Co (3)	30	20	30	50	50	50
Cr (1)	200	150	150	150	20	20
Cu (10)	69	75	68	25	16	61
Nb (11)	15	26	24	20	29	24
Ni (4)	113	80	80	51	26	36
Pb (10)	<10	50	<10	<10	<10	<10
Rb (2)	58	74	5	77	86	73
Sc (5)	20	15	15	15	15	15
Sr (2)	442	437	137	570	137	69
V (7)	300	200	300	300	200	150
Y (5)	19	26	17	10	35	35
Yb (1)	2	2	2	3	3	3
Zn (4)	155	179	126	133	195	325
Zr (5)	313	343	391	352	310	304

Table 2 continued; sample descriptions.

1. Pillow lava, 3.4 m up from basal contact, Hole-in-the-Wall.
2. Pillow lava, at basal contact, Hole-in-the-Wall.
3. Pillow lava, center of coalesced-pillow zone, Fifty Mountain.
4. Pillow lava, small pillow, Fifty Mountain.
5. Pillow lava, center of pillow, 70 cm from basal contact, Granite Park
6. Pillow lava, Apgar Mountains.
7. Interpillow hyaloclastite breccia, Granite Park.
8. Interpillow hyaloclastite breccia, Fifty Mountain.
9. Lower flow unit, Hole-in-the-Wall.
10. Middle flow unit, Hole-in-the-Wall.
11. Upper flow unit, Hole-in-the-Wall.
12. Flow unit(?), Redhorn Peak.
13. Lowermost flow unit, Fifty Mountain.
14. Middle flow unit, Fifty Mountain.
15. Upper flow unit, Fifty Mountain.
16. Lower flow unit, Granite Park.
17. Upper flow unit, Granite Park.
18. Flow unit, Apgar Mountain.
19. Lower portion of hypabyssal sill, Hole-in-the-Wall.
20. Middle of hypabyssal sill, Hole-in-the-Wall.
21. Hypabyssal sill(?), Red Horn Peak.
22. Late-phase intrusive into uppermost flow-unit, Hole-in-the-Wall.
23. Vent facies matrix, Redhorn Peak.
24. Vent facies matrix, Redhorn Peak.
25. Sill in Helena Formation (middle Belt carbonate sill), 2 m up from base, Thunderbird Mountain (Hole-in-the-Wall).
26. Sill in Helena Formation (middle Belt carbonate sill), chilled margin, Redhorn Peak.
27. Sill in Helena Formation (middle Belt carbonate sill), chilled lower margin, Fifty Mountain.
28. Sill in Helena Formation (middle Belt carbonate sill), chilled upper margin, Granite Park.
29. Dike cutting Helena, Snowslip and Purcell Lava Formations, chilled margin, Grinnell Glacier overlook, Granite Park.
30. Dike cutting Helena, Snowslip and Purcell Lava Formations, center, Grinnell Glacier overlook, Granite Park.
31. Amygdaloidal lava flow (approximately 12 m thick) in Mt. Shields Formation, 210 m stratigraphically above the Purcell Lava; chilled lower margin, Hole-in-the-Wall.
32. Amygdaloidal lava flow in Mt. Shields Formation, center, Hole-in-the-Wall.

Table 3. Previously reported chemical analyses of the Purcell Lava outside of Glacier National Park, and average of middle Belt carbonate sill analyses from Glacier National Park.

Analysis	1	2	3	4
	Major oxides (weight percent)			
SiO_2	41.5	47.6	49.9	48.9
TiO_2	3.3	4.0	3.9	4.2
Al_2O_3	17.1	16.7	12.8	12.5
Fe_2O_3	3.3	1.9	--	--
FeO	10.1	7.8	12.4	12.2
MgO	12.7	6.2	7.0	7.9
CaO	1.0	.95	9.2	9.4
Na_2O	2.8	.26	4.4	4.5
K_2O	.22	9.5	1.4	1.4
H_2O+	7.0	4.2	--	--
H_2O-	.21	.25	--	--
P_2O_5	1.1	.74	--	--
MnO	tr	.08	--	--
CO_2	--	.02	--	--
Total	100.03	100.20	101.00	101.00

1. Lava, Yahk River, British Columbia, porphyritic amygdaloid (Daly, 1912, p. 209).

2. Lava, Mt. Rowe, Waterton Park just north of Glacier National Park, amygdaloid (Hunt, 1964).

3. Average of 9 analyses of middle Belt carbonate sill at Siyeh Pass, Dawson Pass, and Yarrow Creek, Glacier National Park (Mejstrick, 1975). The 9 analyses are reported individually in Appendix C.

4. Average of 3 analyses of the chill zone of the middle Belt carbonate sill at Siyeh Pass, Dawson Pass, and Yarrow Creek, Glacier National Park (Mejstrick, 1975). The 3 analyses are reported individually in Appendix C.

Table 4. Representative chemical analyses of selected igneous rock types for comparison with analyses of the Purcell Lava.

	1	2	3	4	5	6	7	8	9	10
	Major oxides (weight percent)									
SiO_2	50.7	49.3	49.3	50.8	45.2	47.1	45.8	46.8	48.8	57.6
TiO_2	2.0	1.8	1.5	2.0	2.3	2.7	2.6	3.0	1.3	.77
Al_2O_3	14.4	15.2	17.0	14.1	16.0	15.3	14.6	14.6	15.7	17.3
Fe_2O_3	3.2	2.4	2.0	2.9	6.5	4.3	3.2	3.7	3.8	3.1
FeO	9.8	8.0	6.8	9.0	8.1	8.3	8.7	7.9	6.6	4.3
MgO	6.2	8.3	7.2	6.3	7.6	7.0	9.4	6.8	6.1	3.6
CaO	9.4	10.8	11.7	10.4	9.3	9.0	10.7	12.4	7.1	7.2
Na_2O	2.6	2.6	2.7	2.2	3.2	3.4	2.6	2.6	4.4	3.2
K_2O	1.0	.24	.16	.82	.81	1.2	.95	1.1	1.0	1.5
H_2O+	—	—	.69	.91	1.0	—	.76	.51	—	1.0
H_2O-	—	—	.58	—		—	—	—	—	
P_2O_5	—	.21	—	.23	.39	.41	.39	.37	.34	.21
MnO	.20	.17	.17	.18	.17	.17	.20	.15	.15	.15

1. Continental tholeiites, average of 144 analyses (Hyndman, 1972, p. 533).
2. Oceanic tholeiites, average of 161 analyses (Hyndman, 1972, p. 533).
3. Average oceanic tholeiite (Engel and others, 1965, p. 721).
4. Tholeiite basalt, average of 137 analyses (Nockolds, 1954)
5. Alkaline olivine basalt (Carmichael and others, 1974, p. 499).
6. Average alkaline olivine basalt (Hyndman, 1972, p. 171).
7. Alkaline basalt, average of 96 analyses (Nockolds, 1954).
8. Alkaline basalt without olivine, average of 22 analyses, (Nockolds, 1954).
9. Average spilite (Hyndman, 1972, p. 99).
10. Aversge andesite, based on 2500 analyses (Gill, 1981, p. 3).

Table 5. Average chemical compositions from Cenozoic basalts of selected elements considered to be relatively immobile during low-grade metamorphism. From Bloxam and Lewis (1972) except Ni which is from Engel and others (1965).

	Oceanic Tholeiite	Island Arc Tholeiite	Calc-Alkaline Basalt	Alkaline Basalt
Wt. %				
TiO_2	1.5	.80	1.1	2.9
P_2O_5	.16	.11	.21	.92
ppm				
Cr	297	50	40	67
Zr	95	70	100	333
Y	43	--	20	54
Ni	97	--	--	51

Table 6. Composition range and average of Purcell Lava and average alkaline basalts. Major oxides and trace elements for the Purcell Lava are from Table 2, and major oxides of average alkaline basalts are from Table 4. Selected trace elements and a few major oxides, in parantheses, for average alkaline basalts are from Engel and others (1975). Samples of the hyaloclastite breccia (analyses 7, 8, Table 2) and those in close proximity to the vent facies (analyses 12, 22, 23, and 24) were not included because of their anomalously high and low concentrations of certain elements.

	Purcell Lava	Ave.	Alkaline Basalts
Wt. %			
SiO_2	36.9 -- 48.7	42.9	45.8 -- 47.1
TiO_2	3.5 -- 4.2	3.8	2.3 -- 3.0
Al_2O_3	14.0 -- 16.7	15.3	14.6 -- 16.0
Fe_2O_3	1.2 -- 8.1	3.6	3.2 -- 6.5
FeO	9.0 -- 14.0	10.9	7.9 -- 8.7
MgO	6.8 -- 10.1	8.5	6.8 -- 9.4
CaO	1.1 -- 5.5	2.8	9.0 -- 12.4
Na_2O	.98 -- 2.9	2.0	2.6 -- 3.4 (4.0)
K_2O	1.1 -- 5.5	3.0	.81 -- 1.2 (1.7)
H_2O+	3.5 -- 6.9	5.2	<1.0 (.79)
H_2O-	.13 -- .45	.26	(.61)
P_2O_5	.70 -- 1.8	.84	.37 -- .41(.92)
MnO	.05 -- .23	.11	.15 -- .20
ppm			
Ba	315 -- 2705	814	498
Co	20 -- 50	35	25
Cr	10 -- 30	20	67
Cu	<10 -- 185	30	36
Nb	7 -- 40	27	72
Ni	24 -- 49	36	51
Rb	19 -- 57	39	33
Sr	40 -- 200	89	815
V	100 -- 200	150	252
Y	23 -- 80	39	54
Yb	2 -- 3	3	4
Zr	305 -- 488	356	333

Table 7. Range and average chemical content of the Purcell Lava, and middle Belt carbonate sill and dike.

	Purcell Lava		Middle Belt carbonate sill		Dike
	range	ave.	range	ave.	ave.
Wt. %					
SiO_2	36.9 - 48.7	42.9	47.0 - 48.4	47.9	49.7
TiO_2	3.5 - 4.2	3.8	3.9 - 4.3	4.1	3.5
Al_2O_3	14.0 - 16.7	15.3	11.2 - 12.4	11.7	13.0
Fe_2O_3	1.2 - 8.1	3.6	2.6 - 3.8	3.2	2.3
FeO	7.0 - 14.0	10.9	8.4 - 9.5	9.0	9.8
MgO	6.8 - 10.1	8.5	6.5 - 7.8	7.3	6.2
CaO	1.1 - 5.5	2.8	8.4 - 10.1	9.3	8.1
Na_2O	.98 - 2.9	2.0	2.1 - 2.6	2.3	2.6
K_2O	1.1 - 5.5	3.0	1.1 - 1.7	1.4	1.1
H_2O+	3.5 - 6.9	5.2	2.0 - 2.3	2.1	2.8
H_2O-	.13 - .45	.26	.13 - .23	.17	.31
P_2O_5	.70 - 1.8	.84	.49 - .56	.51	.49
MnO	.05 - .23	.11	.16 - .17	.16	.15
ppm					
Ba	315 - 2705	814	204 - 391	274	335
Co	20 - 50	35	20 - 30	30	40
Cr	10 - 30	20	150 - 200	200	150
Cu	<10 - 185	30	69 - 75	72	47
Nb	7 - 40	27	8 - 26	17	22
Ni	24 - 49	36	80 - 137	109	66
Rb	19 - 57	39	44 - 74	56	41
Sr	40 - 200	89	437 - 583	480	354
V	100 - 200	150	200 - 300	300	300
Y	23 - 80	39	16 - 26	20	14
Yb	2 - 3	3	2	2	3
Zr	305 - 488	356	308 - 343	321	372

Table 8. Measured thicknesses of the Purcell Lava (total) and the pillowed facies. Where the diabase sill is present (Hole-in-the-Wall, Boulder Peak, and Mt. Cleveland) thicknesses include the sedimentary interval (generally about 5 m thick) that separates the sill from the pillow lava. NM = not measured.

Location	Total Thickness (m)	Thickness of Pillow Lava (m)
Hole-in-the-Wall		
East wall	84	NM
West wall	77	12
North wall	92	NM
Boulder Peak (southwest flank)	76	11
Fifty Mountain	41	11
Mt. Cleveland (west face)	65	9
Trapper Peak	63	NM
Flattop Mountain	26	NM
Granite Park (Swiftcurrent Pass)	19	10
Apgar Mountains (Huckleberry Mtn.)		
North flank	40	13
Southwest flank	18	13
Near pinchout, southwest flank	15	15